DEVELOPMENT OF CHIRALITY SENSORS FOR THE DETERMINATION OF ABSOLUTE STEREOCHEMISTRY OF CHIRAL MOLECULES VIA ECCD

By

Mercy Anyika

A DISSERTATION

Submitted to
Michigan State University
In partial fulfillment of the requirements
for the degree of

DOCTOR OF PHILOSOPHY

Chemistry

2012

ABSTRACT

DEVELOPMENT OF CHIRALITY SENSORS FOR THE DETERMINATION OF ABSOLUTE STEREOCHEMISTRY OF CHIRAL MOLECULES VIA ECCD

By

Mercy Anyika

A quality of molecules that causes them to be non-superimposable on their mirror images is known as Chirality. Because of the effects that chirality can have on the chemical and pharmacological properties of molecules, there is an increased interest in developing methods for use in assigning the absolute stereochemistry of chiral molecules. This thesis will detail some of the work we have accomplished using exciton coupled circular dichroism to probe chirality in organic molecules.

This dissertation focuses on two parts. The first part introduces the concept of exciton coupled circular dichroism (Chapter I) and introduces the electronically tuned porphyrin tweezer TPFP, which has enhanced sensitivity for chirality sensing (Chapter II). We were able to employ analugues of this tweezer to develop working mnemonics for assigning the absolute stereochemistry of chiral hydroxyl ketones and sulfoxides, two important classes of functional groups commonly encountered as building block in the synthesis of complex molecules.

In using tweezers in the study of absolute stereochemistry of molecules, in order to study molecules with only one site of attachment, the molecules are first derivatized with an achiral carrier molecule to provide the second requisite site of attachment. The second part of this dissertation focuses on addressing this group of molecules and the rationale about how we

designed and synthesized the MAPOL host molecule that would allow for the assignment of absolute stereochemistry of mono-coordinating molecules, without requiring derivatization with carrier molecules (Chapter III). Lastly, chapter IV will describe the successful application of MAPOL host as a chirality reporter for a number of chiral molecules including mono amines, carboxylic acids and alcohols which would otherwise require derivatization in order to employ conventional methods.

Dedicated to my beloved family for their love and support.

ACKNOWLEDGEMENTS

I would like to first express my deepest gratitude to my advisor, Professor Babak Borhan, for his guidance, continuing encouragement and patience during my graduate career. Professor Borhan's mentorship and criticism helped me improve as a research scientist and will continue to benefit me during my whole life.

I am thankful to my committee members, Professor William Wulff, Professor James Jackson and Professor Milton Smith, for their help and suggestions during my graduate work.

I would like to thank all the members of the Borhan group for their invaluable help and friendship during the past five years. I especially would like to thank the people who worked with me on the CD project: Dr. Chrysoula Vasileiou, Dr. Marina Tanasova, Dr. Xiaoyong Li and Carmin Burrell. The academic discussions we had always drove me to think hard and critically. I especially want to thank Carmin for patiently reading through my entire thesis, understanding what it was I was trying to say, and giving suggestions. I look forward to returning the favor soon.

I would like to thank Robert Acho, a very talented and patient undergraduate student who worked with me on the MAPOL project. He was the best undergraduate student I could ever ask for.

I also wish to thank everyone who sat in room 524 at one time or the other: Xiaoyong Li, Marina Tanasova, Carmin Burrell, Calvin Grant and Bardia Soltanzadeh: thank you for allowing me the freedom to play my loud music when I needed some stress relief. I especially thank Dr. Wenjing Wang for being a good friend from when we first joined the lab, and willingly coming

along to dance even when she felt embarrassed to do so. I also wish to thank Roozbeh Yousefi for introducing me to salsa dancing. I will really miss those Saturday nights of dancing.

A special group of people deserve special acknowledgements. They were there when I needed a friend to laugh with, or a shoulder to cry on. Luis Mori Quiroz, Camille Watson, Carmin Burrell and Calvin Grant. Thank you for the hugs, laughter and for your prayers.

Last but not least, I want to express my gratitude to my mum and sisters Lois, Zet and Sarah for being very understanding and supporting my carrer. Even though you are far away, you are always in my heart.

TABLE OF CONTENTS

LIST OF TABLES

LIST OF FIGURES

LIST OF SCHEMES

Key to Symbols and Abbreviations

α	angle of rotation
$[\alpha]$	specific rotation
Å	angstrom
A	CD amplitude
ACN	acetonitrile
AcOH	acetic acid
Ar	aromatic
$BF_3 \bullet OEt_2$	boron trifluoride diethyl ether
BINOL	1,1'-Bi-2-naphthol
Bn	benzyl
BnBr	benzyl bromide
BnCl	benzyl chloride
CD	circular dichroism
CE	Cotton effect
p-chloranil	tetrachloro-1,4-benzoquinone
cm	centimeter
d	doublet
DCM	dichloromethane
DDQ	2,3-dichloro-5,6-dicyano-1,4-benzoquinone
DET	diethyl tartrate
DFT	density functional theory
DIPT	diisobutylaluminum hydride

DMAP	4-diaminopyridine
DMF	N,N-dimethylformamide
ee	enantiomeric excess
Et_3N	triethylamine
ε	molar absorption coefficient
ECCD	Exciton Coupled Circular Dichroism
Et_2O	diethyl ether
EtOAc	ethyl acetate
eq	equivalents
g	gram(s)
h	hour(s)
HKR	hydrolytic kinetic resolution
HPLC	high pressure liquid chromatography
HRMS	high resolution mass spectrometry
Hz	hertz
*i*Pr	isopropyl
IR	infrared
J	NMR coupling constant
K_{assoc}	association constant
LAH	lithium aluminum hydride
m	magnetic dipole transition moment
m	multiplet

mCPBA	3-chloroperoxybenzoic acid
MeOH	methanol
min	minute
mg	milligram
MHz	megahertz
M	molar
μM	micromolar
MS	mass spectrometry
m/*z*	mass to charge ratio
n	refractive index
NaOH	sodium hydroxide
nm	nanometer
NMR	nuclear magnetic resonance
ORD	optical rotatory dispersion
PCC	pyridinium chlorochromate
Ph	phenyl
PMB	*para*-methoxybenzyl
q	quartet
R	rotational strength
s	singlet
SAD	Sharpless asymmetric dihydroxylation
SAE	Sharpless asymmetric epoxidation
rt	room temperature

t	triplet
TBAF	tetrabutylammonium fluoride
TBS	*t*-butyldimethylsilyl
TFA	trifluoroacetic acid
THF	tetrahydrofuran
TPP-tz	5-(4-carboxyphenyl)-10,15,20-triphenylporphyrin tweezer
UV-vis	ultraviolet-visible spectroscopy
Zn-TPP	zinc tetraphenylporphyrin
Zn-TPP-tweezer	zinc 5-(4-carboxyphenyl)-10,15,20- triphenylporphyrin tweezer
$Zn(OAc)_2$	zinc acetate

Chapter 1

Introduction to ECCD

1-1 Chirality

Man's fascination with asymmetric objects goes back to the 1800's. With the discovery of the existence of two forms of tartrate by Louis Pasteur in 1847,[1] the art of exploring dissymmetry in molecules became a molecular science. This fascination grew into an intriguing problem to be solved when in 1874, Van't Hoff and LeBel suggested[2,3] that molecules possess a three-dimensional structure that may result in dissymmetry. The introduction of the word "chiral" by Lord Kelvin,[4] forty years after Pasteur's discovery represents a milestone in the history of absolute configuration, and marked the beginning of a new era in the determination of absolute stereochemistry of chiral molecules. The word "chiral" originates[5] from the Greek word for hand (cheir) and introduces the concept of "handedness" in reference to a pair of non-superimposable mirror images.

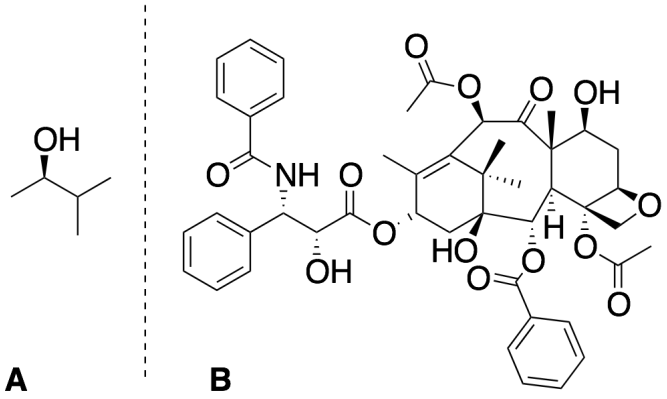

Figure 1-1. Representative chiral molecules: 3-methylbutan-2-ol (**A**) and Taxol® (**B**).

Examples of chiral molecules can range from simple molecules like 3-methylbutan-2-ol that possesses point chirality, to large natural products with multiple chiral centers, such as Taxol® (Figure 1-1). The two mirror images of the molecule are referred to as "enantiomers" and, despite their identity in chemical composition, they may be of different abundance and possess different physical and/or biological properties. For instance, living organisms use exclusively one chiral form of a molecule (homochirality). Virtually all active forms of amino acids are of the L-form (D-serine being a notable exception), while most biologically relevant sugars are of the D-form. Enzymes being chiral, often distinguish between two enantiomers, and preferentially bind to a single enantiomer since it can fit inside an enzyme's binding cavity, while the other cannot.

Changes in chirality affect chemical and biological properties of some chiral molecules. For instance, while (*S*)-mercaptohexanal (Figure 1-2) has a pleasant, fruity odor, its R enantiomer has a pungent sulfur smell. Similarly, the S enantiomer of Carvone has the odor of caraway seeds, while its (*R*) enantiomer has the odor of spearmint.

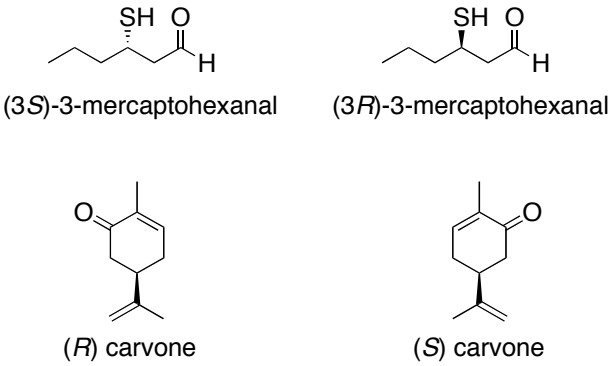

Figure 1-2. Enantiomeric forms of 3-mercapto hexanal and carvone.

Chiral organic molecules are of extreme interest to the pharmaceutical, agrochemical and other industries.[19] Drugs generally work by interacting with receptors on cell surfaces, or enzymes within cells. Receptors have a specific three-dimensional structure which will allow only the isomer that fits precisely to bind preferentially while the other has little or no activity. Considering that the two enantiomers of a natural product or synthetic drug may have different physiological properties, the resolution and clinical testing of both enantiomers is a prerequisite to the development of the optimum drug.[19]

Most of the pharmaceuticals sold commercially contain one or more chiral centers. Drugs obtained from natural sources or those prepared from natural materials are produced as pure enantiomers, because chiral compounds from nature usually occur as the pure form of one of the enantiomers. However, until recently (1970s) most chiral drugs produced synthetically from achiral starting materials were produced and sold in their racemic form, even though their therapeutic effect was mainly due to only one isomer. In most cases, the unwanted isomer was physiologically inactive and did not cause any serious side effects. However, that was not always the case. One tragic example of historical note is thalidomide.

(*S*)-Thalidomide (*R*)-Thalidomide

Figure 1-3. Structures of (*R*)- and (*S*)-Thalidomide.

Thalidomide was developed and sold from 1957 - 1961 in almost 50 countries. It was mainly prescribed to pregnant women as an antiemetic to treat morning sickness and as a sleep

aid. As shown in Figure 1-3, thalidomide contains a stereocenter and so exists in its two enantiomeric forms.[4] Tragically, while the (*S*)-isomer had the desired anti-nausea effects, the (*R*)-form was teratogenic and caused fetal abnormalities, such as severely deformed limbs.

Chirality is not only becoming an important issue in the pharmaceutical industry, but also in the agrochemical and other industries as well.[19] As a result, there is a need for simple and effective ways for the determination of absolute configuration.

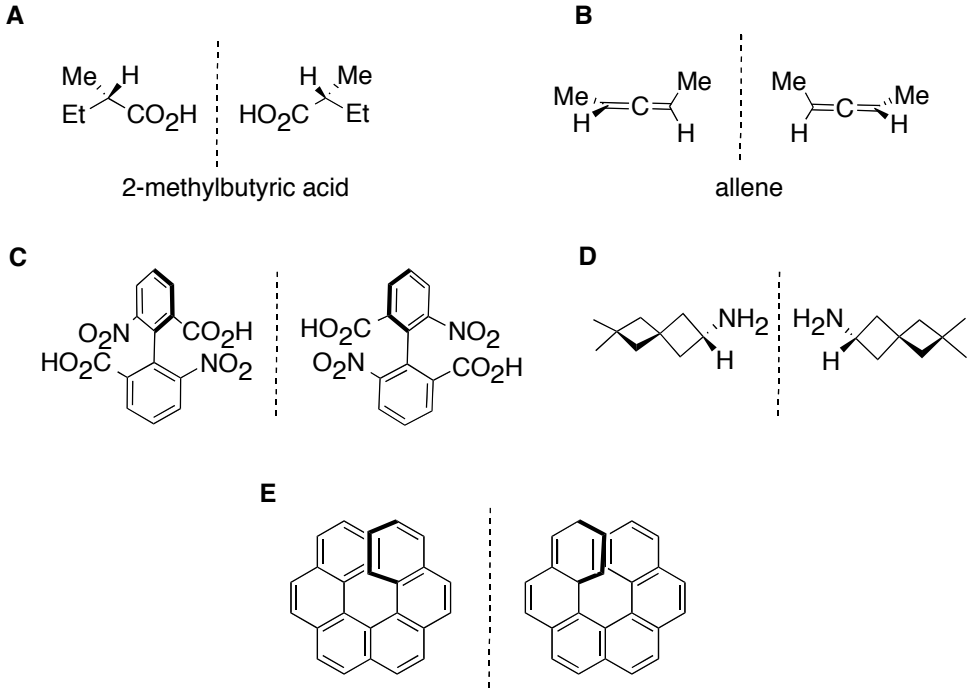

Figure 1-4. Examples of some chiral molecules and their mirror images.

The variety of chiral molecules is complemented by different types of chirality. Point chirality arises when four different substituents are attached to a tetrahedral carbon making the carbon a chiral center (Figure 1-4A). The letters *R* (from Latin "*rectus*" meaning right) and *S*

(from Latin "*sinister*" meaning left) are used to indicate the configuration (arrangement of groups) on the chiral center, based on priorities set in place by Cahn, Ingold and Prelog.[6] The classic point chirality is represented by 2-methylbutyric acid (Figure 1A). As shown, (*S*)-2-methylbutyric acid is not superimposable on its mirror image (*R*)-2-methylbutanoic acid. This non-superimposability of mirror images is the only necessary requirement for chirality. However, molecules do not need to have a chiral center to be chiral. Figure 1-4 A-C shows the various forms of chirality.

Figure 1-4B shows an allene[7] where the overall molecule is not planar, but rather the two π bonds are perpendicular to each other causing the molecule to lack any plane of symmetry when both ends are unsymmetrically substituted. Figure 1-4C shows a biphenyl molecule, bearing large groups on each side of the C-C single bond. This molecule is chiral because of restricted rotation around the single bond, hence it is "locked" into a chiral conformation since steric hindrance between the *ortho*-substituents prevents bond rotation. This restriction of rotation is the source of geometric isomerism (atropisomerism). Restricted rotation can also be found in spiranes, which are compounds that have two rings with a common carbon atom, as shown in Figure 1-4D. Because of this, the rings are perpendicular to each other giving rise to axial chirality.[8] Figure 1-4E shows a classic example of an inherently chiral chromophore,[9] hexahelicene. Despite the fact that this molecule does not have any asymmetric carbons, it is not planar, but rather lacks a plane of symmetry as it traces a helix when one side of the molecule lies above the other due to crowding of the rings. The defined helix can be either right-handed (+)-hexahelicene, or left-handed (-)-hexahelicene and therefore, non-superimposable on its mirror image.[10]

1-1.2 Methods for Assigning Absolute Configuration

Due to the role of chirality in physical, biochemical and physiological properties of chiral molecules, there is an increasing interest in determining molecular chirality,[1] and the need for simple and effective ways for the determination of absolute configuration is more prominent than ever. There are several methods that are used to establish the absolute stereochemistry of chiral molecules including: chemical correlation with known chiral compounds,[5] NMR Mosher ester method,[13] as well as X-ray crystallography.

NMR-based configurational assignment of chiral compounds has been the most widely used approach to determining chirality. The method originated by Mosher and co-workers[13] involves derivatization of a chiral alcohol with two enantiomers of a chiral acid, bearing an aromatic group at the chiral center. The ^{1}H-NMR spectra of the two obtained diastereomers are then compared, and the anisotropic shielding ($\Delta\delta^{RS}$) for the protons neighboring the chiral center are measured. The scope of the Mosher ester method has been extended further to amines and carboxylic acids,[5] however, discrepancies with conformational stability of diastereomers, and the resulting misinterpretation of the data may introduce error in the analysis. In addition, a small limitation is posed by the need for chemical derivatization, that requires multi-milligram quantities of material.

X-ray crystallography is the most unambiguous method for absolute stereochemical determination. Although X-ray crystallography provides full stereochemical analysis of chiral compounds in a single experiment, several shortcomings associated with the method, such as the need to obtain an X-ray quality crystal, the need for multi milligram amounts of the compound of

interest, and the requirement of a heavy atom in order to obtain absolute stereochemistry make this method less desirable. These limitations necessitate the development of a general and more accessible protocol that allows for easy stereochemical determination.

1-2 Optical Rotatory Dispersion (ORD) and Circular Dichroism (CD) spectroscopy

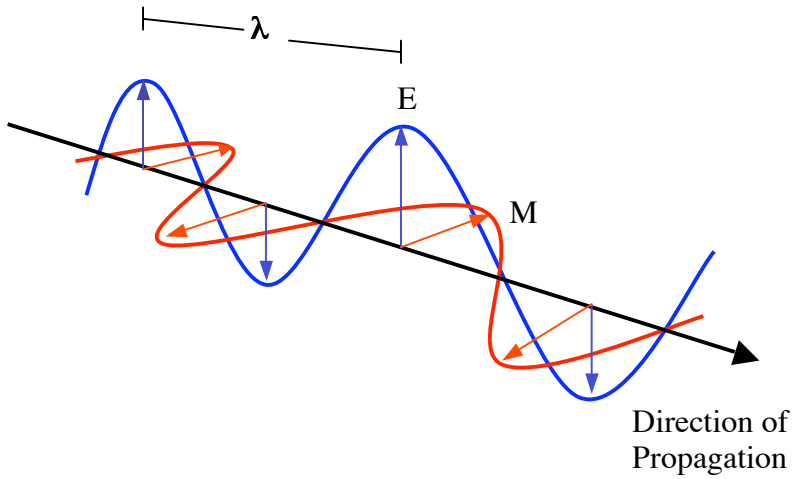

Figure 1-5. Light as electromagnetic radiation.
For interpretation of the references to color in this and all other figures, the reader is referred to the electronic version of this dissertation.

Chiroptical methods based on optical rotatory dispersion (ORD) and circular dichroism (CD) spectroscopy have been employed for the absolute stereochemical determination of chirality. The advantage of chiroptical analysis is the high sensitivity, generally requiring only μM concentrations of compound.

Optical Rotatory Dispersion and Circular Dichroism are based on the ability of chiral molecules to interact with polarized light. Polarized light is a transverse wave, consisting of both an electric

and magnetic component, which oscillate perpendicular to one another in the direction of the propagation of light, thus forming a right handed coordinate system.[18] The polarization of light is defined by the direction of its electric field vector.[18] (Figure 1-5)

Ordinary light sources such as the sun or a light bulb are unpolarized, since light waves propagate in all directions. On the other hand, when unpolarized light passes through a polarizing filter, only the light waves with oscillation parallel to the direction of the filter pass through.

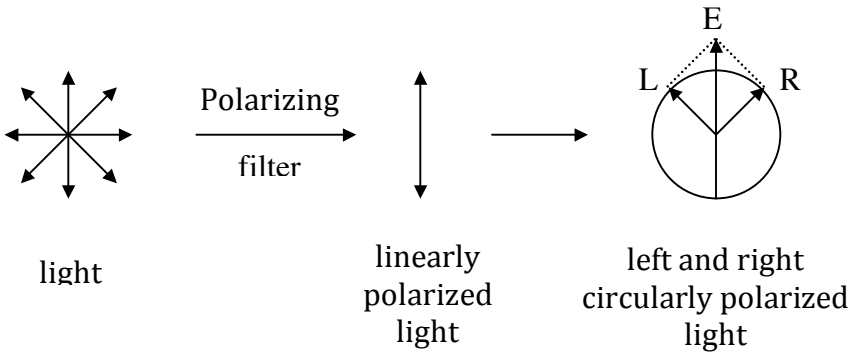

Figure 1-6. Linearly and circularly polarized light.

The light passing through the filter is now aligned in one plane of oscillation, and is defined as linearly polarized light. Linearly polarized light only oscillates in one specific direction, where the electric field (E) remains constant in magnitude, but traces out a helix as a function of time,[20] and can be resolved into two circularly polarized light beams: a left circular component (L) and a right circular component (R) as shown in Figure 1-6.

The two basic phenomena of the interaction of light and matter, *absorption* (or extinction (ε)) and a decrease in *velocity* (c), are caused by the interaction of the electric (E) vector of the propagating wave with the electrons of the component atoms. This interaction has two effects:

reducing the velocity of propagation (also called *retarding* the light) and decreasing the amplitude of the E vector. Reducing the velocity of propagation is called *refraction* and is described by the *index of refraction, n* (first described by Fresnel in 1825), and decreasing the amplitude of the vector E is called *absorption* and is described by the *molar absorption coefficient,* ε.

For most substances, simple refraction and absorption are the only detectable results of such an interaction even if the light is polarized. However, when polarized light interacts with chiral matter, its properties such as intensity (amplitude), polarization, velocity (c) or refraction (n), wavelength (λ), etc may change.[21] For instance, when plane polarized light passes through an achiral or racemic compound, refraction or absorbance of the left and right circularly polarized light is equally affected. On the other hand, if it passes through an optically active medium (Figure 1-7) the refraction (equation 1-1)[18] and absorbance of either one of the circularly polarized components is altered to a greater extent as compared to the other component.[21]

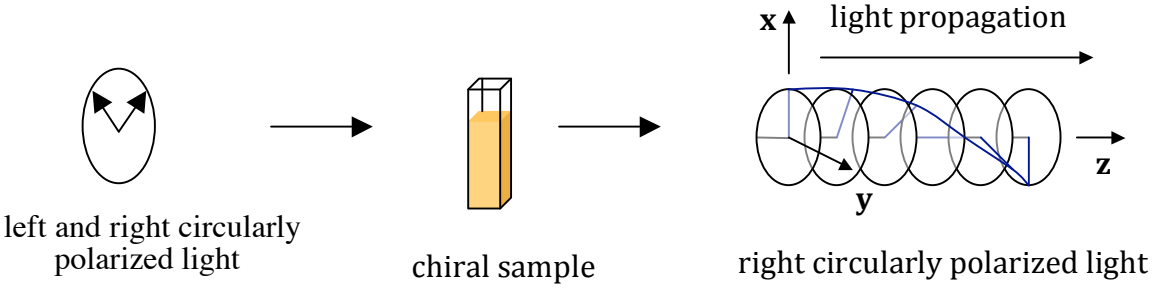

Figure 1-7. Circularly polarized light passing through a chiral medium, which absorbs the left circularly polarized component more than the right.

$$\Delta n = n_L - n_R \neq 0 \qquad (1\text{-}1)$$

$$\Delta \varepsilon = \varepsilon_L - \varepsilon_R \neq 0 \qquad (1\text{-}2)$$

Symbols n_L and n_R are the refractive indices for left and right circularly polarized light, respectively. Because the left and right circularly polarized light travels through the optically active medium at different velocities, i.e. they are characterized by the different *refraction indexes n*, the two components are no longer in phase, and the resultant vector is rotated by an angle α relative to the original plane of polarization. The angle α, reflecting this rotation of the vector is called an *optical rotation*. *Optical rotation* is the oldest of chiroptical methods that is used as a criterion for enantiomeric purity only if optical rotation data of the compound had been previously identified. When specific optical rotation [α] is plotted as a function of wavelength, an Optical Rotatory Dispersion (ORD) spectrum is generated, which can be used for absolute stereochemical determinations.[34] The specific optical rotation can be calculated from the observed angle of rotation α, as expressed by equation 1-3[18] where α is the angle of rotation (degree units), *c* is the mass-based concentration of the sample (g mL^{-1}), and *l* is the path length (decimeters).

$$[\alpha] = \alpha / cl \qquad (1\text{-}3)$$

The difference in refractive indices for left and right circularly polarized light is related to the angle of rotation, α, and is represented by equation 1-4:[18]

$$\alpha = (n_L - n_R)\ 1800\ l / \lambda_0 \qquad (1\text{-}4)$$

where α is the angle of rotation, in degrees, n_L and n_R are the refractive indices for left and right circularly polarized light, l is the path length in decimeters, and λ_0 is the wavelength in vacuum of the light beams, in centimeters.

Because ORD is only based on the difference in the refractive indices, and all chiral molecules exhibit a molecular refraction at almost any wavelength of irradiation, theoretically, ORD can be detected over all wavelengths. Typically, the sodium D-line (589 nm) is used to detect and quantitate optical activity. In contrast to ORD, Circular Dichroism (CD) is based on the difference in absorption between the left and the right circularly-polarized components of a circularly-polarized light (equation 1-2).[18] Due to nonequivalent absorption, the two circularly polarized components are not only out of phase, but also of unequal amplitude. Consequently, the resulting electric field vector E (Figure 1-6) does not oscillate along a straight line but rotates along an ellipsoid path and produces *elliptically polarized light*. Both ORD and CD effects are manifestations of the same phenomenon and are also referred to as the Cotton Effect (CE), in honor of French physicist Aimé Cotton who first observed both phenomena. CD is an absorptive process and therefore, it can be detected for chromophore-containing molecules in the vicinity of an absorption band, and plots Δε vs. wavelength.[18] The molar amplitude A of an ORD can be related to the intensity of the CD curve, Δε, by equation 1-5:[22]

$$A \approx 40.28\Delta\varepsilon \qquad (1\text{-}5)$$

The shape and appearance of a CD curve is similar to that of the ordinary UV-vis absorption curve of the electronic transition to which it corresponds. The only difference is that, unlike the ordinary UV-vis absorption curves, CD curves may be positive or negative as shown in Figure 1-

8, depending on the absorptive properties of the chiral media and, subsequently, the outcome of Equation 1-2.

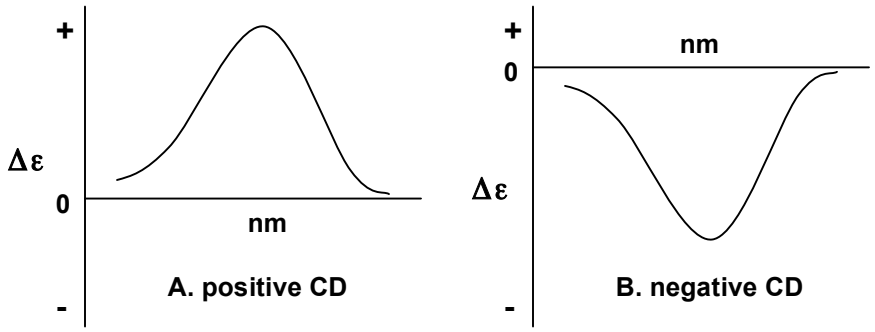

Figure 1-8. Positive (A) and negative (B) Cotton effects.

The sign of CD depends on the direction of a momentary dipole called electric dipole transition moment (edtm) μ, resulting from the excitation of the chromophore from its ground state to an excited state. The direction of μ is the same as the direction in which the electrons are pushed during the transition.

In an achiral molecule (Figure 1-9A), the net electron redistribution upon interaction with the light is always planar, and the net μ is nulled (Figure 1-9A). In a chiral molecule (Figure 1-9B) the electron rearrangement is always helical[23] and the electronic transition causes the charge displacement, which generates the electron dipole transition moment. If the helix of electron motion is right-handed then a positive *CD* is observed, and *vice versa*, i.e. if the helix of electron motion is left-handed then a negative *CD* is observed.

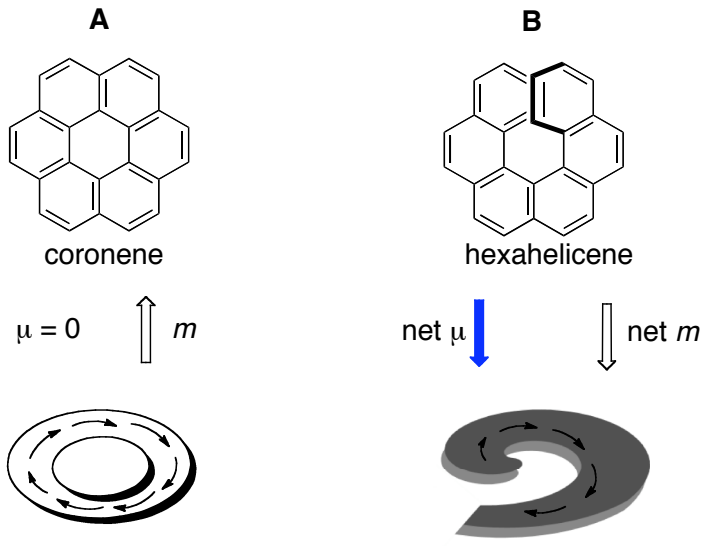

Figure 1-9. Electron redistribution upon light excitation for a transition of **A** achiral and **B** chiral molecule.

The rotation of the electric charge creates a magnetic field, the strength and direction of which may be described by the magnetic transition dipole moment denoted by the vector . (Figure 1-9).[5] The direction of a magnetic transition moment, can be determined by application of the "right hand rule" (Figure 1-10[24]) to the rotation of the charge (circular electric current). Instructively, the outstretched thumb points to the direction of the magnetic transition dipole moment when the right hand fingers are curved in the direction of electron flow.[25]

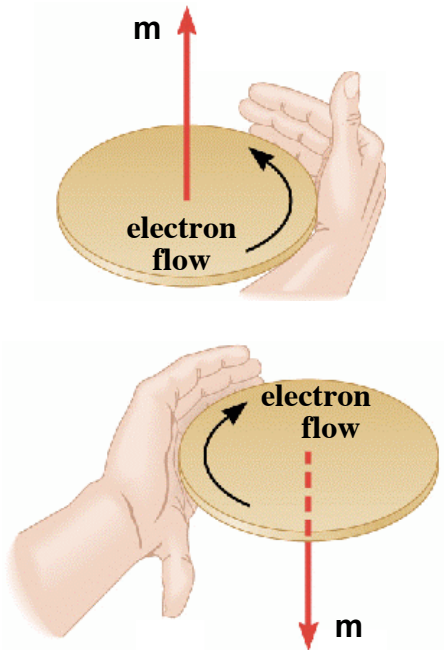

Figure 1-10. The right hand rule to determine the direction of magnetic dipole transition moment (*m*).

The fact that left-handed circularly polarized light induces a right-handed transition follows from the interaction of the electric vector, and the component of the magnetic field, referred to as rotational strength, *R*. The rotational strength, *R*, which is a theoretical parameter representing the sign and strength of a CD Cotton effect (CE), is given by the scalar product of the electric and magnetic transition moments (Equation 1-6):[5]

$$R = \vec{\mu} \cdot \vec{m} = |\mu|\,|m| \cos\beta \qquad (1\text{-}6)$$

Where μ and *m* are the electric and magnetic transition dipole moments, respectively, and β is the angle between the two transition moments. The sign of the CE is positive when the angle is acute ($0 < \beta < 90^{\circ}$) or in the limiting case, parallel, and it is negative when the angle is obtuse ($90^{\circ} < \beta < 180^{\circ}$) or in the limiting case, antiparallel. Dextrorotation results when $R > 0$, together with positive CD, and levorotation is generated when $R < 0$, together with negative CD curve. There is no CE when the electric and magnetic transition dipole moments are perpendicular to each other.

1-2.1 A brief introduction to Circular Dichrometers (spectropolarimeter)

Circular dichrometers are used to record both ORD and CD spectroscopy. The essential features of a spectropolarimeter are shown in Figure 1-11.

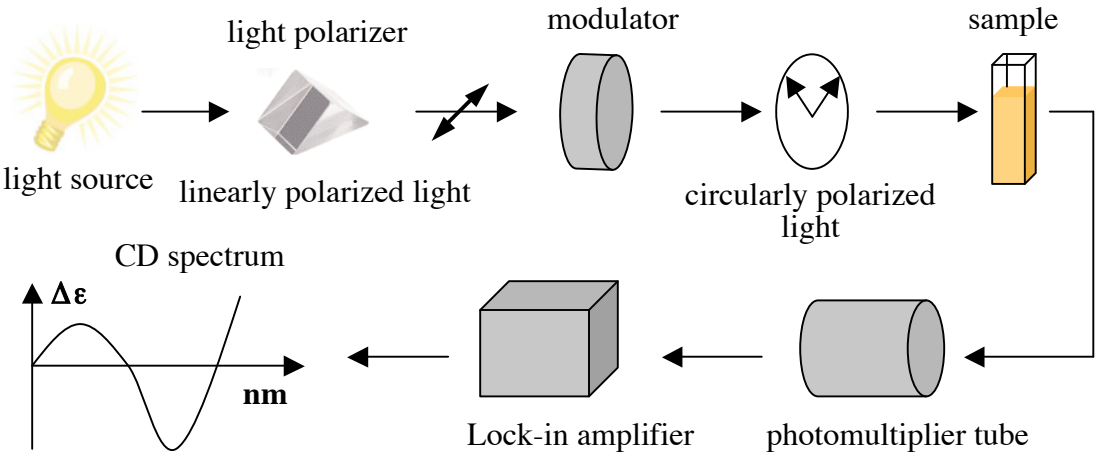

Figure 1-11. Schematic representation of a CD spectropolarimeter.

A xenon lamp is typically used as the source of light. This light passes through a monochromator consisting of a series of crystal prisms to produce linearly polarized light. In the CD spectropolarimeter, the optical system is comprised of two monochromators (a double monochromator), which helps in reducing stray light. The linearly polarized light is then modulated into left and right circularly polarized light. The modulator consists of a thin crystalline plate known as a wave plate. When linearly polarized light is incident on a wave plate at 45°, the light is divided into two equal electric field components, one of which is retarded by a quarter wavelength by the plate. This throws the two components 90° out of phase with each other such that upon emerging, one is always maximum, while the other is always zero and vice versa. The effect is to produce circularly polarized light. The 90° phase shift is produced by a

precise thickness *d* of the birefringent crystal, which, because of the 90° shift, is referred to as a quarter wave plate. This then passes through the sample chamber. The light transmitted through the sample is measured by a photomultiplier tube, which produces a current whose magnitude depends on the number of incident photons. This current is then detected by a lock-in amplifier and recorded. (Figure 1-11)

Most CD spectropolarimeters measure differential absorbance, *ΔA,* between the left and right circularly polarized light, which can then be converted to Δε based on the Beer-Lambert law, using Equation 1-7.[5]

$$\Delta A = \Delta\varepsilon\, c\, l \qquad (1\text{-}7)$$

Where ΔA is the difference in absorbance and Δε is the difference in molar extinction coefficients ($M^{-1}L^{-1}$). Since Optical Rotatory Dispersion (ORD) and Circular Dichroism (CD) are manifestations of chiral substances and are not observed for achiral compounds or racemic mixtures, they can be used to detect and quantitate optical activity. However, ORD and CD by themselves do not allow the configuration of a given product to be defined.

1-3 Exciton Coupled Circular Dichroism (ECCD)

1-3-1 Theoretical background of ECCD

Excitation of a chiral system with a single chromophore results in ORD or CD. For chiral systems containing two or more chromophores, excitation with polarized light induces a through-space interaction referred to as the Exciton Coupled Circular Dichroism (ECCD) and results in a bisignate CD curve - *ECCD spectrum*. In contrast to ORD and CD, the ECCD method is a non-empirical approach to establishing the absolute configuration of chiral compounds first discovered by Harada and Nakanishi.[34]

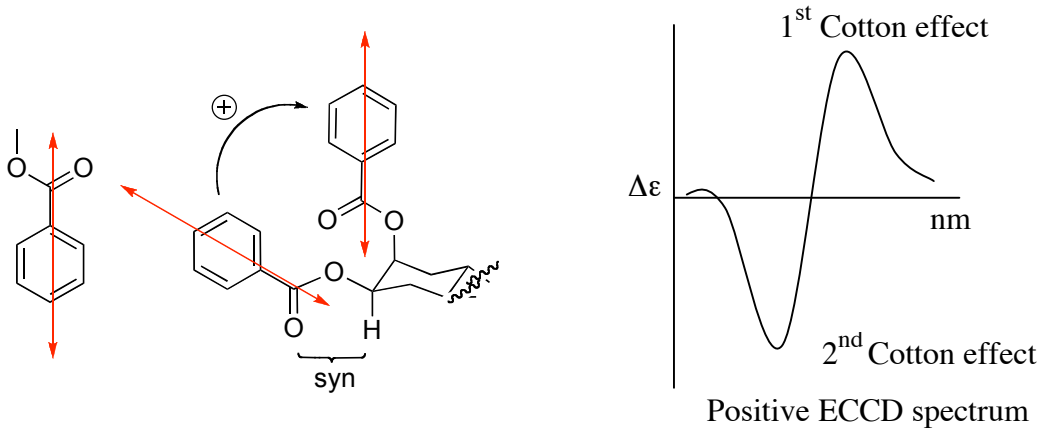

Figure 1-12. Exciton Coupled Circular Dichroism (ECCD) of steroidal 2,3-bisbenzoate.

ECCD is based on the through space exciton coupling between two or more chirally oriented non-conjugated chromophores. The coupling of the chromophores' electric transition dipole moment leads to the observed bisignate CD spectrum and the nonempirical determination of their orientation. Figure 1-12 shows the exciton coupling between two benzoates in steroidal 2,3-bisbenzoate.[26] Due to the oscillation of the main electric transition dipole, excitation of a bis-chromophoric system yields two sets of the through space interaction of edtm: an *in-phase* or an *out-of-phase* interaction. These interactions cause the energy level of the excited state (exciton)[31] to split into two states: the *out-of-phase* stabilizing dipole-dipole interaction (low energy interaction, α-state) and the *in-phase* destabilizing dipole-dipole interaction (high energy interaction, β-state) (Figure 1-13). The difference in the λ_{max} of the two UV-vis peaks is due to the energy gap, $2v_{ij}$, and is called the Davydov splitting,[29] after the Russian physicist who developed the theory of exciton coupling in the electronic spectra of molecular crystals.

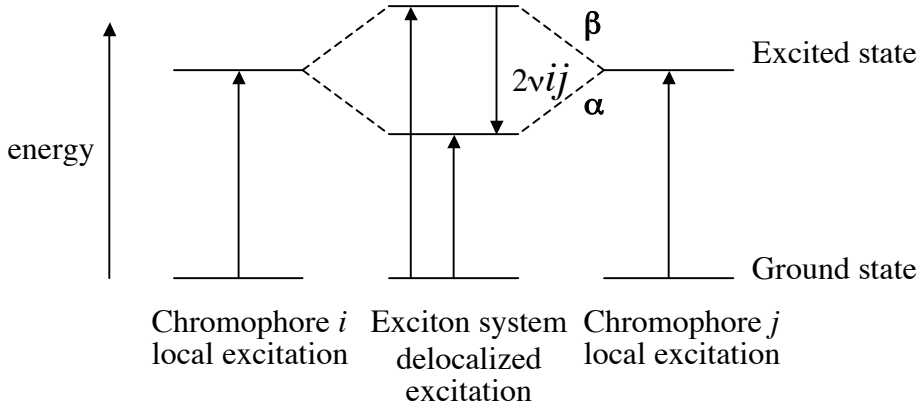

Figure 1-13. Splitting of the excited states of isolated chromophores *i* and *j* by exciton interaction. The energy gap $2\nu_{ij}$ is referred to as the Davydov splitting.

The two split transitions lead to two absorptions that are differentiated by the absorption wavelength: the *out-of-phase* transition is detected at higher wavelength, while the *in-phase* transition, being higher in energy, appears at lower wavelength (Figure 1-14A, dotted lines). The magnitude of $2v_{ij}$ depends on the nature of chromophores. For degenerate chromophores, the difference $2v_{ij}$ is relatively small, and the wavelength of the two transitions may be relatively similar. Alternatively, for different chromophores the energy gap $2v_{ij}$ between the two energy levels is substantial and the two transitions might be observed separately.[29] Figure 1-14 depicts Davydov splitting in the UV-Vis and the CD spectra.

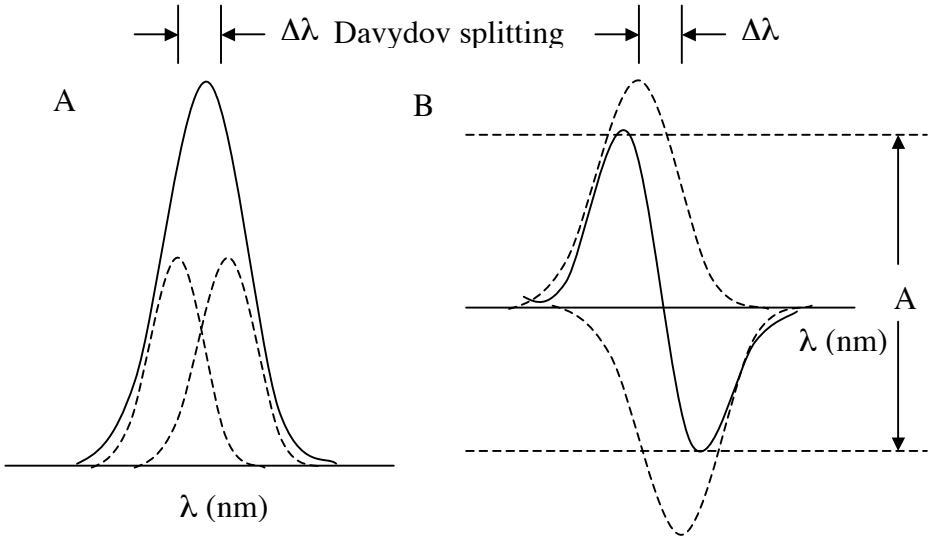

Figure 1-14. The UV-vis spectrum (A) and ECCD spectrum (B) upon through space interaction of two degenerate chromophores. The two observed Cotton effects are shown using dashed lines, while the observed, summation curves are in solid lines.

In case of the plain polarized light (UV-vis spectrum), the interaction of the two excited degenerate chromophores is detected as two component spectra of the same sign, which usually appear as a single absorption with double intensity (Figure 1-13B, solid line), consisting of two transition representing the α and β exciton states (Figure 1-13B, dotted line). In case of circularly polarized light, depending upon whether the edtms are in phase (symmetric) or out of phase (anti symmetric), a Cotton effect of different sign is produced (Figure 1-13C, dotted lines). As a result, a spectrum with two peaks (bisignate curve), one positive and one negative CD couplets is generated. This phenomenon is known as Exciton Coupled Circular Dichroism, leading to a bisignate spectrum (Figure 1-13B, solid line). The difference in λ_{max} of the two peaks is $2v_{ij}$.

An ECCD spectrum may be positive (+) or negative (-). In a positive ECCD spectrum, the positive CD appears at higher wavelength (lower energy), followed by the negative CD at

lower wavelength (higher energy). In the case of a negative ECCD spectrum, the negative CD appears at higher wavelength (lower energy), followed by the positive CD at lower wavelength (higher energy). The overall sign of ECCD generated from a bis-chromophoric exciton coupling depends on the angular arrangement of electric transition dipole moment (etdm). There are two possible orientations of electric transition dipole moments (or chromophores): clockwise or counterclockwise. Positive ECCD is observed for the clockwise orientation, and negative ECCD for the counterclockwise orientation. For example, a clockwise orientation of the chromophores in Figure 1-12 results in a positive ECCD spectrum.

The relationship between helical orientation of chromophores and observed ECCD can be established based on the direction of net charge oscillation in the two coupled systems, or based on the interaction between the electric and magnetic moments of chromophores. Figure 1-15 depicts analysis of exciton coupling interaction of two chromophores or, more precisely, two etms' of the two chromophores that are pre-set in a clockwise helical orientation relativeto one another. The helix associated with the charge rotation generated from the edtm transition can be visualized by placing the partial edtm in a cylinder, aligned along the axis of the "total" edtm, (Figure 1-15). The individual edtm μ of an electric transition, for each chromophore, couples to the other in phase (symmetric) or out of phase (asymmetric), Figure 1-15 **i** and **ii** respectively. In the case **i** where the two electric transition dipole moments couple in phase, the "total" electric transition dipole moments are oriented along the chromophoric C_2 axis, and in case B, where they couple out of phase, the "total" electric transition moments are oriented perpendicular to the chromophoric C_2 axis. As shown in Figure 1-15 (i), the symmetric coupling results in a counter-clockwise helical movement, therefore, according to the right hand rule, the magnetic transition dipole moment (*m*) is anti-parallel to μ, leading

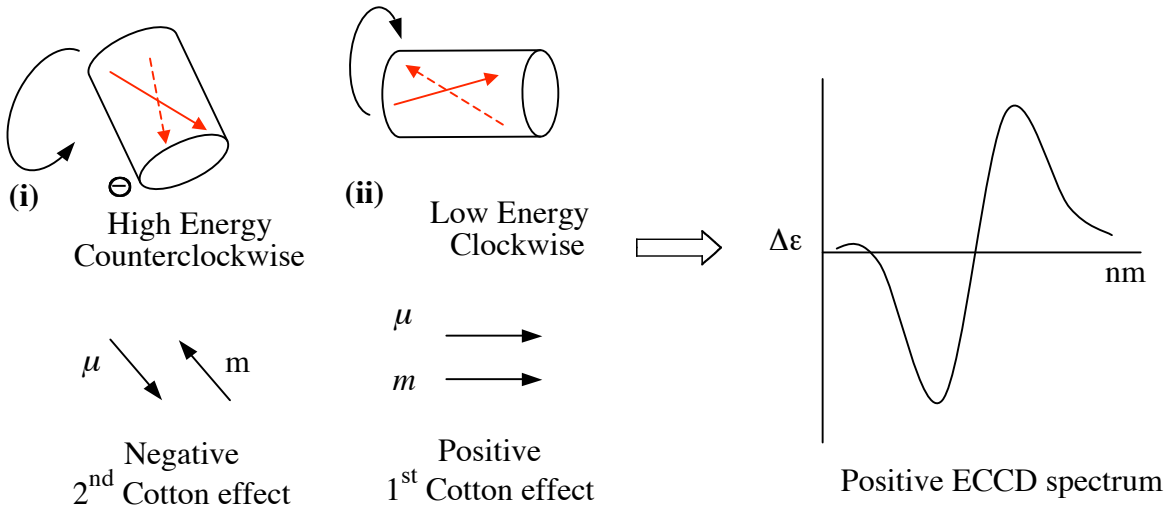

Figure 1-15. The expected ECCD spectrum of dibenzoate and its rationalization.

to a negative Cotton effect (negative CD band). (Figure 1-15 **i**) As expected, the out of phase interaction causes the opposite effect leading to parallel *m* and μ vectors (Figure 1-15 **ii**) leading to a positive Cotton effect (positive CD band). According to Equation 1-6, ($R = \vec{\mu} \cdot \vec{m} = |\mu||m|\cos\beta$) the sign of a Cotton effect depends exclusively on the angle between the electric and the magnetic transition dipole moment. Therefore, the symmetric coupling of the edtm will result in a negative peak ($\beta = 180^\circ$, $\cos\beta = -1$), while the anti-symmetric will result in a positive one ($\beta = 0^\circ$, $\cos\beta = 1$), both of equal magnitude. The positions of these two Cotton effects relative to each other (which defines whether the overall ECCD spectrum is positive or negative) depends on the relative energies of the two occurring transitions. The in phase coupling is of higher energy because of the repulsion between like charges, and so the corresponding negative Cotton effect will appear at a shorter wavelength. Because nomenclature dictates that the

bisignate ECCD curve be named after the lower energy 1st Cotton effect, the spectrum of the dibenzoate discussed above (Figures 1-15) will be referred to as a positive ECCD curve.

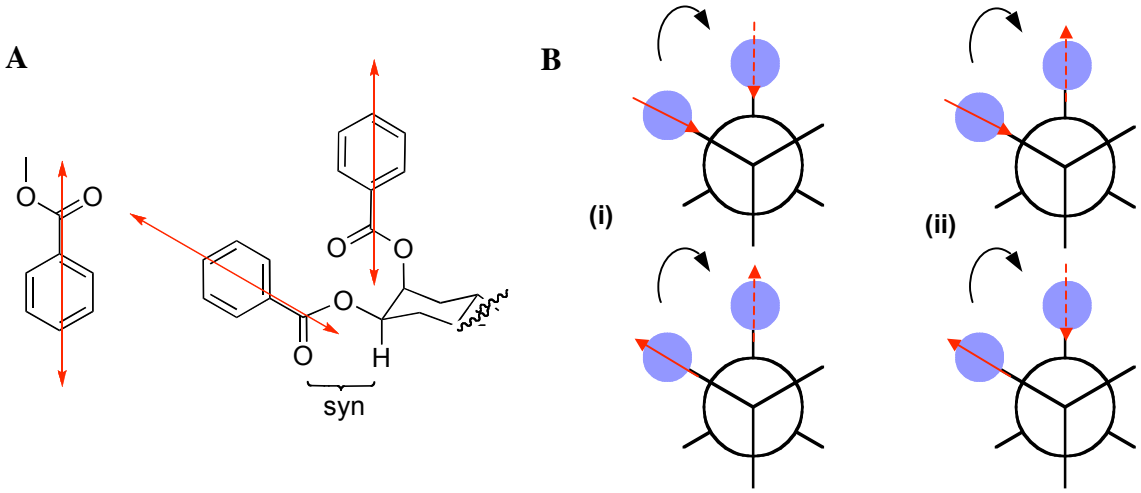

Figure 1-16. A qualitative explanation of ECCD. **A**. Structures of benzoate and dibenzoate esters. edtm's are shown in red; **B**. Possible in phase (i) and out of phase (ii) interactions of the edtm's of the degenerate chromophores (shown in blue).

Exciton Coupled Circular Dichroism can be further explained by examining its application to a specific molecule, bearing two identical benzoate groups[25] shown in Figure 1-16, where benzoate esters of a vicinal cyclohexanediol are interacting. Benzoate esters have a strong UV-Vis absorption band at around 230 nm, arising from the $\pi \rightarrow \pi^*$ transition of the conjugated aromatic ring with the carbonyl group.[30] The large electric dipole transition moment μ of each benzoate group is oriented collinearly with the long axis of the molecule, almost parallel to the direction of the C-O bond, and oscillates in both directions (Figure 1-16A). Determination of absolute configuration means determination of the absolute sense of chirality between the C(2)-O and C(3)-O bonds, by looking down the C-C bonds from front to back, the orientation of the two

benzoate groups is set in a clockwise manner, which leads to positive chirality. The absolute sense of twist stays the same regardless of whether it is viewed from C(3) to C(2) o*r vice versa*.

1.3-2 The Quantum Mechanics Explanation of ECCD

The ECCD theory can also be explained by Quantum Mechanical considerations. As mentioned previously, when a molecule contains two identical chromophores, as a result of their through space interactions, excitation is delocalized between the two chromophores, and the excited state[31] is split into two α and β states (Figure 1-13).

$$R_{\alpha,\beta} = \pm\frac{1}{2}\pi\sigma_0\vec{R}_{ij}\bullet(\vec{\mu}_{ioa}\times\vec{\mu}_{joa}) \qquad 1\text{-}8$$

Based on theoretical calculations on the binary system, the rotational strength, R, which represents the sign and the strength of a CD Cotton effect, can be defined by Equation 1-8,[26] where the positive and negative signs correspond to α- and β- state, respectively, R_{ij} is the distance vector between two chromophores, μ_{ioa} and μ_{joa} are the etdm of excitations, and σ_o is the excitation number of transition from 0 to α state.

Table 1-1. Definition of Exciton Chirality for a Binary System.

	Qualitative Definition	Quantitative Definition	Cotton effects
Positive Chirality	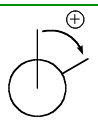	$Rij\bullet(\mu ioa\times\mu joa)Vij>0$	positive first and negative second Cotton effects
Negative Chirality	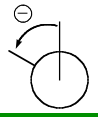	$Rij\bullet(\mu ioa\times\mu joa)Vij<0$	negative first and positive second Cotton effects

If Equation 1-8 is positive (+) the observed ECCD spectrum is positive, and if it is negative (-) then the observed ECCD spectrum is negative. From the equation above, the sign of the bisignate curve completely depends on the spatial orientation of the two chromophores.[32] As shown in Table 1-1,[33] if the electric transition dipole moments of the two chromophores from front to back constitutes a clockwise orientation, then according to Equation 1-8 above, a positive bisignate spectrum will be observed, which refers to a positive 1st and negative 2nd Cotton effects, while an opposite but otherwise identical spectrum is produced by the counterclockwise orientation.[34,35] Therefore, the sign of an ECCD spectrum for a chiral molecule can be predicted as long as the spatial orientation of two chromophores is known. Moreover, the sign of a bisignate ECCD spectrum can enable the determination of the absolute orientation of two chromophores in space in a non-empirical manner.

The difference in $\Delta\varepsilon$ between the 1st and 2nd Cotton effects is called the amplitude, A, of the ECCD couplet (Figure 1-14). This amplitude depends on several factors:[36]

a. *Molar absorption coefficient (ε) of the interacting chromophores*. The amplitude is proportional to ε^2. Therefore, in order to have increased sensitivity with ECCD methods, chromophores with strong absorptions are preferred. These highly active chromophores enable CD measurements to be performed at micro-molar concentrations, which make it an extremely useful property when only limited amount of chiral compound is available.
b. *Interchromophoric distance (R)*. The amplitude is inversely proportional to the distance *R*, between the interacting chromophores.[37,38] To achieve enhanced interaction, the coupling chromophores should be oriented close to each other in space. This tendency is

exemplified by a series of dibenzoates as shown by Nakanishi,[29] (Figure 1-17) where remote dibenzoates generally exhibit weaker amplitudes.

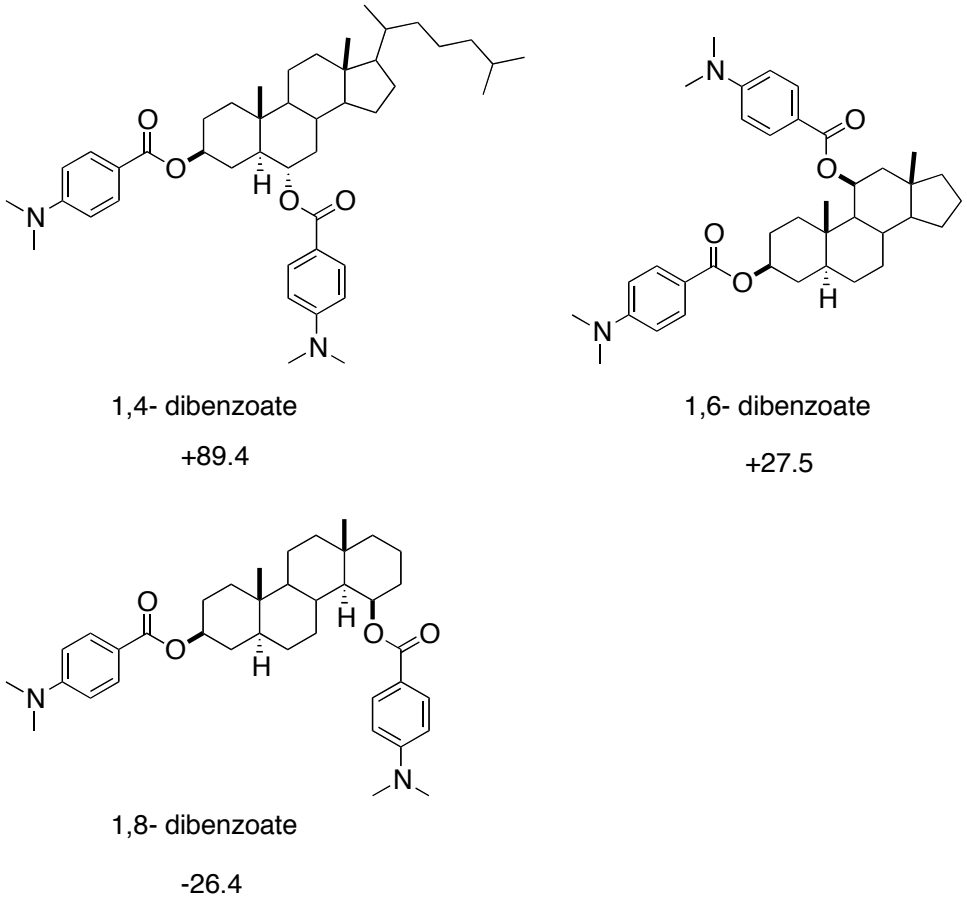

Figure 1-17. Dibenzoate chirality method – Distance effect.

Although the 1,8-dibenzoate has an interchromophoric distance of 12.8 Å, a relatively strong ECCD is still observed. Generally, a distance of about 13 Å is enough to observe ECCD for most organic molecules. However, strong chromophores such as porphyrins (Soret band λ_{max} at 415 nm, ε = 350,000 M^{-1} cm^{-1}) are known to couple at distances of up to 50 Å.[39-41]

c. *Projection angle between the interacting chromophores*. The *A* value is maximal at a chromophoric projection angle of around 70°. There is no exciton coupling when the chromophores are either parallel or 180° to each other.

d. *Number of interacting chromophores (X, Y, Z)*. The *A* value of the system is the summation of the *A* values of each pair of interacting chromophores, i.e. the principle of pair-wise additivity holds in systems comprising three or more chromophores: $A_{total} = A_{xy}+A_{xz}+A_{yz}$. This observation has been proven by experiments and theoretical calculations.[42-44]

Exciton coupling is not limited to degenerate chromophores, and can occur between different chromophores if the UV-Vis absorption λ_{max} values for the interacting chromophores are relatively close. In systems containing two different chromophores, two opposite Cotton effects appear, slightly red- and blue-shifted from the respective maxima of the interacting chromophores.[26] The interacting chromophores do not have to be within the same molecule, as long as they are in close proximity in space. In particular, supramolecular compounds, like stacking of anthocyanins[45] and porphyrin containing brevetoxins[41] have been reported to give rise to exciton coupled CD bands.

1.3-3 ECCD method in determining absolute stereochemistry of chiral molecules

The solid correlation between the sign of the ECCD spectrum and the absolute orientation of chromophores, signifies the non-empirical character of the ECCD method. Considering the dependence of ECCD on the presence of chromophores, ECCD spectroscopy can be applied to

the characterization of a wide variety of chromophore-containing molecules. Alternatively, in the absence of a chromophore, chemical modification with appropriate chromophoric groups can provide a conjugate that is amenable for ECCD analysis. As a result, non-empirical chirality determination of substrates of chemical and biological interest has been achieved.[29, 46-49] Figure 1-18 is an example of determining the absolute stereochemistry of (+)-abscisic acid by the ECCD method.[50,51] Abscisic acid, a plant hormone, contains two non-conjugated chromophores, an enone and a dienoic acid, separated by the only chiral center, a tertiary alcohol.

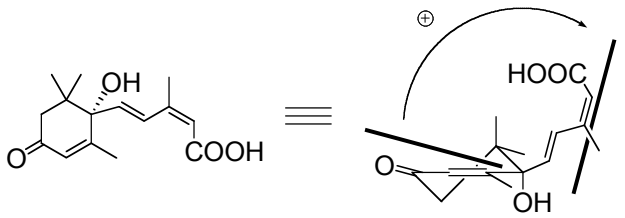

Figure 1-18. ECCD active abscisic acid.

The enone and the dienoic acid moieties interact through space, resulting in a positive ECCD couplet. Based on the sign of the spectrum, the two chromophores must be oriented in a clockwise manner, which directly indicates the β-configuration of the hydroxyl group.

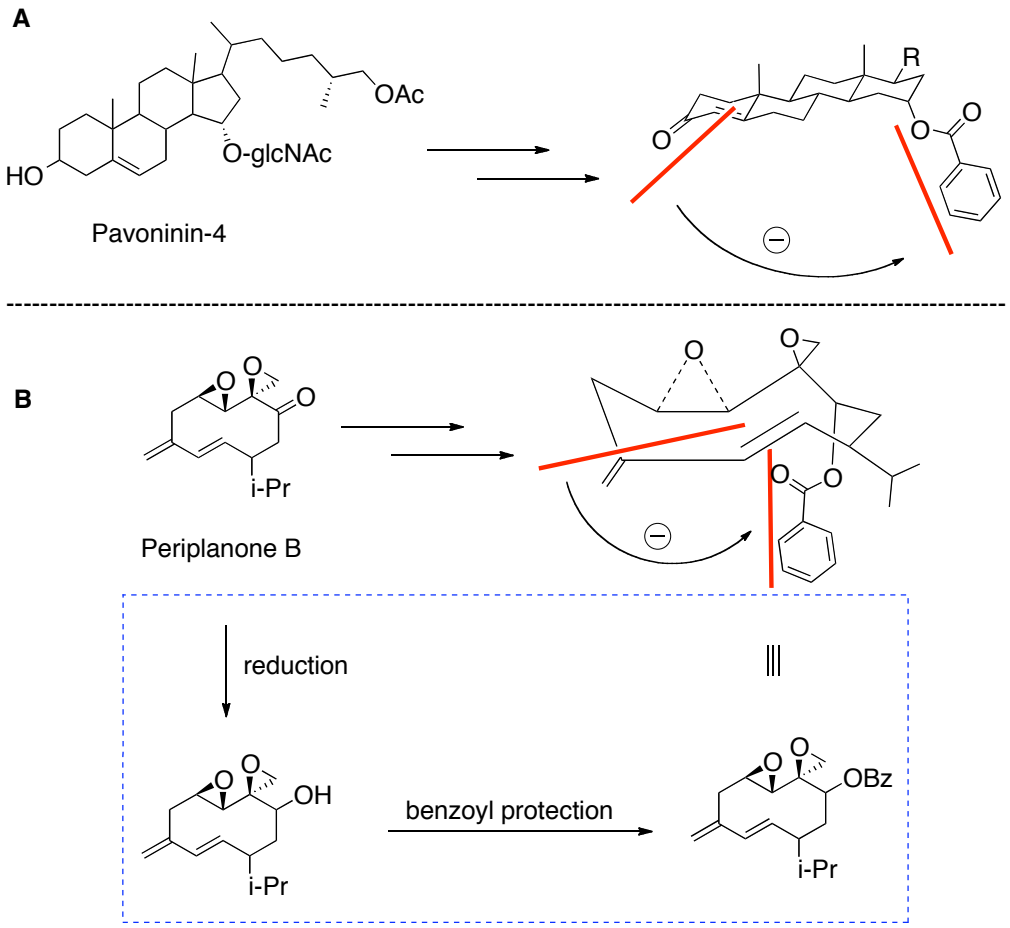

Figure 1-19. Application of the ECCD method in absolute configurational assignment of natural products.

Figure 1-19 shows two examples where introduction of a benzoyl group via hydroxyl derivatization allowed for ECCD detection, as a result of the coupling of Bz with a preexisting chromophore in the molecule. In A, the configuration of the 15-glcNAc group in Pavoninin-4, which is a shark repellant, was determined according to the observed ECCD couplet between the enone and the introduced bromobenzoate moiety.[52]

Figure 1-19B depicts stereochemical determination of the potent cockroach sex excitant periplanone B, containing only one chromophore (the diene). The absolute stereochemistry of the

macrocycle was determined after reduction of the carbonyl and derivatization of the resulting secondary alcohol with a chromophore. The observed negative ECCD established the counterclockwise correlation of the secondary hydroxyl group with respect to the diene in the favored conformation of the macrolactone. Subsequently, the orientation of the epoxide and the *i*-Pr were defined.[53]

1-4 Alternative Chromophoric Hosts in ECCD Studies

As mentioned earlier, the ECCD method requires the presence of at least two interacting chromophores in the molecule. This requirement limits the use of ECCD method with inherently achromophoric molecules that also lack a point of derivatization. In order to address this issue, chromophoric receptors have been designed to act as hosts for non-chromophoric, chiral molecules. Once the chiral substrate binds to the host receptor, either covalently or non-covalently, it will induce the host to adopt a preferred chiral conformation, which can then be observed as an ECCD couplet. This chiral induction was first demonstrated on dyes bound to polypeptides in their helical conformations.[54] This binding induced a helical orientation within the chromophoric molecule producing an ECCD-active species. The process for transmission of configurational information comprises at least two elementary processes: (1) complex formation between the chiral molecule (guest) and the chromophoric receptor (host) and (2) some dynamic processes associated with it, usually a conformational change of interacting molecules[55,56] that can induce the signal. If the interactions between the two molecules are strong enough this will lead to efficient transmission of information. In order to simplify the observed ECCD signal, the chromophoric hosts used for ECCD studies are either achiral or in the form of racemates. When

an achiral host is used, it can adopt the dictated chirality of the chiral substrate that binds to it through chiral induction. This induction leads to the formation of a preferred helical conformer, the orientation of which can be determined by ECCD. In the case of a chiral host, preferential binding of the chiral substrate with one of the enantiomers of the ECCD active host yields an induced ECCD spectrum.

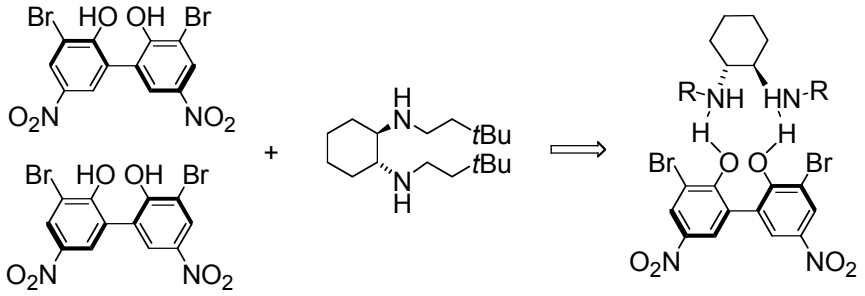

Figure 1-20. The induced chirality of biphenol upon binding to chiral amine.

Binding between the host and guest molecules can either be covalent or non-covalent, depending on the complex being formed. One example of induced chirality on a prochiral host, upon interaction with a chiral guest, is shown in Figure 1-20.[57] The biphenol shown is an ECCD active molecule (atropisomeric molecule), however, the racemic mixture of the two enantiomers is ECCD silent. When the chiral trans-1,2-cyclohexane diamine is added to the racemic mixture of the biphenyl, a matched complex

with one enantiomer of biphenol is formed as shown due to the hydrogen bonding between the phenols and the amine groups.[58-60] Formation of an optically active complex is observed as an ECCD spectrum, the sign of which is dictated by the absolute stereochemistry of the chiral diamine.[57] This is an example of non-covalent complex formation. In a similar manner, covalent

bonding has been used to determine the absolute stereochemistry of chiral secondary alcohols.[61]

As shown in Figure 1-21, the chromophoric reagent, 3-cyanocarbonyl-3'-methoxycarbonyl-2,2'-binapthalene, can be esterified with chiral secondary alcohols and the resultant complex exhibits induced ECCD as a result of favoring one atropisomer, due to restricted rotation about the C-C phenyl bonds. The chirality has been transferred from the chiral alcohols to the binaphthylene system by minimizing the steric interaction between the substituents on the chiral alcohols with the methyl ester group in the binaphthylene.

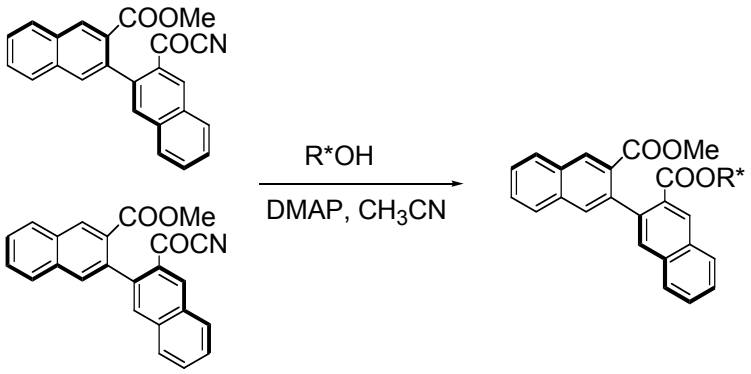

Figure 1-21. Determination of stereochemistry of chiral alcohols by ECCD.

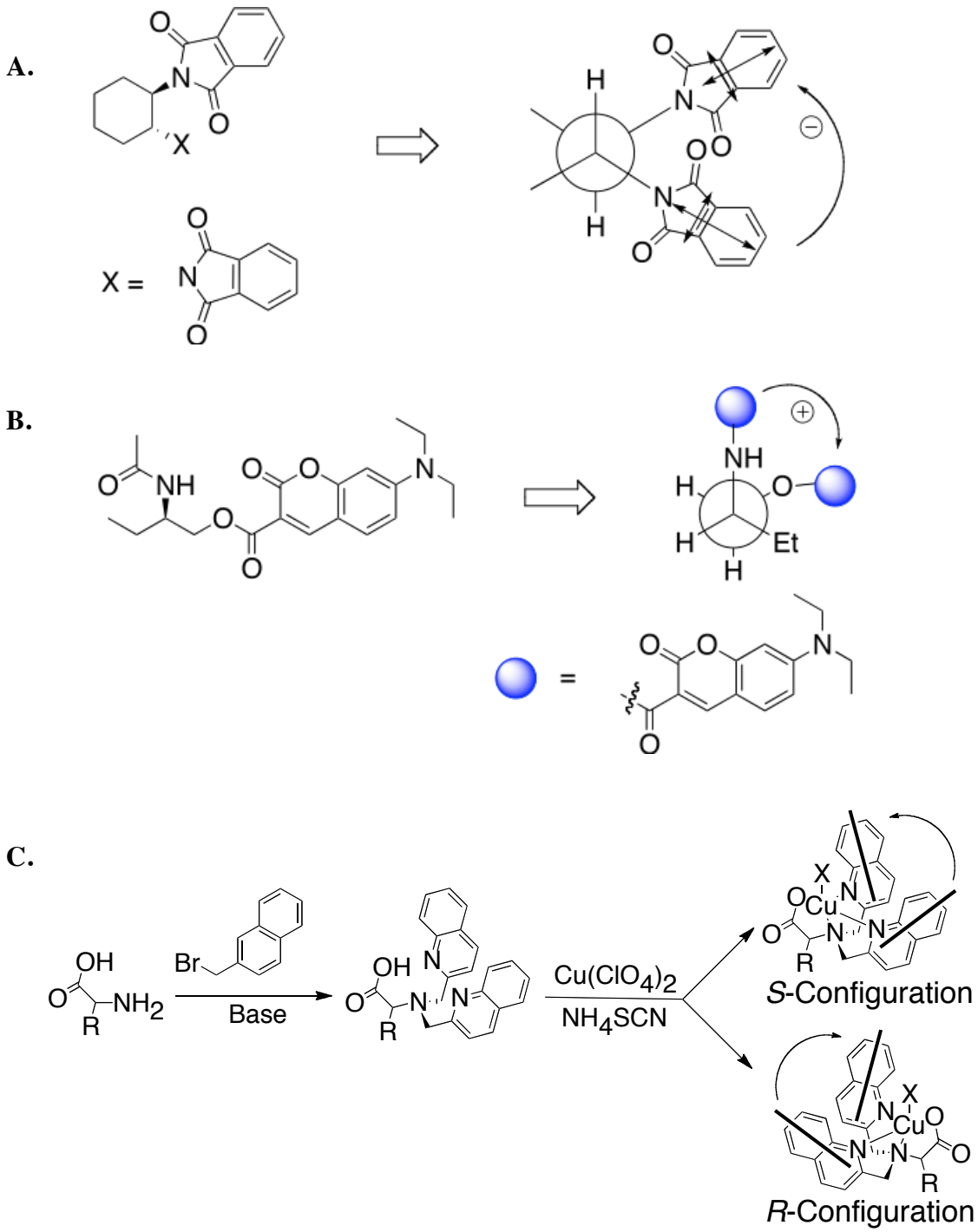

Figure 1-22. Derivatization methods for analysis of absolute configurations with various chromophores.

In recent years, several methods for the determination of absolute stereochemistry of difunctional amines by the ECCD method have been developed, after derivatization of the functional groups to introduce the required chromophores. Figure 1-22 shows a few examples of chromophores that have been applied.

In A, Gawronski et. al.[62] used pthalimide to study the absolute stereochemistry of diamines. Their study also included the use of benzoate as the chromophore for hydroxyl and carboxyl groups to include the study of absolute stereochemistry of amino acids and amino alcohols. Lo et al.[63] have used 7-diethylaminocoumarin-3-carboxylate shown in B for amines, hydroxyl and carboxyl functional groups.

Canary and coworkers have published a number of systems,[64-66] one of which is shown in C, where they make use of quinoline chromophores for the formation of chiral propellers. In these systems, a tripodal system bearing a chiral group on one of the arms is synthesized. Upon complexation of Cu(II) or Zn(II), one of the two possible propeller conformations (P or M) is formed, depending on the chirality of the original molecule, giving rise to the corresponding characteristic ECCD couplet.

1-4.1 Use of Zinc Porphyrins as Chromophoric Hosts

Throughout the literature, there is a predominance of porphyrin-based systems as chromophoric hosts for application in the ECCD method of stereochemical determination. The study of porphyrins has received increased interest in recent years since they have been utilized for the development of various projects, both of chemical and biochemical interest.[67] Especially

in the case of chromophoric receptors for the determination of stereochemistry using ECCD, the unique features of these highly conjugated rings have made them extremely attractive targets:[68]

(1) Their planar structures provide a well-defined binding pocket that is accentuated by substitutions on the ring. There are many sites that can be derivatized, such as the *meso* and β-positions, the central metal and the inner nitrogen atoms. By varying the substituents on the periphery of porphyrins, the solubility of the porphyrin containing compounds can be easily modified, for use in both polar and non-polar solvents.

(2) Porphyrins have a large extinction coefficient of around 400,000 M^{-1} cm^{-1}; the amplitude (*A*) of the Cotton effects depend on the extinction coefficient of the chromophores and hence the intense absorption of the porphyrins greatly enhance the sensitivity of CD.

(3) Absorption maximum of porphyrins rests around 418 nm for the main absorption band (Soret band), located in a region of the spectrum far red shifted than most chromophores that likely preexist in the system under investigation (typically carbonyls and olefins). This prevents the unwanted interaction between the introduced chromophore and the chiral substrate that can potentially complicate the spectral analysis.

(4) Metal incorporation into the porphyrin ring can be easily achieved, providing a coordination center for the binding of the chiral molecule. Metalloporphyrins, such as zinc porphyrins and magnesium porphyrins, can provide extra stereodifferentiation with their Lewis acidic binding sites. Therefore, porphyrins have been recognized as the ideal chromophores for detecting subtle changes in their close environment, including chirality induction.

(5) Porphyrins have efficient electric transition dipole moments that can couple over a distance of ~50Å.[26]

TPP Porphyrins have been widely utilized in stereochemical studies by CD. These include absolute configurational assignments,[40,69,70] stereochemical differentiations of sugars and amino acids,[71,72] and interactions with bio-macromolecules.[73,74]

Porphyrins, such as the alkyl connected bis-metalloporphyrins shown in Figure 1-23, can be used as chromophoric host systems for stereochemical determination of chiral compounds because of their ability to bind to the chiral compounds at the metal centers and report the chirality of bound guests based on Exciton Coupled Circular Dichroic Spectroscopy (ECCD).[67,75-78]

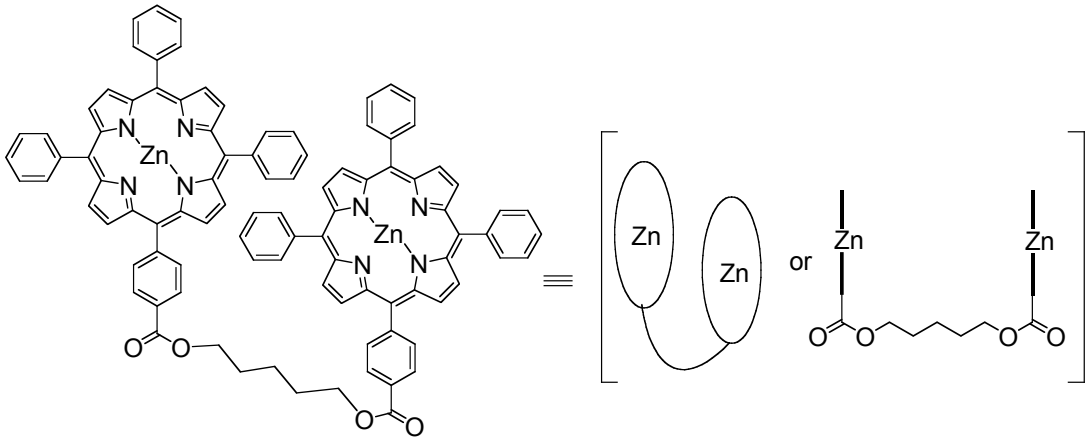

Figure 1-23. Structure and schematic representation of a porphyrin tweezer.

For instance, upon complexation with a chiral L-lysine methyl ester (through Zn-N coordination, Figure 1-24) the two porphyrins of the achiral tweezer adopt a helical orientation induced by the helicity of the bound diamine. The two possible ECCD active conformations are clockwise ((+)-helicity) or counterclockwise ((-)-helicity), yielding a positive or a negative ECCD, respectively. It is now accepted that induction of helicity directly correlates with the difference in the relative

sizes of the substituents, defined by their A-values. Viewing the system depicted in Figure 1-24, the bound diamine bears two substituents at the chiral center that are not involved in binding and, therefore, create an asymmetric environment in the tweezer binding pocket. Those are the ester group and the hydrogen. According to the A-values, hydrogen is considered as the small group, while the ester group (COOMe) plays the role of the large substituent. The porphyrin closest to the chiral center ('stereo-differentiating" porphyrin) faces the most steric interaction that dictates the final helical disposition of the two porphyrins. Steric interaction within the complex is expected to be alleviated upon positioning the stereodifferentiating porphyrin away from the larger substituent towards the smaller one. This discrimination generates the "chiral screw" that is detected by the CD spectrometer. Thus, the presented (*S*)-diamine differentiation between the small "H" and large "COOMe" is expected to induce a counterclockwise helical twist between the two porphyrins. Indeed, the ZnTPP-tweezer complex with (*S*)-lysine methyl ester exhibits a negative ECCD. The alternative, clockwise helical twist, in which porphyrin positions closer to the larger substituent, can be considered disfavored, relative to the counterclockwise twist.

Direct correlation between the experimentally-observed sign of ECCD and the A-values of the substituents at the chiral center has been established in screening of a variety of chiral substrates. The role of A-values in stereo-differentiations allows for a direct translation of the observed ECCD sign into the appropriate special distribution of the substituents at the chiral center and, therefore to establishing the absolute chirality of the bound guest. Such direct correlation defines porphyrin tweezer-based analysis as a non-empirical and highly reliable and appealing tool for the absolute stereochemical determination of other classes of chiral substrates.

Use of porphyrin tweezers, however, is limited by the requirement of dual coordination. Therefore, compounds that have one site of attachment such as chiral primary and secondary

amines, alcohols and carboxylic acids cannot be directly used in the stereo-determination with the porphyrin tweezer because the single site of attachment means coordination to only one metalloporphyrin. This does not lead to the formation of a sandwiched host-guest complex, where the chiral substrate is locked inside the tweezer. Consequently, the relative orientation of the two porphyrin chromophores as well as the electric dipole transition moments will be random due to the free rotation around the pentylene linker resulting in unpredictable or zero CD signal. In order to solve this problem, these molecules have been derivatized with "carriers" which offer the required extra binding sites (usually nitrogen-containing functionality) for ditopic complexation. (Figure 1-25)

Various carriers designed for binding and analysis of molecules, such as alcohols, monoamines, carboxylic acids, allow for the systematic analysis of these substrates and introduction of working mnemonics correlating the observed ECCD sign with the ECCD active conformation (i.e. the spatial orientation of the substituents at the chiral center) of the bound guest.

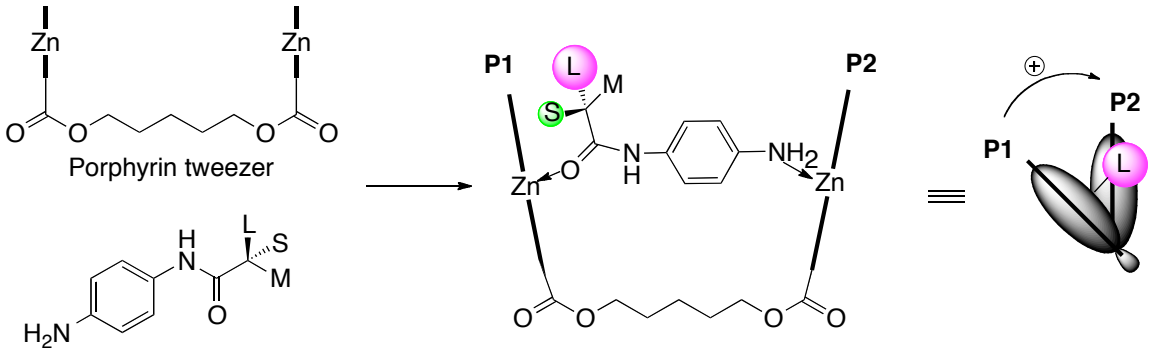

Figure 1-25. Determination of chirality for derivatized α-carboxylic acid.

While the carrier methodology enables wide use of tweezers as chirality sensors, direct complexation of chiral molecules (without derivatization) is one of our primary goals. In pursuit of this goal, Inoue and co-workers designed an octaethyl substituted porphyrin tweezer linked by an ethylene linker (Figure 1-26) for use with mono alcohols and amines for ECCD measurements.[81,82] Upon binding with this tweezer, the steric interaction between the chiral center and the ethyl groups at the 3,7 positions of the non-bound porphyrin to slide away generating a right-handed screw for *S*- substrates and a left-handed screw for *R*- substrates leading to ECCD signals. However this method requires a large excess of chiral substrates 1,000-10,000 equivalents, and the signals for alcohols were weak.

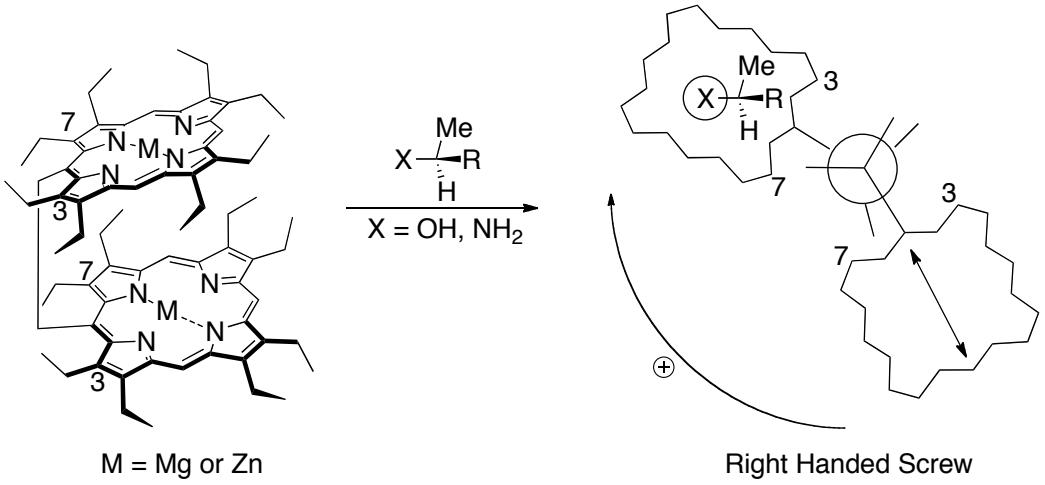

Figure 1-26. Inoue's porphyrin tweezer for stereochemical determination.

The signal strength is often used as a criterion of sensitivity for the receptor molecule. One of our primary goals is to improve the sensitivity of the receptor and to develop more widely applicable chirality sensors.

1-5 Research Aim

The use of porphyrin tweezers for assignment of absolute stereochemistry has grown a lot in the last decade. However, a key challenge and, moreover, the aim of this thesis work, is the study of mono coordinating compounds, such as carboxylic acids, primary and secondary amines and alcohols. These compounds cannot be directly used in the stereo-determination with the porphyrin tweezers because the one site of attachment means coordination to only one metalloporphyrin. This does not single to the formation of a helical twist within the complex, hence, they cannot be studied in this way. To date, the lion's share of research in this area requires derivatization of the compounds with "carrier" molecules in order to introduce a second coordination site. Consequently, the aims of this thesis can be summarized as follows:

- Design, synthesis and study of a range of electronically and sterically tuned tweezers to afford useful candidates with enhanced binding affinity as well as sensitivity. With the improved binding affinity, these porphyrin tweezers would be applied for ECCD study of several different classes of oxygen containing compounds as well as remote chirality sensing.
- Design, synthesis and evaluation of novel host molecules that will allow for the absolute stereochemical assignment of compounds containing one coordination site without the need for derivatization.

The outcome of this research will provide chemists facile and reliable methods for nonempirical assignment of chirality for a series of important organic molecules at the microscale devoid of any chemical derivatization, which is a challenging task for conventional methods. This study will open a broad pathway for absolute stereochemical determination using the exciton coupled circular dichroism protocol.

REFERENCES

References:

1. Pasteur, L. "The Assymmetry of Natural Occuring Compounds" *American Book Company, New York*, **1901**.

2. Allenmark, S.; Gawronski, J. "Determination of Absolute Configuration - An Overview Related to This Special Issue" *Chirality* **2008**, *20*, 606-608.

3. Stephens, P. J.; Devlin, F. J.; Pan, J. J. "The Determination of the Absolute Configurations of Chiral Molecules Using Vibrational Circular Dichroism (VCD) Spectroscopy" *Chirality* **2008**, *20*, 643-663.

4. Thomson, W. "Kelvin's Baltimore Lectures and Modern Theoretical Physics. Historical and Philosophical Perspectives" *MIT Press* **1987**.

5. Eliel, E. L. W., S. W. "Stereochemistry of Organic Compounds" *Wiley: New York* **1994**.

6. Bruice, P. Y. "Organic Chemistry 3rd ed." *Prentice-Hall, Inc.: Upper Saddle Rivevr, New Jersey* **2001**.

7. Rossi, R.; Diversi, P. "Synthesis, Absolute Configuration, and Optical Purity of Chiral Allenes" *Synthesis-Stuttgart* **1973**, 25-36.

8. Oki, M. "In Topics in Stereochemistry (Eds.: Allinger, N. L.; Eliel, E. L.; Wilen, S. W. " *Interscience Publication, New York* **1983**.

9. Laarhoven, W. H.; Prinsen, W. J. C. "Carbohelicenes and Heterohelicenes" *Topics in Current Chemistry* **1984**, *125*, 63-130.

10. Prinsen, W. J. C.; Laarhoven, W. H. "Determination of the Enantiomeric Excess of Hexahelicene and its Methyl-Substituted Derivatives by High-Performance Liquid-Chromatography" *Journal of Chromatography* **1987**, *393*, 377-390.

11. Bada, J. L. "Meteoritics - Extraterrestrial Handedness?" *Science* **1997**, *275*, 942-943.

12. Bonner, W. A.; Kavasmaneck, P. R. "Asymmetric Adsorption of dl-alanine Hydrochloride by Quartz" *Journal of Organic Chemistry* **1976**, *41*, 2225-2226.

13. Bonner, W. A.; Kavasmaneck, P. R.; Martin, F. S.; Flores, J. J. "Asymmetric Adsorption by Quartz - Model for Prebiotic Origin of Optical-Activity" *Origins of Life and Evolution of the Biosphere* **1975**, *6*, 367-376.

14. Cronin, J. R.; Pizzarello, S. "Enantiomeric Excesses in Meteoritic Amino Acids" *Science* **1997**, *275*, 951-955.

15. Dale, J. A.; Mosher, H. S. "Nuclear Magnetic Resonance Enantiomer Reagents - Configurational Correlations via Nuclear Magnetic Resonance Chemical Shifts of Diastereomeric Mandelate, o-Methylmandelate, and Alpha-Methoxy-Alpha-Trifluoromethylphenylacetate (mtpa) esters" *Journal of the American Chemical Society* **1973**, *95*, 512-519.

16. Feringa, B. L.; van Delden, R. A. "Absolute Asymmetric Synthesis: The Origin, Control, and Amplification of Chirality" *Angewandte Chemie-International Edition* **1999**, *38*, 3419-3438.

17. Freire, F.; Seco, J. M.; Quinoa, E.; Riguera, R. "The Assignment of the Absolute Configuration of 1,2-diols by Low-Temperature NMR of a Single MPA Derivative" *Organic Letters* **2005**, *7*, 4855-4858.

18. Hazen, R. M.; Filley, T. R.; Goodfriend, G. A. "Selective Adsorption of L- and D-Amino Acids on Calcite: Implications for Biochemical Homochirality" *Proceedings of the National Academy of Sciences of the United States of America* **2001**, *98*, 5487-5490.

19. Kavasmaneck, P. R.; Bonner, W. A. "Adsorption of Amino-Acid Derivatives by d-Quartz and l-Quartz" *Journal of the American Chemical Society* **1977**, *99*, 44-50.

20. Lambert, J. B. S., J. F.; Lightner, D. A.; Cooks,R. G. "Organic Structural Spectroscopy" *Prentice Hall, Upper Saddle River* **1998**.

21. Stinson, S. C. "Chiral chemistry" *Chemical & Engineering News* **2001**, *79*, 45-+.
22. Solomons, T. W. "*Organic Chemistry*" *John Wiley & Sons Inc., New York* **1978**.

23. Velluz, L. L., M.; Grosjean, M. "*Optical Circular Dichroism*" *Academic Press, New York* **1965**.

24. Mislow, K.; Glass, M. A. W.; Obrien, R. E.; Rutkin, P.; Djerassi, C.; Weiss, J.; Steinber.Dh "Configuration Conformation and Rotatory Dispersion of Optically Active Biaryls" *Journal of the American Chemical Society* **1962**, *84*, 1455-&.

25. Snatzke, G. "Semi-Empirical Rules in Circular Dichroism of Natural Products" *Pure and Applied Chemistry* **1979**, *51*, 769-785.

26. Vasileiou, C. *PhD Thesis* **2006**.

27. Snatzke, G. "Circular Dichroism and Absolute Conformation - Application of Qualitative mo Theory to Chiroptical Phenomena" *Angewandte Chemie-International Edition in English* **1979**, *18*, 363-377.

28. Harada, N. N., K. "Circular Dichroic Spectroscopy: Exciton Coupling in Organic Stereochemistry" *University Science Books: Mill Valley* **1983**.

29. Kuhn, W. "The Physical Significance of Optical Rotatory Power" *Transactions of the Faraday Society* **1930**, *26*, 0293-0307.

30. Kirkwood, J. G. "On the Theory of Optical Rotatory Power" *Journal of Chemical Physics* **1937**, *5*, 479-491.

31. Nakanishi, K. "Circular Dichroism Principles and Applications" **1994**.

32. Wiesler, W. T.; Vazquez, J. T.; Nakanishi, K. "Pairwise Additivity in Exciton Coupled cd Curves of Multichromophoric Systems" *Journal of the American Chemical Society* **1987**, *109*, 5586-5592.

33. Chen, S. M. L.; Harada, N.; Nakanishi. K. "Long-Range Effect in Exciton Chirality Method" *Journal of the American Chemical Society* **1974**, *96*, 7352-7354.

34. Harada, N.; Nakanishi, K. "Exciton Chirality Method and its Application to Configurational and Conformational Studies of Natural Products" *Accounts of Chemical Research* **1972**, *5*, 257-&.

35. Harada, N.; Chen, S. L.; Nakanishi, K. "Quantitative Definition of Exciton Chirality and Distant Effect in Exciton Chirality Method" *Journal of the American Chemical Society* **1975**, *97*, 5345-5352.

36. Hug, W.; Wagniere, G. "Optical Activity of Chromophores of Symmetry C2" *Tetrahedron* **1972**, *28*, 1241-&.

37. Wagniere, G.; Hug, W. "Polarization and Sign of Long Wavelength Cotton Effects in Chromophores of Symmetry C2" *Tetrahedron Letters* **1970**, 4765-&.

38. Weckerle, B.; Schreier, P.; Humpf, H. U. "A New one-step Strategy for the Stereochemical Assignment of Acyclic 2-and 3-Sulfanyl-1-Alkanols Using the CD Exciton Chirality Method" *Journal of Organic Chemistry* **2001**, *66*, 8160-8164.

39. Oancea, S.; Formaggio, F.; Campestrini, S.; Broxterman, Q. B.; Kaptein, B.; Toniolo, C. "Distance Dependency of Exciton Coupled Circular Dichroism Using Turn and Helical Peptide Spacers" *Biopolymers* **2003**, *72*, 105-115.

40. Pescitelli, G.; Gabriel, S.; Wang, Y. K.; Fleischhauer, J.; Woody, R. W.; Berova, N. "Theoretical Analysis of the Porphyrin - Porphyrin Exciton Interaction in Circular Dichroism Spectra of Dimeric Tetraarylporphyrins" *Journal of the American Chemical Society* **2003**, *125*, 7613-7628.

41 Matile, S.; Berova, N.; Nakanishi, K. "Intramolecular Porphyrin pi, pi-Stacking: Absolute Configurational Assignment of Acyclic Compounds with Single Chiral Centers by Exciton Coupled Circular Dichroism" *Enantiomer* **1996**, *1*, 1-12.

42. Matile, S.; Berova, N.; Nakanishi, K. "Exciton Coupled Circular Dichroic Studies of Self-Assembled Brevetoxin - Porphyrin Conjugates in Lipid Bilayers and Polar Solvents" *Chemistry & Biology* **1996**, *3*, 379-392.

43. Matile, S.; Berova, N.; Nakanishi, K.; Fleischhauer, J.; Woody, R. W. "Structural Studies by Exciton Coupled Circular Dichroism Over a Large Distance: Porphyrin Derivatives of

Steroids, Dimeric Steroids, and Brevetoxin B" *Journal of the American Chemical Society* **1996**, *118*, 5198-5206.

44. Dong, J. G.; Akritopoulou-Zanze, I.; Guo, J. S.; Berova, N.; Nakanishi, K.; Harada, N. "Theoretical Calculation of Circular Dichroic Exciton-Split Spectra in Presence of Three Interacting 2-Naphthoate Chromophores" *Enantiomer* **1997**, *2*, 397-409.

45. Lichtenthaler, F. W.; Sakakibara, T.; Oeser, E. "Sugar Enolones .6. "Tetra-o-Benzoyl-2-Halohexopyranosyl Halides - Preparation, Assignment of Configuration, and Hydrolysis to Enolones" *Carbohydrate Research* **1977**, *59*, 47-61.

46. Liu, H. W.; Nakanishi, K. "A Micro Method for Determining the Branching Points in Oligosaccharides Based on Circular Dichroism" *Journal of the American Chemical Society* **1981**, *103*, 7005-7006.

47. Goto, T.; Kondo, T. "Structure and Molecular Stacking of Anthocyanins - Flower Color Variation" *Angewandte Chemie-International Edition in English* **1991**, *30*, 17-33.

48. Rele, D.; Zhao, N.; Nakanishi, K.; Berova, N. "Acyclic 1,2-/1,3-Mixed Pentols. Synthesis and General Trends in Bichromophoric Exciton Coupled Circular Dichroic Spectra" *Tetrahedron* **1996**, *52*, 2759-2776.

49. Wiesler, W. T.; Nakanishi, K. "Relative and Absolute Configurational Assignments of Acyclic Polyols by Circular Dichroism .1. Rationale for a Simple Procedure Based on the Exciton Chirality Method" *Journal of the American Chemical Society* **1989**, *111*, 9205-9213.

50. Zhao, N.; Berova, N.; Nakanishi, K.; Rohmer, M.; Mougenot, P.; Jurgens, U. J. "Structures of two Bacteriohopanoids with Acyclic Pentol Side-Chains From the Cyanobacterium Nostoc PCC 6720" *Tetrahedron* **1996**, *52*, 2777-2788.

51. Gimple, O.; Schreier, P.; Humpf, H. U. "A new Exciton Coupled Circular Dichroism Method for Assigning the Absolute Configuration in Acyclic Alpha- and Beta-Hydroxy Carboxylic Acids" *Tetrahedron-Asymmetry* **1997**, *8*, 11-14.

52. Harada, N. "Absolute Configuration of (+)-Trans-Abscisic Acid as Determined by a Quantitative Application of Exciton Chirality method" *Journal of the American Chemical Society* **1973**, *95*, 240-242.

53. Koreeda, M.; Weiss, G.; Nakanish, K. "Absolute Configuration of Natural (+)-Abscisic Acid" *Journal of the American Chemical Society* **1973**, *95*, 239-240.

54. Tachibana, K.; Sakaitani, M.; Nakanishi, K. "Pavoninins, Shark-Repelling and Ichthyotoxic Steroid n-Acetylglucosaminides From the Defense Secretion of the Sole Paradachirus-Pavoninus (Soleidae)" *Tetrahedron* **1985**, *41*, 1027-1037.

55. Adams, M. A.; Nakanishi, K.; Still, W. C.; Arnold, E. V.; Clardy, J.; Persoons, C. J. "Sex-Pheromone of the American Cockroach - Absolute Configuration of Periplanone-B" *Journal of the American Chemical Society* **1979**, *101*, 2495-2498.

56. Blout, E. R.; Stryer, L. "Anomalous Optical Rotatory Dispersion of Dye - Polypeptide Complexes" *Proceedings of the National Academy of Sciences of the United States of America* **1959**, *45*, 1591-1593.

57. Beer, P. D.; Rothin, A. S. "A new Allosteric Bis Crown Ether Ligand That Displays Negative Binding Co-operativity of the Diquat Dication by the Complexation of a Transition-Metal Guest" *Journal of the Chemical Society-Chemical Communications* **1988**, 52-54.

58. Mizutani, T.; Yagi, S.; Honmaru, A.; Ogoshi, H. "Interconversion Between Point Chirality and Helical Chirality Driven by Shape-Sensitive Interactions" *Journal of the American Chemical Society* **1996**, *118*, 5318-5319.

59. Mizutani, T.; Takagi, H.; Hara, O.; Horiguchi, T.; Ogoshi, H. "Axial Chirality Induction in Flexible Biphenols by Hydrogen Bonding and Steric Interactions" *Tetrahedron Letters* **1997**, *38*, 1991-1994.

60. Bell, C. L.; Barrow, G. M. "Evidence for a Low-Lying 2nd Potential Minimum in Hydrogen-Bonded systems" *Journal of Chemical Physics* **1959**, *31*, 1158-1163.

61. Hanessian, S.; Simard, M.; Roelens, S. "Molecular Recognition and Self-Assembly by Non-Amidic Hydrogen-Bonding - An Exceptional Assembler of Neutral and Charged

Supramolecular Structures" *Journal of the American Chemical Society* **1995**, *117*, 7630-7645.

62. Kramer, R.; Lang, R.; Brzezinski, B.; Zundel, G. "Proton-Transfer in Intramolecular Hydrogen-Bonds with Large Proton Polarizability in 1-Piperidinecarboxylic Acids - Temperature, Solvent and Concentration-Dependence" *Journal of the Chemical Society-Faraday Transactions* **1990**, *86*, 627-630.

63. Hosoi, S.; Kamiya, M.; Ohta, T. "Novel Development of Exciton-Coupled Circular Dichroism Based on Induced Axial Chirality" *Organic Letters* **2001**, *3*, 3659-3662.

64. Skowronek, P.; Gawronski, J. "A Simple Circular Dichroism Method for the Determination of the Absolute Configuration of Allylic Amines" *Tetrahedron Letters* **2000**, *41*, 2975-2977.

65. Lo, L. Y., C.; Tsai, C. "A CD Exciton Chirality Method for Determination of the Absolute Configuration of *threo*-beta-Aryl-beta-hydroxy-alpha-aminoAcid Derivatives" *J. Org. Chem.* **2002**, *4*, 1368 - 1371.

66. Canary, J. W.; Allen, C. S.; Castagnetto, J. M.; Chiu, Y. H.; Toscano, P. J.; Wang, Y. H. "Solid State and Solution Characterization of Chiral, Conformationally Mobile Tripodal Ligands" *Inorganic Chemistry* **1998**, *37*, 6255-6262.

67. Canary, J. W.; Allen, C. S.; Castagnetto, J. M.; Wang, Y. H. "Conformationally Driven, Propeller-Like Chirality in Labile Coordination-Complexes" *Journal of the American Chemical Society* **1995**, *117*, 8484-8485.

68. Holmes, A. E.; Zahn, S.; Canary, J. W. "Synthesis and Circular Dichroism Studies of N,N-bis(2-quinolylmethyl)amino Acid Cu(II) Complexes: Determination of Absolute Configuration and Enantiomeric Excess by the Exciton Coupling Method" *Chirality* **2002**, *14*, 471-477.

69. Huang, X. F.; Nakanishi, K.; Berova, N. "Porphyrins and Metalloporphyrins: Versatile Circular Dichroic Reporter Groups for Structural Studies" *Chirality* **2000**, *12*, 237-255.

70. Ogoshi, H.; Mizutani, T. "Multifunctional and Chiral Porphyrins: Model Receptors for Chiral Recognition" *Accounts of Chemical Research* **1998**, *31*, 81-89.

71. Arimori, S.; Takeuchi, M.; Shinkai, S. "Sugar-Controlled Aggregate Formation in Boronic Acid-Appended Porphyrin Amphiphiles" *Journal of the American Chemical Society* **1996**, *118*, 245-246.

72. Matile, S.; Berova, N.; Nakanishi, K.; Novkova, S.; Philipova, I.; Blagoev, B. "Porphyrins - Powerful Chromophores for Structural Studies by Exciton-Coupled Circular-Dichroism" *Journal of the American Chemical Society* **1995**, *117*, 7021-7022.

73. Crossley, M. J.; Hambley, T. W.; Mackay, L. G.; Try, A. C.; Walton, R. "Porphyrin Analogs of Trogers Base - Large Chiral Cavities with a Bimetallic Binding-Site" *Journal of the Chemical Society-Chemical Communications* **1995**, 1077-1079.

74. Crossley, M. J.; Mackay, L. G.; Try, A. C. "Enantioselective Recognition of Histidine and Lysine Esters by Porphyrin Chiral Clefts and Detection of Amino-Acid Conformations in the Bound-State" *Journal of the Chemical Society-Chemical Communications* **1995**, 1925-1927.

75. Foster, N.; Singhal, A. K.; Smith, M. W.; Marcos, N. G.; Schray, K. J. "Interactions of Porphyrins and Tranfser-RNA" *Biochimica Et Biophysica Acta* **1988**, *950*, 118-131.

76. Suenaga, H.; Arimori, S.; Shinkai, S. "Sugar-Controlled Association Dissociation Equilibria Between DNA and Boronic Acid-Appended Porphyrin" *Journal of the Chemical Society-Perkin Transactions 2* **1996**, 607-612.

77. Huang, X. F.; Borhan, B.; Rickman, B. H.; Nakanishi, K.; Berova, N. "Zinc Porphyrin Tweezer in Host-Guest Complexation: Determination of Absolute Configurations of Primary Monoamines by Circular Dichroism" *Chemistry-a European Journal* **2000**, *6*, 216-224.

78. Huang, X. F.; Fujioka, N.; Pescitelli, G.; Koehn, F. E.; Williamson, R. T.; Nakanishi, K.; Berova, N. "Absolute Configurational Assignments of Secondary Amines by CD-Sensitive Dimeric Zinc Porphyrin Host" *Journal of the American Chemical Society* **2002**, *124*, 10320-10335.

79. Huang, X. F.; Rickman, B. H.; Borhan, B.; Berova, N.; Nakanishi, K. "Zinc Porphyrin Tweezer in Host-Guest Complexation: Determination of absolute Configurations of

Diamines, Amino Acids, and Amino Alcohols by Circular Dichroism" *Journal of the American Chemical Society* **1998**, *120*, 6185-6186.

80. Proni, G.; Pescitelli, G.; Huang, X. F.; Quraishi, N. Q.; Nakanishi,K.;Berova, N. "Configurational Assignment of Alpha-Chiral Carboxylic Acids by Complexation to Dimeric Zn-porphyrin: Host-guest Structure, Chiral Recognition and Circular Dichroism" *Chemical Communications* **2002**, 1590-1591.

81. Yang, Q.; Olmsted, C.; Borham, B. "Absolute Stereochemical Determination of Chiral Carboxylic Acids" *Organic Letters* **2002**, *4*, 3423-3426.

82. Proni, G.; Pescitelli, G.; Huang, X. F.; Nakanishi, K.; Berova, N. "Magnesium tetraarylporphyrin tweezer: A CD-Sensitive Host for Absolute Configurational Assignments of Alpha-Chiral Carboxylic Acids" *Journal of the American Chemical Society* **2003**, *125*, 12914-12927.

83. Borovkov, V. V.; Lintuluoto, J. M.; Inoue, Y. "Supramolecular Chirogenesis in Zinc Porphyrins: Mechanism, Role of Guest Structure, and Application for the Absolute Configuration Determination" *Journal of the American Chemical Society* **2001**, *123*, 2979-2989.

84. Borovkov, V. V.; Yamamoto, N.; Lintuluoto, J. M.; Tanaka, T.; Inoue, Y. "Supramolecular Chirality Induction in bis(Zinc Porphyrin) by Amino Acid Derivatives: Rationalization and Applications of the Ligand Bulkiness Effect" *Chirality* **2001**, *13*, 329-335.

85. Kano, K.; Fukuda, K.; Wakami, H.; Nishiyabu, R.; Pasternack, R. F. "Factors Influencing Self-Aggregation Tendencies of Cationic Porphyrins in Aqueous Solution" *Journal of the American Chemical Society* **2000**, *122*, 7494-7502.

86. Kano, K.; Minamizono, H.; Kitae, T.; Negi, S. "Self-Aggregation of Cationic Porphyrins in Water. Can pi-pi Stacking Interaction Overcome Electrostatic Repulsive Force?" *Journal of Physical Chemistry A* **1997**, *101*, 6118-6124.

87. Koti, A. S. R.; Periasamy, N. "Cyanine Induced Aggregation in Meso-Tetrakis(4-sulfonatophenyl)Porphyrin Anions" *Journal of Materials Chemistry* **2002**, *12*, 2312-2317.

88. Kubat, P.; Lang, K.; Prochakova, K.; Anzenbacher, P. "Self-Aggregates of Cationic Meso-Tetratolylporphyrins in Aqueous Solutions" *Langmuir* **2003**, *19*, 422-428.

89. Wang, Y. T.; Jin, W. J. "H-Aggregation of Cationic Palladium-Porphyrin as a Function of Anionic Surfactant Studied Using Phosphorescence, Absorption and RLS Spectra" *Spectrochimica Acta Part a-Molecular and Biomolecular Spectroscopy* **2008**, *70*, 871-877.

90. Yu, W.; Li, Z. S.; Wang, T. Y.; Liu, M. H. "Aggregation and Supramolecular Chirality of Achiral Amphiphilic Metalloporphyrins" *Journal of Colloid and Interface Science* **2008**, *326*, 460-464.

91. Tanasova, M.; Vasileiou, C.; Olumolade, O. O.; Borhan, B., "Enhancement of Exciton Coupled Circular Dichroism with Sterically Encumbered Bis-Porphyrin Tweezers" *Chirality* **2009,** 21, (3), 374-382.

92. Li, X. *PhD Thesis* **2009**.

Chapter 2

Use of Zn-TPFP tweezers for assignment of absolute stereochemistry of compounds

2-1 Development of electron deficient porphyrin tweezers

Zn-TPP tweezer has successfully been applied for the evaluation of several groups of molecules.[1] However use of this tweezer is limited in two ways. First it requires the chiral guests to possess dual coordination sites, (for example diamines) and second, oxygen functionalities demonstrated low or no binding to this tweezer.[2] Its use in mono coordinating compounds like monoamines and carboxylic acids has been achieved by use of "carrier" molecules, such as 1,4-diamino benzene, which are used to derivatize the chiral molecules.[3] (Figure 1-25) Because of these shortcomings, we adopted two approaches towards the development of more sensitive porphyrin tweezers.

As shown in Figure 2-1, the steric and electronic properties of porphyrins can be easily tuned to afford optimal binding affinity as well as sensitivity. This could greatly increase the use and substrate scope of porphyrin tweezers. Our goal was to tune these properties in order to obtain the most optimal tweezers. One approach is based on the hypothesis that increasing the bulk of the porphyrin host could lead to a larger steric interaction between the host porphyrin and the chiral guest molecule. Consequently, stronger ECCD signals are expected. An extra benefit of this approach is that the bulky porphyrin host may sense subtle size differences of substituents at the chiral center, making it capable of effectively differentiating between substituents of similar sizes.[4] Another way[5] to approach the goal of achieving a more sensitive porphyrin tweezer is to increase the binding affinity of the tweezer by either introducing electron-

withdrawing groups at the *para* positions of the *meso* phenyl rings within the porphyrin, or using metal cations with higher affinity for nitrogen and oxygen.

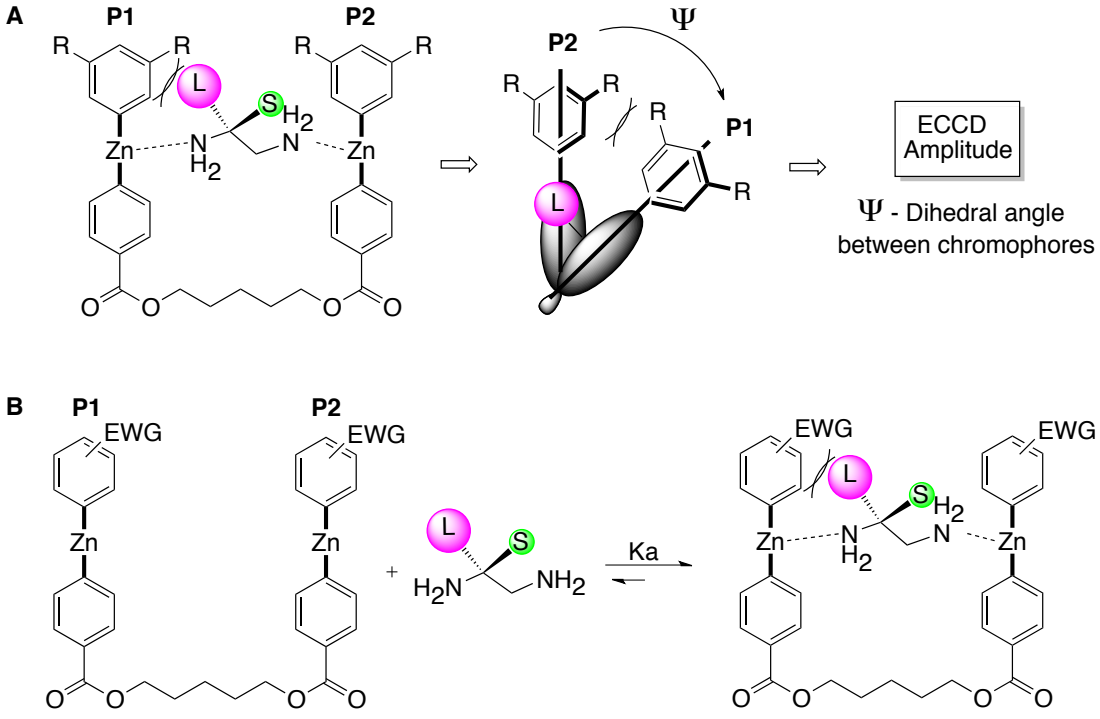

Figure 2-1. Proposed strategies for improving porphyrin sensitivity: A) increasing the steric bulk and B) introducing electron withdrawing groups.

It was hypothesized that increasing the electrostatic interaction between the metal center of the porphyrin with the bound chiral guest would lead to a stronger binding interaction between the porphyrin and the substrates. The more Lewis acidic tweezer could then be employed towards substrates that bind weakly to zinc TPP. As a result, the complexation equilibrium between the Lewis-acidic metallo tweezer and the guest would be strengthened, and enhanced ECCD amplitudes would be expected. Most importantly, we anticipated that the enhanced binding affinity would enable the direct attachment of non-derivatized amino alcohols and diols,

which would tremendously expand the applications of porphyrin tweezer methodology. A series of novel electron-rich and electron-deficient porphyrin tweezers were synthesized by Dr. Xiaoyong Li of our group, and employed in ECCD studies (Figure 2-2).[5] The electron-deficient zinc porphyrin tweezers (TPFP, TTFP, and TFP) demonstrated greatly improved sensitivity in absolute stereochemical determination. Of these, the highly electron deficient Zn-TPFP tweezer demonstrated the most improvement in sensitivity, yielding increased amplitudes for most substrates as compared to Zn-TPP tweezer. (Table 2-1)[5]

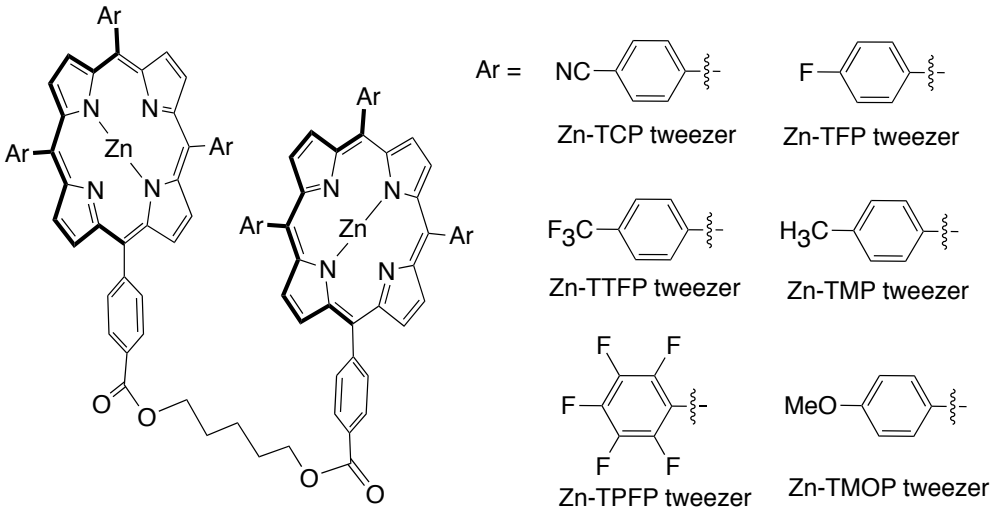

Figure 2-2. Electronically tuned tweezers for ECCD studies.

The observed ECCD signs obtained with Zn-TPFP are consistent with the ones obtained with Zn-TPP tweezer (Table 2-1) suggesting the two tweezers follow a similar mechanism[2] for stereochemical differentiation as illustrated in Figure 1-25. Dr. Li then employed this electron

deficient tweezer for the absolute stereochemical determination of *erythro* and *threo* diols, amino alcohols, and diamines[5] as well as epoxy alcohols,[6] 1,n diols[7] and aziridines.[7]

Following the success of Zn-TPFP tweezer with these functional groups, we naturally thought to extend its application to other functional groups that have not succumbed to ECCD studies yet, including hydroxyl ketones, sulfoxides, and cyanohydrins. Each of these will be discussed in more detail.

2-2 Determination of Absolute Stereochemistry for Chiral Hydroxy Ketones

2-2-1 Background

The value of enantiopure hydroxy ketones lies in their increasing utility both as important building blocks in organic synthesis and as substructures in many biologically important compounds.[8] Hydroxy ketones are particularly attractive intermediates because further elaboration provides an expedient route to highly functionalized and stereochemically complex polyoxygenated backbones. Because of this, they are frequently employed in the synthesis of pharmaceuticals, such as Indinovir, a HIV protease inhibitor.[9] Figure 2-4 shows a small sampling of natural products that contain hydroxyl ketones.

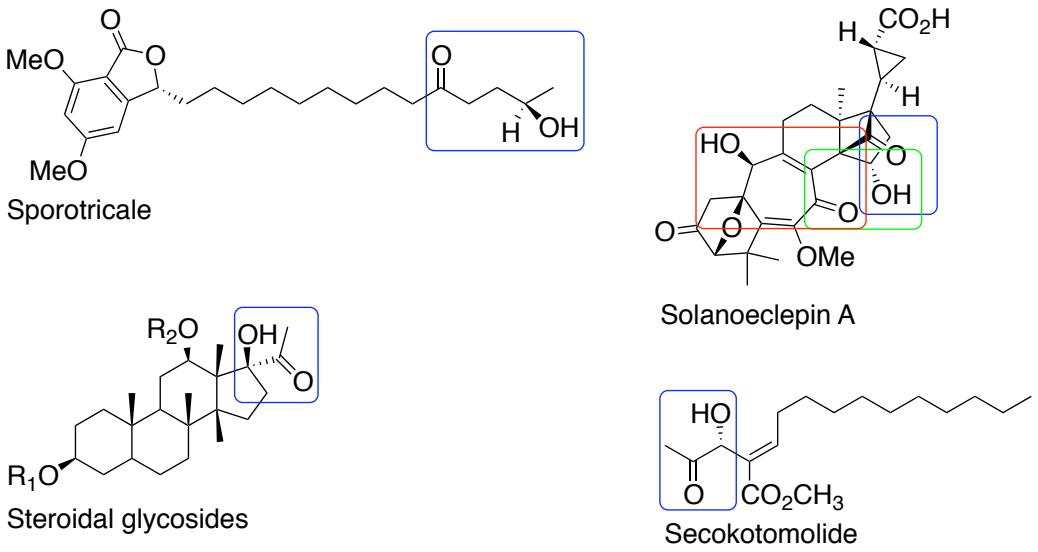

Figure 2-4. The hydroxy ketone moiety in natural products.

One example employing a hydroxy ketone in natural product synthesis is shown in the work by List and co-workers (Scheme 2-1).[10] They developed an asymmetric synthesis of the

bark beetle pheromone (*S*)-Ipsenol via a 1,3-hydroxy ketone intermediate. This molecule is of interest due to its use in insect traps and is needed in kilogram quantities.

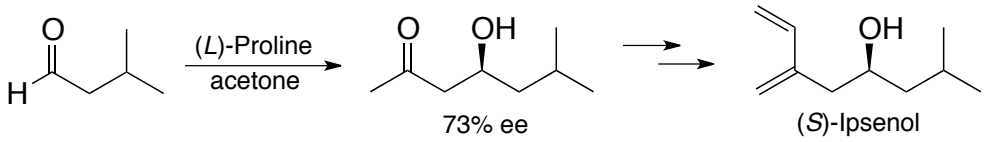

Scheme 2-1. Use of chiral hydroxyl ketone in the synthesis of (*S*)-Ipsenol.

A more elaborate use of hydroxy ketones in natural product synthesis was shown in the first total synthesis of Taxol by Holton and co-workers.[11] Over a number of steps, the C-ring hydroxy ketone precursor was used as an essential handle for elaboration and construction of the D-ring in the natural product. (Figure 2-5)

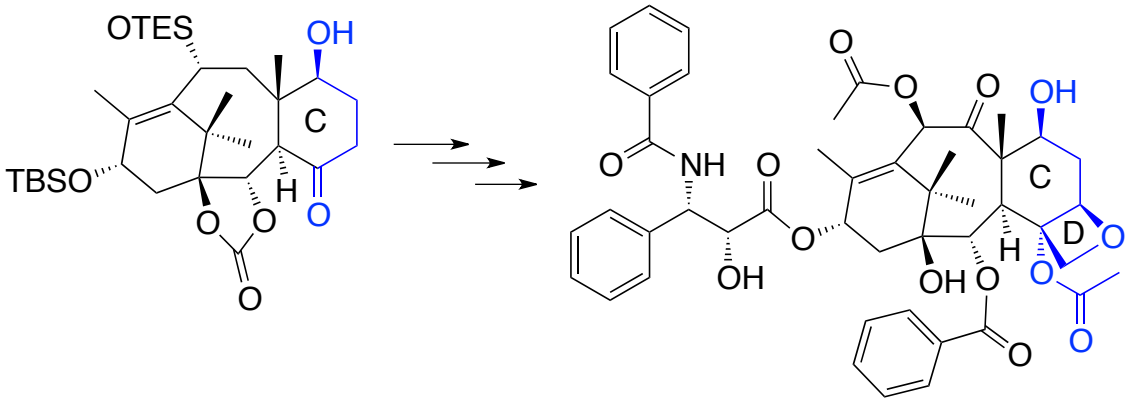

Figure 2-5. Use of hydroxy ketone in the synthesis of Taxol's ring D.

Assignment of absolute stereochemistry for hydroxy ketones relies heavily on X-ray crystallography, stereoselective synthesis and ^{1}H-NMR spectroscopy, particularly the Mosher

ester analysis.[12] As mentioned in chapter one, the difficulty of growing pure single crystals makes X-ray crystallography much less practical in the case of compounds that are not solid or that are difficult to crystallize. The simplest and most commonly used method of stereoselective synthesis is the asymmetric α-hydroxylation of enolates and enol derivatives. Scheme 2-2 shows an example of a catalytic approach to enantioselective synthesis of α-hydroxy ketones. Yamamoto[13] and co-workers introduced an oxy group at the α-position of ketone enolates using nitrosobenzene, and were able to obtain α-hydroxy ketones in up to 97% ee.

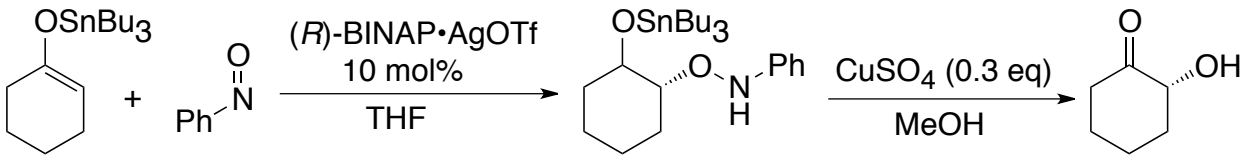

Scheme 2-2. Yamamoto's synthesis of α-hydroxy ketones using nitrosobenzene.

Mosher ester analysis has been used for the assignment of hydroxy ketones, where the hydroxy ketones are treated as chiral alcohols and derivatized with a chiral derivatizing agent. For example, Thiericke[14] and co-workers assigned the absolute stereochemistry of Streptoketol A (Scheme 2-3) by employing the Mosher ester protocol using 2-phenylbutanoic acid (PBA) as the chiral derivatizing agent.

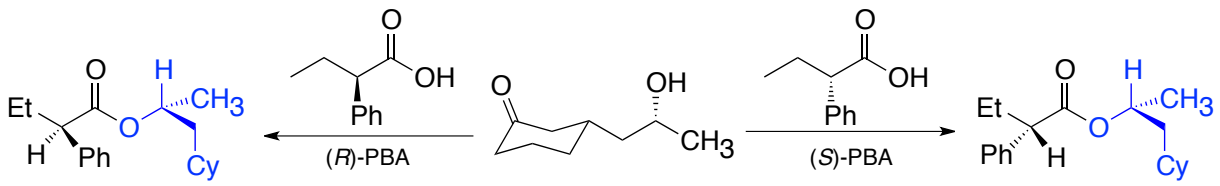

Scheme 2-3. Stereochemical assignment of Streptoketol A using Mosher ester analysis.

The Mosher ester methodology is not always convenient, especially in cases where limited amount of compound is available. Furthermore, there are few reports in the literature detailing the absolute stereochemistry determination of hydroxy ketones,[14b, 15] and these reports are limited to α-hydroxy ketones and even so, they are not general for application to all α hydroxy ketones.

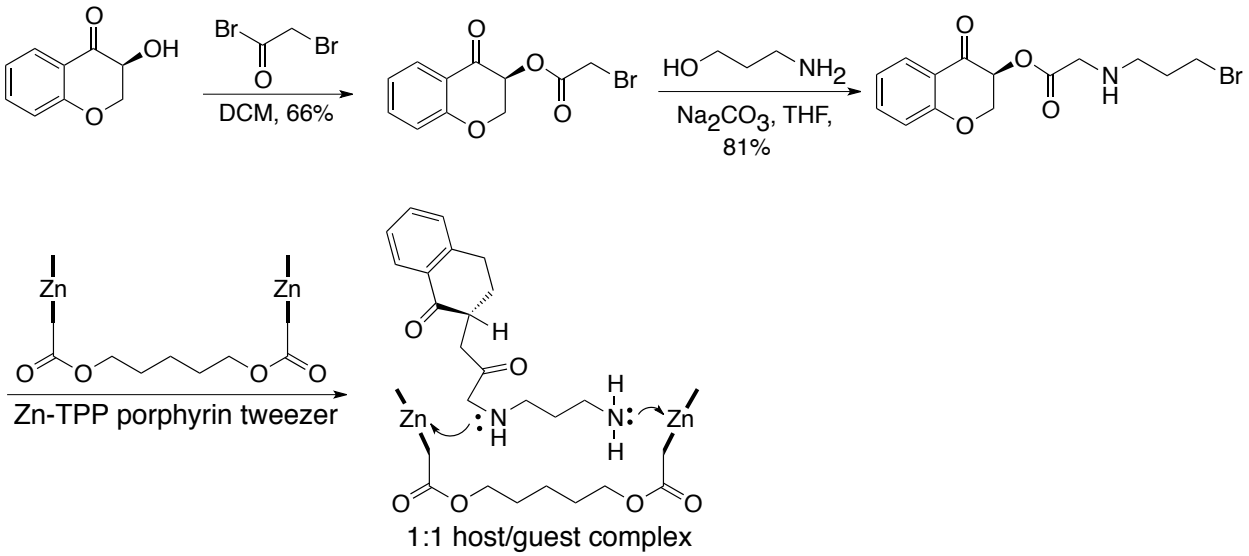

Scheme 2-4. Assignment of absolute stereochemistry of *cyclic* α- hydroxy ketones.

Recently, Ishi and co-workers reported the absolute stereochemical assignment of *cyclic* α- hydroxy ketones.[16] In their report, the hydroxy ketones are derivatized with a (3-hydroxypropylamino)acetyl group to act as a "carrier" molecule in order to provide an "amino alcohol-like or hydroxyconjugate" functionality necessary for binding (Scheme 2-4). While their protocol shows promise it is limited to cyclic α-hydroxy ketones, and like Mosher ester, requires derivatization.

We aimed to develop a system that would require minimum amounts of material, be nonempirical and require no derivatizations prior to employing the exciton coupled circular dichroism protocol. The desired methodology should be general enough to be applicable to any hydroxy ketone, cyclic or acyclic, and applicable to 1, n hydroxy ketones as well. In order to achieve this, we needed to use a porphyrin tweezer capable of binding efficiently with hydroxy ketones. Prior to the use of Zn-TPFP tweezer for diols and epoxy alcohols, we had not imagined that chiral hydroxy ketones could be bound directly with a porphyrin tweezer; in fact they were considered as substrates with only one site of attachment (the hydroxyl group), and thus we would have resorted to derivatization with carrier. The enhanced Lewis acidity of the metallocenter in the Zn-TPFP tweezer makes it feasible to consider the binding of molecules such as hydroxy ketones with the idea that both the hydroxyl and ketone functionalities will bind to the tweezer.

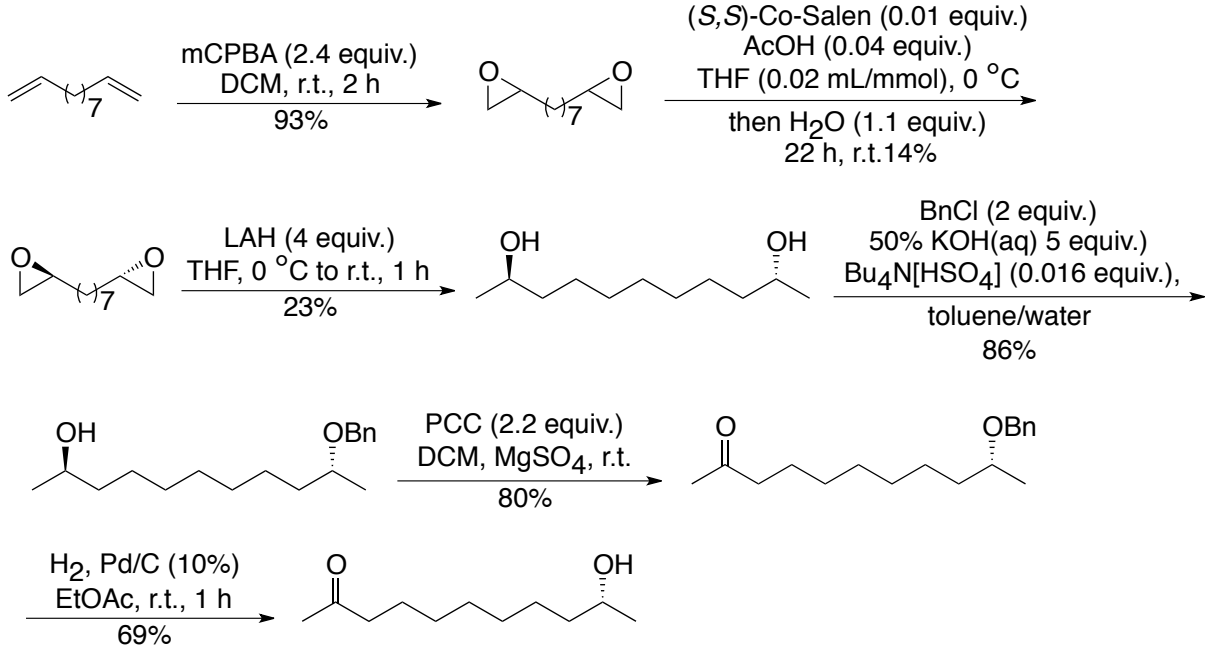

Scheme 2-5. Synthesis of chiral hydroxyl ketones via Jacobsen epoxidation.

2-2-2 Synthesis of Chiral Hydroxy Ketones

Chiral hydroxyl ketones **3** and **4** were synthesized by asymmetric aldol reaction following known procedure.[17] substrates **7**, **8** and **9** were readily accessed in three steps from their chiral diol counterparts that were synthesized by Dr. Li via regioselective ring opening of chiral bisepoxides.[7] The chiral bisepoxides were prepared by the Jacobsen hydrolytic kinetic resolution of racemic bisepoxides.[18] Monobenzylation of the chiral diols,[19] followed by PCC oxidation and finally de-benzylation gave the chiral hydroxy ketones (Scheme 2-5). It is worth noting that these extra manipulations do not erode the ee's as shown for the case of 9-hydroxydecan-2-one, **7(*R*)**. ($[\alpha]^{20}_{D}$ = -8.9, (*c* = 0.50, $CHCl_3$; *ee* = 92%; lit $[\alpha]^{20}_{D}$ -9.7 *ee* > 95%)). **4** was obtained from reduction of 2,5-hexanedione by yeast.[20] Substrates **6** and **10** were purchased from Sigma Aldrich and used without further purification.

2-2-3 ECCD Studies of Chiral Hydroxy Ketones Using Zn-TPFP Tweezer

2-2.3.1 Binding Affinity of Zn-TPFP Tweezer to Hydroxy Ketones

As mentioned above, Zn-TPFP tweezer was successfully used to determine the stereochemistry of oxygen containing functionalities (*erythro* and *threo* diols, amino alcohols, diamines and epoxy alcohols).[5-6] The principle advantage of the porphyrin tweezer system is its capacity for non-covalent binding of the chiral guest, thus avoiding the need for chemical derivatizations. Since the tweezer strategy is based on the steric interaction between the substituents at the chiral center and one of the two porphyrins, we believed that hydroxyl ketones would behave much like other systems that contain two sites of attachment with one stereocenter

such as diamines with one chiral center.[1c] Therefore, we predicted that the porphyrins would bind to the hydroxyl and carbonyl functionalities, and the helicity of the bound porphyrin tweezer would depend on the steric differentiation experienced by the porphyrin bound to the hydroxyl group attached to the stereocenter. This porphyrin would bind *anti* to the largest substituent on the chiral center and stereodifferentiate between the two remaining groups attached to the same chiral carbon. The porphyrin bound to the oxygen atom of the carbonyl (an sp^2 center) does not take part in the stereodifferentiation. Upon steric differentiation at the chiral center, the two porphyrins would adopt a specific helicity.

Ketones have not previously been shown to bind with zinc porphyrin tweezers and could be a potential problem. For this approach to work, a strong binding between hydroxyl ketone and tweezer is required so that a large population of the chiral guest would bind and thus increase the observed signal. If weakly binding complexes are formed, it could lead to small energetic differences between a number of complexed conformations leading to inconsistent results in the observed ECCD.

We gathered information on the binding affinity for ketones by UV-Vis titration analysis of benzophenone with Zn-TPFP ester (Figure 2-6). The association constant of ketone was found to be 73 M^{-1}, about 30 times weaker than that of alcohol[5] K_a = 2170 M^{-1}.[5] With this in mind, there exists the possibility of the porphyrin tweezer not binding to the hydroxy ketones strongly enough to be suitable for our purposes.

A

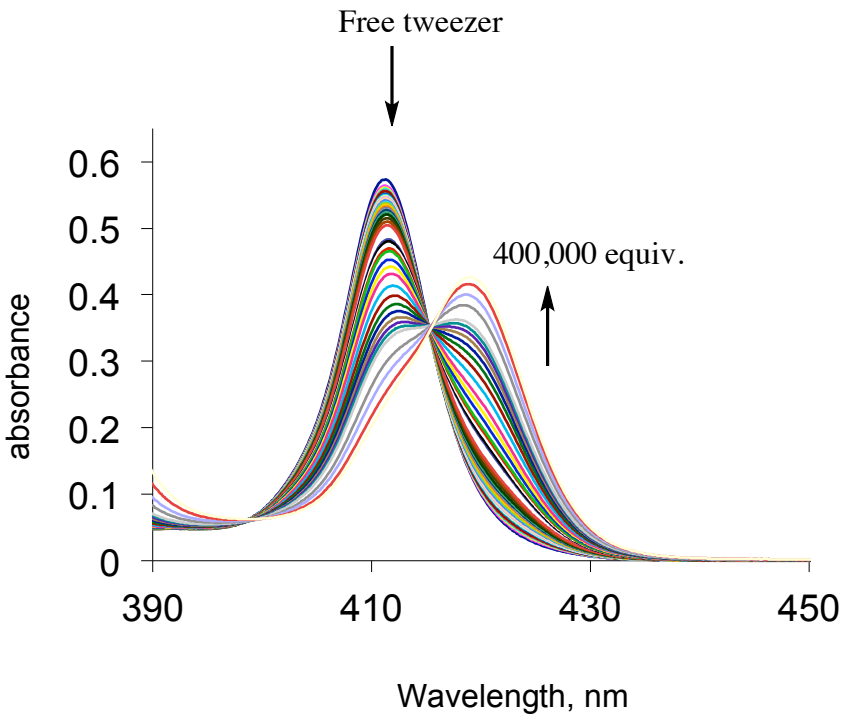

B

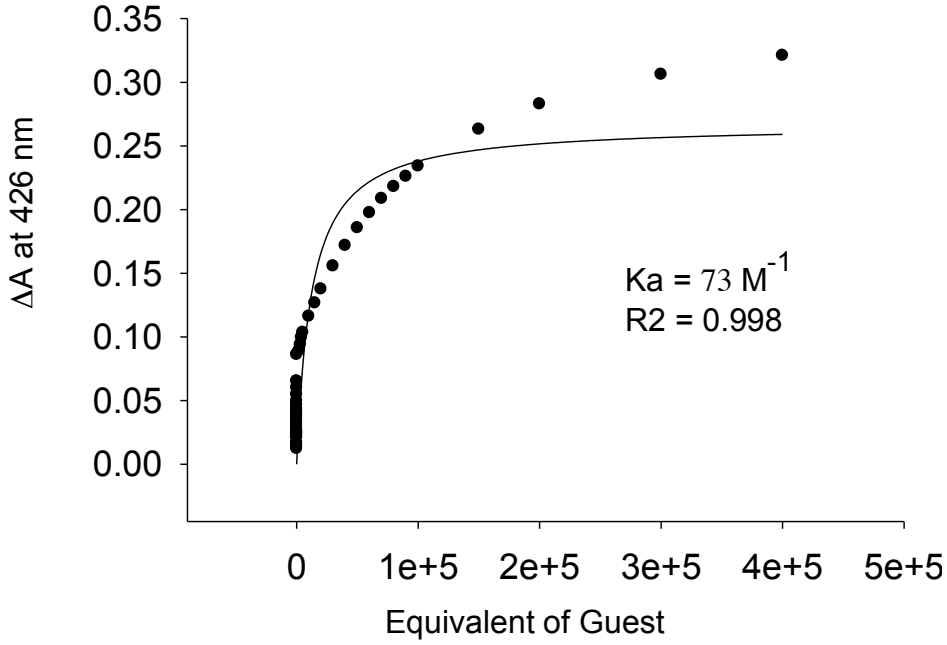

Figure 2-6. A) Titration of Zn-TPFP ester with phenyl methyl ketone (0-400,000 equiv) in hexane. B) The non-linear least square fit of the change in absorption vs. equiv of ligand provides the binding constant.

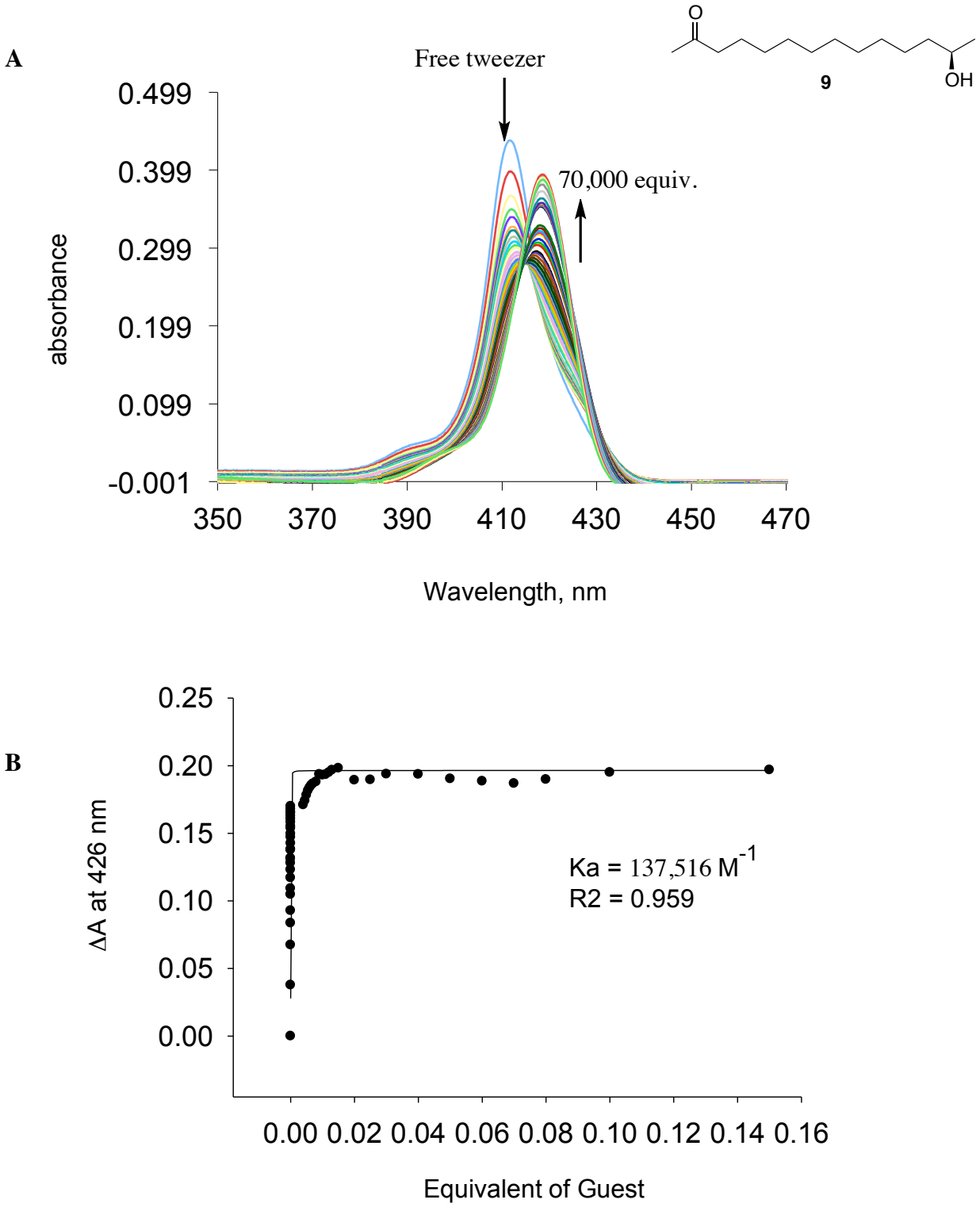

Figure 2-7. A) Titration of Zn-TPFP porphyrin tweezer with 1,12-hydroxy ketone (0-70,000 equiv) in hexane. B) The non-linear least square fit of the change in absorption vs. equiv of ligand provides the binding constant.

Interestingly however, as depicted in figure 2-7, the binding of hydroxy ketones with TPFP tweezer was measured to be 137,516 M^{-1} in hexane, which is comparable to diols $K_{assoc.}$ = 152,000 M^{-1} in hexane.[5] Based on this $K_{assoc.}$ value, contrary to our initial concern, we expected hydroxy ketones to bind effectively.

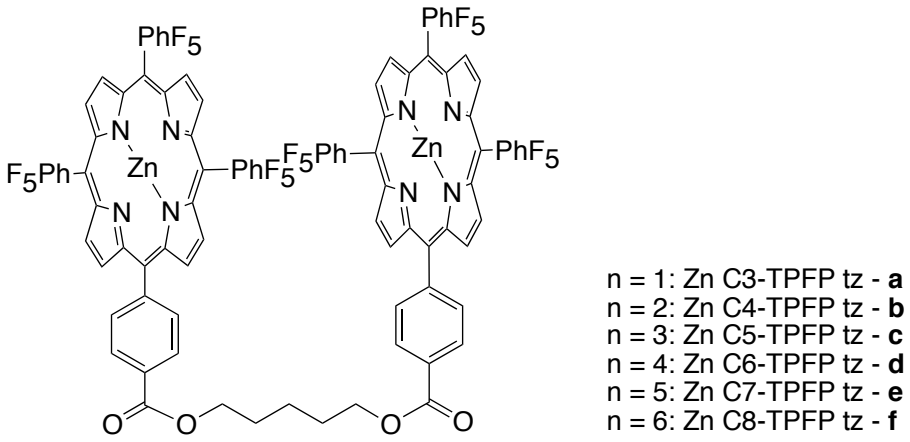

Figure 2-8. A series of porphyrin tweezers of varying linker lengths.

Assuming that the chirality in the hydroxyl ketones is transferred to the tweezer upon steric interactions between the substituents at the chiral center and one of the porphyrins, we predicted that during complexation the porphyrins would bind to the hydroxyl and carbonyl functionalities, and the helicity of the porphyrin tweezer would depend on the steric differentiation experienced by the porphyrin bound to the hydroxyl group attached to the stereocenter. This porphyrin would bind *anti* to the largest substituent at the chiral center and stereodifferentiate between the two remaining groups attached to the same chiral carbon. Upon steric differentiation, the two porphyrins would adopt a specific helicity that we could then relate back to the stereochemistry of the bound substrate.

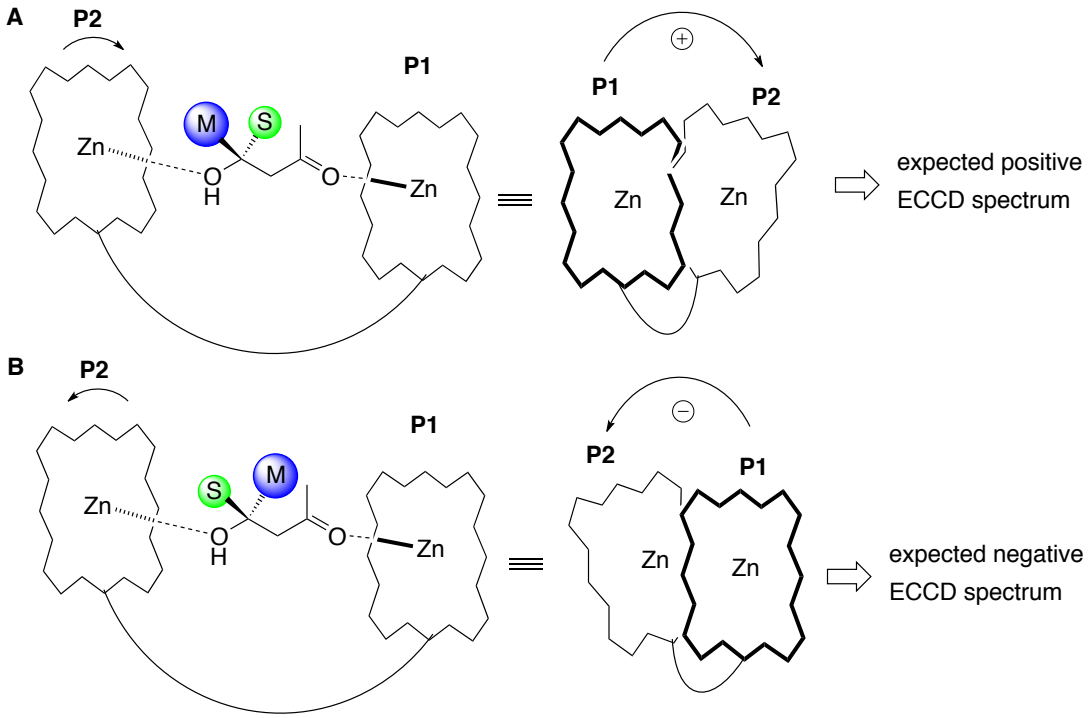

Figure 2-9. Proposed binding of hydroxy ketones with Zn-TPFP tweezer. In A) the S- chirality results in a predicted positive ECCD spectrum, while the R-chirality results in a predicted negative ECCD spectrum as shown in B.

Figure 2-9 shows a proposed binding model for hydroxy ketones with Zn-TPFP tweezer. In A), (an *S*-hydroxy ketone), the stereodifferentiation would be between the small substituent in back and the medium substituent in front. To avoid unfavorable steric interactions with the larger medium substituent, the porphyrin **P2** would rotate towards the smaller (S) group pointing back, away from the larger medium group. The porphyrin **P2** bound to the oxygen atom of the carbonyl (an sp^2 center) does not take part in the stereodifferentiation process. Overall, a clockwise (positive) helicity of **P2** relative to **P1** is generated, resulting in a predicted positive ECCD spectrum. Likewise, in B) (an *R*-hydroxy ketone) the stereodifferentiation would be between the small substituent in the front and the medium substituent in back. Porphyrin **P2**

would rotate towards the smaller (S) group in front, away from the larger medium group, leading to the overall counterclockwise (negative) helicity of **P2** relative to **P1**, resulting in an expected negative ECCD spectrum.

However, when hydroxy-ketones were subjected to ECCD studies with C5-Zn-TPFP tweezer (**e**) (Figure 2-8), we failed to observe ECCD. The same was the case with the C3 tweezer[1] (**c**) (Figure 2-8), which has been successfully used for the absolute stereochemical determination of chiral 1,n-glycols.[1] The fact that both these tweezers failed to induce a detectable signal upon substrate binding, led us to investigate the possibility that the linker length could be playing a significant role in chirality amplification, especially given the weaker binding of the ketone to the porphyrin. We set out to find a suitable linker length that would lead to orientation of the porphyrins in such a way that we could obtain amplification of chirality.

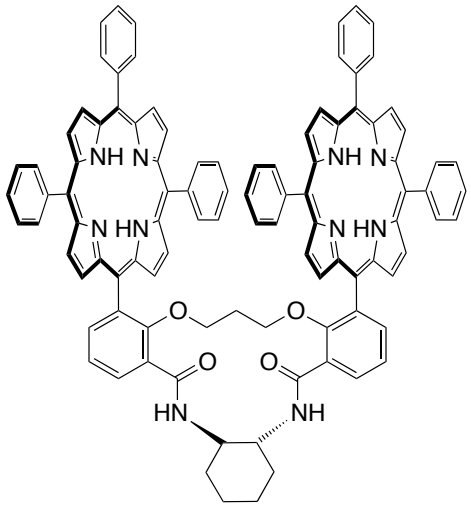

Figure 2-10. Utaka's porphyrin tweezer.

It has been shown in the literature that linker length can play a crucial role in chirality recognition and transfer.[21] Of particular note are the studies by Utaka and Colquhoun who have each shown that it is possible to control the substrates that tweezers can recognize by varying the length and nature of linkers: In Utaka's study of diamines,[21c] with a chiral porphyrin tweezer linked through a fairly rigid macrocyclic spacer (Figure 2-10), they observed that binding of short chain terminal diamines (2-4 methylenes) is detrimental for the ECCD active conformation and using guests with more than six carbons also diminishes the CD amplitude.

Therefore, further rigidifying the linker was considered not to be beneficial since it might lead to selective recognition for guests only with certain chain lengths. They found that having a fairly short linker, (C3) greatly diminished the amplitudes of shorter diamines (2-4 methylenes), and slightly reduces that of diamines with more than 6 methylenes.

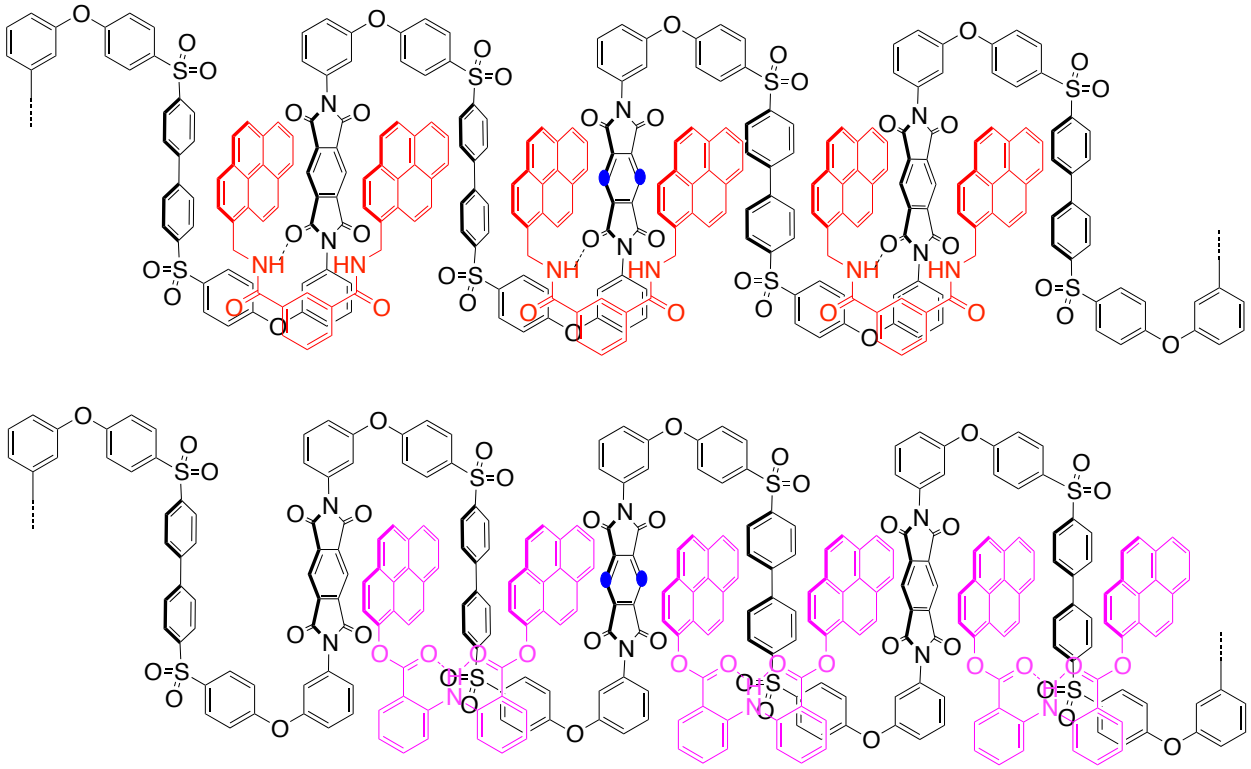

Figure 2-11. Colquhoun's tweezer systems (red and pink) showing chain folding and multiple binding to different polyimide triplet sequences (black) by the different tweezer molecules each tweezer molecule binds either to a different monomer sequence. Red tweezer, by hydrogen bonding to the imide carbonyls, and pink tweezer, which lacks hydrogen bonding ability, recognizing different polyimide sequences.

In a more recent study by Colquhoun et al., they demonstrated that by changing the nature and length of linker, they could target specific imide site from among many.[21a] As shown in Figure 2-11, by removing the hydrogen bonding ability from one tweezer, (pink) they are able to change the polyimide sequence the tweezer is able to recognize.

These investigations show that the linker plays a crucial role in controlling both the distance and the geometry of the two porphyrins relative to each other, and hence in addition to other factors like binding affinity, plays a crucial role in chirality recognition.

We hypothesized that because of the rather weak binding affinity of ketones to zincated porphyrin, the steric environment that increases upon coordination may overcome the binding, and so a longer linker could relax the strain. Upon close investigation, an interesting trend is observed, where it appears that a combination of both the tweezer linker as well as the length of the hydroxy ketone play an important role.

Figure 2-12 shows an overlay of tweezers C3-C9 with A) a short hydroxy ketone (1,3) and B) a long hydroxy ketone (1,8). As shown, for the short chiral guests, it was found that none of the porphyrin tweezers yield reproducible ECCD, except C8 tweezer that gave a large positive ECCD curve. Increasing the length to C9 causes this amplitude to drop dramatically (Figure 2-12A). For the longer chiral guest, while there is no observable ECCD signal with shorter linker tweezers, (C3, C4, and C5) we start to obtain ECCD signal with the longer C6 linker. Importantly, the obtained amplitude increases with increasing linker length, with C9 giving the largest amplitude (Figure 2-12B). An important point is that all obtained ECCD signs are consistently of the same sign meaning that the tweezers follow the same stereodifferentiation mechanism.

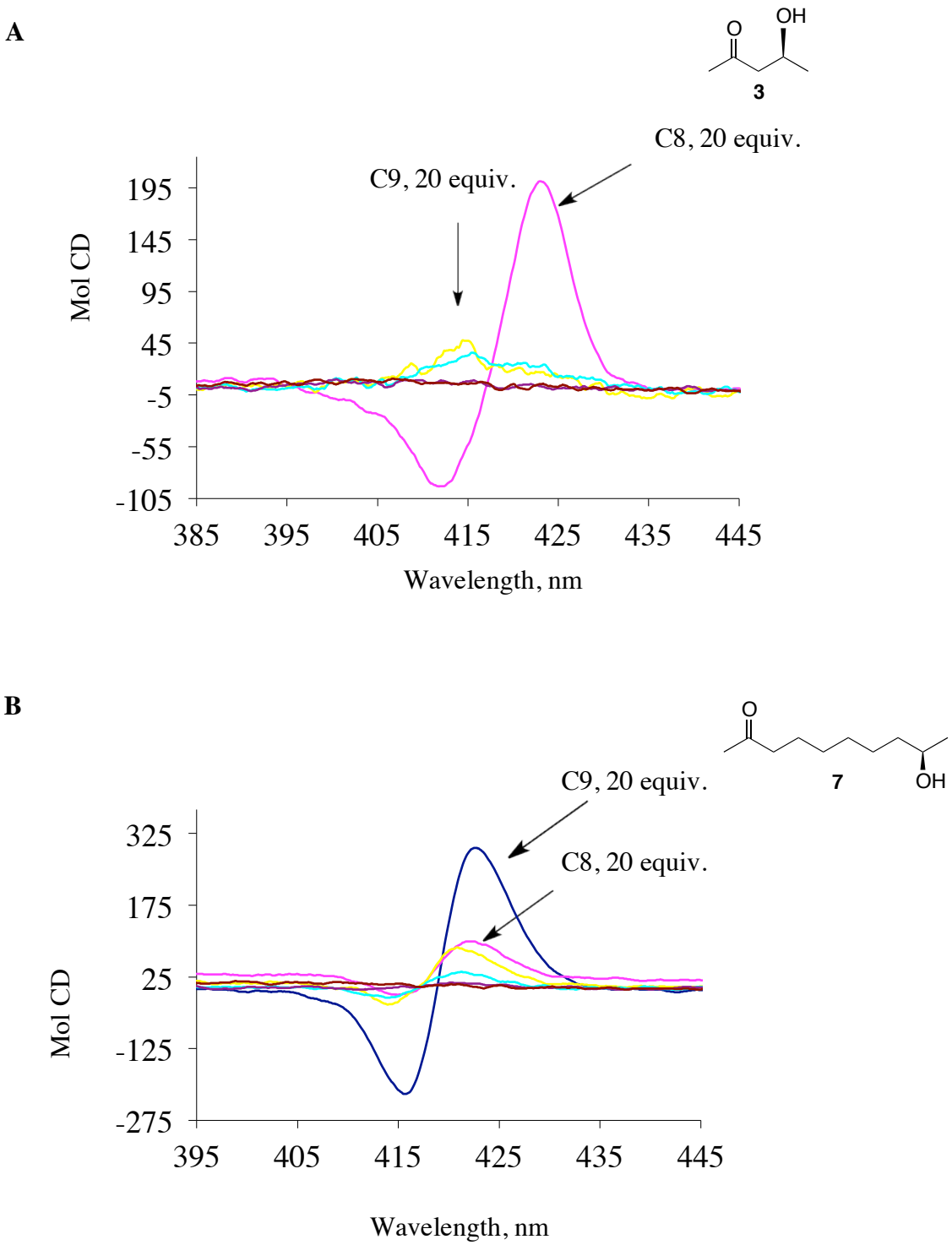

Figure 2-12. Overlay of ECCD signals obtained for A) 1,3 hydroxy ketone **3**(*S*) and B) 1,8 hydroxy ketone **7**(*R*) with Zn-TPFP tweezers C3-C8 in hexane at 0°C. For both the short and long tweezers, C-8 give the highest amplitude.

Table 2-2. ECCD data for chiral hydroxy ketones in hexane.

entry		hydroxy ketone	predicted sign	λ nm, (Δε)	A
1	**2** (*R*)	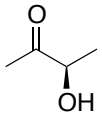	neg	424, -13 413, +15	-28
2	**3** (*S*)	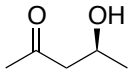	pos	423, +201 412, -93	+294
3	**4** (*R*)	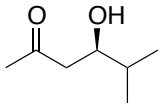	pos	423, +78 411, -32	+110
4	**5** (*S*)	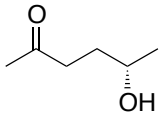	neg	422, -11 411, +21	-32
5	**6** (*S*)	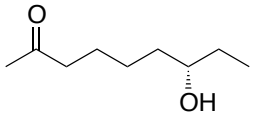	neg	421, +-41 413, +44	-85
6	**7** (*R*)	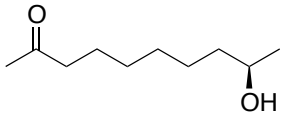	pos	422, +99 414, -13	+112
7	**8** (*R*)	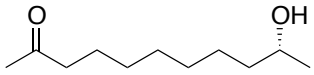	pos	422, +23 415, -14	+37
8	**9** (*R*)	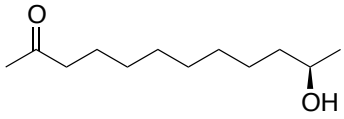	pos	422, +48 415, -27	+76
9	**10** (*S*)	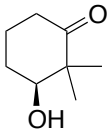	neg	421, -4 413, +7	-111

Tweezer:substrate ratio – 1:20, 1 μM tweezer concentration at 0 °C was used for all measurements. All measurements were done in hexane as solvent.

To our delight, prominent bisignate CD signals (ECCD) at the Soret region were observed upon complexation of C8-Zn-TFPF tweezer (**f**) with all the chiral hydroxy ketones at

micromolar concentrations, and so with these results in hand, we used the optimized C8 Zn-TPFP tweezer for our studies.

As shown in Table 2-2, the (*R*) and (*S*) assignments of the hydroxy ketones are not an important factor in correlating the chirality and the obtained sign of ECCD. Comparing entry 2 and 3, which are pseudo enantiomers, they both result in a positive ECCD signal. This shows that the size of the group at the chiral center is important. To illustrate this, Figure 2-13 A) shows a proposed binding model for **3**(*S*) and **4**(*R*) that are pseudo enantiomers. The binding interactions occur between the hydroxyl group and the carbonyl oxygen with the zincated porphyrins. It is assumed that the binding of **P1** to the hydroxyl group happens first because the hydroxyl group binds more strongly to Zn than the carbonyl oxygen. **P1** approaches the hydroxyl group from the side opposite the large group (methyl or *i*Pr) then **P2** coordinates to the ketone oxygen lone pair, anti to the sterically demanding **P1**. **P2** faces no steric bias since this carbon is not chiral. **P1** then relieves steric strain by rotating away from the larger group (alkyl chain) towards the smaller group (hydrogen) in both cases resulting in the more favored complex in which the two chromophores have a clockwise chiral twist. This orientation of the two porphyrins results in the observed positive ECCD spectra for both entries 2 and 3.

On the other hand, Figure 2-13 B) shows a proposed binding model for **5**(*S*). Again, the binding interactions occur between the hydroxyl group and the carbonyl oxygen with the zincated porphyrins. In this case, **P1** approaches the hydroxyl group from the side opposite the large group (methyl), then **P2** coordinates to the ketone oxygen lone pair, *anti* to the sterically demanding **P1**. **P1** then relieves steric strain by rotating away from the larger group (alkyl chain) towards the smaller group (hydrogen) resulting in the more favored complex in which the two

chromophores have a counterclockwise chiral twist. This orientation of the two porphyrins results in the observed positive ECCD spectrum for entry 4.

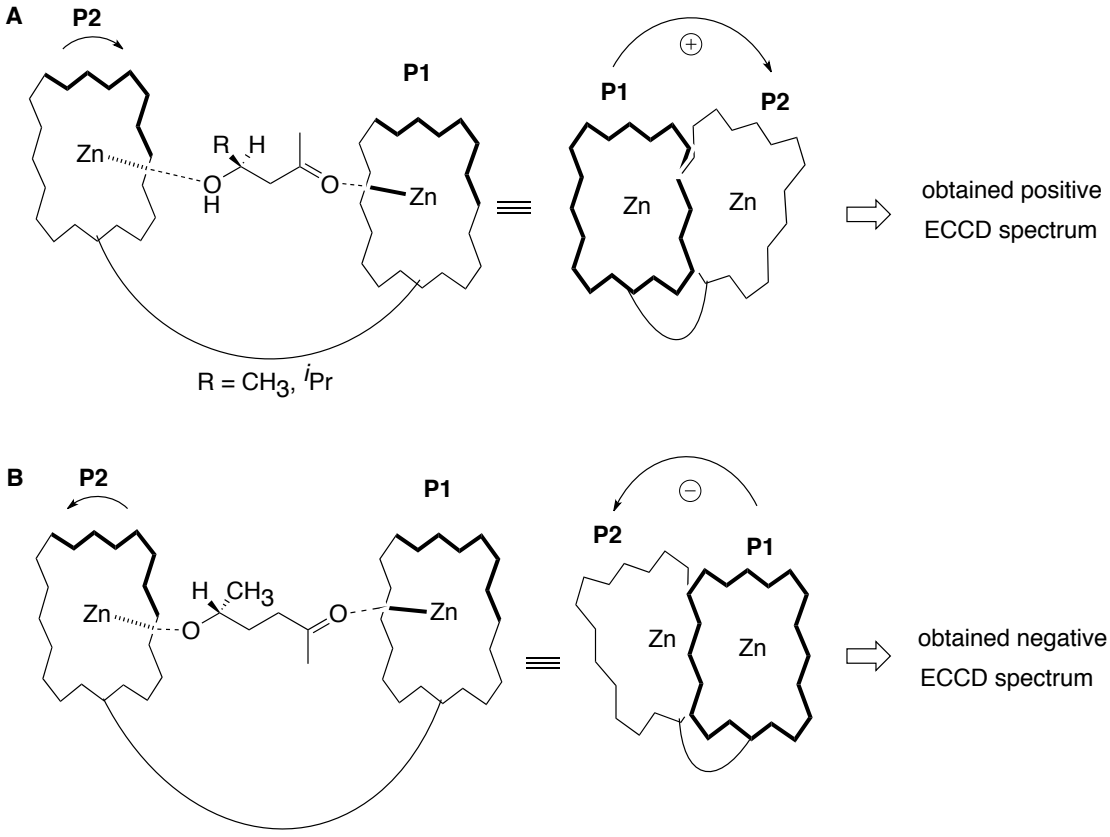

Figure 2-13. Proposed complexation between tweezer and hydroxy ketones A) **3*S*** and **4*R*** that yield positive ECCD and B) **5*S*** that yields negative ECCD spectra.

The nature of acyclic systems can lead to a number of rotamers, making it difficult to predict whether or not the conformation of the complexed guest molecules retains the lowest energy conformation of unbound molecules; since complexation with the large tweezer can result in compensating interactions with an overall effect of the host-guest complex adopting a higher energy conformation.

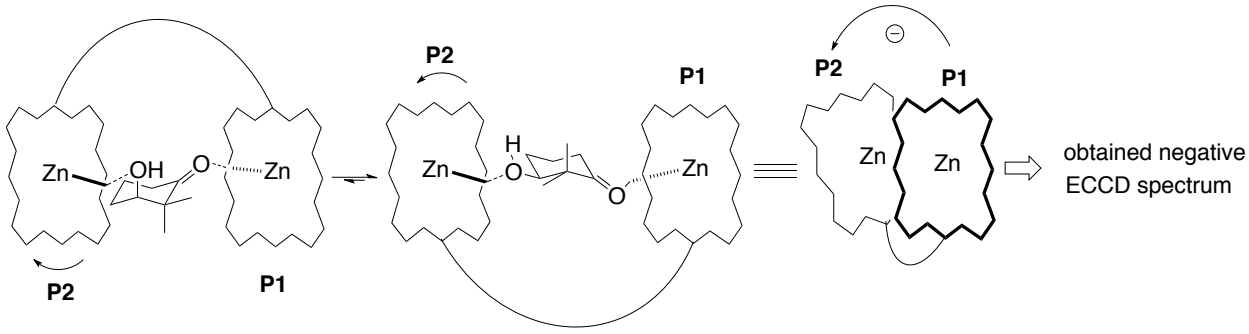

Figure 2-14. Proposed conformation of the complex formed between Zn-TPFP tweezer and (*S*)-(+)-3-hydroxy-2,2-dimethylcyclohexananone **10(*S*)**, resulting in a negative ECCD spectrum (421 nm, -4; 413 nm, 7; A = -11). **P1** rotates towards the smallest H group, away from the bulky ring CH_2 alkyl group.

We investigated (*S*)-(+)-3-hydroxy-2,2-dimethylcyclohexananone (entry 9), and were delighted to find that the trend is not affected by changing the substrate to a more rigid cyclic hydroxy ketone. (*S*)-(+)-3-hydroxy-2,2-dimethylcyclohexananone can exist in the two possible chair conformations shown (Figure 2-14).

Since there is no free rotation around the bonds, the relative positions of the two binding sites: ketone and hydroxy are fixed. This forces the two porphyrins **P1** and **P2** to approach from opposite sides to avoid steric clash. This translates to an arrangement where the porphyrins are bound *anti* to one another. Steric differentiation by **P1** leads to the rotation of **P1** towards the smaller H group at the chiral center (counterclockwise). Note that **P2** is not attached to a chiral center and so has no effect on the stereodifferentiation process. This leads to a negative helicity. The observed ECCD of (*S*)-(+)-3-hydroxy-2,2-dimethylcyclohexananone bound to C8-TPFP tweezer results in a negative signal in accordance with the proposed model.

It is worth noting that this trend is not affected by the length of the alkyl chain connecting the carbonyl to the hydroxy group. The proposed mnemonic is applicable for both short chain

hydroxy ketones and long chain hydroxy ketones. Also, of important note is the fact that the trend is not affected by the substituents at the chiral center. For example entry 3 that has an isopropyl group at the stereocenter gives the expected positive ECCD sign, and also entry 5 that bears an ethyl group also results in the expected negative ECCD sign. These results show that the system is not limited to only methyl substituents at the chiral center. As mentioned above, ketones have weaker binding affinity with zincated porphyrin than alcohol. This, together with the fixed lone pairs on ketone could be invoking a need for **P2** to loop around to find the lone pairs on the ketone oxygen, so the porphyrin linker has to be long enough to wrap around comfortably, and relax the strain within the complex.

In the case of the short tweezers, an increase in steric bulk as the two porphyrins approach one another could disfavor complex formation, causing a reduced, or no coordination with the ketone, hence, we see no ECCD signal. Note that this is not the case for diols with the same short tweezer,[7] probably because with the higher binding affinity an alcohol has to zinc, the complex formed is strong enough to overcome this steric issue. Comparing Figure 2-12A, C8 and C9 with the 1,3 hydroxy ketone, the amplitude drops dramatically, yet going from C8 to C9 with the 1,8 substrate, there is a dramatic increase in amplitude. Here, the complex will not experience as much steric clash.

Considering the importance of hydroxy ketones in organic chemistry, this developed protocol is particularly useful for organic chemists who are seeking to determine the absolute stereochemistry of hydroxy ketones. More importantly, the success of the hydroxy ketone case prompted us to look into the ECCD study of complex molecules that contain hydroxy ketones in their framework such as steroids, which are an important class of molecules. The results of this study will be discussed later.

2-3 Determination of Absolute Stereochemistry for Chiral Sulfoxides

2-3-1 Background

Exciton Coupled Circular Dichroism[2] has been applied for the determination of absolute stereochemistry of chiral diamines, amino alcohols and amino acids[1c] epoxy alcohols,[6] diols,5 mono amines and mono alcohols,[1a, 22] carboxylic acids,[2-3, 23] as well as lactams.[24] Notably absent from this list are sulfoxides.

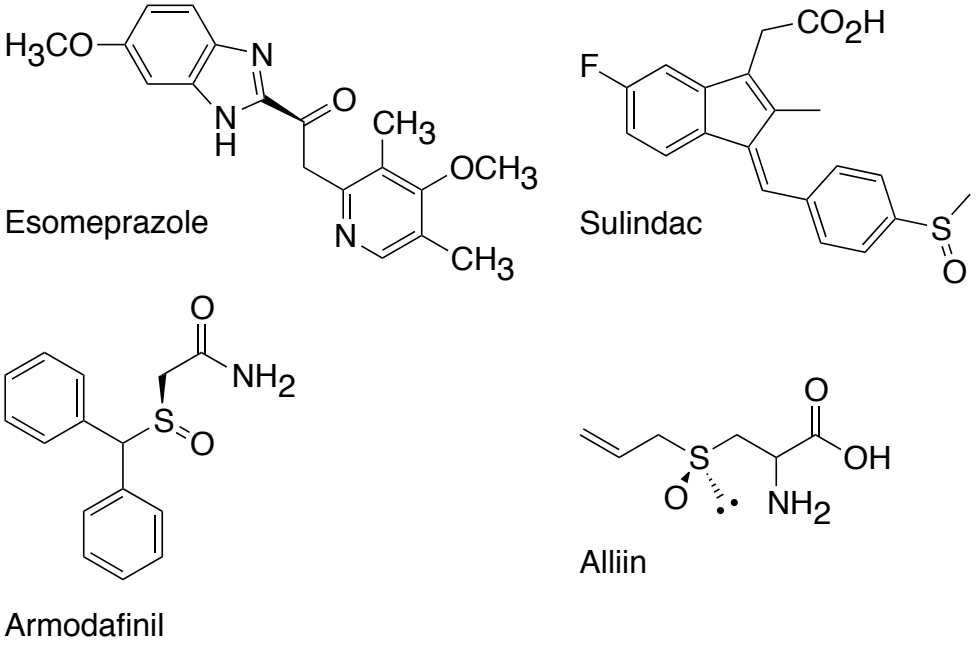

Figure 2-15. Synthetic and naturally occurring compounds containing a Sulfoxide moiety.

A sulfoxide is a molecule that contains a sulfinyl attached to two carbon atoms. They are structurally similar to carbonyls, with sulfur replacing the carbonyl carbon. Sulfoxides have some interesting characteristics. First, the bond between the sulfur and oxygen atoms differs

from the conventional double bond between carbon and oxygen in carbonyls. There has been considerable debate over the nature of the S=O bond, with comparison to other well-known molecules bearing the similar (C=O and P=O) motif (Figure 2-16).

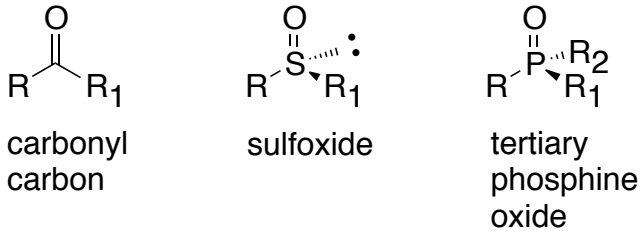

Figure 2-16. Geometric comparison of a sulfoxide to a carbonyl and tertiary phosphine oxide.

In the carbon analogue, the carbon atom forms a typical *p-p* π-bond with oxygen. In the sulfoxide and phosphine oxide cases, it is believed that the oxygen contributes electrons from its unshared lone pairs, in the *2p* orbital to the empty *3d* orbital of the sulfur or phosphorus. i.e. *d-p* π-bonding. However, there is some debate about the compatibility of the energy level overlap of the *3d* orbital with the oxygen *2p* orbital. The best representation of a sulfoxide bond is shown in the resonance structures shown in Figure 2-17.

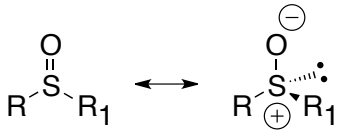

Figure 2-17. Resonance structures of a sulfoxide bond.

A second interesting and important characteristic of sulfoxides is their ability to be chiral. Chiral centers are mainly associated with tetrahedral carbons. However, with sulfoxides, a lone pair of electrons resides on the sulfur atom, giving it tetrahedral molecular geometry analogous

to an sp^3 carbon. When sulfur is bound to two different R groups, the sulfur atom becomes a chiral center. The Cahn-Ingold-Prelog priority rules are followed when assigning stereochemistry of chiral sulfoxides, and the lone pair of electrons is assigned the lowest priority.

Chiral sulfoxides have, and continue to receive considerable attention in organic and medicinal chemistry.[25] They are present in many synthetic bioactive compounds and pharmaceuticals because they have shown a wide range of biological activities such as regulation of cholesterol metabolism.[25a, 26] Furthermore, enantiopure sulfoxides are commonly employed as valuable intermediates in the synthesis of natural products,[27] as well as ligands for asymmetric synthesis in a wide range of carbon-carbon or carbon-heteroatom bond forming reactions.[25b, 28]

Sulfoxides are widely used to modulate pharmacological properties of drugs,[25a, 29] thereby increasing their importance in the pharmaceutical industry. Because of the tetrahedral geometry and anionic character of the oxygen of S=O, sulfoxides are used as mimics of the alkoxide functionality. Such substitution allows for modulating chemical stability and reactivity of a drug, while retaining, and in some cases enhancing, their biological activity.[30] For example, if a target protein recognizes a particular chirality of an alkoxide, it might enjoy enhanced recognition of the sulfoxide analogue due to the strong polar nature of the S-O bond.[29a, 30a, 30c]

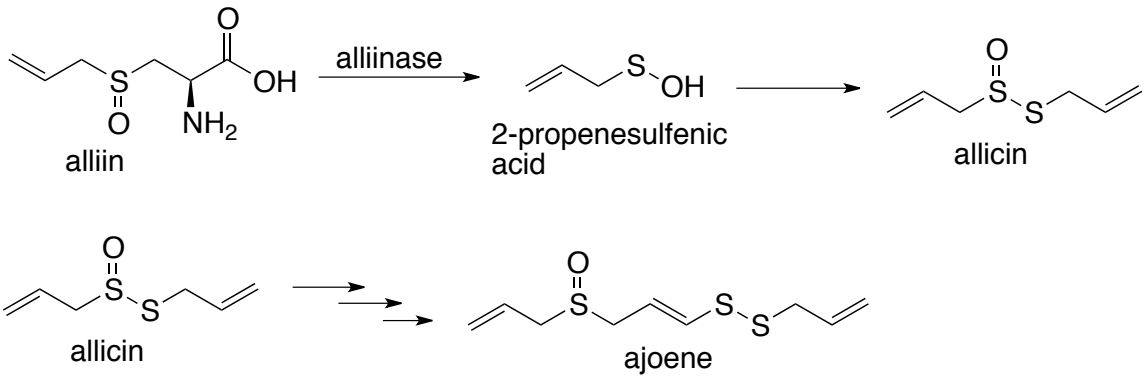

Figure 2-18. Conversion of alliin to ajoene via allicin.

Just like their synthetic counterparts, naturally occurring sulfoxides are also of importance. For instance, garlic has long been used as a therapeutic remedy. When raw garlic is chopped or crushed, the enzyme alliinase which is usually stored in a separate compartment in the garlic, combines with a compound called alliin, (*S*-2-propenylcysteine S-oxide) and converts it into the intermediate compound 2-propenesulfenic acid, which immediately condenses to give the antibiotic substance allicin (allyl 2-propenethiosulfinate) (Figure 2-18). Allicin is responsible for the aroma of fresh garlic and has antimicrobial and antifungal properties; it also inhibits lipid synthesis *in vitro*. Allicin can be transformed into an unsaturated sulfoxide disulfide called ajoene, which has anticlotting (antithrombotic) properties.

When an onion bulb is cut or crushed, an odourless substance in the bulb, S-1-propenylcysteine S-oxide, is similarly transformed into 1-propenesulfenic acid, $CH_3CH{=}CH{-}S{-}O{-}H$, which rearranges to (Z)-propanethial S-oxide, $CH_3CH_2CH{=}S^{+}O^{-}$, the tear-inducing substance of the onion.

Despite their increasing importance, there remain very few reports investigating the determination of chirality for sulfoxides. Moreover, there is no direct method for the assignment of their absolute stereochemistry.

2-3-2 Conventional Methods for Assigning Absolute Stereochemistry of Sulfoxides

There are a number of developed methods for establishing the absolute stereochemistry of sulfoxides. One such method utilizes enantioselective synthesis,[31] most commonly, enantioselective oxidation of sulfides (Figure 2-19).[32]

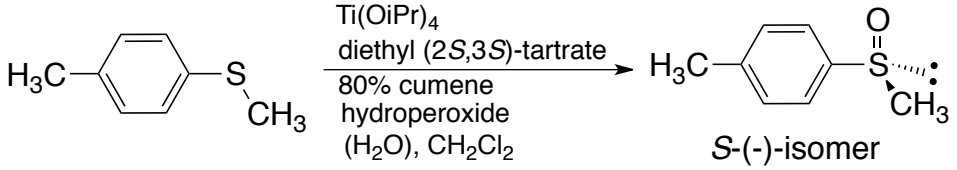

Figure 2-19. Asymmetric synthesis of sulfoxides by oxidation of sulfides.

Other methods for determining absolute stereochemistry of chiral sulfoxides include chiroptical methods like electron circular dichroism and vibrational circular dichroism.[33] However, these are empirical methods that require computations/calculations of a predicted spectrum in order to compare with the obtained experimental spectrum.

X-ray crystallography is of great importance in the assignment of absolute stereochemistry of chiral sulfoxides.[34] The first sulfoxide whose absolute stereochemistry was assigned by the X-ray analysis was (+)-methyl-L-cysteine sulfoxide.[35] This breakthrough then made X-ray analysis of fundamental importance in the early studies of chiral sulfoxides, allowing for the assignment of absolute stereochemistry of some optically active sulfoxides that were then used as reference compounds for assigning the absolute stereochemistry of related chiral sulfoxides.[36] Although X-ray crystallography is the most unambiguous and reliable

method for determining absolute stereochemistry of molecules, the difficulty of growing pure single crystals makes it much less practical in the case of compounds that are not solid or are difficult to crystallize. For these reasons, spectroscopic methods have been developed as alternative approaches for assigning absolute configuration of optically active sulfoxides.

The Mosher ester analysis method, which has been widely used for assigning the absolute stereochemistry of chiral molecules,[12] involves the use of a chiral solvating agent (CSA) for derivatization. For sulfoxides however, the use of Mosher ester analysis is limited to only a few cases.[37] The most common modification employs chiral solvating agents for studying chiral sulfoxides such as 9-anthryl-1,1,1-trifluoroethanol,[38] α-methoxyphenylacetic acid,[39] and (*R*)-(-)-*N*-(3,5-dinitrobenzoyl)-α-phenylethylamine.[40] These reagents form non-covalent interactions with sulfoxides via hydrogen bonding, inducing chemical shift changes in the protons neighboring the chiral sulfoxide moiety. The optically active sulfoxide gives rise to diastereomeric complexes when interacting with both enantiomers of CSA. The absolute stereochemistry of the sulfoxide is empirically related to the sign of the difference in chemical shift for the same ^{1}H-NMR signal when comparing the complexes. Therefore, in order to determine the absolute stereochemistry of a sulfoxide, it is necessary to record the NMR spectrum for both diastereomeric adducts with a CSA. In the pioneering work by Pirkle and Beare,[38a] they used (-)-(R)-2,2,2-trifluoro-phenylethanol as the CSA for assignment of absolute stereochemistry of alkyl methyl and aryl methyl sulfoxides.

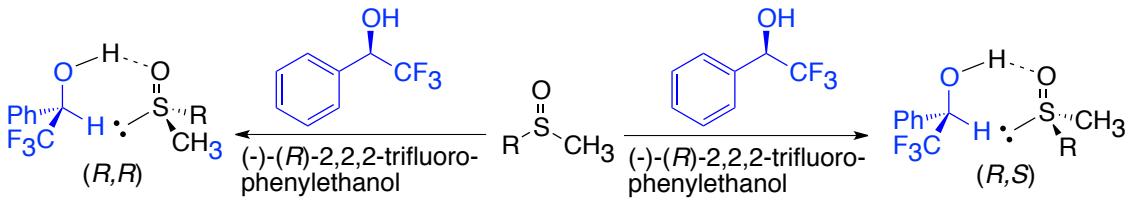

Figure 2-20. Solvation model for the interaction of (*R*)-2,2,2-trifluoro-phenylethanol with both (*R*) and (*S*) configurations of aryl methyl sulfoxides.

They proposed the solvation model shown in Figure 2-20 to rationalize the observed chemical shifts. In the proposed model, the chiral alcohol and the sulfoxide form a complex by a hydrogen-bond between the hydroxyl hydrogen and sulfoxide sulfur lone pair electrons. The inductive effects of the proximal electron withdrawing CF_3 group causes an increase in the acidity of the hydroxyl hydrogen, making it more prone to interact with the basic S=O group. In the solvate (*R*,*R*), the methyl group faces the CF_3 group, while the R group is *syn* to the phenyl ring. The opposite is true for the diastereomeric solvate (*R*,*S*). Due to the shielding caused by the phenyl group, the methyl NMR signal will shift to higher field for (*R*,*S*) than for (*R*,*R*). The converse is expected for the protons of the R alkyl moiety, whose resonances will shift to higher field for (*R*,*R*) than for (*R*,*S*). In this way, the absolute stereochemistry of the sulfoxide can be related to the sign of the difference in chemical shift for the same ^{1}H-NMR signal when comparing the diastereomeric complexes.

While this approach is rather simple and fast, it has some significant drawbacks like the requirement of derivatization of chiral sulfoxide before analysis. Moreover, in order to achieve a reliable correlation, the prevalent conformation of the complexes must be known. Given that these are hydrogen-bonded complexes, the conformation can be difficult to predict. With such labile adducts a fast equilibrium exists between several species and conformations in solution,

resulting in small (or in some cases nonsystematic) chemical shift differences between the diastereomeric complexes, leading to an inability to predict the most prevalent conformation.

In 1999, Yabuuchi and co-workers developed[37] an elegant modification to this methodology. This method involves the conversion of sulfoxides into *N*-(methoxyphenylacetyl sulfoximines, by amination of the sulfoxide with *O*-mesitylsulfonylhydroxylamine, which occurs with complete retention of chirality at the sulfur atom. After formation of the *N*-(methoxyphenylacetyl sulfoximines, (*R*)- and (*S*)-MPA are introduced at the nitrogen atom (Figure-2-21). This approach leads to the formation of more stable complexes due to the introduction of a covalent bond. However, even though this methodology is more reliable than the previous methods, there is the need for derivatization. Hence, the absolute stereochemistry of chiral sulfoxides remains a challenge. As such, we pursued the development of a microscale, nonempirical and efficient protocol to determine the absolute stereochemistry of sulfoxy alcohols without the need for any derivatization.

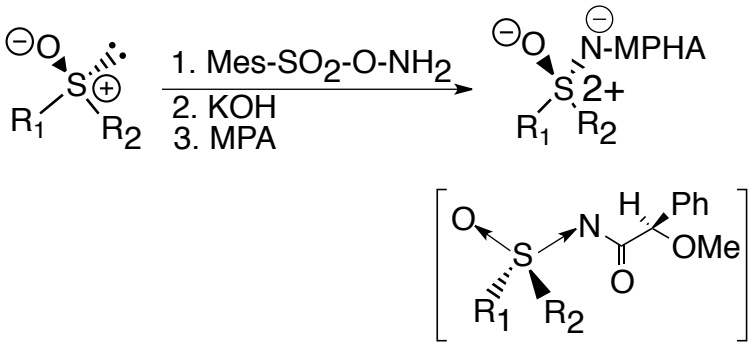

Figure 2-21. Formation of *N*-(methoxyphenylacetyl) sulfoximines from sulfoxides.

As mentioned previously, we have introduced the highly Lewis acidic fluorinated Zn-TPFP porphyrin tweezer that showed high binding affinity for hydroxyl and epoxide groups.[5-6]

Following its successful use for the assignment of hydroxy ketones, we hypothesized that the use of this fluorinated tweezer would also lead to a successful methodology in the assignment of sulfoxy alcohols.

Initially, one concern for developing mnemonics was determining if the tweezer would bind with the sulfur or the oxygen lone pairs of the sulfoxide (Figure 2-17). Central to the success of this proposed methodology would be the use of a tweezer that is capable to bind to the alcohol as well as keep a consistent binding mode with the sulfoxide (either the sulfur or oxygen lone pair electrons).

2-3-3 ECCD Studies of Chiral Sulfoxides Using C3-TPFP Tweezer

2-3-3.1 Binding Affinity of Sulfoxides with Zn-TPFP Tweezer

Porphyrin tweezer (**a**) employed in this study was synthesized according to literature procedure[5] substituting 1,3-propanediol for 1,5-pentanediol.

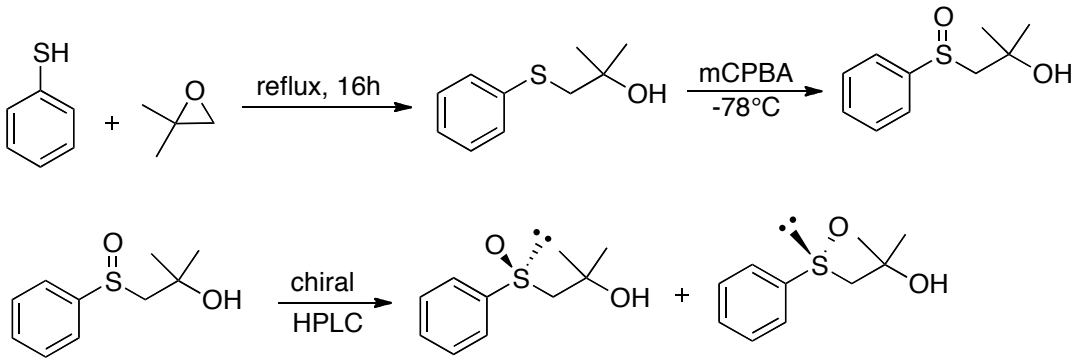

Scheme 2-6. Representative scheme for synthesis of chiral sulfoxy alcohols.

Racemic sulfoxy alcohols were synthesized following basic organic chemistry procedures and the pure enantiomeric forms were obtained by HPLC separation, as shown in Scheme 2-6 for phenyl sulfoxy alcohol. First, the thioether was obtained by refluxing an epoxide with benzene thiol neat. This was then followed by *m*CPBA oxidation of the thio ether in methylene chloride to give the racemic sulfoxide. Individual enantiomers were then obtained after chiral HPLC separation, and all absolute stereochemistry was confirmed by X-ray crystallography. (See experimental details).

The binding constant was determined using UV-vis analysis by titration of Zn TPFP porphyrin with phenylmethyl sulfoxide. The UV spectrum shown in figure 2-22 below shows the change observed in the Soret band absorption upon binding of the sulfoxide. Plotting the equivalents of sulfoxide added as a function of the change in absorption at 426 nm leads to a saturation curve which provides the binding constant of the complex formed upon non-linear least square analysis using Sigma plot 2001 program. Calculations of binding constants follows protocols described for diols[5] and was determined as $1.08 \times 10^4\ M^{-1}$ in hexane. The value obtained is comparable to that of epoxy alcohols $2.88 \times 10^4\ M^{-1}$ in hexane[6] suggesting a good binding affinity.

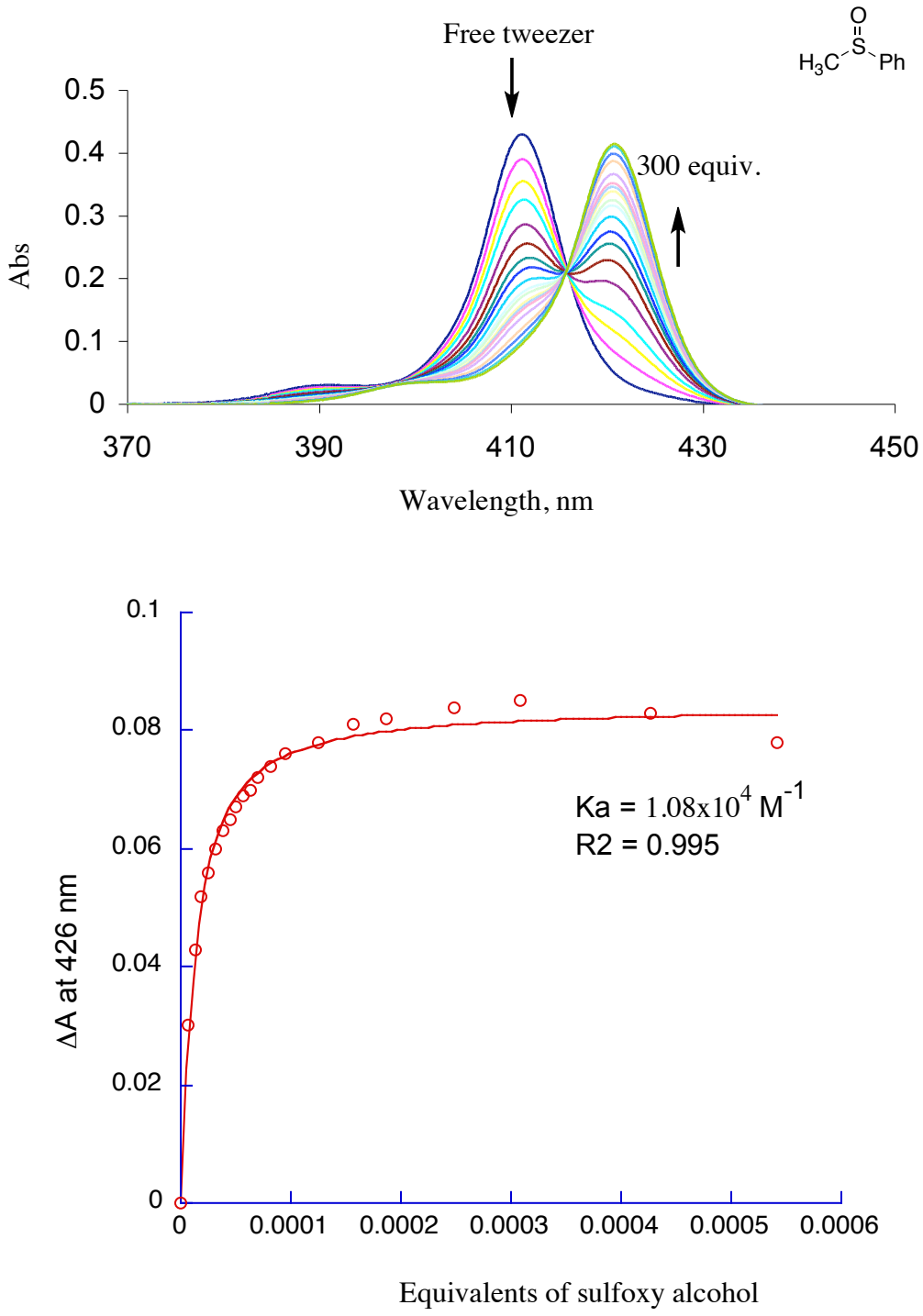

Figure 2-22. A) Titration of Zn-TPFP porphyrin with phenylmethyl sulfoxide (0-300 equiv) in hexane. B) The non-linear least square fit of the change in absorption vs. equiv of ligand provides the binding constant.

2-3-3.2 Probing the Zinc-Sulfoxide Binding

As mentioned, sulfoxides can exist in two resonance forms (Figure 2-17). Because of this, sulfoxides are polarized molecules that possess two potential sites for coordination to metals: the lone pair of electrons on sulfur or the negative charge on oxygen. As shown in Figure 2-23, switching the coordination point of the sulfoxide from sulfur to oxygen could result in a switch in the predicted ECCD sign, hence, it is important to understand the sulfoxide binding mode to the Zn in order to correctly interpret the obtained results.

Assuming that the porphyrin tweezer binds with the sulfoxy alcohols in a similar mode as is proposed for hydroxy ketones, there are two possible scenarios: One where porphyrin **P1** binds to the oxygen of the sulfoxide (Figure 2-23 A) and the other where porphyrin **P1**, binds to the sulfur atom (Figure 2-23 B).

In A the sulfoxide coordinates to the zinc via the oxygen. Here, **P1** approaches to the hydroxyl oxygen from the front (same side as small lone pair group) leaving the second porphyrin **P2** to approach the oxygen from the back to avoid sterics from the first porphyrin and thereby sliding away from the larger R group, to avoid the unfavorable steric interactions; this results in a predicted positive ECCD curve for the *R* enantiomer shown. However, if the binding were to occur via the sulfur lone pairs, as in case B, then the predicted ECCD sign would be negative. Here, porphyrin **P1** approaches the sulfur from the front as shown causing **P2** to approach the alcohol from the back, avoiding bulky **P1**. **P2** slides away from the larger OH group resulting in an expected negative ECCD sign. These conflicting results from the proposed possible binding mnemonics stress the importance of understanding the preferred binding mode of the sulfoxide to the zinc. i.e. S-Zn vs O-Zn binding of sulfoxide.

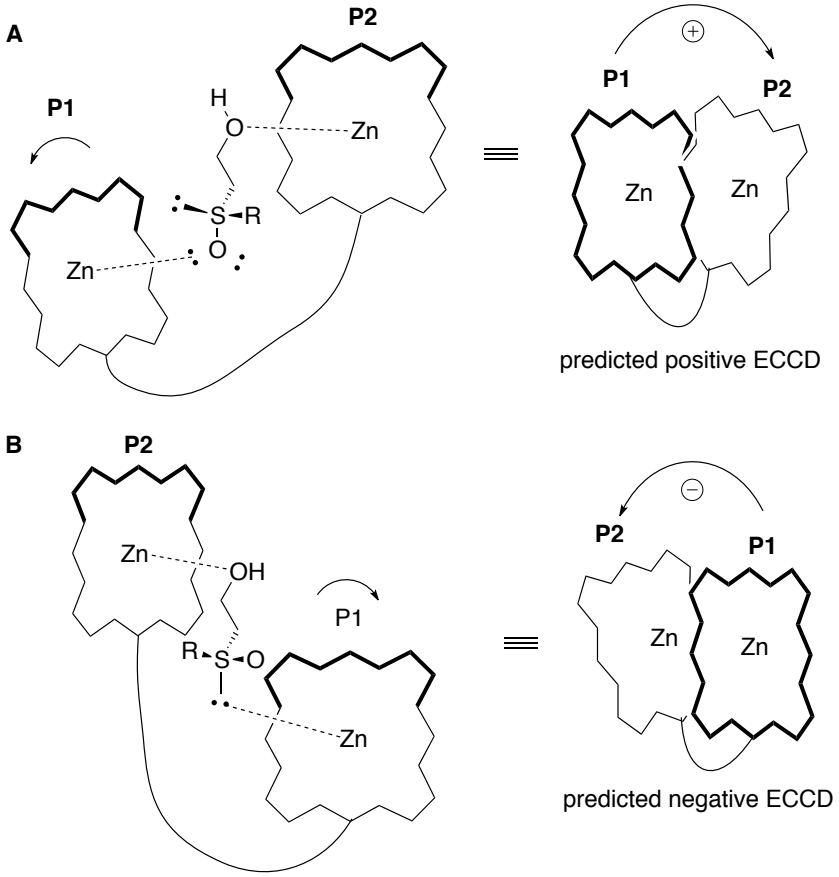

Figure 2-23. Proposed binding of a sulfoxy alcohol to Zn-TPFP tweezer. In A) sulfoxide coordinates to porphyrin via oxygen lone pairs yielding a predicted positive ECCD signal. In B) sulfoxide coordinates to zinc via sulfur lone pairs yielding a

Several X-ray crystallographic studies of the chemistry of transition metals complexes with sulfoxides, specifically, dimethyl sulfoxide (DMSO), have been done.[41] However, because of the difficulty in obtaining an X-ray quality crystal, in addition to the fact that not all compounds are crystalline, it becomes difficult to use X-ray crystallography, therefore, IR spectroscopy has become very important in determining the metal-sulfoxide bonding.

DMSO is structurally similar to acetone, with sulfur replacing the carbonyl carbon. The normal absorption of the S=O bond occurs at 1050 cm^{-1}. This is lower than the C=O frequency, since the SO bond has a larger reduced mass than the CO bond resulting in the frequency shift. Metals can bond to DMSO either through its oxygen or its sulfur lone pairs. If the binding is to the sulfur, the metal donates electrons from its 1*t* orbitals (the *t2g)* into an empty 1*t* orbital on the DMSO ligand, thereby increasing the S--O bond order. Thus, if the metal is bonded to the DMSO at the sulfur, the frequency of the S=O absorption increases. If the bonding is to the oxygen of the DMSO, the metal forms a bond with one of the lone pairs on the oxygen, and thereby withdraws electron density from the oxygen. This favors the second resonance form in Figure 2-17, since the oxygen will "seek" to gain electrons to compensate for the electrons donated to the metal. The net effect is the lowering of the S=O bond order, and the S=O absorption appears at lower frequency. This shift of the S-O stretching frequency to lower values on binding to oxygen and to higher values on binding to sulfur has been well established.[42]

Figure 2-24 shows a sketch[41] of the periodic table showing the preference of O- or S-bonding as inferred from IR spectroscopy. A close look at this table reveals that there's a general preference of O-bonding over S-bonding, based on the Hard/Soft acid/base principle. However, it is important to remember that the hardness and softness of a metal ion can be dramatically modified by the nature of the coordinated ligands.

H *o*													
Li												B	
Na													
K		Sc *o*	Ti *o*	V *o*	Cr *o*	Mn *o*	Fe *s, o*	Co *o*	Ni *o*	Cu *o*	Zn *o*		
	Sr	Y *o*	Zr *o*	Nb *o*	Mo *o*	Tc	Ru *s, o*	Rh *s, o*	Pd *s, o*	Ag *o*	Cd	In	Sn
		La *o*	Hf *o*	Ta *o*		Re *o*	Os	Ir *s, o*	Pt *s*		Hg *o*	Tl	Pb
		Ac *o*											

Figure 2-24. Sketch of the periodic table showing the preference of O- and S- bonding sulfoxide complexes as suggested by IR spectroscopy.

Attempts to crystallize sulfoxides bound to porphyrin were unsuccessful, and so we turned to IR spectroscopy in order to understand the binding of S=O to zinc. IR spectroscopy analysis of monomeric A4 Zn-TPFP complexed with phenyl methyl sulfoxide was used to gain insight into the binding mode of fluorinated tweezer system with sulfoxide. In this experiment, our main interest was the behavior of the SO stretching frequency, since this should be the most informative with respect to the nature of the zinc-sulfoxide bonding. As shown in figure 2-25, upon coordination of sulfoxide to porphyrin, the peak corresponding to the S=O stretch (1048 cm^{-1}) decreased in intensity with increasing equivalents of porphyrin, until complete disappearance at 1 equivalents of porphyrin. Addition of sulfoxide to this saturated complex resulted in the re-appearance of S=O at the same frequency (1048 cm^{-1}). (See SI for full experimental details).

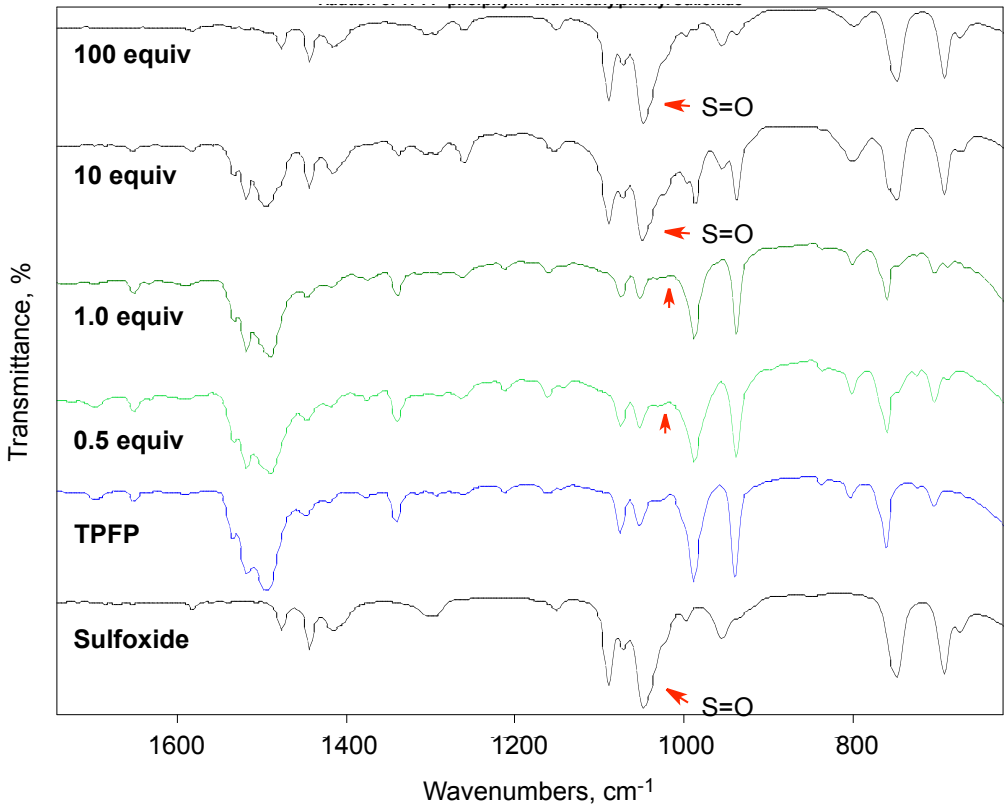

Figure 2-25. IR titration of methyl phenyl sulfoxide with TPFP porphyrin. From 0.5 eq to 100 eq. in methylene chloride. The S=O stretch disappears at high porphyrin concentration, and re-appears with addition of excess sulfoxide.

Usually, the S-O stretch gives rise to a distinct intense peak in IR. However, due to overlap or mixing with other bands such as C-H rocking, it is usually hard or complicated to identify its location. Moreover, the shift of the S-O stretch can sometimes be small, making it very difficult or impossible to determine.[43] However, there is no precedence in literature for the preference for sulfur coordination by zinc metal, based on this, we expected Zn-porphyrin to coordinate to oxygen. Looking at the IR data, the S=O stretch disappears upon complexation, but, there are several bands where we would expect the S-O stretch to be (800-1000 cm^{-1}). We do not however observe the appearance of S=O stretch at higher frequencies that would indicate

a sulfur coordination. (1120-1170 cm^{-1}). With this in mind, we proposed that the porphyrin tweexer preferably binds to the oxygen lone pairs of the sulfoxide. This information was useful for us to derive the binding model and working mnemonic for the absolute stereochemical determination for chiral sulfoxides.

Following these observations, we proposed that Zn-TPFP tweezer would bind to the sulfoxy alcohols via the oxygen lone pairs as depicted in Figure 2-23 B, and not via the sulfur atom. With this in mind, Zn-TPFP tweezer was examined for configurational assignment of a variety of sulfoxy alcohols via the Exciton Coupled Circular Dichroism protocol. To our delight, prominent and reproducible bisignate CD signals at the Soret region were observed upon complexation of the tweezer with micromolar concentrations of a number of chiral sulfoxy alcohols (Table 2-3).

As shown in Table 2-3, the obtained amplitudes are reasonably large and as expected, the enantiomers give opposite signals. The sulfoxides **2**, **3**, **4**, **5-ent**, **6** and **7-ent** resulted in negative ECCD spectra, while positive signals were observed for sulfoxides **2-ent**, **3-ent**, **4-ent**, **5**, **6-ent** and **7**. It is noteworthy that the observed ECCD signals remain constant regardless of the presence or absence of substituents at the hydroxyl binding site.

Figure 2-26 shows a proposed binding conformation that correlates the chirality of the sulfoxy alcohols and the sign of ECCD obtained. Here, one binding interaction occurs between the hydroxyl group and one porphyrin of the tweezer, while the other is between the sulfoxide oxygen and the other porphyrin of the tweezer. It is assumed that the porphyrin bound to the hydroxyl group approaches opposite the largest substituent on the sulfoxy alcohol. Since **P2** is bound to the sulfoxide oxygen, invariably, this will be the largest group so that P**1** and **P2** avoid

Table 2-3. ECCD data for chiral sulfoxy alcohols in hexane.

entry		sulfoxy alcohol	predicted sign	λ nm, (Δε)	A
1	**2** (*S*)	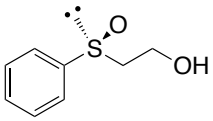	neg	432, -27 419, +30	-53
2	**2-ent**(*R*)	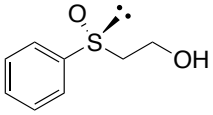	pos	432, +39 421, -31	+70
3	**3** (*S,S*)	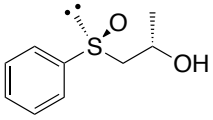	neg	425, -34 414, +36	-70
4	**3-ent**(*R,S*)	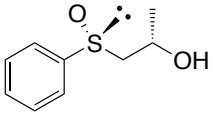	pos	426, +37 414, -43	+80
5	**4** (*S,R*)	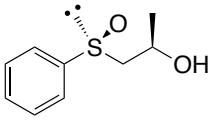	neg	422, +199 414, -13	-25
6	**4-ent**(*R,R*)	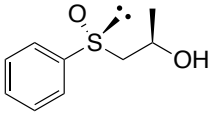	pos	427, +88 414, -82	+170
7	**5** (*S*)	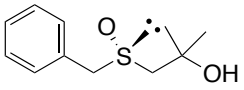	pos	426, +55 414, -12	+67
8	**5-ent**(*R*)	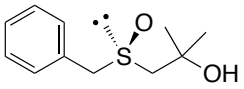	neg	426, -39 413, +76	-115
9	**6** (*S*)	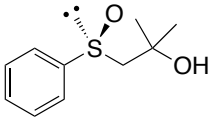	neg	423, -65 413, +55	-120
10	**6-ent**(*R*)	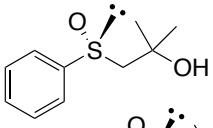	pos	424, +70 415, -60	+130
11	**7** (*R*)	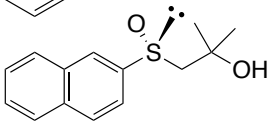	pos	421, +27 415, -23	+50
12	**7-ent**(*S*)	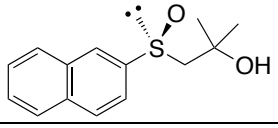	neg	425, -10 416, +39	-49

Tweezer:substrate ratio – 1:20, 1 μM tweezer concentration at 0 °C was used for all measurements.

steric clash with each other. In the case of substrates **2**, **5**, **6** and **7**, steric relief of **P1** is achieved through rotation/sliding of the porphyrin ring away from the largest substituent on the chiral center. Considering substrate **2** depicted in Figure 2-26 A, **P1** slides away from phenyl group, in preference of the smaller lone pair of electrons, generating the energetically favored complex in which the two porphyrins are twisted in a clockwise fashion. Consequently, a positive ECCD spectrum is obtained for the **2R**, **6R** and **7R** substrates.

For substrates with two chiral centers, **3** and **4**, it is assumed that each porphyrin undergoes independent steric differentiation, keeping in mind that the observed ECCD spectrum is the result of the helical twist of the two porphyrins. This is shown in Figure 2-26 B with the binding of sulfoxy alcohol **3(*S*,*S*)**. We propose that **P1** approaches the sulfoxide oxygen opposite to the largest substituent at the chiral center, in this case the phenyl group. This way, the phenyl group is anti to the porphyrin and does not participate in the steric differentiation. The two remaining groups, the lone pair of electrons and the alkyl CH_2 chain dictate the rotation of the porphyrin ring. Because lone pair electrons are smaller, **P1** will rotate clockwise, away from the CH_2 chain. In a similar manner, **P2** goes anti to the methyl group when binding to the hydroxyl group. Steric differentiation of the remaining substituents (H and CH_2 chain) causes the counterclockwise rotation of **P2** away from bulky CH_2 chain towards the smaller hydrogen. This causes a clockwise helical twist between **P1** and **P2** which would predict a negative ECCD spectrum. Figure 2-30 shows the positive and negative ECCD spectra obtained with substrates **2 (R)** and **3 (S,S)** upon complexation with tweezer.

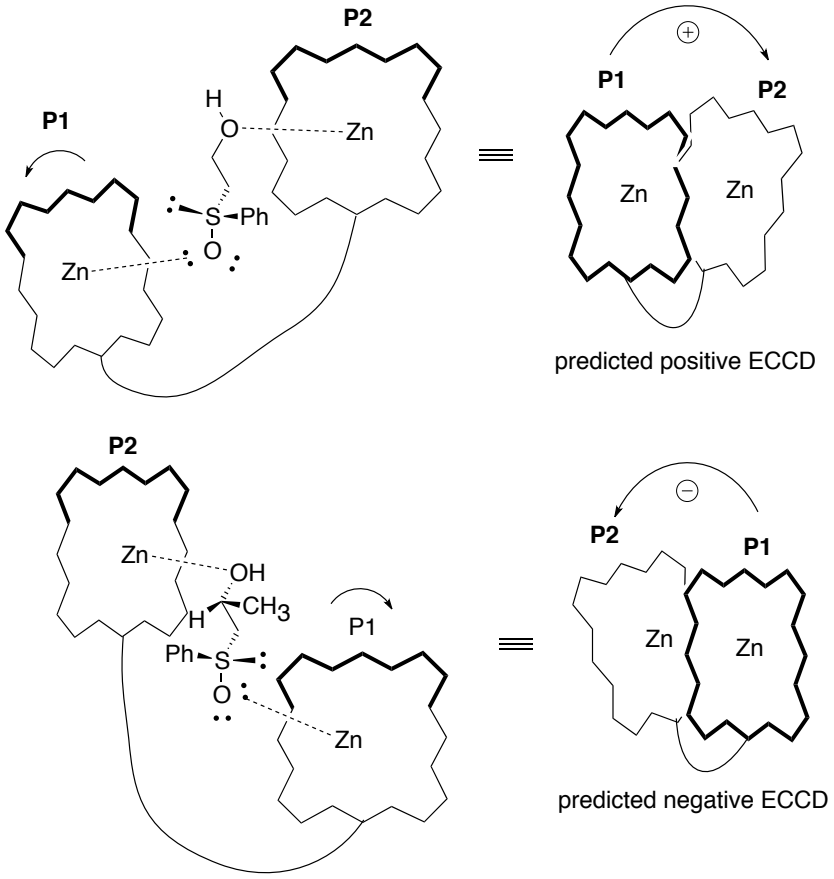

Figure 2-26. Proposed working mnemonic as shown for **2-ent(*R*)** and **3(*S*,*S*)**

The sign does not depend on the chain length or the groups on the substrates. It is also independent of the alcohol, with primary, secondary and tertiary centers behaving in a similar manner. This leads us to believe that the stereodifferentiation is governed only by the groups directly attached at the chiral centers and the porphyrin coordinating to the sulfoxide oxygen achieves the stereodifferentiation based on the sizes of the groups attached directly to the sulfoxide.

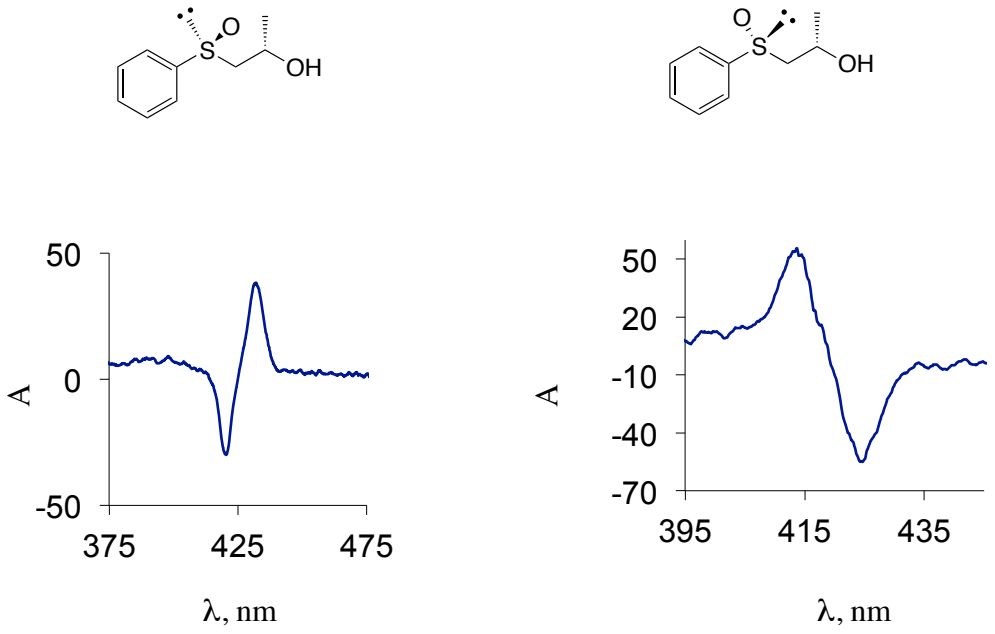

Figure 2-27. Obtained ECCD spectra of **3** (*S*,*S*), and **3-ent** (R,*S*) respectively.

In conclusion, we have successfully applied the tweezer methodology to determine the absolute stereochemistry of chiral sulfoxides, using very little substrate (milligram quantities) and without requiring any derivatizations.

EXPERIMENTAL:

Materials and methods

Anhydrous CH_2Cl_2 was dried and redistilled over CaH_2. The solvents used for CD measurements were purchased from Aldrich and were spectra grade. All reactions were performed in dried glassware under nitrogen. Column chromatography was performed using SiliCycle silica gel (230-400 mesh). ^{1}H-NMR and ^{13}C-NMR spectra were obtained on Varian Inova 300 and 500 MHz instrument and are reported in parts per million (ppm) relative to the solvent resonances (δ), with coupling constants (*J*) in Hertz (Hz). IR studies were performed on a Nicolet FT-IR 42 instrument. UV/Vis spectra were recorded on a Perkin-Elmer Lambda 40 spectrophotometer, and are reported as λmax [nm]. CD spectra were recorded on a JASCO J-810 spectropolarimeter, equipped with a temperature controller (Neslab 111) for low temperature studies, and were reported as λ[nm] ($\Delta\varepsilon_{max}$ [L mol^{-1} cm^{-1}]). Optical rotations were recorded at 20 °C on a Perkin Elmer 341 Polarimeter (λ = 589 nm, 1 dm cell). HRMS analyses were performed on a Q-TOF Ultima system using electrospray ionization in positive mode.

General procedure for CD measurement:

Zinc porphyrin tweezer **1** (1 μL of a 1 mM solution in anhydrous CH_2Cl_2) was added to hexane (1 mL) in a 1.0 cm cell to obtain a 1 μM tweezer **1** solution. The background spectrum was recorded from 350 nm to 550 nm with a scan rate of 100 nm/min at 0 °C. Chiral hydroxy ketone (1 to 20 μL of a 1 mM solution in anhydrous CH_2Cl_2) was added into the prepared tweezer solution to afford the host/guest complex. The CD spectra were measured immediately

(minimum of 5 accumulations). The resultant ECCD spectra recorded in millidegrees were normalized based on the tweezer concentration to obtain the molecular CD (Mol CD).

Binding affinity measurements of hydroxyl ketone upon complexation with Zn-TPFP-tz 1.

The binding affinities for porphyrin tweezer complexes were determined through titration of porphyrin tweezer **1** with corresponding guest. The UV spectrum of the titration of hydroxy ketone **8** shown below (Figure S1) demonstrates the change in the Soret band absorption upon binding of the guest to the host. Plot of the equivalence of the hydroxy ketone added as a function of the change in absorption (426 nm) leads to a saturation curve, which provides the binding constant of complex formed upon non-linear least square analysis. Calculations of binding constants via the latter procedure follows previously published protocols and analysis.[5]

Investigation of importance of linker length.

Synthesis of chiral hydroxy ketones

Compound **6** and **10** are commercially available from Aldrich. Hydroxy ketones **2-8** were synthesized from their corresponding chiral diols by monobenzylation,[19] followed by oxidation and deprotection. This procedure does not significantly affect the ee's. as shown by comparing the $[\alpha]^{20}_{D}$ obtained for (*R*)-9-hydroxydecan-2-one (***6R***) to the reported literature value (**[**α**]** $^{20}_{D}$ = -8.5, (*c* = 0.50, $CHCl_3$; *ee*= 92% (lit -9.7 >95%))

Typical procedure for synthesis of chiral hydroxy ketones from chiral diols as described for the synthesis of 2:

1) Procedure for mono benzylation:

Reactions were performed at 50 °C.

To a flame-dried 5mL round bottom flask equipped with a stir bar was added diol (200 mg, 1.69 mmol) and freshly distilled toluene (2 mL). 0.74 mL of a 50% w KOH aqueous solution (0.5 equiv. pure KOH) and tetrabutylammonium bisulfate (9.2 mg, 1.6 mmol) were subsequently added to the flask and stirred for 15 min to equilibrate. Then, benzyl chloride (0.38 mL, 3.3 mmol) was added and the mixture stirred for 24 h, monitored by TLC until completion. The organic layer was extracted into CH_2Cl_2 and solvent removed under reduced pressure. The residue was purified by flash chromatography (20% EtOAc/hexane) to afford the mono protected diol (0.3 g, 91%) as a colorless oil.

(2*R*,9*R*)-9-(benzyloxy)decan-2-ol

^{1}H-NMR (CDCl3, 300 MHz) δ 0.95 (t, 3H, *J*= 7.2 Hz), 1.46 (m, 4H), 1.78 (t, 1H, *J* = 6.3 Hz), 2.91 (m, 2H), 3.61 (m, 1H), 3.91 (m, 1H).

(2*R*,10*R*)-10-(benzyloxy)undecan-2-ol

^{1}H-NMR ($CDCl_3$, 300 MHz) δ 1.16-12.10 (m, 18H), 2.11 (s, 3H), 2.39 (t, 2H, *J* = 7.5 Hz), 3.44 (m, 1H), 4.48 (dd, 2H, *J* = 12.9 Hz and 11.7Hz), 7.32-7.23 (m, 5H).

(2*R*,13*R*)-13-(benzyloxy)tetradecan-2-ol

^{1}H-NMR (CDCl3, 300 MHz) δ 1.60-1.15 (m, 23H), 3.49-3.44 (m, 1H), 3.78-3.76 (m, 1H), 2.91 (m, 2H), 3.61 (m, 1H), 4.48 (dd, 2H, *J* = 12.9 Hz and 11.7Hz), 7.33-7.24 (m, 5H); ^{13}C-NMR

(CDCl3, 75 MHz) δ 19.8, 23.7, 25.7, 26.0, 26.4, 29.7, 29.82, 29.84, 29.85, 29.88, 29.9, 30.0, 36.9, 39.6, 68.4, 70.5, 70.7, 73.0, 75.1, 127.5, 127.7, 127.8, 128.53, 128.57, 139.4.

2) Procedure for oxidation:

To a flame-dried round bottom flask was added PCC (0.61 g, 2.2 eq), $MgSO_2$ (5 times PCC) and freshly distilled CH_2Cl_2 (enough to just cover the reagents). This was stirred vigorously and then alcohol (0.27 g, 1 eq) dissolved in CH_2Cl_2 (10 mL) was added in one portion. This was stirred at room temperature under niterogen atmosphere and monitored by TLC. After completion of the reaction, ether (2 times CH_2Cl_2) was added in and stirred for 2 min, then suction filtered. Solvent was removed under reduced pressure and product purified by flash chromatography (20% EtOAc/hexane) to give desired ketone (0.21 g, 80%)

(*R*)-9-(benzyloxy)decan-2-one

^{1}H-NMR (CDCl3, 300 MHz) δ 1.16 (d, 3H, *J*= 6 Hz), 1.59-1.21 (m, 10H), 2.10 (s, 3H), 2.38 (t, 2H, *J*=7.2 Hz), 3.48 (m, 1H), 4.48 (dd, 2H, *J*= 11.7 and 23.1 Hz), 7.32-7.25 (m, 5H); ^{13}C-NMR (CDCl3, 75 MHz) δ 19.6, 23.8, 25.3, 29.1, 29.4, 29.8, 36.6, 43.8, 70.3, 74.8, 103.9, 127.3, 127.6, 128.3, 139.1.

(*R*)-10-(benzyloxy)undecan-2-one

^{1}H-NMR (CDCl3, 300 MHz) δ 0.95 (t, 3H, *J*= 7.2 Hz), 1.46 (m, 4H), 1.78 (t, 1H, *J* = 6.3 Hz), 2.91 (m, 2H), 3.61 (m, 1H), 3.91 (m, 1H).

(*R*)-13-(benzyloxy)tetradecan-2-one

^{1}H-NMR (CDCl3, 300 MHz) δ 1.16-12.10 (m, 18H), 2.11 (s, 3H), 2.39 (t, 2H, *J* = 7.5 Hz), 3.44 (m, 1H), 4.48 (dd, 2H, *J* = 12.9 Hz and 11.7Hz), 7.32-7.23 (m, 5H);

3) Procedure for deprotection:

To a flame-dried flask containing ketone dissolved in EtOAc was added Pearlman's catalyst (10%) and stirred at room temperature until completion of reaction as observed by TLC. After completion, the reaction mixture was filtered by vaccum filtration and solvent removed under reduced pressure. Hydroxy ketone was obtained in quantitative yield after flash chromatography (20% EtOAc/hexane)

Note: the additional manipulations (protection, oxidation, deprotection) do not affect the ee values as shown from comparison of $[\alpha]^{20}_{D}$ Values to known compounds.

(*S*)-4-hydroxypentan-2-one (2*S*)

^{1}H-NMR (CDCl3, 300 MHz) δ 0.95 (t, 3H, *J*= 7.2 Hz), 1.46 (m, 4H), 1.78 (t, 1H, *J* = 6.3 Hz), 2.91 (m, 2H), 3.61 (m, 1H), 3.91 (m, 1H).

(*R*)-4-hydroxy-5-methylhexan-2-one (3*R*)

^{1}H-NMR (CDCl3, 300 MHz) δ 0.95 (t, 3H, *J*= 7.2 Hz), 1.46 (m, 4H), 1.78 (t, 1H, *J* = 6.3 Hz), 2.91 (m, 2H), 3.61 (m, 1H), 3.91 (m, 1H).

(*S*)-5-hydroxyhexan-2-one (4*S*)

^{1}H-NMR (CDCl3, 300 MHz) δ 0.95 (t, 3H, *J*= 7.2 Hz), 1.46 (m, 4H), 1.78 (t, 1H, *J* = 6.3 Hz), 2.91 (m, 2H), 3.61 (m, 1H), 3.91 (m, 1H).

(*R*)-9-hydroxydecan-2-one (6*R*)

$[\alpha]^{20}_{D}$= -8.5, (*c* = 0.50, CHCl3; *ee*= 92% (lit -9.7 >95%); ^{1}H-NMR (CDCl3, 300 MHz) δ 1.15 (d, 3H, *J*= 6.3 Hz), 1.59-1.23 (m, 10H), 2.1 (s, 3H), 2.39 (t, 2H, *J*=7.2Hz), 3.77-3.73(m, 1H); ^{13}C-NMR (CDCl3, 75 MHz) δ 14.5, 18.0, 23.5, 23.7, 25.5, 29.1, 29.3, 29.8, 39.2, 43.7, 68,1, 111.1;

(*R*)-10-hydroxyundecan-2-one (7*R*)

^{1}H-NMR (CDCl3, 300 MHz) δ 0.95 (t, 3H, *J*= 7.2 Hz), 1.46 (m, 4H), 1.78 (t, 1H, *J* = 6.3 Hz), 2.91 (m, 2H), 3.61 (m, 1H), 3.91 (m, 1H).

(*R*)-13-hydroxytetradecan-2-one (8*R*)

^{1}H-NMR (CDCl3, 300 MHz) δ 0.95 (t, 3H, *J*= 7.2 Hz), 1.46 (m, 4H), 1.78 (t, 1H, *J* = 6.3 Hz), 2.91 (m, 2H), 3.61 (m, 1H), 3.91 (m, 1H).

Synthesis of chiral sulfoxy alcohols:

To obtain pure enantiomers, the racemic chiral sulfoxides were separated on chiral HPLC column.

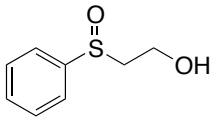

To a stirred solution of benzene thiol (1 g, 9.07 mmol) and triethyl amine (2.5 mL, 18 mol) in acetonitrile (26 mL) was added 2-bromoethanol (0.71 mL, 9.98 mmol). The reaction was stirred at room temperature for 24 h, treated with saturated NH_4Cl (20 mL) and extracted into ethyl acetate (3x20 mL). The combined organic layers were dried (Na_2SO_4). Solvent was removed and desired thio-ether obtained by flash chromatography (hex/EtOAc 2:1) as a colorless oil in 75% yield.

^{1}H NMR ($CDCl_3$, 500 MHz) δ 2.12-2.16 (t, 1H J = 5.7), 3.13-3.17 (t, 2H J = 3.3 Hz), 3.75-3.81 (q, 2H, J = 6.0 Hz), 7.22-7.36 (m, 3H), 7.40-7.44 (m, 2H); ^{13}CNMR (CDCl3, 75 MHz) δ;

This was then treated with MCPBA (1:1 eq) in freshly distilled DCM at room temperature for 4 h to give the racemic sulfoxide as a clear oil in 45% yield. ^{1}H-NMR ($CDCl_3$, 500 MHz) δ 2.81-3.21 (ddd, 2H J_1 = 3.6, J_2 = 13.8, J_3 =), 3.37 (br s, 1H), 3.97-4.19 (ddd, 2H, J_1 = 2.7, J_2 = 11.7, J_3 = Hz), 3.97 (s, 1H), 7.57-7.61 (m, 3H), 7.88-7.99 (m, 3H), 8.19 (s, 1Hr); ^{13}C-NMR (CDCl3, 75 MHz) δ 56.6, 58.9, 123.9, 129.4, 131.2, 143.1.

HPLC separation was done using OD column, eluting with 4% IPA/hex, at 0.8 mL/min

Retention times:

Enantiomer 1: 36 min

Enantiomer 2: 44 min

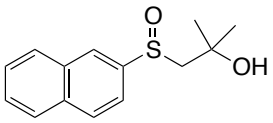

2-naphthalenethiol (1 g, 6.93 mmol) was dissolved in 2,2-dimethyloxirane (0.5 g, 6.93 mmol) and refluxed for 16 h. After this, the reaction mixture was directly poured onto a silica gel column and pruduct eluted with 20% EtOAC/hex as a crystalline white solid in 29% yield.

^{1}H-NMR ($CDCl_3$, 500 MHz) δ 1.50 (s, 6H), 3.41 (s, 3H), 7.65-7.73 (m, 2H), 7.91 (d, 2H J = 8.5), 7.95 (d, 2H J = 8.0 Hz), 8.08 (t, 2H J = 8.5 Hz), 8.53 (s, 1H); ^{13}C-NMR (CDCl3, 75 MHz) δ 29.1, 30.9, 68.0, 71.2, 119.8, 124.7, 127.7, 128.2, 128.3, 128.7, 130.0, 133.1, 134.7, 141.1;

This was then treated with MCPBA (1:1 eq) in freshly distilled DCM at room temperature for 4 h to give the racemic sulfoxide as a clear oil in 50% yield.

^{1}H-NMR ($CDCl_3$, 500 MHz) δ 1.36 (s, 3H), 1.64 (s, 3H), 2.80-3.09 (dd, 2H, J_1 = 13.5, J_2 = Hz), 3.97 (s, 1H), 7.57-7.61 (m, 3H), 7.88-7.99 (m, 3H), 8.19 (s, 1Hr); ^{13}C-NMR (CDCl3, 75 MHz) δ 29.1, 30.9, 68.0, 71.2, 119.8, 124.7, 127.7, 128.2, 128.3, 128.7, 130.0, 133.1, 134.7, 141.1;

HPLC separation was done using OD column, eluting with 5% IPA/hex, at 0.8 mL/min

Retention times:

Enantiomer 1: 30 min

Enantiomer 2: 40 min

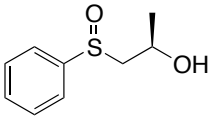

Benzenethiol (0.88 mL, 8.62 mmol) was dissolved in (*R*)-(-)-1,2-epoxypropane (1 mL, 8.62 mmol) and refluxed for 16 h. After this, the reaction mixture was directly poured onto a silica gel column and product eluted with 10% EtOAC/hex as a crystalline white solid in 29% yield.

^{1}H-NMR ($CDCl_3$, 500 MHz) δ 1.24 (d, 3H J = 6 Hz), 2.15 (br, s 1H), 2.80-2.84 (dd, 1H J_1 = 8.5, J_2 = 13.5), 3.07-3.11 (dd, 1H, J_1 = 3.5, J_2 = 13.5Hz), 3.82-3.83 (m, 1H), 7.18-7.21 (m, 1H), 7.26-

7.29 (m, 2H), 7.36-7.38 (m, 2H); ^{13}C-NMR (CDCl3, 75 MHz) δ 22.1, 43.8, 65.7, 126.9, 129.3, 130.3, 136.4;

This was then treated with MCPBA (1:1 eq) in freshly distilled DCM at room temperature for 4h to give the racemic sulfoxide as a clear oil in 40% yield.

HPLC separation was done using HPLC column, eluting with 5% IPA/hex, at 1.5 mL/min

Retention times:

Enantiomer 1: 30 min

Enantiomer 2: 40 min

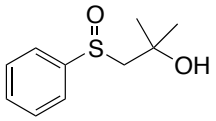

Benzenethiol (1.42 mL, 13.86 mmol) was dissolved in 2,2-dimethyloxirane (1 g, 13.86 mmol) and refluxed for 16 h. After this, the reaction mixture was directly poured onto a silica gel column and product eluted with 10% EtOAC/hex as a crystalline white solid in 59% yield.

^{1}H-NMR (CDCl3, 300 MHz) δ 1.34 (s, 3H), 1.61 (s, 3H), 2.71-3.02 (dd, 2H, J_1 = 7.8, J_2 = Hz), 3.89 (s, 1H), 7.49-7.54 (m, 3H), 7.63-7.64 (m, 2H); ^{13}C-NMR (CDCl3, 75 MHz) δ 28.9, 38.4, 45.8, 70.8, 127.4, 128.8, 129.1, 138.5;

This was then treated with MCPBA (1:1 eq) in freshly distilled DCM at room temperature for 2 h to give the racemic sulfoxide as a white solid in 44% yield.

^{1}H-NMR (CDCl3, 300 MHz) δ 1.34 (s, 3H), 1.61 (s, 3H), 2.71-3.02 (dd, 2H, J_1 = 7.8, J_2 = Hz), 3.89 (s, 1H), 7.49-7.54 (m, 3H), 7.63-7.64 (m, 2H); ^{13}C-NMR (CDCl3, 75 MHz) δ 28.9, 38.4, 45.8, 70.8, 127.4, 128.8, 129.1, 138.5.

HPLC separation was done using HPLC column, eluting with 5% IPA/hex, at 1.5 mL/min

Retention times:

Enantiomer 1:

Enantiomer 2:

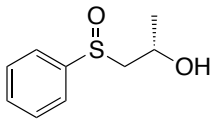

Benzenethiol (0.88 mL, 8.62 mmol) was dissolved in (*S*)-(-)-1,2-Epoxypropane (1mL, 8.62 mmol) and refluxed for 16 h. After this, the reaction mixture was directly poured onto a silica gel column and product eluted with 10% EtOAC/hex as a crystalline white solid in 29% yield.

^{1}H-NMR (CDCl3, 300 MHz) δ 1.30 (d, 3H *J* = 10.5 Hz), 2.47 (d, 1H *J* = 5.5 Hz), 2.84-2.91 (dd, 1H, J_1 = 14, J_2 = Hz), 3.86-3.91 (m, 1H), 7.25-7.44 (m, 5H); ^{13}C-NMR (CDCl3, 75 MHz) δ;

This was then treated with MCPBA (1:1 eq) in freshly distilled DCM at room temperature for 4h to give the racemic sulfoxide as a colorless oil in 40% yield.

^{1}H-NMR ($CDCl_3$, 300 MHz) δ 1.31 (s, 3H), 1.45 (s, 3H), 2.54-2.84 (dd, 2H, J_1 = 12.9, J_2 = Hz), 3.71 (s, 1H), 3.97-4.13 (dd, 2H J_1 = 12.9, J_2 =), 3.91 (m, 1H); ^{13}C-NMR (CDCl3, 75 MHz) δ 28.9, 38.4, 45.8, 70.8, 127.4, 128.8, 129.1, 138.5;

HPLC separation was done using HPLC column, eluting with 10% IPA/hex, at 1.5 mL/min

Retention times:

Enantiomer 1: 14 min

Enantiomer 2: 19 min

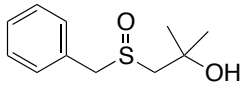

Benzyl mercaptan (1.7 g, 13.86 mmol) was dissolved in 2,2-dimethyloxirane (1 g, 13.86 mmol) and some solid NaOH pellets added in. The mixture was then refluxed for 16h, after which the reaction mixture was directly poured onto a silica gel column and product eluted with 20% EtOAC/hexanes as a crystalline white solid in 89% yield.

^{1}H-NMR ($CDCl_3$, 300 MHz) δ 1.31 (s, 3H), 1.45 (s, 3H), 2.54-2.84 (dd, 2H, J_1 = 12.9, J_2 = Hz), 3.71 (s, 1H), 3.97-4.13 (dd, 2H J_1 = 12.9, J_2 =), 3.91 (m, 1H); ^{13}C-NMR (CDCl3, 75 MHz) δ 28.9, 38.4, 45.8, 70.8, 127.4, 128.8, 129.1, 138.5;

This was then treated with MCPBA (1:1 eq) in freshly distilled DCM at room temperature for 2 h to give the racemic sulfoxide as a white solid in 74% yield.

HPLC separation was done using OD-H column, eluting with 2% IPA/hex, at 1.5 mL/min

Retention times:

Enantiomer 1: 45 min

Enantiomer 2: 60 min

X-Ray Crystallography Data

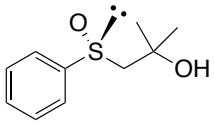

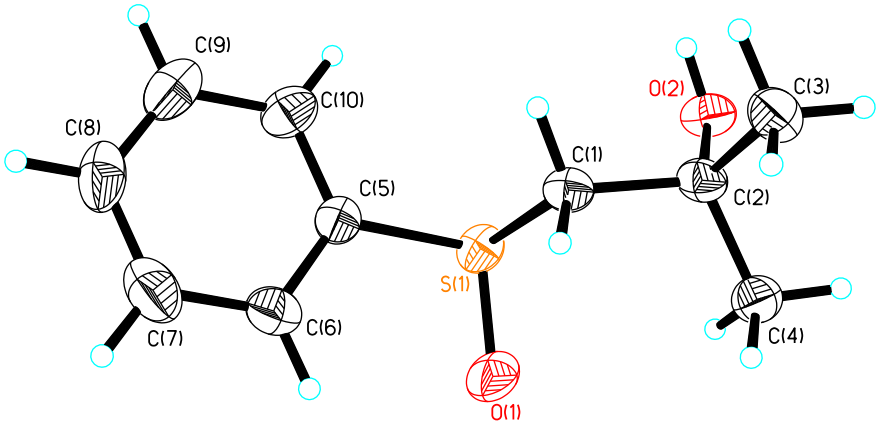

Table 2-4. Crystal data and structure refinement for bb58_0m.

Identification code	bb58_0m	
Empirical formula	C10 H14 O2 S	
Formula weight	198.27	
Temperature	173(2) K	
Wavelength	1.54178 Å	
Crystal system	Monoclinic	
Space group	P 21	
Unit cell dimensions	a = 5.6789(2) Å	a= 90°.
	b = 9.9447(3) Å	b= 99.182(2)°.
	c = 9.2621(3) Å	g = 90°.
Volume	516.37(3) $Å^3$	
Z	2	
Density (calculated)	1.275 Mg/m^3	
Absorption coefficient	2.512 mm^{-1}	
F(000)	212	
Crystal size	0.68 x 0.09 x 0.09 mm^3	
Theta range for data collection	4.84 to 68.05°.	

Table 2-4 (cont'd)

Index ranges	-6<=h<=6, -11<=k<=11, -7<=l<=10
Reflections collected	7022
Independent reflections	1804 [R(int) = 0.0449]
Completeness to theta = 68.05°	97.5 %
Absorption correction	Semi-empirical from equivalents
Max. and min. transmission	0.8148 and 0.2791
Refinement method	Full-matrix least-squares on F^2
Data / restraints / parameters	1804 / 1 / 121
Goodness-of-fit on F^2	1.063
Final R indices [I>2sigma(I)]	R1 = 0.0310, wR2 = 0.0749
R indices (all data)	R1 = 0.0344, wR2 = 0.0766
Absolute structure parameter	-0.001(19)
Largest diff. peak and hole	0.164 and -0.225 e.$Å^{-3}$

Table 2-5. Atomic coordinates (x 10^4) and equivalent isotropic displacement parameters ($Å^2$x 10^3)
for bb58_0m. U(eq) is defined as one third of the trace of the orthogonalized U^{ij} tensor.

	x	y	z	U(eq)
S(1)	2056(1)	1134(1)	1997(1)	30(1)
O(1)	4368(3)	1129(2)	1404(2)	43(1)
O(2)	-2301(3)	37(2)	-138(2)	34(1)
C(1)	-70(4)	2044(2)	705(2)	28(1)
C(2)	-1205(3)	1213(3)	-625(2)	29(1)
C(3)	-3064(4)	2105(3)	-1535(3)	38(1)
C(4)	611(4)	708(2)	-1537(3)	36(1)
C(5)	2430(4)	2395(2)	3409(3)	29(1)
C(6)	4340(4)	3272(3)	3513(3)	38(1)
C(7)	4669(5)	4207(3)	4629(3)	50(1)
C(8)	3112(5)	4256(3)	5628(3)	47(1)
C(9)	1212(5)	3386(3)	5511(3)	46(1)
C(10)	852(5)	2438(3)	4403(3)	39(1)

Table 2-6. Bond lengths [Å] and angles [°] for bb58_0m.

S(1)-O(1)	1.5014(15)
S(1)-C(5)	1.800(2)
S(1)-C(1)	1.802(2)
O(2)-C(2)	1.431(3)
O(2)-H(2)	0.8400
C(1)-C(2)	1.537(3)
C(1)-H(1A)	0.9900
C(1)-H(1B)	0.9900
C(2)-C(4)	1.519(3)
C(2)-C(3)	1.526(3)
C(3)-H(3A)	0.9800
C(3)-H(3B)	0.9800
C(3)-H(3C)	0.9800
C(4)-H(4A)	0.9800
C(4)-H(4B)	0.9800
C(4)-H(4C)	0.9800
C(5)-C(6)	1.383(3)
C(5)-C(10)	1.384(3)
C(6)-C(7)	1.380(4)
C(6)-H(6)	0.9500
C(7)-C(8)	1.379(4)
C(7)-H(7)	0.9500
C(8)-C(9)	1.374(4)
C(8)-H(8)	0.9500
C(9)-C(10)	1.385(4)
C(9)-H(9)	0.9500
C(10)-H(10)	0.9500
O(1)-S(1)-C(5)	105.02(11)
O(1)-S(1)-C(1)	106.95(10)
C(5)-S(1)-C(1)	97.00(10)
C(2)-O(2)-H(2)	109.5
C(2)-C(1)-S(1)	114.39(15)
C(2)-C(1)-H(1A)	108.7

Table 2-6 (cont'd)

S(1)-C(1)-H(1A)	108.7
C(2)-C(1)-H(1B)	108.7
S(1)-C(1)-H(1B)	108.7
H(1A)-C(1)-H(1B)	107.6
O(2)-C(2)-C(4)	105.9(2)
O(2)-C(2)-C(3)	110.57(16)
C(4)-C(2)-C(3)	110.86(19)
O(2)-C(2)-C(1)	109.54(17)
C(4)-C(2)-C(1)	112.88(16)
C(3)-C(2)-C(1)	107.2(2)
C(2)-C(3)-H(3A)	109.5
C(2)-C(3)-H(3B)	109.5
H(3A)-C(3)-H(3B)	109.5
C(2)-C(3)-H(3C)	109.5
H(3A)-C(3)-H(3C)	109.5
H(3B)-C(3)-H(3C)	109.5
C(2)-C(4)-H(4A)	109.5
C(2)-C(4)-H(4B)	109.5
H(4A)-C(4)-H(4B)	109.5
C(2)-C(4)-H(4C)	109.5
H(4A)-C(4)-H(4C)	109.5
H(4B)-C(4)-H(4C)	109.5
C(6)-C(5)-C(10)	121.2(2)
C(6)-C(5)-S(1)	119.36(18)
C(10)-C(5)-S(1)	119.41(18)
C(7)-C(6)-C(5)	119.2(2)
C(7)-C(6)-H(6)	120.4
C(5)-C(6)-H(6)	120.4
C(8)-C(7)-C(6)	120.1(3)
C(8)-C(7)-H(7)	119.9
C(6)-C(7)-H(7)	119.9
C(9)-C(8)-C(7)	120.3(3)
C(9)-C(8)-H(8)	119.8
C(7)-C(8)-H(8)	119.8

Table 2-6 (cont'd)

C(8)-C(9)-C(10)	120.5(3)
C(8)-C(9)-H(9)	119.7
C(10)-C(9)-H(9)	119.7
C(5)-C(10)-C(9)	118.7(2)
C(5)-C(10)-H(10)	120.7
C(9)-C(10)-H(10)	120.7

Symmetry transformations used to generate equivalent atoms:

Table 2-7. Anisotropic displacement parameters ($Å^2 x\ 10^3$) for bb58_0m. The anisotropic displacement factor exponent takes the form: $-2p^2[\ h^2\ a^{*2}U^{11} + ... + 2\ h\ k\ a^*\ b^*\ U^{12}\ ]$

	U^{11}	U^{22}	U^{33}	U^{23}	U^{13}	U^{12}
S(1)	36(1)	25(1)	31(1)	0(1)	7(1)	7(1)
O(1)	35(1)	57(1)	38(1)	-6(1)	8(1)	17(1)
O(2)	32(1)	24(1)	47(1)	-5(1)	15(1)	-4(1)
C(1)	26(1)	23(1)	34(1)	1(1)	7(1)	2(1)
C(2)	26(1)	24(1)	37(1)	-2(1)	7(1)	-4(1)
C(3)	32(1)	41(1)	39(2)	0(1)	2(1)	-3(1)
C(4)	34(1)	36(1)	38(2)	-7(1)	10(1)	-6(1)
C(5)	30(1)	28(1)	28(1)	1(1)	3(1)	6(1)
C(6)	28(1)	44(2)	44(2)	-2(1)	5(1)	0(1)
C(7)	37(2)	49(2)	59(2)	-9(1)	-8(1)	-1(1)
C(8)	53(2)	46(2)	36(2)	-10(1)	-10(1)	14(1)
C(9)	58(2)	48(2)	34(2)	1(1)	12(1)	16(1)
C(10)	45(1)	35(1)	40(2)	3(1)	15(1)	2(1)

Table 2-8. Hydrogen coordinates (x 10^4) and isotropic displacement parameters ($Å^2$x 10^3) for bb58_0m.

	x	y	z	U(eq)
H(2)	-3425	266	299	50
H(1A)	-1355	2383	1216	33
H(1B)	737	2834	354	33
H(3A)	-3827	1606	-2397	56
H(3B)	-2287	2909	-1849	56
H(3C)	-4273	2371	-945	56
H(4A)	1714	85	-954	53
H(4B)	1506	1472	-1842	53
H(4C)	-216	242	-2405	53
H(6)	5411	3233	2824	46
H(7)	5970	4817	4709	60
H(8)	3353	4895	6400	56
H(9)	136	3435	6197	56
H(10)	-451	1829	4327	46

Table 2-9. Torsion angles [°] for bb58_0m.

O(1)-S(1)-C(1)-C(2)	81.01(17)
C(5)-S(1)-C(1)-C(2)	-170.90(14)
S(1)-C(1)-C(2)-O(2)	56.12(19)
S(1)-C(1)-C(2)-C(4)	-61.6(2)
S(1)-C(1)-C(2)-C(3)	176.10(15)
O(1)-S(1)-C(5)-C(6)	12.8(2)
C(1)-S(1)-C(5)-C(6)	-96.9(2)
O(1)-S(1)-C(5)-C(10)	-164.95(19)
C(1)-S(1)-C(5)-C(10)	85.3(2)
C(10)-C(5)-C(6)-C(7)	0.0(4)
S(1)-C(5)-C(6)-C(7)	-177.7(2)
C(5)-C(6)-C(7)-C(8)	0.2(4)
C(6)-C(7)-C(8)-C(9)	-0.6(4)
C(7)-C(8)-C(9)-C(10)	0.8(4)
C(6)-C(5)-C(10)-C(9)	0.2(4)
S(1)-C(5)-C(10)-C(9)	177.93(19)
C(8)-C(9)-C(10)-C(5)	-0.6(4)

Symmetry transformations used to generate equivalent atoms:

Table 2-10. Hydrogen bonds for bb58_0m [Å and °].

D-H...A	d(D-H)	d(H...A)	d(D...A)	<(DHA)
O(2)-H(2)...O(1)#1	0.84	1.94	2.768(2)	168.1

Symmetry transformations used to generate equivalent atoms:
#1 x-1,y,z

Table 2-10 (cont'd)

Space Group P21
Wavelength 1.54178
Flack x .... -0.001
Flack (su) . 0.019

Bijvoet Pairs 834
Coverage ... 95.0
DiffCalcMax. 120.08
Outlier Crit 240.17
Sigma Crit.. 0.25
Select Pairs 599
Number Plus 502
Number Minus 97
Aver. Ratio 1.053
RC 1.016

Normal Prob. Plot
Sample Size. 834
Corr. Coeff. 0.996
Intercept .. -0.189
Slope 0.990

Bayesian Statistics
Type ..... Gaussian
Select Pairs 834
P2(true).... 1.000
P3(true).... 1.000
P3(rac-twin) 0.0E+00
P3(false) .. 0.0E+00
G 1.0168
G (su) 0.0264

Table 2-10 (cont'd)

Hooft y .... -0.008
Hooft (su) . 0.013

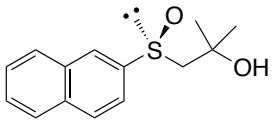

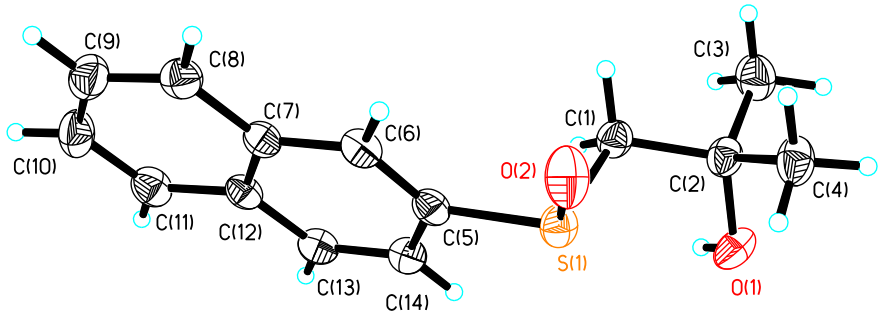

Table 2-11. Crystal data and structure refinement for bb64_0m.

Identification code	bb64_0m	
Empirical formula	C14 H16 O2 S	
Formula weight	248.33	
Temperature	173(2) K	
Wavelength	1.54178 Å	
Crystal system	Orthorhombic	
Space group	P 21 21 21	
Unit cell dimensions	a = 5.69360(10) Å	a= 90°.
	b = 10.0348(3) Å	b= 90°.
	c = 22.1186(5) Å	g = 90°.
Volume	1263.73(5) $Å^3$	
Z	4	
Density (calculated)	1.305 Mg/m^3	
Absorption coefficient	2.167 mm^{-1}	

Table 2-11 (cont'd)

F(000)	528
Crystal size	0.33 x 0.11 x 0.08 mm^3
Theta range for data collection	4.84 to 67.71°.
Index ranges	-6<=h<=6, -12<=k<=12, -15<=l<=26
Reflections collected	9193
Independent reflections	2276 [R(int) = 0.0616]
Completeness to theta = 67.71°	99.8 %
Absorption correction	Semi-empirical from equivalents
Max. and min. transmission	0.8457 and 0.5367
Refinement method	Full-matrix least-squares on F^2
Data / restraints / parameters	2276 / 0 / 157
Goodness-of-fit on F^2	1.027
Final R indices [I>2sigma(I)]	R1 = 0.0359, wR2 = 0.0831
R indices (all data)	R1 = 0.0397, wR2 = 0.0848
Absolute structure parameter	0.02(2)
Largest diff. peak and hole	0.450 and -0.206 e.$Å^{-3}$

Table 2-12. Atomic coordinates (x 10^4) and equivalent isotropic displacement parameters ($Å^2$x 10^3)
for bb64_0m. U(eq) is defined as one third of the trace of the orthogonalized U^{ij} tensor.

	x	y	z	U(eq)
S(1)	7037(1)	6755(1)	8222(1)	28(1)
O(1)	2938(3)	5661(2)	7364(1)	33(1)
O(2)	9513(3)	7026(2)	8026(1)	39(1)
C(1)	5125(4)	7596(2)	7693(1)	26(1)
C(2)	4366(4)	6732(2)	7154(1)	28(1)
C(3)	2971(5)	7623(3)	6725(1)	39(1)
C(4)	6432(4)	6084(3)	6828(1)	34(1)
C(5)	6472(4)	7834(2)	8850(1)	25(1)
C(6)	8057(4)	8783(2)	9015(1)	26(1)
C(7)	7614(3)	9590(2)	9531(1)	24(1)
C(8)	9202(4)	10583(2)	9730(1)	30(1)
C(9)	8775(5)	11289(3)	10243(1)	36(1)
C(10)	6726(5)	11058(2)	10583(1)	36(1)
C(11)	5119(4)	10132(2)	10398(1)	32(1)
C(12)	5514(4)	9374(2)	9866(1)	26(1)
C(13)	3902(4)	8389(2)	9669(1)	28(1)
C(14)	4352(4)	7624(2)	9175(1)	27(1)

Table 2-13. Bond lengths [Å] and angles [°] for bb64_0m.

S(1)-O(2)	1.4994(18)
S(1)-C(5)	1.790(2)
S(1)-C(1)	1.807(2)
O(1)-C(2)	1.425(3)
O(1)-H(1)	0.8400
C(1)-C(2)	1.536(3)
C(1)-H(1A)	0.9900
C(1)-H(1B)	0.9900
C(2)-C(4)	1.526(3)
C(2)-C(3)	1.526(3)
C(3)-H(3A)	0.9800
C(3)-H(3B)	0.9800
C(3)-H(3C)	0.9800
C(4)-H(4A)	0.9800
C(4)-H(4B)	0.9800
C(4)-H(4C)	0.9800
C(5)-C(6)	1.362(3)
C(5)-C(14)	1.421(3)
C(6)-C(7)	1.423(3)
C(6)-H(6)	0.9500
C(7)-C(8)	1.416(3)
C(7)-C(12)	1.424(3)
C(8)-C(9)	1.359(4)
C(8)-H(8)	0.9500
C(9)-C(10)	1.407(4)
C(9)-H(9)	0.9500
C(10)-C(11)	1.367(4)
C(10)-H(10)	0.9500
C(11)-C(12)	1.418(3)
C(11)-H(11)	0.9500
C(12)-C(13)	1.418(3)
C(13)-C(14)	1.361(3)
C(13)-H(13)	0.9500

Table 2-13 (cont'd)

C(14)-H(14)	0.9500
O(2)-S(1)-C(5)	106.50(10)
O(2)-S(1)-C(1)	107.12(11)
C(5)-S(1)-C(1)	96.39(10)
C(2)-O(1)-H(1)	109.5
C(2)-C(1)-S(1)	114.10(15)
C(2)-C(1)-H(1A)	108.7
S(1)-C(1)-H(1A)	108.7
C(2)-C(1)-H(1B)	108.7
S(1)-C(1)-H(1B)	108.7
H(1A)-C(1)-H(1B)	107.6
O(1)-C(2)-C(4)	105.78(19)
O(1)-C(2)-C(3)	110.32(18)
C(4)-C(2)-C(3)	110.95(19)
O(1)-C(2)-C(1)	109.50(17)
C(4)-C(2)-C(1)	112.97(18)
C(3)-C(2)-C(1)	107.34(19)
C(2)-C(3)-H(3A)	109.5
C(2)-C(3)-H(3B)	109.5
H(3A)-C(3)-H(3B)	109.5
C(2)-C(3)-H(3C)	109.5
H(3A)-C(3)-H(3C)	109.5
H(3B)-C(3)-H(3C)	109.5
C(2)-C(4)-H(4A)	109.5
C(2)-C(4)-H(4B)	109.5
H(4A)-C(4)-H(4B)	109.5
C(2)-C(4)-H(4C)	109.5
H(4A)-C(4)-H(4C)	109.5
H(4B)-C(4)-H(4C)	109.5
C(6)-C(5)-C(14)	122.1(2)
C(6)-C(5)-S(1)	120.77(16)
C(14)-C(5)-S(1)	117.13(17)
C(5)-C(6)-C(7)	119.7(2)

Table 2-13 (cont'd)

C(5)-C(6)-H(6)	120.1
C(7)-C(6)-H(6)	120.1
C(8)-C(7)-C(6)	122.5(2)
C(8)-C(7)-C(12)	118.8(2)
C(6)-C(7)-C(12)	118.7(2)
C(9)-C(8)-C(7)	120.8(2)
C(9)-C(8)-H(8)	119.6
C(7)-C(8)-H(8)	119.6
C(8)-C(9)-C(10)	120.6(2)
C(8)-C(9)-H(9)	119.7
C(10)-C(9)-H(9)	119.7
C(11)-C(10)-C(9)	120.5(2)
C(11)-C(10)-H(10)	119.8
C(9)-C(10)-H(10)	119.8
C(10)-C(11)-C(12)	120.5(2)
C(10)-C(11)-H(11)	119.8
C(12)-C(11)-H(11)	119.8
C(13)-C(12)-C(11)	121.8(2)
C(13)-C(12)-C(7)	119.3(2)
C(11)-C(12)-C(7)	118.9(2)
C(14)-C(13)-C(12)	121.3(2)
C(14)-C(13)-H(13)	119.4
C(12)-C(13)-H(13)	119.4
C(13)-C(14)-C(5)	118.9(2)
C(13)-C(14)-H(14)	120.6
C(5)-C(14)-H(14)	120.6

Symmetry transformations used to generate equivalent atoms:

Table 2-14. Anisotropic displacement parameters ($Å^2 x\ 10^3$) for bb64_0m. The anisotropic displacement factor exponent takes the form: $-2p^2[\ h^2\ a^{*2}U^{11} + ... + 2\ h\ k\ a^*\ b^*\ U^{12}\ ]$

	U^{11}	U^{22}	U^{33}	U^{23}	U^{13}	U^{12}
S(1)	26(1)	30(1)	27(1)	-4(1)	0(1)	4(1)
O(1)	28(1)	24(1)	47(1)	-8(1)	9(1)	-4(1)
O(2)	26(1)	55(1)	37(1)	-14(1)	4(1)	6(1)
C(1)	27(1)	24(1)	28(1)	-2(1)	0(1)	3(1)
C(2)	26(1)	28(1)	28(1)	-4(1)	3(1)	-4(1)
C(3)	40(1)	44(1)	32(1)	-2(1)	-7(1)	0(1)
C(4)	30(1)	40(1)	32(1)	-10(1)	7(1)	-4(1)
C(5)	25(1)	28(1)	23(1)	4(1)	-2(1)	4(1)
C(6)	21(1)	31(1)	25(1)	4(1)	2(1)	2(1)
C(7)	22(1)	27(1)	24(1)	3(1)	-1(1)	2(1)
C(8)	28(1)	31(1)	32(1)	3(1)	-4(1)	0(1)
C(9)	38(1)	32(1)	38(1)	-3(1)	-10(1)	-1(1)
C(10)	42(1)	36(1)	31(1)	-10(1)	-4(1)	6(1)
C(11)	34(1)	35(1)	28(1)	2(1)	5(1)	6(1)
C(12)	26(1)	27(1)	24(1)	4(1)	-2(1)	4(1)
C(13)	22(1)	31(1)	29(1)	5(1)	3(1)	1(1)
C(14)	24(1)	29(1)	28(1)	2(1)	-1(1)	-1(1)

Table 2-15. Hydrogen coordinates (x 10^4) and isotropic displacement parameters (Å^{2}x 10^3) for bb64_0m.

	x	y	z	U(eq)
H(1)	1748	5969	7540	50
H(1A)	3704	7900	7911	31
H(1B)	5942	8397	7537	31
H(3A)	2451	7100	6376	58
H(3B)	3968	8359	6588	58
H(3C)	1599	7983	6937	58
H(4A)	7200	5446	7099	51
H(4B)	7561	6772	6708	51
H(4C)	5863	5617	6468	51
H(6)	9452	8906	8786	31
H(8)	10583	10759	9503	36
H(9)	9869	11944	10373	43
H(10)	6458	11549	10944	44
H(11)	3729	9995	10627	39
H(13)	2480	8261	9887	33
H(14)	3267	6960	9049	32

Table 2-16. Torsion angles [°] for bb64_0m.

O(2)-S(1)-C(1)-C(2)	91.46(17)
C(5)-S(1)-C(1)-C(2)	-159.05(16)
S(1)-C(1)-C(2)-O(1)	65.6(2)
S(1)-C(1)-C(2)-C(4)	-52.0(2)
S(1)-C(1)-C(2)-C(3)	-174.65(16)
O(2)-S(1)-C(5)-C(6)	7.2(2)
C(1)-S(1)-C(5)-C(6)	-102.78(19)
O(2)-S(1)-C(5)-C(14)	-170.76(16)
C(1)-S(1)-C(5)-C(14)	79.23(18)
C(14)-C(5)-C(6)-C(7)	0.6(3)
S(1)-C(5)-C(6)-C(7)	-177.27(16)
C(5)-C(6)-C(7)-C(8)	179.3(2)
C(5)-C(6)-C(7)-C(12)	0.4(3)
C(6)-C(7)-C(8)-C(9)	-176.7(2)
C(12)-C(7)-C(8)-C(9)	2.2(3)
C(7)-C(8)-C(9)-C(10)	-0.8(4)
C(8)-C(9)-C(10)-C(11)	-0.9(4)
C(9)-C(10)-C(11)-C(12)	1.1(4)
C(10)-C(11)-C(12)-C(13)	178.8(2)
C(10)-C(11)-C(12)-C(7)	0.3(3)
C(8)-C(7)-C(12)-C(13)	179.5(2)
C(6)-C(7)-C(12)-C(13)	-1.5(3)
C(8)-C(7)-C(12)-C(11)	-1.9(3)
C(6)-C(7)-C(12)-C(11)	177.0(2)
C(11)-C(12)-C(13)-C(14)	-176.8(2)
C(7)-C(12)-C(13)-C(14)	1.7(3)
C(12)-C(13)-C(14)-C(5)	-0.7(3)
C(6)-C(5)-C(14)-C(13)	-0.5(3)
S(1)-C(5)-C(14)-C(13)	177.48(17)

Symmetry transformations used to generate equivalent atoms:

Table 2-17. Hydrogen bonds for bb64_0m [Å and °].

D-H...A	d(D-H)	d(H...A)	d(D...A)	<(DHA)
O(1)-H(1)...O(2)#1	0.84	1.97	2.797(2)	165.8

Symmetry transformations used to generate equivalent atoms:
#1 x-1,y,z
Space Group P212121
Wavelength 1.54178
Flack x 0.02
Flack (su) . 0.02

Bijvoet Pairs 920
Coverage ... 99.4
DiffCalcMax. 240.32
Outlier Crit 480.65
Sigma Crit.. 0.25
Select Pairs 679
Number Plus 560
Number Minus 119
Aver. Ratio 0.955
RC 0.931

Normal Prob. Plot
Sample Size. 920
Corr. Coeff. 0.999
Intercept .. -0.071
Slope 0.870

Bayesian Statistics
Type ..... Gaussian

Table 2-17 (cont'd)

Select Pairs	920
P2(true)....	1.000
P3(true)....	1.000
P3(rac-twin)	0.0E+00
P3(false) ..	0.0E+00
G	0.9274
G (su)	0.0325
Hooft y	0.036
Hooft (su) .	0.016.

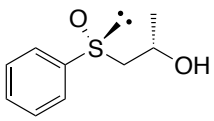

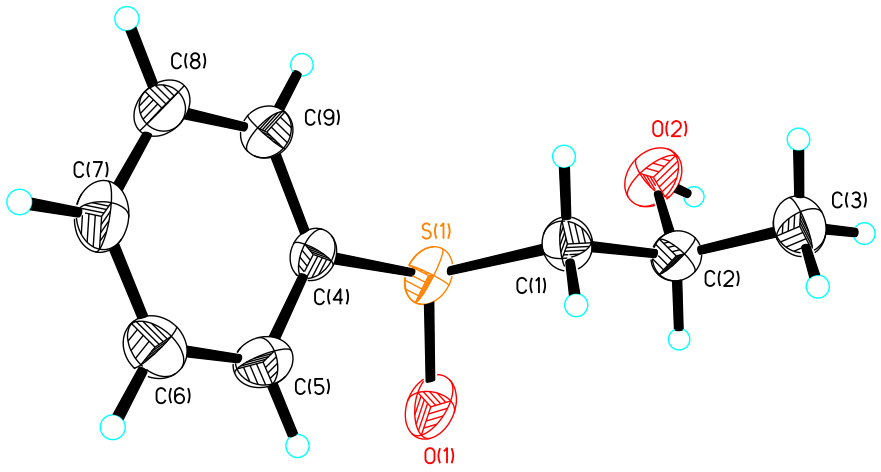

Table 2-18. Crystal data and structure refinement for bb48_0m.

Identification code	bb48_0m
Empirical formula	C9 H12 O2 S

Table 2-18 (cont'd)

Formula weight	184.25	
Temperature	173(2) K	
Wavelength	1.54178 Å	
Crystal system	Orthorhombic	
Space group	P 21 21 21	
Unit cell dimensions	a = 5.48730(10) Å	a= 90°.
	b = 8.3275(2) Å	b= 90°.
	c = 20.4046(4) Å	g = 90°.
Volume	932.40(3) $Å^3$	
Z	4	
Density (calculated)	1.313 Mg/m^3	
Absorption coefficient	2.743 mm^{-1}	
F(000)	392	
Crystal size	0.18 x 0.08 x 0.08 mm^3	
Theta range for data collection	4.33 to 67.83°.	
Index ranges	-6<=h<=6, -9<=k<=8, -20<=l<=24	
Reflections collected	6464	
Independent reflections	1672 [R(int) = 0.0369]	
Completeness to theta = 67.83°	99.5 %	
Absorption correction	Semi-empirical from equivalents	
Max. and min. transmission	0.8104 and 0.6380	
Refinement method	Full-matrix least-squares on F^2	
Data / restraints / parameters	1672 / 0 / 111	
Goodness-of-fit on F^2	1.050	
Final R indices [I>2sigma(I)]	R1 = 0.0306, wR2 = 0.0798	
R indices (all data)	R1 = 0.0322, wR2 = 0.0807	
Absolute structure parameter	-0.01(2)	
Largest diff. peak and hole	0.235 and -0.194 e.$Å^{-3}$	

Table 2-19. Atomic coordinates (x 10^4) and equivalent isotropic displacement parameters ($Å^2$x 10^3)
for bb48_0m. U(eq) is defined as one third of the trace of the orthogonalized U^{ij} tensor.

	x	y	z	U(eq)
S(1)	-215(1)	7942(1)	8713(1)	34(1)
O(1)	818(3)	9254(2)	9135(1)	46(1)
O(2)	-2565(3)	5582(2)	9602(1)	43(1)
C(1)	1064(4)	6081(2)	9017(1)	33(1)
C(2)	11(4)	5667(2)	9682(1)	36(1)
C(3)	1047(5)	4091(3)	9929(1)	46(1)
C(4)	1448(3)	8008(2)	7954(1)	28(1)
C(5)	3558(4)	8906(3)	7914(1)	35(1)
C(6)	4741(4)	9013(3)	7316(1)	40(1)
C(7)	3836(4)	8216(3)	6771(1)	40(1)
C(8)	1723(4)	7309(3)	6822(1)	38(1)
C(9)	509(4)	7213(2)	7418(1)	34(1)

Table 2-20. Bond lengths [Å] and angles [°] for bb48_0m.

S(1)-O(1)	1.5018(17)
S(1)-C(4)	1.7979(19)
S(1)-C(1)	1.811(2)
O(2)-C(2)	1.425(3)
O(2)-H(2)	0.8400
C(1)-C(2)	1.515(3)
C(1)-H(1A)	0.9900
C(1)-H(1B)	0.9900
C(2)-C(3)	1.516(3)
C(2)-H(2A)	1.0000
C(3)-H(3A)	0.9800
C(3)-H(3B)	0.9800
C(3)-H(3C)	0.9800
C(4)-C(9)	1.379(3)
C(4)-C(5)	1.381(3)
C(5)-C(6)	1.384(3)
C(5)-H(5)	0.9500
C(6)-C(7)	1.387(3)
C(6)-H(6)	0.9500
C(7)-C(8)	1.388(3)
C(7)-H(7)	0.9500
C(8)-C(9)	1.387(3)
C(8)-H(8)	0.9500
C(9)-H(9)	0.9500
O(1)-S(1)-C(4)	106.24(10)
O(1)-S(1)-C(1)	106.24(9)
C(4)-S(1)-C(1)	97.18(9)
C(2)-O(2)-H(2)	109.5
C(2)-C(1)-S(1)	110.74(15)
C(2)-C(1)-H(1A)	109.5
S(1)-C(1)-H(1A)	109.5
C(2)-C(1)-H(1B)	109.5

Table 2-20 (cont'd)

S(1)-C(1)-H(1B)	109.5
H(1A)-C(1)-H(1B)	108.1
O(2)-C(2)-C(1)	106.67(16)
O(2)-C(2)-C(3)	111.57(18)
C(1)-C(2)-C(3)	110.58(19)
O(2)-C(2)-H(2A)	109.3
C(1)-C(2)-H(2A)	109.3
C(3)-C(2)-H(2A)	109.3
C(2)-C(3)-H(3A)	109.5
C(2)-C(3)-H(3B)	109.5
H(3A)-C(3)-H(3B)	109.5
C(2)-C(3)-H(3C)	109.5
H(3A)-C(3)-H(3C)	109.5
H(3B)-C(3)-H(3C)	109.5
C(9)-C(4)-C(5)	121.74(19)
C(9)-C(4)-S(1)	118.62(15)
C(5)-C(4)-S(1)	119.58(15)
C(4)-C(5)-C(6)	118.72(19)
C(4)-C(5)-H(5)	120.6
C(6)-C(5)-H(5)	120.6
C(5)-C(6)-C(7)	120.5(2)
C(5)-C(6)-H(6)	119.7
C(7)-C(6)-H(6)	119.7
C(6)-C(7)-C(8)	119.95(19)
C(6)-C(7)-H(7)	120.0
C(8)-C(7)-H(7)	120.0
C(9)-C(8)-C(7)	119.90(19)
C(9)-C(8)-H(8)	120.0
C(7)-C(8)-H(8)	120.0
C(4)-C(9)-C(8)	119.18(19)
C(4)-C(9)-H(9)	120.4
C(8)-C(9)-H(9)	120.4

Symmetry transformations used to generate equivalent atoms:

Table 2-21. Anisotropic displacement parameters ($Å^2 x\ 10^3$) for bb48_0m. The anisotropic displacement factor exponent takes the form: $-2p^2[\ h^2\ a^{*2}U^{11} + ... + 2\ h\ k\ a^*\ b^*\ U^{12}\ ]$

	U^{11}	U^{22}	U^{33}	U^{23}	U^{13}	U^{12}
S(1)	34(1)	41(1)	26(1)	1(1)	0(1)	9(1)
O(1)	72(1)	39(1)	28(1)	-3(1)	-4(1)	14(1)
O(2)	36(1)	63(1)	31(1)	0(1)	5(1)	-2(1)
C(1)	32(1)	33(1)	34(1)	3(1)	0(1)	0(1)
C(2)	40(1)	37(1)	31(1)	1(1)	-3(1)	-4(1)
C(3)	49(1)	42(1)	48(1)	13(1)	-7(1)	-9(1)
C(4)	29(1)	30(1)	26(1)	2(1)	-3(1)	4(1)
C(5)	33(1)	36(1)	36(1)	-4(1)	-7(1)	0(1)
C(6)	34(1)	40(1)	45(1)	2(1)	3(1)	-3(1)
C(7)	51(1)	40(1)	30(1)	4(1)	6(1)	6(1)
C(8)	52(1)	36(1)	27(1)	-2(1)	-9(1)	3(1)
C(9)	35(1)	34(1)	32(1)	2(1)	-6(1)	-1(1)

Table 2-22. Hydrogen coordinates (x 10^4) and isotropic displacement parameters ($Å^2$x 10^3) for bb48_0m.

	x	y	z	U(eq)
H(2)	-3243	5650	9970	65
H(1A)	706	5203	8704	40
H(1B)	2856	6187	9053	40
H(2A)	415	6541	10000	43
H(3A)	326	3833	10356	70
H(3B)	2819	4187	9975	70
H(3C)	667	3235	9616	70
H(5)	4186	9440	8289	42
H(6)	6184	9637	7279	47
H(7)	4662	8291	6363	49
H(8)	1109	6755	6451	46
H(9)	-951	6607	7455	40

Table 2-23. Torsion angles [°] for bb48_0m.

O(1)-S(1)-C(1)-C(2)	70.27(16)
C(4)-S(1)-C(1)-C(2)	179.56(14)
S(1)-C(1)-C(2)-O(2)	57.37(19)
S(1)-C(1)-C(2)-C(3)	178.86(15)
O(1)-S(1)-C(4)-C(9)	-164.26(16)
C(1)-S(1)-C(4)-C(9)	86.45(18)
O(1)-S(1)-C(4)-C(5)	12.82(18)
C(1)-S(1)-C(4)-C(5)	-96.47(17)
C(9)-C(4)-C(5)-C(6)	0.4(3)
S(1)-C(4)-C(5)-C(6)	-176.54(17)
C(4)-C(5)-C(6)-C(7)	-0.8(3)
C(5)-C(6)-C(7)-C(8)	0.3(3)
C(6)-C(7)-C(8)-C(9)	0.6(3)
C(5)-C(4)-C(9)-C(8)	0.4(3)
S(1)-C(4)-C(9)-C(8)	177.40(15)
C(7)-C(8)-C(9)-C(4)	-0.9(3)

Symmetry transformations used to generate equivalent atoms:

Table 2-24. Hydrogen bonds for bb48_0m [Å and °].

D-H...A	d(D-H)	d(H...A)	d(D...A)	<(DHA)
O(2)-H(2)...O(1)#1	0.84	1.90	2.729(2)	169.3

Symmetry transformations used to generate equivalent atoms:
#1 x-1/2,-y+3/2,-z+2
Space Group P212121
Wavelength 1.54178
Flack x .... -0.01
Flack (su) . 0.02

Table 2-24 (cont'd)

Bijvoet Pairs 655
Coverage ... 97.3
DiffCalcMax. 159.66
Outlier Crit 319.31
Sigma Crit.. 0.25
Select Pairs 518
Number Plus 423
Number Minus 95
Aver. Ratio 1.019
RC 1.010

Normal Prob. Plot
Sample Size. 655
Corr. Coeff. 0.997
Intercept .. 0.204
Slope 1.074

Bayesian Statistics
Type ..... Gaussian
Select Pairs 655
P2(true).... 1.000
P3(true).... 1.000
P3(rac-twin) 0.0E+00
P3(false) .. 0.0E+00
G 1.0096
G (su) 0.0292
Hooft y .... -0.005
Hooft (su) . 0.015

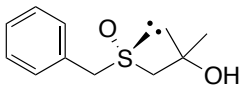

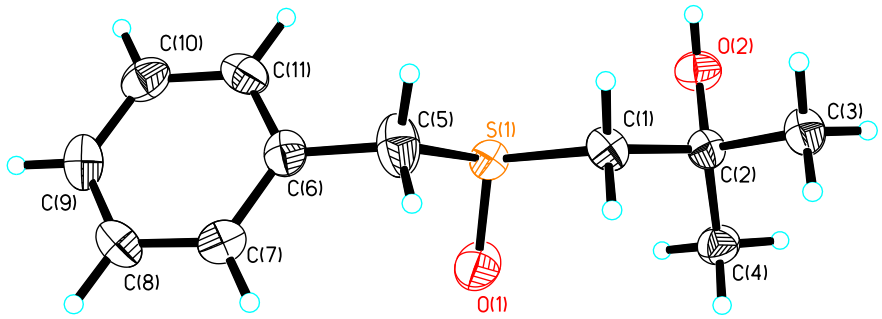

Table 2-25. Crystal data and structure refinement for BB73_0m.

Identification code	bb73_0m	
Empirical formula	C11 H16 O2 S	
Formula weight	212.30	
Temperature	173(2) K	
Wavelength	1.54178 Å	
Crystal system	Monoclinic	
Space group	P 21	
Unit cell dimensions	a = 5.70270(10) Å	a= 90°.
	b = 8.9995(2) Å	b= 90.611(2) °.
	c = 10.7011(2) Å	g = 90°.
Volume	549.165(19) $Å^3$	
Z	2	
Density (calculated)	1.284 Mg/m^3	
Absorption coefficient	2.395 mm^{-1}	
F(000)	228	
Crystal size	0.28 x 0.15 x 0.05 mm^3	
Theta range for data collection	4.13 to 67.76°.	
Index ranges	-6<=h<=6, -10<=k<=10, -12<=l<=12	
Reflections collected	7577	
Independent reflections	1796 [R(int) = 0.0583]	
Completeness to theta = 67.76°	95.8 %	

Table 2-25 (cont'd)

Absorption correction	Semi-empirical from equivalents
Max. and min. transmission	0.8957 and 0.5484
Refinement method	Full-matrix least-squares on F^2
Data / restraints / parameters	1796 / 1 / 130
Goodness-of-fit on F^2	1.037
Final R indices [I>2sigma(I)]	R1 = 0.0372, wR2 = 0.0904
R indices (all data)	R1 = 0.0445, wR2 = 0.0936
Absolute structure parameter	0.03(2)
Largest diff. peak and hole	0.196 and -0.167 e.$Å^{-3}$

Table 2-26. Atomic coordinates (x 10^4) and equivalent isotropic displacement parameters ($Å^2$x 10^3)
for BB73_0m. U(eq) is defined as one third of the trace of the orthogonalized U^{ij} tensor.

	x	y	z	U(eq)
S(1)	991(1)	7850(1)	5549(1)	27(1)
O(1)	-1446(3)	7813(4)	5031(2)	50(1)
O(2)	4746(4)	8556(2)	3502(2)	33(1)
C(1)	2786(5)	6599(3)	4656(3)	27(1)
C(2)	3531(5)	7179(4)	3362(3)	27(1)
C(3)	5142(5)	5999(4)	2812(3)	32(1)
C(4)	1489(5)	7467(3)	2482(3)	32(1)
C(5)	926(6)	6662(4)	6917(3)	44(1)
C(6)	-537(5)	7312(4)	7952(3)	31(1)
C(7)	-2672(5)	6662(4)	8257(3)	34(1)
C(8)	-3929(5)	7218(4)	9257(3)	35(1)
C(9)	-3112(6)	8407(4)	9934(3)	40(1)
C(10)	-1012(6)	9074(4)	9625(3)	37(1)
C(11)	278(5)	8518(4)	8634(3)	35(1)

Table 2-27. Bond lengths [Å] and angles [°] for BB73_0m.

S(1)-O(1)	1.491(2)
S(1)-C(1)	1.803(3)
S(1)-C(5)	1.813(3)
O(2)-C(2)	1.427(4)
O(2)-H(2)	0.8400
C(1)-C(2)	1.544(4)
C(1)-H(1A)	0.9900
C(1)-H(1B)	0.9900
C(2)-C(4)	1.513(4)
C(2)-C(3)	1.526(4)
C(3)-H(3A)	0.9800
C(3)-H(3B)	0.9800
C(3)-H(3C)	0.9800
C(4)-H(4A)	0.9800
C(4)-H(4B)	0.9800
C(4)-H(4C)	0.9800
C(5)-C(6)	1.511(4)
C(5)-H(5A)	0.9900
C(5)-H(5B)	0.9900
C(6)-C(11)	1.386(5)
C(6)-C(7)	1.393(4)
C(7)-C(8)	1.387(4)
C(7)-H(7)	0.9500
C(8)-C(9)	1.371(5)
C(8)-H(8)	0.9500
C(9)-C(10)	1.383(5)
C(9)-H(9)	0.9500
C(10)-C(11)	1.390(5)
C(10)-H(10)	0.9500
C(11)-H(11)	0.9500
O(1)-S(1)-C(1)	108.72(15)
O(1)-S(1)-C(5)	105.06(17)

Table 2-25 (cont'd)

C(1)-S(1)-C(5)	94.36(14)
C(2)-O(2)-H(2)	109.5
C(2)-C(1)-S(1)	115.3(2)
C(2)-C(1)-H(1A)	108.4
S(1)-C(1)-H(1A)	108.4
C(2)-C(1)-H(1B)	108.4
S(1)-C(1)-H(1B)	108.4
H(1A)-C(1)-H(1B)	107.5
O(2)-C(2)-C(4)	106.6(2)
O(2)-C(2)-C(3)	110.6(2)
C(4)-C(2)-C(3)	110.0(2)
O(2)-C(2)-C(1)	109.8(2)
C(4)-C(2)-C(1)	113.5(2)
C(3)-C(2)-C(1)	106.4(2)
C(2)-C(3)-H(3A)	109.5
C(2)-C(3)-H(3B)	109.5
H(3A)-C(3)-H(3B)	109.5
C(2)-C(3)-H(3C)	109.5
H(3A)-C(3)-H(3C)	109.5
H(3B)-C(3)-H(3C)	109.5
C(2)-C(4)-H(4A)	109.5
C(2)-C(4)-H(4B)	109.5
H(4A)-C(4)-H(4B)	109.5
C(2)-C(4)-H(4C)	109.5
H(4A)-C(4)-H(4C)	109.5
H(4B)-C(4)-H(4C)	109.5
C(6)-C(5)-S(1)	112.3(2)
C(6)-C(5)-H(5A)	109.1
S(1)-C(5)-H(5A)	109.1
C(6)-C(5)-H(5B)	109.1
S(1)-C(5)-H(5B)	109.1
H(5A)-C(5)-H(5B)	107.9
C(11)-C(6)-C(7)	119.6(3)
C(11)-C(6)-C(5)	120.3(3)

Table 2-25 (cont'd)

C(7)-C(6)-C(5)	120.0(3)
C(8)-C(7)-C(6)	119.3(3)
C(8)-C(7)-H(7)	120.4
C(6)-C(7)-H(7)	120.4
C(9)-C(8)-C(7)	120.9(3)
C(9)-C(8)-H(8)	119.5
C(7)-C(8)-H(8)	119.5
C(8)-C(9)-C(10)	120.1(3)
C(8)-C(9)-H(9)	119.9
C(10)-C(9)-H(9)	119.9
C(9)-C(10)-C(11)	119.5(3)
C(9)-C(10)-H(10)	120.2
C(11)-C(10)-H(10)	120.2
C(6)-C(11)-C(10)	120.5(3)
C(6)-C(11)-H(11)	119.8
C(10)-C(11)-H(11)	119.8

Symmetry transformations used to generate equivalent atoms:

Table 2-28. Anisotropic displacement parameters ($Å^2 x\ 10^3$) for BB73_0m. The anisotropic displacement factor exponent takes the form: $-2p^2[\ h^2\ a^{*2}U^{11} + ... + 2\ h\ k\ a^*\ b^*\ U^{12}\ ]$

	U^{11}	U^{22}	U^{33}	U^{23}	U^{13}	U^{12}
S(1)	29(1)	25(1)	27(1)	0(1)	0(1)	2(1)
O(1)	32(1)	80(2)	38(1)	-10(2)	-10(1)	23(1)
O(2)	34(1)	29(1)	36(1)	4(1)	-3(1)	-4(1)
C(1)	26(1)	23(2)	33(2)	5(1)	2(1)	5(1)
C(2)	27(2)	28(2)	26(2)	0(1)	2(1)	0(1)
C(3)	32(2)	34(2)	30(2)	2(1)	4(1)	5(1)
C(4)	31(2)	36(2)	30(2)	-1(1)	-5(1)	2(1)
C(5)	49(2)	50(2)	35(2)	12(2)	10(2)	19(2)
C(6)	31(2)	34(2)	27(2)	8(1)	-2(1)	9(1)
C(7)	35(2)	32(2)	35(2)	-1(2)	-5(1)	0(1)
C(8)	27(2)	33(2)	44(2)	6(2)	7(1)	1(1)
C(9)	48(2)	39(2)	32(2)	3(2)	10(2)	7(2)
C(10)	45(2)	33(2)	34(2)	4(2)	-10(2)	-1(2)
C(11)	25(2)	38(2)	42(2)	12(2)	-1(1)	-2(1)

Table 2-29. Hydrogen coordinates (x 10^4) and isotropic displacement parameters (Å^{2}x 10^3) for BB73_0m.

	x	y	z	U(eq)
H(2)	5932	8433	3962	50
H(1A)	4218	6370	5151	33
H(1B)	1915	5657	4537	33
H(3A)	5683	6326	1991	48
H(3B)	4280	5062	2723	48
H(3C)	6496	5851	3370	48
H(4A)	502	8257	2823	49
H(4B)	560	6557	2386	49
H(4C)	2082	7774	1665	49
H(5A)	279	5681	6677	53
H(5B)	2548	6508	7229	53
H(7)	-3262	5846	7786	41
H(8)	-5376	6770	9475	42
H(9)	-3991	8774	10618	48
H(10)	-454	9906	10086	45
H(11)	1728	8967	8423	42

Table 2-30. Torsion angles [°] for BB73_0m.

O(1)-S(1)-C(1)-C(2)	76.6(3)
C(5)-S(1)-C(1)-C(2)	-175.9(2)
S(1)-C(1)-C(2)-O(2)	56.9(3)
S(1)-C(1)-C(2)-C(4)	-62.3(3)
S(1)-C(1)-C(2)-C(3)	176.6(2)
O(1)-S(1)-C(5)-C(6)	-67.9(3)
C(1)-S(1)-C(5)-C(6)	-178.6(3)
S(1)-C(5)-C(6)-C(11)	-72.7(4)
S(1)-C(5)-C(6)-C(7)	109.9(3)
C(11)-C(6)-C(7)-C(8)	-1.1(5)
C(5)-C(6)-C(7)-C(8)	176.3(3)
C(6)-C(7)-C(8)-C(9)	0.8(5)
C(7)-C(8)-C(9)-C(10)	0.2(5)
C(8)-C(9)-C(10)-C(11)	-0.9(5)
C(7)-C(6)-C(11)-C(10)	0.5(5)
C(5)-C(6)-C(11)-C(10)	-177.0(3)
C(9)-C(10)-C(11)-C(6)	0.5(5)

Symmetry transformations used to generate equivalent atoms:

Table 2-31. Hydrogen bonds for BB73_0m [Å and °].

D-H...A	d(D-H)	d(H...A)	d(D...A)	<(DHA)
O(2)-H(2)...O(1)#1	0.84	1.95	2.786(3)	170.9

Symmetry transformations used to generate equivalent atoms:
#1 x+1,y,z
Space Group P21
Wavelength 1.54178
Flack x 0.03
Flack (su) . 0.02

Table 2-31 (cont'd)

Bijvoet Pairs 776
Coverage ... 83.7
DiffCalcMax. 152.30
Outlier Crit 304.59
Sigma Crit.. 0.25
Select Pairs 515
Number Plus 425
Number Minus 90
Aver. Ratio 1.105
RC 1.085

Normal Prob. Plot
Sample Size. 773
Corr. Coeff. 0.985
Intercept .. 0.181
Slope 1.192

Bayesian Statistics
Type ..... Gaussian
Select Pairs 773
P2(true).... 1.000
P3(true).... 1.000
P3(rac-twin) 0.0E+00
P3(false) .. 0.0E+00
G 1.0824
G (su) 0.0314
Hooft y .... -0.041
Hooft (su) . 0.016

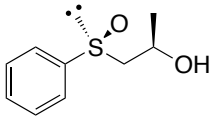

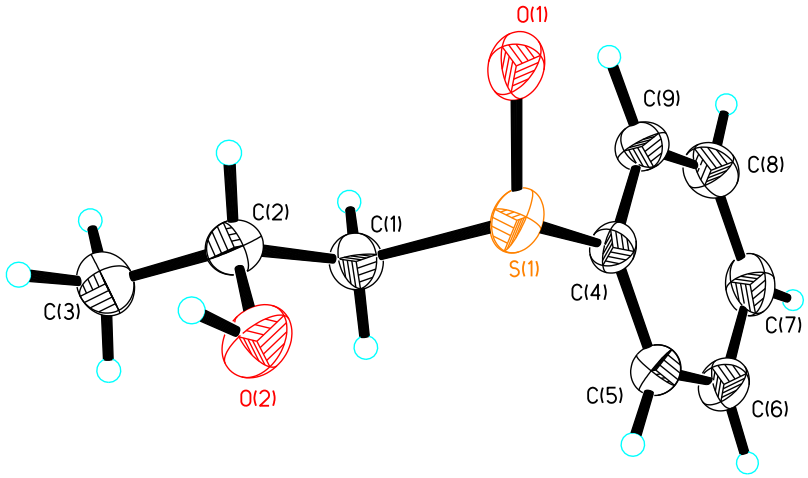

Table 2-32. Crystal data and structure refinement for BB42_0m.

Identification code	bb42_0m	
Empirical formula	C9 H12 O2 S	
Formula weight	184.25	
Temperature	173(2) K	
Wavelength	1.54178 Å	
Crystal system	Orthorhombic	
Space group	P 21 21 21	
Unit cell dimensions	a = 5.48550(10) Å	a= 90°.
	b = 8.32920(10) Å	b= 90°.
	c = 20.4080(4) Å	g = 90°.
Volume	932.44(3) $Å^3$	
Z	4	
Density (calculated)	1.312 Mg/m^3	
Absorption coefficient	2.743 mm^{-1}	
F(000)	392	
Crystal size	0.33 x 0.20 x 0.08 mm^3	
Theta range for data collection	4.33 to 67.86°.	
Index ranges	-6<=h<=6, -9<=k<=9, -24<=l<=24	

Table 2-32 (cont'd)

Reflections collected	6308
Independent reflections	1682 [R(int) = 0.0298]
Completeness to theta = 67.86°	99.8 %
Absorption correction	Semi-empirical from equivalents
Max. and min. transmission	0.8104 and 0.4610
Refinement method	Full-matrix least-squares on F^2
Data / restraints / parameters	1682 / 0 / 157
Goodness-of-fit on F^2	1.106
Final R indices [I>2sigma(I)]	R1 = 0.0263, wR2 = 0.0670
R indices (all data)	R1 = 0.0273, wR2 = 0.0676
Absolute structure parameter	0.029(19)
Largest diff. peak and hole	0.248 and -0.174 e.$Å^{-3}$

Table 2-33. Atomic coordinates (x 10^4) and equivalent isotropic displacement parameters ($Å^2$x 10^3)
for BB42_0m. U(eq) is defined as one third of the trace of the orthogonalized U^{ij} tensor.

	x	y	z	U(eq)
S(1)	-216(1)	7058(1)	8713(1)	33(1)
O(1)	810(3)	5749(1)	9135(1)	46(1)
O(2)	-2568(2)	9417(2)	9602(1)	42(1)
C(1)	1069(3)	8921(2)	9016(1)	32(1)
C(2)	3(3)	9332(2)	9682(1)	35(1)
C(3)	1044(4)	10907(3)	9932(1)	47(1)
C(4)	1447(3)	6988(2)	7956(1)	28(1)
C(5)	510(3)	7785(2)	7416(1)	33(1)
C(6)	1731(4)	7697(2)	6822(1)	38(1)
C(7)	3836(4)	6785(2)	6772(1)	41(1)
C(8)	4743(4)	5992(2)	7316(1)	39(1)
C(9)	3555(3)	6092(2)	7915(1)	34(1)

Table 2-34. Bond lengths [Å] and angles [°] for BB42_0m.

S(1)-O(1)	1.4991(13)
S(1)-C(4)	1.7942(16)
S(1)-C(1)	1.8128(18)
O(2)-C(2)	1.421(2)
O(2)-H(2)	0.88(2)
C(1)-C(2)	1.518(2)
C(1)-H(1A)	0.96(2)
C(1)-H(1B)	0.92(2)
C(2)-C(3)	1.519(3)
C(2)-H(2A)	0.951(18)
C(3)-H(3A)	1.01(2)
C(3)-H(3B)	0.92(3)
C(3)-H(10)	0.99(3)
C(4)-C(9)	1.379(2)
C(4)-C(5)	1.386(2)
C(5)-C(6)	1.387(2)
C(5)-H(5)	0.95(2)
C(6)-C(7)	1.386(3)
C(6)-H(6)	0.95(2)
C(7)-C(8)	1.385(3)
C(7)-H(7)	1.01(2)
C(8)-C(9)	1.388(3)
C(8)-H(8)	0.92(2)
C(9)-H(9)	1.03(2)
O(1)-S(1)-C(4)	106.24(8)
O(1)-S(1)-C(1)	106.29(8)
C(4)-S(1)-C(1)	97.14(8)
C(2)-O(2)-H(2)	102.4(17)
C(2)-C(1)-S(1)	110.40(12)
C(2)-C(1)-H(1A)	111.5(11)
S(1)-C(1)-H(1A)	106.0(12)
C(2)-C(1)-H(1B)	110.9(12)

Table 2-34 (cont'd)

S(1)-C(1)-H(1B)	104.9(12)
H(1A)-C(1)-H(1B)	113.0(17)
O(2)-C(2)-C(1)	106.92(13)
O(2)-C(2)-C(3)	111.62(15)
C(1)-C(2)-C(3)	110.52(16)
O(2)-C(2)-H(2A)	108.6(11)
C(1)-C(2)-H(2A)	109.0(10)
C(3)-C(2)-H(2A)	110.1(10)
C(2)-C(3)-H(3A)	108.8(15)
C(2)-C(3)-H(3B)	111.5(14)
H(3A)-C(3)-H(3B)	107(2)
C(2)-C(3)-H(10)	112.4(14)
H(3A)-C(3)-H(10)	104.2(18)
H(3B)-C(3)-H(10)	112(2)
C(9)-C(4)-C(5)	121.43(16)
C(9)-C(4)-S(1)	119.78(12)
C(5)-C(4)-S(1)	118.72(13)
C(4)-C(5)-C(6)	119.41(16)
C(4)-C(5)-H(5)	120.5(11)
C(6)-C(5)-H(5)	120.0(11)
C(7)-C(6)-C(5)	119.74(15)
C(7)-C(6)-H(6)	119.2(12)
C(5)-C(6)-H(6)	121.0(12)
C(8)-C(7)-C(6)	120.08(16)
C(8)-C(7)-H(7)	122.2(12)
C(6)-C(7)-H(7)	117.7(12)
C(7)-C(8)-C(9)	120.65(17)
C(7)-C(8)-H(8)	124.7(13)
C(9)-C(8)-H(8)	114.6(13)
C(4)-C(9)-C(8)	118.67(16)
C(4)-C(9)-H(9)	118.5(11)
C(8)-C(9)-H(9)	122.8(11)

Symmetry transformations used to generate equivalent atoms:

Table 2-35. Anisotropic displacement parameters ($Å^2 x\ 10^3$) for BB42_0m. The anisotropic displacement factor exponent takes the form: $-2p^2[\ h^2\ a^{*2}U^{11} + ... + 2\ h\ k\ a^*\ b^*\ U^{12}\ ]$

	U^{11}	U^{22}	U^{33}	U^{23}	U^{13}	U^{12}
S(1)	35(1)	40(1)	26(1)	-1(1)	0(1)	-9(1)
O(1)	71(1)	36(1)	29(1)	3(1)	-5(1)	-14(1)
O(2)	37(1)	61(1)	29(1)	0(1)	5(1)	2(1)
C(1)	33(1)	31(1)	33(1)	-1(1)	0(1)	-2(1)
C(2)	38(1)	35(1)	31(1)	0(1)	-3(1)	5(1)
C(3)	50(1)	41(1)	48(1)	-11(1)	-8(1)	9(1)
C(4)	30(1)	27(1)	26(1)	0(1)	-3(1)	-4(1)
C(5)	35(1)	31(1)	32(1)	-1(1)	-7(1)	1(1)
C(6)	52(1)	35(1)	28(1)	3(1)	-7(1)	-3(1)
C(7)	51(1)	40(1)	32(1)	-5(1)	6(1)	-5(1)
C(8)	34(1)	38(1)	45(1)	-2(1)	2(1)	2(1)
C(9)	33(1)	33(1)	35(1)	3(1)	-6(1)	-1(1)

Table 2-36. Hydrogen coordinates (x 10^4) and isotropic displacement parameters (Å^{2}x 10^3) for BB42_0m.

	x	y	z	U(eq)
H(2)	-3090(50)	9360(30)	10006(12)	52(6)
H(1A)	2790(40)	8750(20)	9041(9)	28(5)
H(1B)	640(40)	9680(20)	8709(9)	38(5)
H(2A)	370(30)	8490(20)	9980(8)	23(4)
H(3A)	300(50)	11150(30)	10373(12)	63(7)
H(3B)	670(50)	11740(30)	9657(11)	53(6)
H(10)	2820(50)	10840(30)	10021(11)	51(6)
H(5)	-910(40)	8420(20)	7455(9)	28(5)
H(6)	1180(40)	8290(20)	6451(10)	36(5)
H(7)	4700(40)	6760(30)	6335(11)	53(6)
H(8)	6120(50)	5350(30)	7317(10)	46(6)
H(9)	4170(40)	5510(20)	8330(9)	39(5)

Table 2-37. Torsion angles [°] for BB42_0m.

O(1)-S(1)-C(1)-C(2)	-70.31(14)
C(4)-S(1)-C(1)-C(2)	-179.59(12)
S(1)-C(1)-C(2)-O(2)	-57.38(16)
S(1)-C(1)-C(2)-C(3)	-179.05(13)
O(1)-S(1)-C(4)-C(9)	-12.90(15)
C(1)-S(1)-C(4)-C(9)	96.42(14)
O(1)-S(1)-C(4)-C(5)	164.22(13)
C(1)-S(1)-C(4)-C(5)	-86.46(14)
C(9)-C(4)-C(5)-C(6)	-0.8(2)
S(1)-C(4)-C(5)-C(6)	-177.84(12)
C(4)-C(5)-C(6)-C(7)	1.5(2)
C(5)-C(6)-C(7)-C(8)	-1.3(3)
C(6)-C(7)-C(8)-C(9)	0.4(3)
C(5)-C(4)-C(9)-C(8)	-0.2(2)
S(1)-C(4)-C(9)-C(8)	176.87(13)
C(7)-C(8)-C(9)-C(4)	0.4(3)

Symmetry transformations used to generate equivalent atoms:

Table 2-38. Hydrogen bonds for BB42_0m [Å and °].

D-H...A	d(D-H)	d(H...A)	d(D...A)	<(DHA)
O(2)-H(2)...O(1)#1	0.88(2)	1.86(2)	2.7311(17)	179(2)

Symmetry transformations used to generate equivalent atoms:
#1 x-1/2,-y+3/2,-z+2
Space Group P212121
Wavelength 1.54178
Flack x 0.029
Flack (su) . 0.019

Table 2-38 (cont'd)

Bijvoet Pairs 662
Coverage ... 98.5
DiffCalcMax. 162.95
Outlier Crit 325.90
Sigma Crit.. 0.25
Select Pairs 551
Number Plus 484
Number Minus 67
Aver. Ratio 0.920
RC 0.892

Normal Prob. Plot
Sample Size. 662
Corr. Coeff. 0.999
Intercept .. 0.078
Slope 0.809

Bayesian Statistics
Type ..... Gaussian
Select Pairs 662
P2(true).... 1.000
P3(true).... 1.000
P3(rac-twin) 0.0E+00
P3(false) .. 0.0E+00
G 0.8925
G (su) 0.0242
Hooft y 0.054
Hooft (su). 0.012

REFERENCES

References.

1. (a) Huang, X. F.; Borhan, B.; Rickman, B. H.; Nakanishi, K.; Berova, N., Zinc porphyrin tweezer in host-guest complexation: Determination of absolute configurations of primary monoamines by circular dichroism. *Chemistry-a European Journal* **2000,** *6* (2), 216-224; (b) Huang, X. F.; Nakanishi, K.; Berova, N., Porphyrins and metalloporphyrins: Versatile circular dichroic reporter groups for structural studies. *Chirality* **2000,** *12* (4), 237-255; (c) Huang, X. F.; Rickman, B. H.; Borhan, B.; Berova, N.; Nakanishi, K., Zinc porphyrin tweezer in host-guest complexation: Determination of absolute configurations of diamines, amino acids, and amino alcohols by circular dichroism. *Journal of the American Chemical Society* **1998,** *120* (24), 6185-6186; (d) Huang, X. F.; Borhan, B.; Berova, N.; Nakanishi, K., UV-vis spectral changes in the binding of acyclic diamines with a zinc porphyrin tweezer. *Journal of the Indian Chemical Society* **1998,** *75* (10-12), 725-728.

2. Proni, G.; Pescitelli, G.; Huang, X. F.; Nakanishi, K.; Berova, N., Magnesium tetraarylporphyrin tweezer: A CD-sensitive host for absolute configurational assignments of alpha-chiral carboxylic acids. *Journal of the American Chemical Society* **2003,** *125* (42), 12914-12927.

3. Yang, Q.; Olmsted, C.; Borham, B., Absolute stereochemical determination of chiral carboxylic acids. *Organic Letters* **2002,** *4* (20), 3423-3426.
4. Tanasova, M.; Vasileiou, C.; Olumolade, O. O.; Borhan, B., Enhancement of Exciton Coupled Circular Dichroism with Sterically Encumbered Bis-Porphyrin Tweezers. *Chirality* **2009,** *21* (3), 374-382.

5. Li, X.; Tanasova, M.; Vasileiou, C.; Borhan, B., Fluorinated porphyrin tweezer: A powerful reporter of absolute configuration for erythro and threo diols, amino alcohols, and diamines. *Journal of the American Chemical Society* **2008,** *130* (6), 1885-1893.

6. Li, X.; Borhan, B., Prompt Determination of Absolute Configuration for Epoxy Alcohols via Exciton Chirality Protocol. *Journal of the American Chemical Society* **2008,** *130* (48), 16126-+.

7. Li, X., PhD Thesis. **2009**.

8. (a) Oppolzer, W., Asymmetric diels-alder and ene reactions in organic-synthesis. *Angewandte Chemie-International Edition in English* **1984,** *23* (11), 876-889; (b) Fujita, M.; Hiyama, T., Highly diastereocontrolled reduction of ketones by means of hydrosilanes - practical synthesis of optically-active 1,2-diols and 2-amino alcohols of threo or erythro configuration. *Journal of the American Chemical Society* **1984,** *106* (16), 4629-4630; (c) Kingston, D. G. I.; Chaudhary, A. G.; Chordia, M. D.; Gharpure, M.; Gunatilaka, A. A. L.; Higgs, P. I.; Rimoldi, J. M.; Samala, L.; Jagtap, P. G.; Giannakakou, P.; Jiang, Y. Q.; Lin, C. M.; Hamel, E.; Long, B. H.; Fairchild, C. R.; Johnston, K. A., Synthesis and biological evaluation of 2-acyl analogues of paclitaxel

(Taxol). *Journal of Medicinal Chemistry* **1998,** *41* (19), 3715-3726; (d) Chaudhary, A. G.; Kingston, D. G. I., Synthesis of 10-deacetoxytaxol and 10-deoxytaxotere. *Tetrahedron Letters* **1993,** *34* (31), 4921-4924; (e) Gala, D.; DiBenedetto, D. J.; Clark, J. E.; Murphy, B. L.; Schumacher, D. P.; Steinman, M., Preparations of antifungal Sch 42427/SM 9164: Preparative chromatographic resolution, and total asymmetric synthesis via enzymatic preparation of chiral alpha-hydroxy arylketones. *Tetrahedron Letters* **1996,** *37* (5), 611-614; (f) Dallavalle, S.; Nannei, R.; Merlini, L.; Bava, A.; Nasini, G., A synthetic approach to sporotricale methylether. *Synlett* **2005,** (17), 2676-2678.

9. (a) Hansen, K. B.; Rabbat, P.; Springfield, S. A.; Devine, P. N.; Grabowski, E. J. J.; Reider, P. J., Asymmetric synthesis of cis-aminochromanol. *Tetrahedron Letters* **2001,** *42* (50), 8743-8745; (b) Ghosh, A. K.; Bilcer, G.; Schiltz, G., Syntheses of FDA approved HIV protease inhihitors. *Synthesis-Stuttgart* **2001,** (15), 2203-2229; (c) Davies, I. W.; Taylor, M.; Marcoux, J. F.; Matty, L.; Wu, J.; Hughes, D.; Reider, P. J., Stereoselective hydrogen bromide-promoted hydrogenation of an alpha-hydroxyoxime. *Tetrahedron Letters* **2000,** *41* (42), 8021-8025; (d) Bava, A.; Dallavalle, S.; Fronza, G.; Nasini, G.; de Pava, O. V., Absolute configuration of sporotricale and structure of 6-hydroxysporotricale. *Journal of Natural Products* **2006,** *69* (12), 1793-1795.

10. List, B.; Pojarliev, P.; Castello, C., Proline-catalyzed asymmetric aldol reactions between ketones and alpha-unsubstituted aldehydes. *Organic Letters* **2001,** *3* (4), 573-575.

11. Holton, R. A.; Kim, H. B.; Somoza, C.; Liang, F.; Biediger, R. J.; Boatman, P. D.; Shindo, M.; Smith, C. C.; Kim, S. C.; Nadizadeh, H.; Suzuki, Y.; Tao, C. L.; Vu, P.; Tang, S. H.; Zhang, P. S.; Murthi, K. K.; Gentile, L. N.; Liu, J. H., First total synthesis of taxol .2. completion of the c-ring and d-ring. *Journal of the American Chemical Society* **1994,** *116* (4), 1599-1600.

12. Dale, J. A.; Mosher, H. S., Nuclear magnetic-resonance enantiomer reagents - configurational correlations via nuclear magnetic-resonance chemical-shifts of diastereomeric mandelate, o-methylmandelate, and alpha-methoxy-alpha-trifluoromethylphenylacetate (mtpa) esters. *Journal of the American Chemical Society* **1973,** *95* (2), 512-519.

13. (a) Momiyama, N.; Yamamoto, H., Catalytic enantioselective synthesis of alpha-aminooxy and alpha-hydroxy ketone using nitrosobenzene. *Journal of the American Chemical Society* **2003,** *125* (20), 6038-6039; (b) Momiyama, N.; Yamamoto, H., Catalytic enantioselective synthesis of alpha-aminooxy and alpha-hydroxy ketone using nitrosobenzene (vol 105, pg 6038, 2003). *Journal of the American Chemical Society* **2004,** *126* (20), 6498-6498.

14. (a) Tang, Y. Q.; Sattler, I.; Grabley, S.; Feng, X. Z.; Thiericke, R., Streptoketol A and B, new secondary metabolites with DNA-binding properties. *Natural Product Letters* **2000,** *14* (5), 341-348; (b) Yang, C.-H.; Chen, J.-W.; Li, Q.; Peng, K.; Pan, X.-F.; Cui, Y.-X., Determination of absolute configuration of alpha-hydroxy ketones using NMR. *Chemical Journal of Chinese Universities-Chinese* **2006,** *27* (7), 1295-1297.

15. Tsuda, Y.; Nunozawa, T.; Nitta, K.; Yamamoto, Y., Utilization of sugars in organic-synthesis .3. stereochemical correlation of dihydroxy-beta-diketone and trihydroxy-beta-diketone fungal metabolites, (-)-terredionol and terremutin hydrate, with sugar alcohols - the absolute-configuration of (-)-terredionol. *Chemical & Pharmaceutical Bulletin* **1980,** *28* (3), 920-925.

16. Ishii, H.; Chen, Y. H.; Miller, R. A.; Karady, S.; Nakanishi, K.; Berova, N., Chiral recognition of cyclic alpha-hydroxyketones by CD-sensitive zinc tetraphenylporphyrin tweezer. *Chirality* **2005,** *17* (6), 305-315.

17. (a) Evans, D. A.; Dart, M. J.; Duffy, J. L.; Yang, M. G., A stereochemical model for merged 1,2- and 1,3-asymmetric induction in diastereoselective Mukaiyama aldol addition reactions and related processes. *Journal of the American Chemical Society* **1996,** *118* (18), 4322-4343; (b) List, B.; Lerner, R. A.; Barbas, C. F., Proline-catalyzed direct asymmetric aldol reactions. *Journal of the American Chemical Society* **2000,** *122* (10), 2395-2396.

18. (a) Schaus, S. E.; Brandes, B. D.; Larrow, J. F.; Tokunaga, M.; Hansen, K. B.; Gould, A. E.; Furrow, M. E.; Jacobsen, E. N., Highly selective hydrolytic kinetic resolution of terminal epoxides catalyzed by chiral (salen)Co(III) complexes. Practical synthesis of enantioenriched terminal epoxides and 1,2-diols. *Journal of the American Chemical Society* **2002,** *124* (7), 1307-1315; (b) Tokunaga, M.; Larrow, J. F.; Kakiuchi, F.; Jacobsen, E. N., Asymmetric catalysis with water: Efficient kinetic resolution of terminal epoxides by means of catalytic hydrolysis. *Science* **1997,** *277* (5328), 936-938.

19. Delazerda, J.; Barak, G.; Sasson, Y., Selective monoetherification and monoesterification of diols and diacids under phase-transfer conditions. *Tetrahedron* **1989,** *45* (5), 1533-1536.

20. Xiao, M.; Ye, J.; Zhang, Y.; Huang, Y., Reaction Characteristics of Asymmetric Synthesis of (2S,5S)-2,5-Hexanediol Catalyzed with Baker's Yeast Number 6. *Chinese Journal of Chemical Engineering* **2009,** *17* (3), 493-499.

21. (a) Zhu, Z.; Cardin, C. J.; Gan, Y.; Colquhoun, H. M., Sequence-selective assembly of tweezer molecules on linear templates enables frameshift-reading of sequence information. *Nature Chemistry* **2010,** *2* (8), 653-660; (b) Leblond, J.; Petitjean, A., Molecular Tweezers: Concepts and Applications. *Chemphyschem* **2011,** *12* (6), 1043-1051; (c) Ema, T.; Misawa, S.; Nemugaki, S.; Sakai, T.; Utaka, M., New optically active diporphyrin having a chiral cyclophane as a spacer. *Chemistry Letters* **1997,** (6), 487-488.

22. (a) Skowronek, P.; Gawronski, J., A simple circular dichroism method for the determination of the absolute configuration of allylic amines. *Tetrahedron Letters* **2000,** *41* (16), 2975-2977; (b) Kurtan, T.; Nesnas, N.; Li, Y. Q.; Huang, X. F.; Nakanishi, K.; Berova, N., Chiral recognition by CD-sensitive dimeric zinc porphyrin host. 1. Chiroptical protocol for absolute configurational assignments of monoalcohols and primary monoamines. *Journal of the American Chemical Society* **2001,** *123* (25), 5962-5973.

23. Proni, G.; Pescitelli, G.; Huang, X. F.; Quraishi, N. Q.; Nakanishi, K.; Berova, N., Configurational assignment of alpha-chiral carboxylic acids by complexation to dimeric Zn-porphyrin: host-guest structure, chiral recognition and circular dichroism. *Chemical Communications* **2002,** (15), 1590-1591.

24. Tanasova, M.; Yang, Q.; Olmsted, C. C.; Vasileiou, C.; Li, X.; Anyika, M.; Borhan, B., An Unusual Conformation of alpha-Haloamides Due to Cooperative Binding with Zincated Porphyrins. *European Journal of Organic Chemistry* **2009,** (25), 4242-4253.

25. (a) Pellissier, H., Use of chiral sulfoxides in asymmetric synthesis. *Tetrahedron* **2006,** *62* (24), 5559-5601; (b) Hanquet, G.; Colobert, F.; Lanners, S.; Solladie, G., Recent developments in chiral non-racemic sulfinyl-group chemistry in asymmetric synthesis. *Arkivoc* **2003**, 328-401.

26. (a) Fernandez, I.; Khiar, N., Recent developments in the synthesis and utilization of chiral sulfoxides. *Chemical Reviews* **2003,** *103* (9), 3651-3705; (b) Holland, H. L.; Brown, F. M., Biocatalytic and chemical preparation of all four diastereomers of methionine sulfoxide. *Tetrahedron-Asymmetry* **1998,** *9* (4), 535-538.

27. Solladie, G.; Almario, A.; Dominguez, C., Asymmetric-synthesis of natural-products monitored by chiral sulfoxides. *Pure and Applied Chemistry* **1994,** *66* (10-11), 2159-2162.

28. Nowaczyk, S.; Alayrac, C.; Reboul, V.; Metzner, P.; Averbuch-Pouchot, M. T., Asymmetric thio-claisen rearrangement induced by an enantiopure alkylsulfinyl group. Unusual preference for a boat transition state in the acyclic series. *Journal of Organic Chemistry* **2001,** *66* (23), 7841-7848.

29. (a) Gurtovenko, A. A.; Anwar, J., Modulating the structure and properties of cell membranes: The molecular mechanism of action of dimethyl sulfoxide. *Journal of Physical Chemistry B* **2007,** *111* (35), 10453-10460; (b) Ternois, J.; Guillen, F.; Piacenza, G.; Rose, S.; Plaquevent, J.-C.; Coquerel, G., Towards a robust and reliable method for the reduction of functionalized sulfoxides. *Organic Process Research & Development* **2008,** *12* (4), 614-617.

30. (a) Walker, L.; Walker, M. C.; Parris, C. N.; Masters, J. R. W., Intravesical chemotherapy - combination with dimethyl-sulfoxide does not enhance cyto-toxicity invitro. *Urological Research* **1988,** *16* (4), 329-331; (b) Choi, S.; Sainz, B., Jr.; Corcoran, P.; Uprichard, S.; Jeong, H., Characterization of increased drug metabolism activity in dimethyl sulfoxide (DMSO)-treated Huh7 hepatoma cells. *Xenobiotica* **2009,** *39* (3), 205-217; (c) Yueh, M. F.; Kawahara, M.; Raucy, J., High volume bioassays to assess CYP3A4-mediated drug interactions: Induction and inhibition in a single cell line. *Drug Metabolism and Disposition* **2005,** *33* (1), 38-48.

31. Andersen, K. K., Synthesis of (+)-ethyl para-tolyl sulfoxide from (-)-menthyl (-)-para-toluenesulfinate. *Tetrahedron Letters* **1962,** (3), 93-95.

32. (a) Brunel, J. M.; Diter, P.; Duetsch, M.; Kagan, H. B., Highly enantioselective oxidation of sulfides mediated by a chiral titanium complex. *Journal of Organic Chemistry* **1995,** *60* (24), 8086-8088; (b) Mislow, K.; Green, M. M.; Raban, M., Absolute configurations of sulfoxides by asymmetric oxidation of sulfides. *Journal of the American Chemical Society* **1965,** *87* (12), 2761-&.

33. (a) Aiello, A.; Fattorusso, E.; Imperatore, C.; Luciano, P.; Menna, M.; Vitalone, R., Aplisulfamines, New Sulfoxide-Containing Metabolites from an Aplidium Tunicate: Absolute Stereochemistry at Chiral Sulfur and Carbon Atoms Assigned Through an Original Combination of Spectroscopic and Computational Methods. *Marine Drugs* **2012,** *10* (1), 51-63; (b) Andersen, K. K.; Foley, J. W.; Gaffield, W.; Papaniko.Ne; Perkins, R. I., Optically active sulfoxides . synthesis + rotatory dispersion of some diaryl sulfoxides. *Journal of the American Chemical Society* **1964,** *86* (24), 5637-&; (c) Mislow, K.; Green, M. M.; Laur, P.; Chisholm, D. R., Optical rotatory dispersion and absolute configuration of dialkyl sulfoxides. *Journal of the American Chemical Society* **1965,** *87* (3), 665-&; (d) Drabowicz, J.; Dudzinski, B.; Mikolajczyk, M.; Wang, F.; Dehlavi, A.; Goring, J.; Park, M.; Rizzo, C. J.; Polavarapu, P. L.; Biscarini, P.; Wieczorek, M. W.; Majzner, W. R., Absolute configuration, predominant conformations, and vibrational circular dichroism spectra of enantiomers of n-butyl tert-butyl sulfoxide. *Journal of Organic Chemistry* **2001,** *66* (4), 1122-1129.

34. (a) Mikolajczyk, M.; Midura, W. H.; Grzejszczak, S.; Montanari, F.; Cinquini, M.; Wieczorek, M. W.; Karolakwojciechowska, J., Alpha-phosphoryl sulfoxides .8. stereochemistry of alpha-chlorination of alpha-phosphoryl sulfoxides. *Tetrahedron* **1994,** *50* (27), 8053-8072; (b) Fuller, A. L.; Aitken, R. A.; Ryan, B. M.; Slawin, A. M. Z.; Woollins, J. D., The X-Ray Structures of Sulfoxides. *Journal of Chemical Crystallography* **2009,** *39* (6), 407-415.

35. Hine, R., Crystal structure and molecular configuration of (+)-s-methyl-l-cysteine sulphoxide. *Acta Crystallographica* **1962,** *15* (JUL10), 635-&.

36. (a) Fleischer, E. B.; Green, M.; Mislow, K.; Axelrod, M., Absolute configuration of menthyl arenesulfinates. *Journal of the American Chemical Society* **1964,** *86* (16), 3395-&; (b) Hope, H.; Delacamp, U.; Homer, G. D.; Messing, A. W.; Sommer, L. H.,

Stereochemical course of grignard reactions at asymmetric sulfur. *Angewandte Chemie-International Edition* **1969,** *8* (8), 612-&; (c) Delacamp, U.; Hope, H., Crystal structure and absolute configuration of (+)-methyl para-tolyl sufoxide. *Acta Crystallographica Section B-Structural Crystallography and Crystal Chemistry* **1970,** *B 26*, 846-&.

37. Yabuuchi, T.; Kusumi, T., NMR spectroscopic determination of the absolute configuration of chiral sulfoxides via N-(methoxyphenylacetyl)sulfoximines. *Journal of the American Chemical Society* **1999,** *121* (45), 10646-10647.

38. (a) Pirkle, W. H.; Beare, S. D., Optically active solvents in nuclear magnetic resonance spectroscopy .9. direct determinations of optical purities and correlations of absolute configurations of alpha-amino acids. *Journal of the American Chemical Society* **1969,** *91* (18), 5150-&; (b) Pirkle, W. H.; Beare, S. D.; Muntz, R. L., Optically active solvents for nuclear magnetic resonance .x. enantiomeric nonequivalence of sulfinamides, sulfinates, sulfites, thiosulfinates, phosphine oxides, and amine oxides. *Journal of the American Chemical Society* **1969,** *91* (16), 4575-&.

39. (a) Buist, P. H.; Marecak, D. M., Stereochemical analysis of a quasisymmetrical dialkyl sulfoxide obtained by a diverted biodehydrogenation reaction. *Journal of the American Chemical Society* **1991,** *113* (15), 5877-5878; (b) Buist, P. H.; Marecak, D. M., Stereochemical analysis of sulfoxides obtained by diverted desaturation. *Journal of the American Chemical Society* **1992,** *114* (13), 5073-5080.

40. Deshmukh, M.; Dunach, E.; Juge, S.; Kagan, H. B., A convenient family of chiral shift-reagents for measurement of enantiomeric excesses of sulfoxides. *Tetrahedron Letters* **1984,** *25* (32), 3467-3470.

41. Calligaris, M.; Carugo, O., Structure and bonding in metal sulfoxide complexes. *Coordination Chemistry Reviews* **1996,** *153*, 83-154.

42. (a) Cotton, F. A.; Francis, R., SULFOXIDES AS LIGANDS .1. A preliminary survey of methyl sulfoxide complexes. *Journal of the American Chemical Society* **1960,** *82* (12), 2986-2991; (b) Meek, D. W.; Straub, D. K.; Drago, R. S., Transition metal ion complexes of dimethyl sulfoxide. *Journal of the American Chemical Society* **1960,** *82* (23), 6013-6016.

43. Drago, R. S.; Meek, D., Infrared spectra of some dimethyl sulfoxide complexes. *Journal of Physical Chemistry* **1961,** *65* (8), 1446-&.

Chapter 3

Determination of Absolute Stereochemistry for Compounds with One Site of Attachment

3-1 Background

3-1.1 Design of MAPOL

As seen in previous chapters, a key challenge facing porphyrin tweezer systems is their use in evaluation of mono coordinating compounds such as carboxylic acids, primary and secondary amines and alcohols. These compounds cannot be directly used in stereo-determination with porphyrin tweezers because porphyrin tweezer systems require the substrates to have two coordination sites in order to form a sandwich structure with the tweezer. Substrates with one binding site can only coordinate to one metalloporphyrin and cannot form the sandwich complex. Therefore, there is no chiral induction into the porphyrin tweezer and no ECCD is observed, hence they cannot be studied in this way.

Conventional approaches to circumvent this limitation involve derivatization of the substrates with "carrier" molecules, (usually small molecules containing nitrogen functionalities) in order to provide the requisite second coordination site.[1] This is not always feasible if the substrates are in short supply as in the case of natural products. Furthermore, addition of synthetic steps in order to install the carrier, and then assign the absolute stereochemistry can prove impractical and time consuming. We have been investigating the design of a host system that can be used for the assignment of absolute configuration of compounds with one site of attachment without the need for chemical derivatization in a fast and convenient manner via exciton coupled circular dichroism.

Information contained in one molecule can be transmitted to another molecule through intermolecular forces. This is seen in processes such as gene transcription, feedback inhibition

and allosteric control. Chiral induction, where a chiral molecule induces chirality in an achiral molecule, is one such process.[1-3] Our group has extensively studied chiral induction in zincated porphyrin tweezers as hosts for chiral guest molecules.[4] In these systems, the chiral information from guest molecules is transmitted to the host tweezer systems upon coordination of the chiral guests to the metallated porphyrin centers; this is ultimately observed as an ECCD signal and enables the assignment of absolute stereochemistry of the bound guests. The information transmission process from the chiral guest to the host comprises of two main processes. First is the complex formation, and second a number of dynamic processes associated with formation of the complex, such as chemical reactions or conformational changes of the interacting molecules. Unlike the porphyrin tweezer systems where the complex formation occurs via metal coordination, complex formation by hydrogen bonding has not been extensively investigated for application in the study of absolute stereochemical assignment using ECCD. With the design of a proper host, it is hypothesized that any molecule capable of hydrogen-bonding could potentially be studied using this system. More importantly, if designed well, mono coordinating compounds could be evaluated without being derivatized.

Our foray into the area of host-guest complexation via hydrogen bonding was inspired by ongoing research in this area, specifically, biphenol systems that form hydrogen-bonding complexes with amines.[3b, 5]

It is known that 2,2'-biphenyl systems are intrinsically chiral and exist in two conformations, *P* and *M*. These two forms differ only by rotation around the central single bond (*atropisomers*). The term atropisomerism, coined by Kuhn,[4] defines isomerism caused by "freezing" the internal rotation about a single bond in a molecule.

Rotation can be hindered by substituents, but this rotation is not impossible and proceeds rapidly at room temperature[5] (Fig 3-1). By convention, a clockwise rotation or right-handed turn of the helix is considered as *P* helicity (plus) and vice versa.

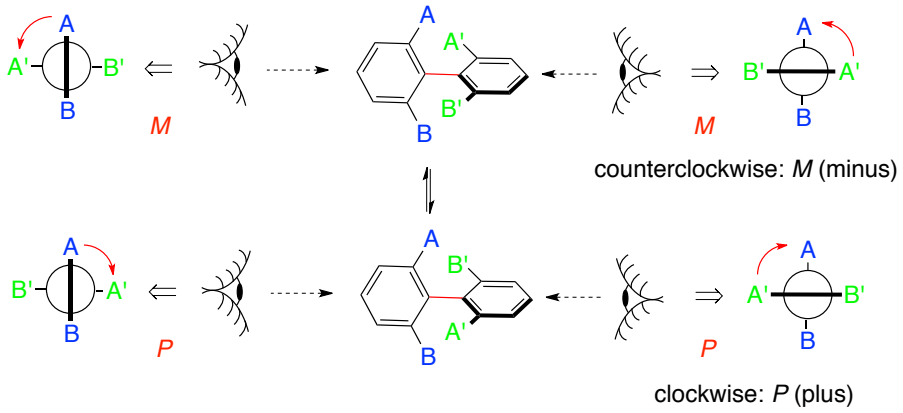

Figure 3-1. Nomenclature for assigning atropisomers. Chirality in biaryl compounds. (Priority:A>B).

In a racemic mixture, the *P* and *M* conformers exist in a 1:1 equilibrating mixture. However, this equilibrium can be disturbed by an external chiral bias, causing one population to be favored over the other as the complex interacts with chiral ligands.[2-3] Binding of these biphenyl systems by hydrogen-bonding to a chiral molecule that possesses an amino or hydroxyl functionality would proceed to favor one helical arrangement over the other. The over-population of either *P* or *M* helicity can then be detected by CD spectroscopy.

One of the initial studies on hydrogen bonding in chiral induction was done by Mizutani and co-workers, who showed that a preferential axial chirality could be induced into flexible biphenols such as **1** upon hydrogen bonding with chiral diamines.[3a] The steric interactions with

chiral *trans*-1,2-diaminocyclohexane derivatives lead to an excess of one atropisomer which is detectable by CD spectroscopy as Cotton effects. These Cotton effects could be assigned to the biphenol chromophore indicating the presence of axial chirality, *i.e.* a preferential axial sense of rotation in the biaryl compound, and they were only observable after the addition of the chiral inducer (chiral diamine).

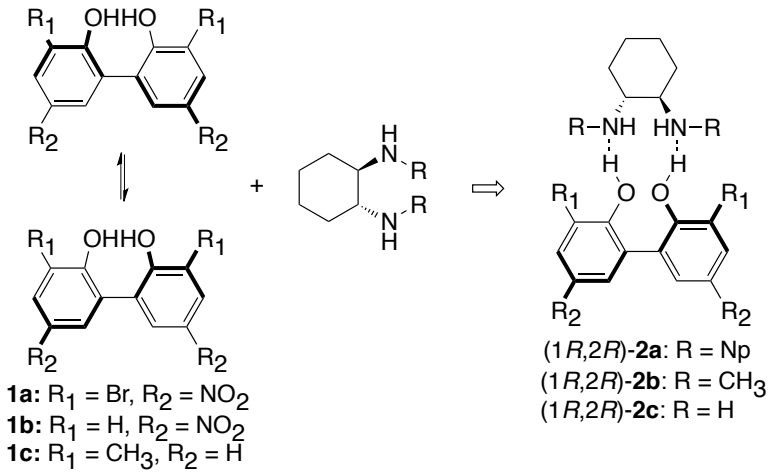

Figure 3-2. The induction of chirality of various biphenols upon binding to chiral diamines by hydrogen bonding.

They further investigated the proton transfer process upon complex formation between biphenols and chiral diamines,[3b] and its effect on the chirality transfer and induction process (Figure 3-3). They showed that at room temperature the complex exists in a 1:1 ratio of biphenol to diamine. This is because the degree of proton transfer is small and relatively independent from the amount of amine present. However, at lower temperatures (-80 °C), the complexation of two molecules of excess diamine with biphenol resulted in a higher degree of proton transfer forming a 1:2 biphenol:diamine complex, presumably of type **3a'**. Interestingly, both the 1:1 and the 1:2

complexes form well-ordered chiral supramolecular structures, accompanied by enhanced chiral induction, as evidenced by the observation of Cotton effects.

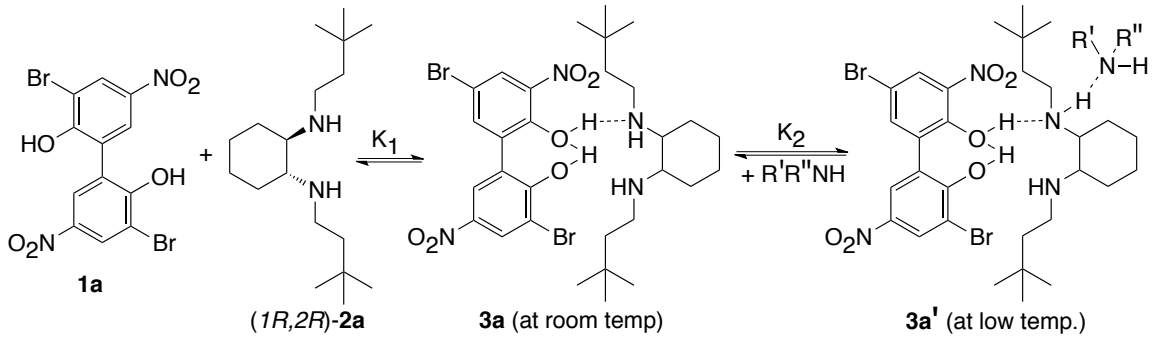

Figure 3-3. Formation of 1:1 complex between diamine **2a** and biphenol **1a** at room temperature, and ternary complex **3a'** at low temperature with excess amine.

Ishii et al. described an elegant potential application of induced atropisomerism for chiroptical probes.[2] (Figure 3-4) They synthesized a 2,2'-biphenyl-bridged bis(free base porphyrin) **4** and employed it as a chirality sensor for chiral amino alcohols. They propose that the host porphyrin system and amino alcohols form a 1:1 complex by hydrogen bonding of the amine and hydroxyl functionalities and the biphenyl unit. Upon stereo differentiation, the chiral information from the stereocenter in the amino alcohols is transferred to the host as a preferential axial twist in the biphenol unit of the host (Figure 3-4). This preferential twist was detected by the appearance of exciton-coupled Cotton effects in the CD curve that were assigned to the intense Soret band of the two porphyrin units. At higher amino alcohol concentrations (10^{-2} M), they were able to determine the absolute stereochemistry of the amino alcohols, with *R* amino alcohols yielding negative ECCD spectra and *S* amino alcohols yielding positive ECCD spectra.

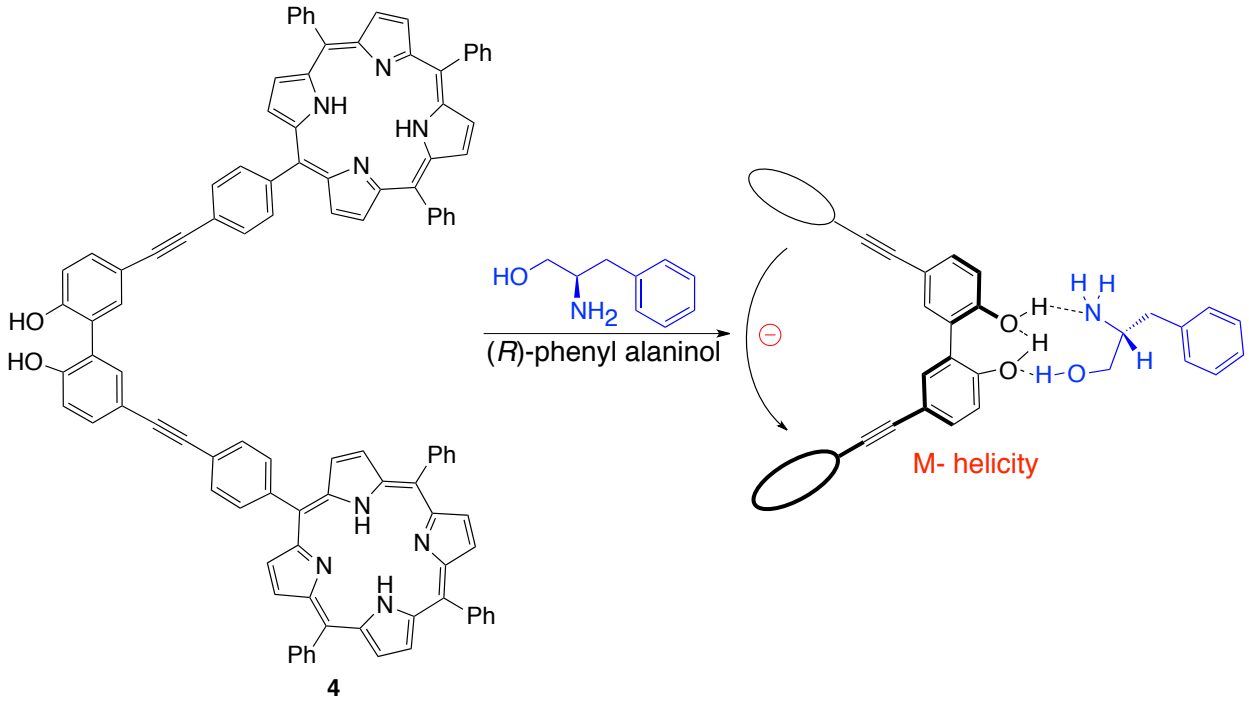

Figure 3-4. Point to axial chirality transfer from amino alcohols to 2,2'-biphenyl-bridged bis(free base porphyrin) **4** via hydrogen bonding.

As mentioned earlier, chirality amplification is of both fundamental and practical importance. It is considered a major factor in the origin of homochirality, triggered from an initial small chiral bias.[6] More importantly however, amplification of chirality is continually being applied in practical ways from asymmetric synthesis to detection of chiral compounds.[3c, 7] One growing application of chirality amplification is in liquid crystalline systems that are widely applied in chiral supramolecular assemblies, smart materials, as well as in the development of liquid crystal displays.[8]

Briefly, achiral nematic liquid crystal solvents can become chiral upon doping with small amounts of suitable dopants (usually enantiopure biphenols or biphenyls).[9] Upon formation of a

complex between host and dopant, a chiral nematic phase (also known as cholesteric phase) is formed with the transfer of molecular chirality of the dopant to the nematic phase organization. This induced chirality affects the optical as well as structural properties of the liquid crystal superstructure.[9]

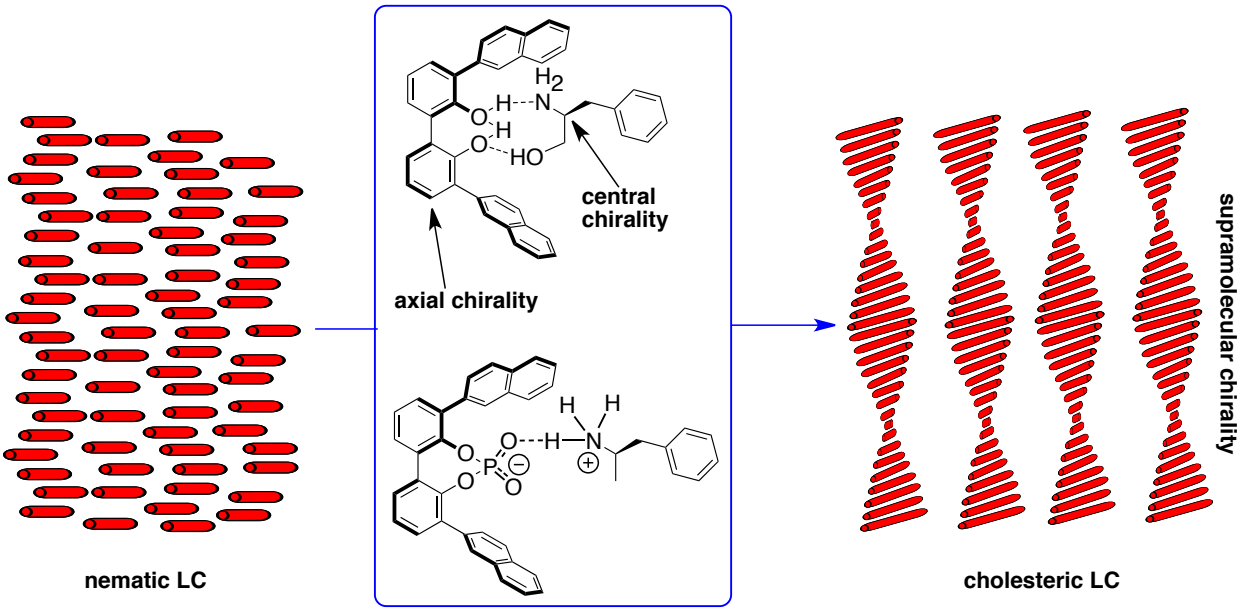

Figure 3-5. Macroscopic expression of the chirality of an amino alcohol and mono amine by a double amplification mechanism in liquid crystalline media via hydrogen bonding.

Eelkema and co-workers reported a modification of this system, enabling the use of racemic biphenols. First, they induce axial chirality to the racemic biphenols using chiral amino alcohols and mono amines.[9a] They then use this chiral complex as the dopant to induce supramolecular chirality in the liquid crystals by a double transfer of chirality from the stereogenic centers of amino alcohols or amines (point chirality) via the biphenols (axial chirality) to the liquid crystals (supramolecular chirality). From IR and ^{1}H-NMR spectroscopic

studies, they propose the formation of complexes of the type shown in Figure 3-5, between the amino alcohols or amines with the biphenyl host. In the proposed structure, the aliphatic part of the amino alcohols is situated within the binding pocket of the 3,3'-substituents of the biaryl. The 1:1 stoichiometry was obtained from Job's plot analysis.[9a, 10]

This model became key for us in designing the two proposed systems, MAPOL **9** and its phosphoric acid derivative, MAPHOS **10** (Figure 3-6). We designed these systems as host molecules to exploit hydrogen-bonding interaction, in forming ECCD active supramolecular complexes upon the addition of chiral guest molecules such as amines. We postulated that MAPOL will form complexes with amines via the OH groups. We also envisioned replacing the two hydroxyl groups with a phosphoric acid moiety. Phosphate groups have been widely used in chemistry and bio chemistry, in recognition of sugars,[11] as chiral resolving agents in the NMR-based determination of enantiomeric excess of chiral amines[12] as well as induction of chirality in helical polymers.[13] By having the phosphoric acid, MAPHOS would act as a proton donor in hydrogen bonding with chiral substrates.

It has been shown that porphyrins are ideal chromophores for ECCD host systems due to their many desirable properties such as high extinction coefficient and far removed red-shifted absorbances that would avoid interference with bound aromatic compounds.[14] Therefore MAPOL and MAPHOS were designed with free base TPP porphyrins at the 2 and 2' positions then with induction of chirality, these chromophores would interact and be responsible for an observed ECCD.[3c]

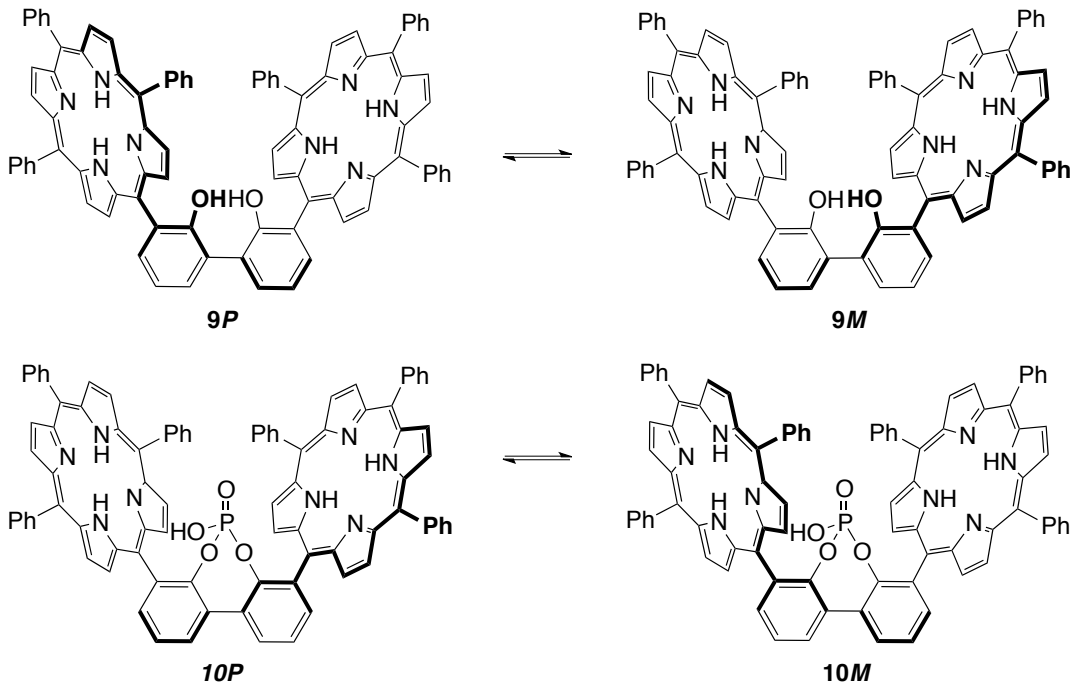

Figure 3-6. Proposed host systems for stereochemical determination of chiral molecules: MAPOL **9** and MAPHOS **10**.

We then expect molecules such as **9** and **10** to act as suitable hosts for detection of chirality by hydrogen bonding using the ECCD protocol. The hydrogen bonding idea is especially ideal, because in theory, any functional group that is capable of hydrogen-bonding could be potentially assigned using this system allowing for ECCD assignment of absolute stereochemistry of small molecules such as monoamines, carboxylic acids, amino acids and alcohols, cyanohydrins, aziridines, sugars and polymers etc. without the need for derivatization.

3-1.2 Synthesis of MAPOL

At first glance, the synthesis of MAPOL seemed very straightforward owing to the intrinsic symmetry of the molecule. We envisioned several possible disconnections for the

synthesis of MAPOL. There are several methods in the literature for the synthesis of porphyrins. The most commonly used method is McDonald's condensation procedure,[15] which consists of the acid-catalyzed condensation of pyrrole and aldehyde, followed by oxidation of the resultant porphyrinogen intermediate to give porphyrin (Figure 3-7).

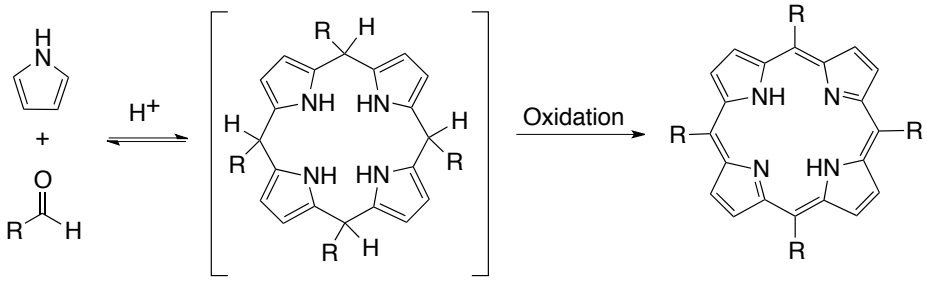

Figure 3-7. The McDonald synthesis of porphyrins.

Initially, our main concern was the low yields associated with this route, (usually yields of 7-13% is typical for one condensation). Considering that the synthesis of MAPOL using this protocol would require two such condensation steps, we expected even more dismal yields. With this in mind, we resorted to alternative routes for the synthesis.

The possible synthetic strategies we initially formulated for the synthesis of MAPOL are highlighted in Scheme 3-1A to Scheme 3-1D. One important thing to note is that we designed MAPOL to have hydrogen atoms at the *meso* positions of the porphyrin. However, because of the different reaction conditions encountered during these synthetic routes, the hydrogens were replaced with phenyl rings, to avoid complication in isolation of the unsubstituted porphyrin. It was hypothesized that these phenyl groups would not be directly involved in the stereo differentiation process, so the identity of the *meso* substituent would not be a major concern for the subsequent ECCD evaluation of small chiral molecules.

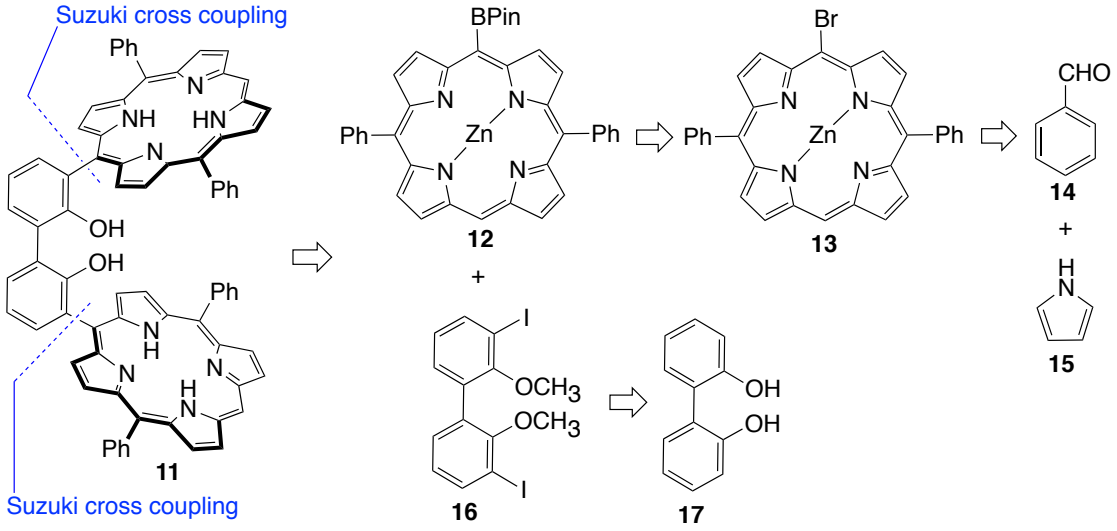

Scheme 3-1A. Retrosythetic analysis **I**. The key disconnection being between porphyrins and the biphenyl unit, utilizing a Suzuki cross coupling reaction to construct the target molecule.

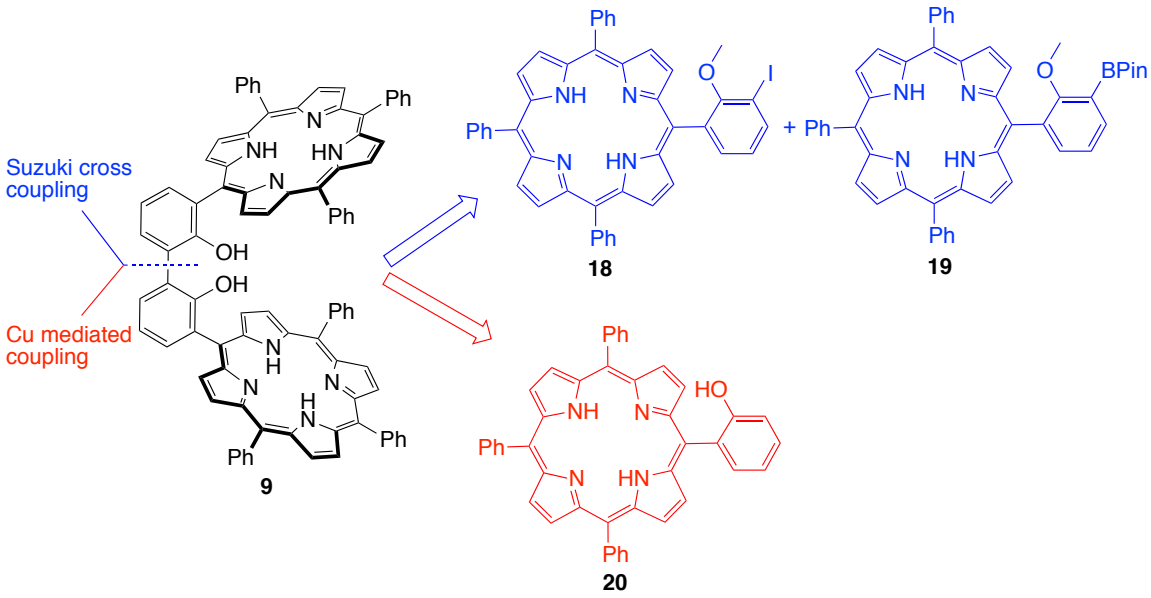

Scheme 3-1B. Retrosynthetic analysis **II**. Disconnection between the biphenyl unit. This is a symmetric disconnection whose forward synthesis could involve Suzuki cross coupling or oxidative coupling reactions.

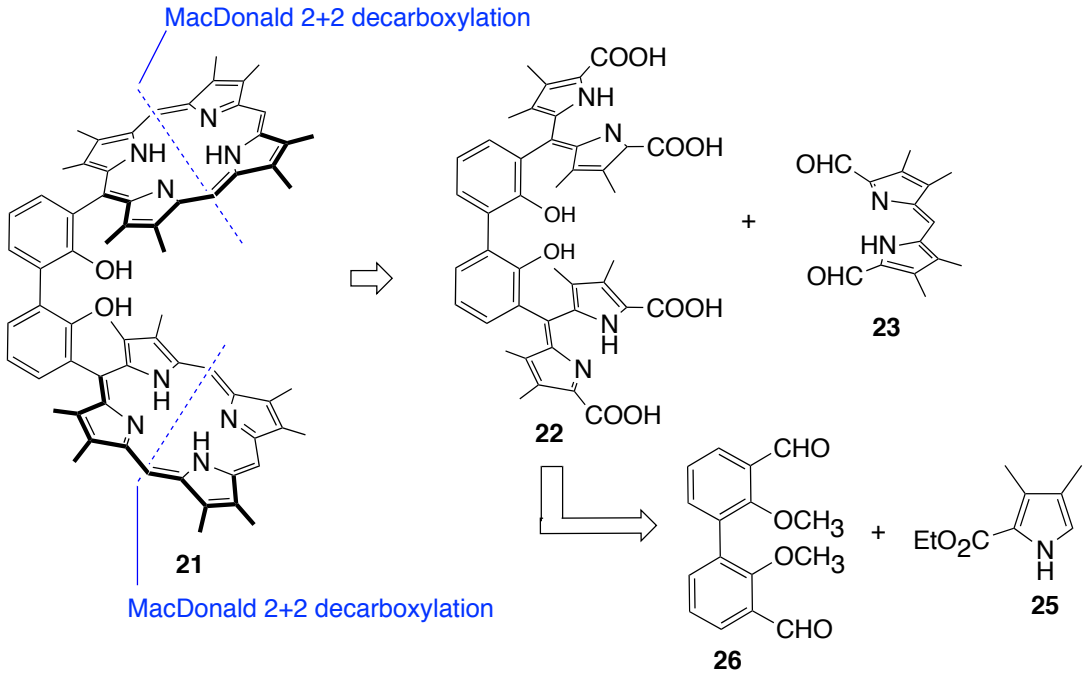

Scheme 3-1C. Retrosynthetic analysis **III**. Disconnection within the porphyrins. The forward synthesis would involve a MacDonald 2+2 condensation reaction.

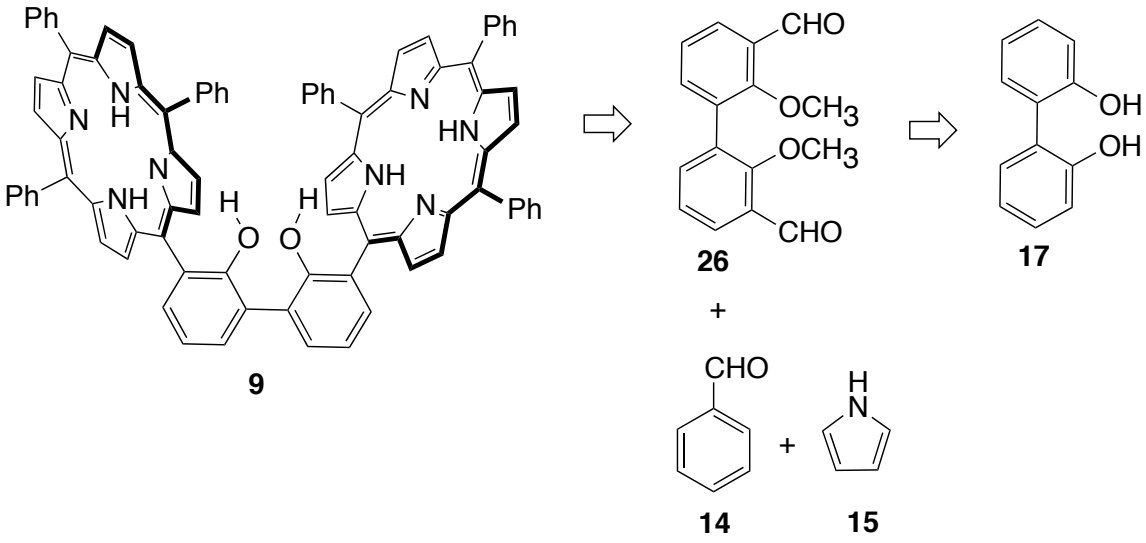

Scheme 3-1D. Retrosynthetic analysis **IV**. No key disconnection, instead, the forward synthesis would be a linear synthesis involving condensation of protected biphenyl-3,3' bisaldehyde, benzaldehyde and pyrrole.

3-1.2-A First generation approach to MAPOL via Suzuki coupling.

Scheme 3-1A shows the first generation retrosynthetic plan **I**. Here, the target molecule **11**, can be split into two parts: the porphyrin unit and the biphenol unit. The key step, a Suzuki cross coupling reaction[16] was envisioned to forge the bond between the porphyrins and biphenol units. While there are several ways to form the sp^2C-sp^2C bond between the two halves, we chose a Suzuki coupling reaction because this reaction has previously been employed in the synthesis of molecules involving porphyrin units.[24] The porphyrin unit could be easily synthesized by a condensation reaction of **14** and **15** followed by bromination to **13**, and subsequent conversion to the pinacol borane **12** via standard procedures. The bisiodo-biphenyl **16** could be synthesized in two steps from the corresponding commercially available 2,2'-biphenol, following known procedures[25] to obtain the two coupling partners.

Cross-coupling reactions have had a tremendous impact in organic synthesis.[17] The 2010 Nobel Prize in Chemistry was awarded to Richard F. Heck, Ei-ichi Negishi, and Akira Suzuki for the discovery and development of palladium catalyzed coupling reactions. The Suzuki coupling reaction was first reported in 1979 by Suzuki and Miyaura as the Pd^0 catalyzed coupling of phenylboronic acid with an aryl bromide to form a series of substituted biaryls.[18] Since its inception, the Suzuki coupling reaction has enjoyed widespread use throughout organic synthesis, due to mild reaction conditions and broad substrate compatibility. In fact, new catalyst and method development have broadened the possible applications so that the scope of the reaction partners is not restricted to arenes, but now includes alkyls, alkenyls and alkynyls. In addition, potassium trifluoroborate salts and organoboranes or boronate esters may be used in

place of boronic acids. Furthermore, organotriflates, iodides, and chlorides can be employed in place of the bromide.[16b] The Suzuki reaction is an extremely versatile and useful reaction for the assembly of biaryl systems, finding wide application in the areas of natural product synthesis, and drug development within academia and the pharmaceutical industry. Figure 3-8 shows an example of two natural products, Korupensamine A and Hippadine, synthesized using a Suzuki reaction as the key step in the formation of the sp^2C-sp^2C bonds indicated.[19] In the synthesis of hippadine for example, the Suzuki coupling works, when other coupling (Kumada and Negishi) reactions failed to provide the desired product.[20]

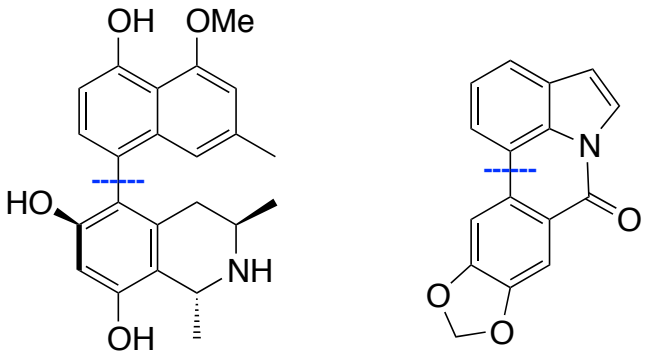

Figure 3-8. Natural products Korupensamine A and Hippadine synthesized by employing Suzuki coupling reaction as the key step.

Suzuki cross-coupling reactions have been widely applied in reactions with porphyrin units, typically proceeding in high yields.[21] One interesting example of Suzuki cross coupling with a porphyrin as one coupling partner was reported by Chng et al. in their synthesis of di-

trimesitylporphyrin xanthene (DTMPX) **30** and di-trimesitylporphyrin dibenzofuran (DTMPD) **32** (Scheme 3-2).[21e]

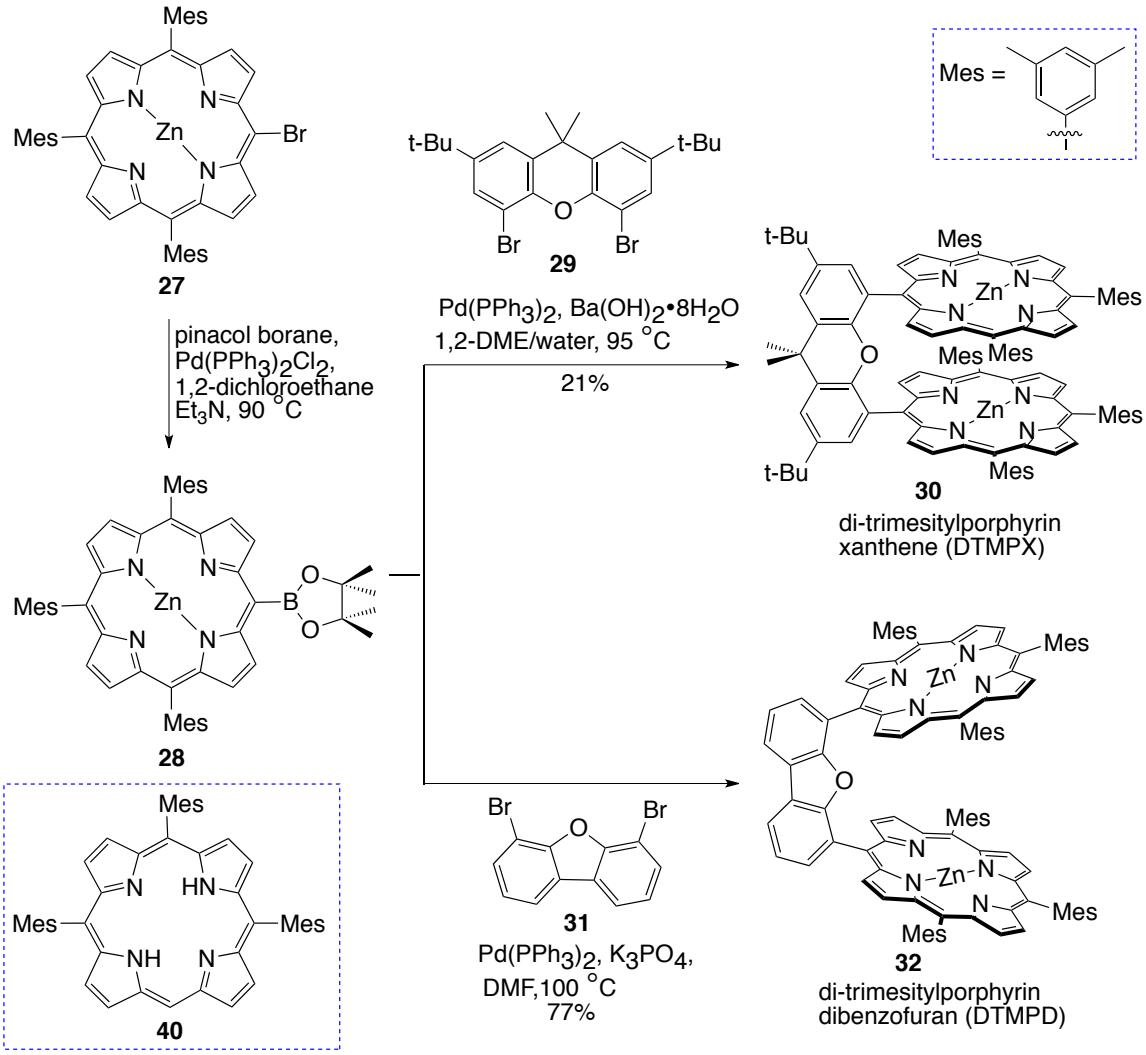

Scheme 3-2. Synthesis of DTMPX and DTMPD, employing Suzuki cross coupling reaction.

In their work, they employ the *meso*-triarylporphyrin 5,10,15-trimesitylporphyrin as the key synthon for the cross coupling approach. By regioselectively brominating **40** with *N*-bromosuccinimide in chloroform at room temperature followed by zinc insertion with

$Zn(OAc)_2 \bullet H_2O$, they are able to quantitatively obtain the zinc(II)bromoporphyrin **27**, which is smoothly converted to boronate **28** in excellent yield by using pinacol borane. This boronate porphyrin then serves as a transmetalating agent for the preparation of DTMPX **30** and DTMPD **32**.

Another elegant use of Suzuki cross coupling reaction with a porphyrin was demonstrated by Hyslop et al.[21f] who employ the boronate porphyrin **12** in the synthesis of several porphyrin-containing supramolecular assemblies **34**, **35** and **36** (Scheme 3-3).

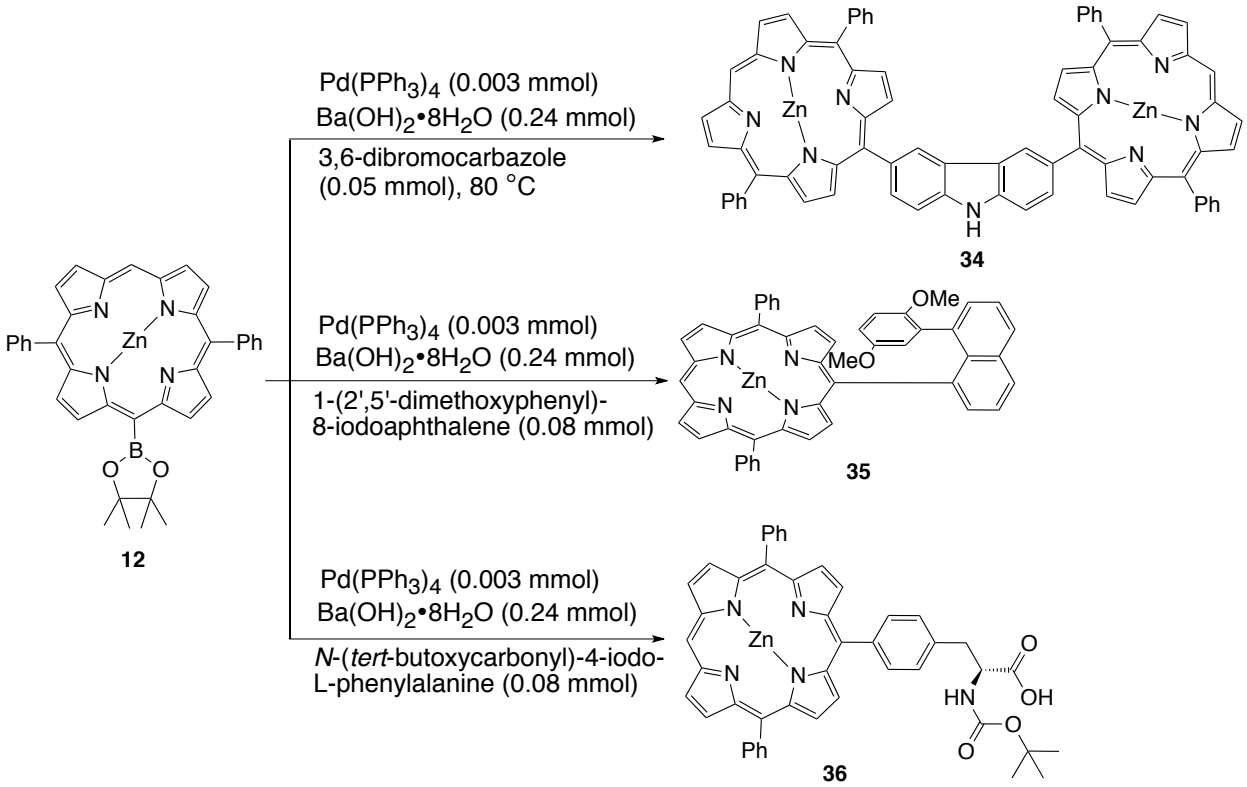

Scheme 3-3. Synthesis of several poprhyrin-containing molecules by Suzuki coupling reaction.

Encouraged by the successful use of the Suzuki cross coupling reaction in the synthesis of porphyrin systems, we set out to begin the synthesis of MAPOL **9**, by Suzuki reaction.

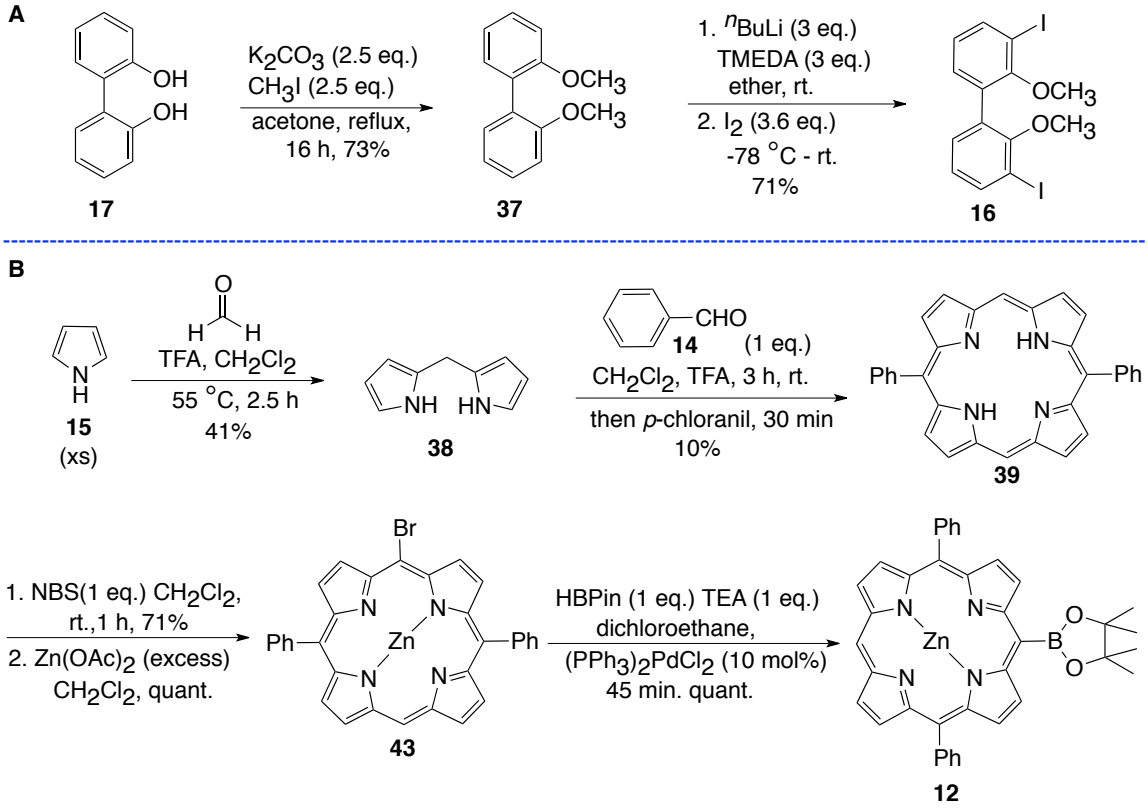

Scheme 3-4. A) Synthesis of bis-iodo biphenyl **16**. B) Synthesis of pinacol borane porphyrin **12** for use in Suzuki coupling.

As suggested by retrosynthetic analysis Scheme **I**, the forward synthesis of MAPOL can be divided into two parts: the porphyrin synthesis and the synthesis of the di-iodo biphenyl **16**. Synthesis of porphyrin begun with the synthesis of dipyrrylmethane **38**[22] which was then used in a trifluoroacetic acid catalyzed condensation with benzaldehyde, followed by oxidation with *p*-chloranil to afford 5,15-phenyl-porphyrin **39** in good yield. Treatment of **39** with NBS provided brominated porphyrin **13**. Metallation with an excess of $Zn(OAc)_2$ gave quantitative yield of the zincated porphyrin **43**, which was then borylated to give pinacol borane porphyrin **12**, for use in the Suzuki coupling.[21f] Synthesis of the bis-iodo biphenyl **16**, begun with bis methylation of

2,2'-biphenol followed by ortho-lithiation and subsequent iodination of methylated biphenol **37** in good yields (Scheme 3-4).[23] Reported procedures were followed in the synthesis of both **12** and **16**.

With the two coupling partners in hand, we set out to carry out the Suzuki coupling reaction. First, Ogoshi's conditions (Scheme 3-2) utilizing 0.5 mol % of palladium catalyst were employed (Table 3-2 entry 1). The reaction was monitored by mass spectroscopy. The reaction proceeded with very low conversion and yields, and unfortunately, the only products observed were mono-coupled biphenyl with either de-halogenation **A**, and/or retention of the second iodine **B**. (The majority of the mass was decomposed starting material). Increasing the catalyst loading to 1 mol % (entry 2) or 10 mol % (entry 3) had no effect on the reaction. We then modified the reaction conditions slightly by changing the base to potassium phosphate and the solvent to DMF. These are the conditions used by Chng et al. that gave them higher yield in their synthesis (Scheme 3-2).[21e] However, this resulted in only the de-halogenated product **A**, still in low yields. Changing the catalyst to the more air-stable $Pd(dppf)Cl_2$ under the original reaction conditions, (entry 4), only resulted in reversing the selectivity in preference to mono-coupled product, without de-iodination **B**. Again, increasing the catalyst loading to 20 mol % had no effect on the reaction outcome. Attempts to re-submit mono-coupled product **B** to a second coupling reaction resulted in decomposition of starting material.

Table 3-2. Conditions tried for Suzuki cross coupling reaction.

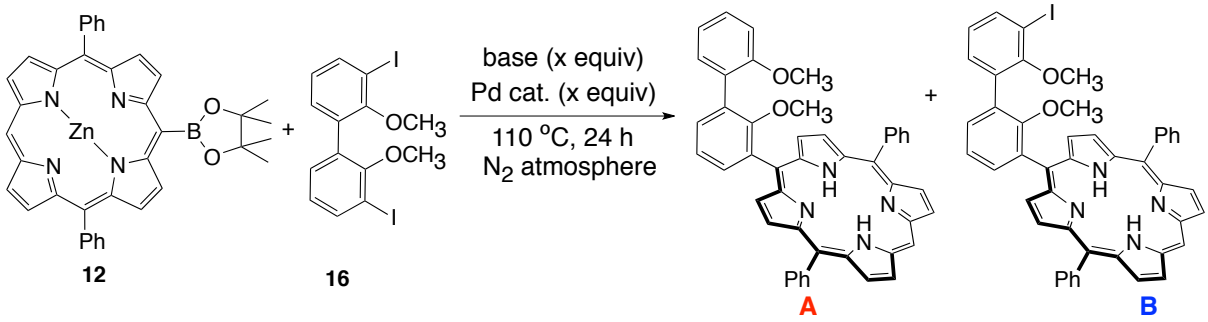

Entry	Conditions	Yield % **A**	Yield % **B**
1	$Ba(OH)_2 \cdot 8H_2O$ (6 eq.) $Pd(PPh_3)_4$, 0.5 mol% DME/H_2O 10:1	3	4
2	$Ba(OH)_2 \cdot 8H_2O$ (6 eq.) $Pd(PPh_3)_4$, 1 mol% DME/H_2O 10:1	3	3
3	$Ba(OH)_2 \cdot 8H_2O$ (6 eq.) $Pd(PPh_3)_4$, 10 mol% DME/H_2O 10:1	3	3
4	$Ba(OH)_2 \cdot 8H_2O$ (6 eq.) $Pd(dppf)Cl_2$,10 mol% DME/H_2O 10:1	0	7
5	K_2PO_4 (12 eq.) $Pd(PPh_3)_4$ (0.3 eq.) DMF	4	0
6	$Ba(OH)_2 \cdot 8H_2O$ $Pd(dppf)Cl_2$ (20 mol%) DME/H_2O 10:1	0	7
7	$Ba(OH)_2 \cdot 8H_2O$ **B** + $Pd(dppf)Cl_2$ (10 mol%) DME/H_2O 10:1	decomposition products	

All these reagents were de-gassed prior to running reaction in a Schlenk flask. We tried changing other factors like reaction times and concentration, but none of these were successful, leading to decomposition of the starting materials. Table 3-2, only shows the more successful conditions that led to formation of coupling products **A** and/or **B**.

Due to the low yields of **38** and **39**, as well as no observation of desired MAPOL under these reaction conditions, we considered the other synthetic routes.

3-1.2-B Second generation approach to MAPOL via Suzuki and oxidative coupling.

Following our second-generation retrosynthetic plan **II** described in Scheme 3-1B, we thought to assemble MAPOL in a convergent manner. There were two different approaches we could take for the synthesis. Taking advantage of the symmetry of the molecule, the main disconnection in this retrosynthetic approach cuts the biaryl motif in half. An oxidative self-coupling or a Suzuki coupling reaction could then be used to forge the bond between the two phenyl rings. Oxidative coupling unit **20** could be easily accessed from condensation of commercially available starting materials **14**, **15** and **33**, while coupling partners **19** and **18**, for use in a Suzuki coupling reaction could be obtained from conversion of **41**. In a forward sense, the two halves of MAPOL are pieced together by a C-C bond formation ortho to the hydroxyl group. In the first approach (Route **A**) the methoxy group in **41** could be used as a handle to install the iodine, providing **18**, which could then be converted to borane **19**. We could then use **18** and **19** in a Suzuki coupling reaction to forge the final bond. The second approach (Route **B**) calls for an oxidative self-coupling reaction of **20**. This route is more desirable because, provided that this coupling reaction works as expected, it would enable the synthesis of MAPOL in one step from the easy to prepare precursor **20**. The most desirable aspect of this second generation

approach is that both routes incorporate the porphyrin into the phenyl right at the beginning making them convergent routes.

Suzuki coupling approach: Route A.

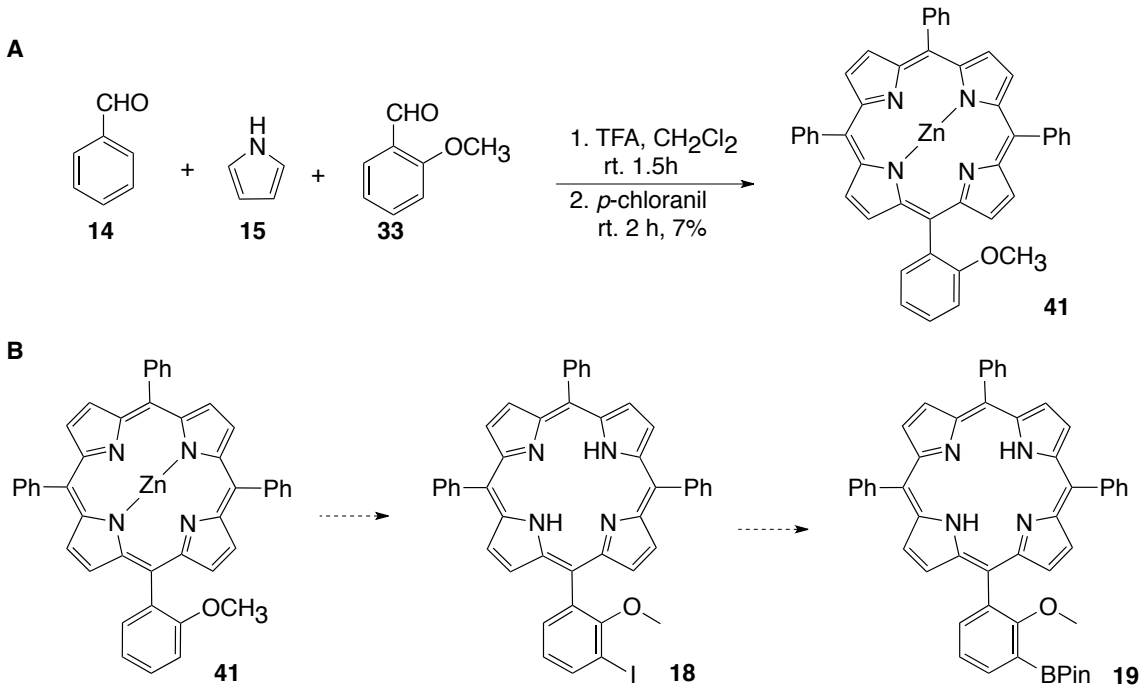

Scheme 3-5. A. Synthesis of **41**. B. Planned elaboration of **41** to **18** and **19**.

We planned to use a Suzuki coupling reaction between the two fully elaborated halves **18** and **19**. These two halves could be prepared from **41**. Porphyrin **41** was accessed in 7% yield by a TFA catalyzed condensation of **14**, **15** and **33**, followed by the *in situ* oxidation by *p*-chloranil. Elaboration of **41** is required to obtain the desired Suzuki coupling partners **18** and **19**. However, all attempts to convert **41** into iodo porphyrin **18**, which would then be further converted to **19** were unsuccessful. The only isolated product was the de-metallated starting material **42**. Despite varying the reaction conditions, **42** was the only isolated product. (Table 3-3)

Table 3-3. Attempts to synthesize **18**.

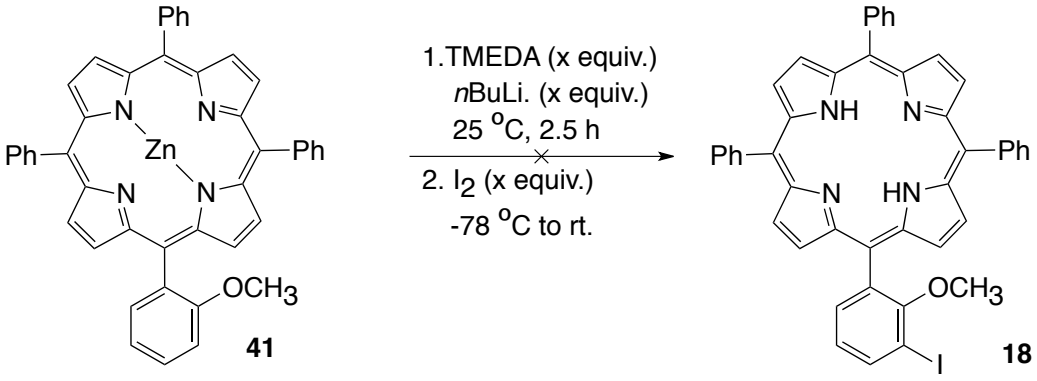

entry	conditions	yield (%)[a]
1	TMEDA (1.5 equiv.) n-BuLi (1.5 equiv.) I_2 (1.5 equiv.)	de-metallation of S.M.
2	TMEDA (2.0 equiv.) n-BuLi (2.0 equiv.) I_2 (2.0 equiv.)	de-metallation of S.M.
3	TMEDA (3.0 equiv.) n-BuLi (3.0 equiv.) I_2 (3.0 equiv.)	de-metallation of S.M.
4	TMEDA (4.0 equiv.) n-BuLi (4.0 equiv.) I_2 (4.0 equiv.)	de-metallation of S.M.
5	TMEDA (5.0 equiv.) n-BuLi (5.0 equiv.) I_2 (5.0 equiv.)	de-metallation of S.M.

[a] product determined by high resolution mass spectroscopy

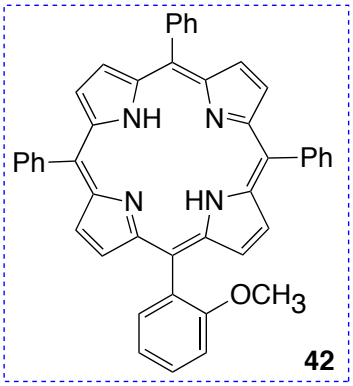

After considering the previous disappointing results with the Suzuki coupling reaction, and issues with the iodination step, we changed our approach to use oxidative coupling reaction.

Oxidative coupling approach: Route B

Oxidative coupling of 2-naphthols is a well-established method for the synthesis of binaphthols.[24] These reactions are usually carried out by treatment of naphthols with a transition metal catalyst in the presence of an oxidant such as oxygen or excess of another transition metal. Frequently employed transition metal catalysts are Fe(III) and Cu(III); although use of Mn(III), Ti(IV), V(V), and Ru(III) have also been reported.[25]

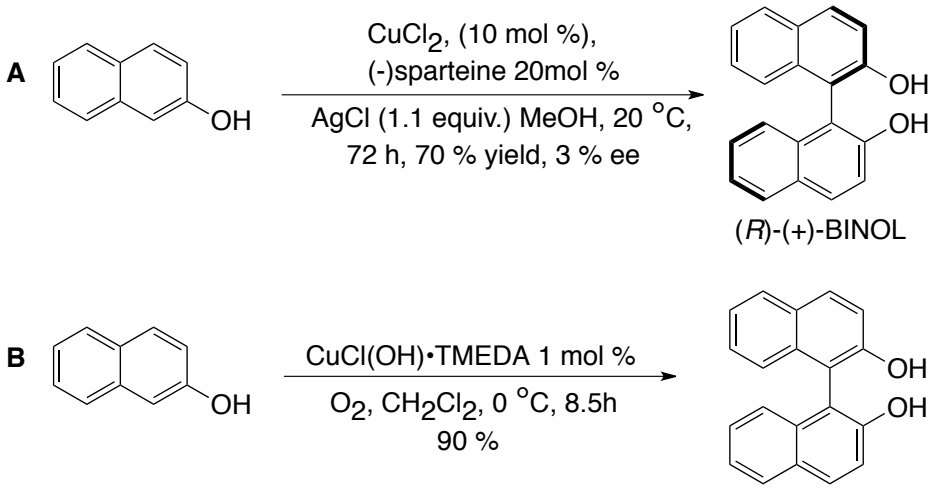

Figure 3-9. Oxidative coupling of 2-naphthol in the synthesis of BINOL. A) $CuCl_2$/(-)sparteine catalyzed system; B) CuCl(OH)•TMEDA complex as catalyst.

This type of chemistry has not been previously employed in the synthesis of porphyrin systems. Additionally, there exists the possibility of formation of multiple coupling products (ortho-ortho coupling, para-para coupling, ortho-para coupling, ortho-ether linkage and para-ether linkage). However, from a strategic sense, we wished to employ oxidative coupling reaction in the synthesis of MAPOL mainly because it would allow faster access to MAPOL

from phenol **20**. First, we synthesized BINOL using this chemistry in order to familiarize ourselves with the chemistry. Upon successful synthesis of BINOL, we then set out to employ these reaction conditions for the synthesis of MAPOL.

For all oxidative coupling reactions attempted, both the free base porphyrin **20**, as well as zincated porphyrin **43** were used. Porphyrin **20** was obtained by BBr_3 de-methylation of **41**, (which simultaneously de-metallates it) and subsequent zincation of **20** using an excess of $Zn(OAc)_2$ provided **43** (Scheme 3-6).

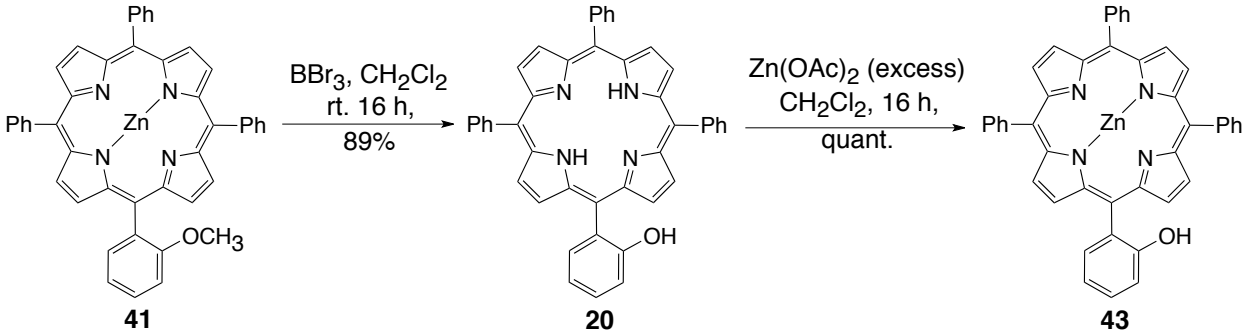

Scheme 3-6. Synthesis of porphyrin **43**.

The first conditions tried utilized CuCl with $BnNH_2$ amine ligand[50] (Table 3-4 entry 1). The reaction was carried out open to air, at room temperature. From mass spectroscopy, the reaction resulted in a single product, which turned out to be the demetallated starting material, **20**. Subsequently, the catalyst was changed to CuCl(OH)•TMEDA complex, using O_2 as the oxidant. CuCl(OH)•TMEDA complex was synthesized as shown in scheme 3-7.[26]

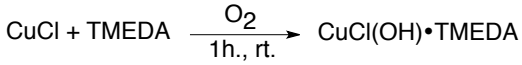

Scheme 3-7. Synthesis of catalyst.

The catalyst loading was gradually increased from 1 mol % to 20 mol %. However, these reactions also resulted in de-metallation of the starting porphyrin when **43** was used. When free porphyrin **20** was used, only unchanged starting material was isolated. In a final effort using CuCl(OH)•TMEDA complex, a stoichiometric amount of catalyst was used. Unfortunately, this did not have a positive effect on the reaction either, providing the same results as before (entries 2, 3, 4 and 5). Next we decided to change the copper salt as well as the amine ligand (entry 6).[27] The reaction of **20** as well as **43**, in the presence of 10 mol % of this catalyst gave some promising results, yielding trace amounts of desired product (detected by mass spectroscopy) after heating at 40 °C in dichloroethane for 9 days. The majority of the mass was recovered starting material **20** and so we decided to push the reaction. Attempts to optimize the reaction conditions, like longer reaction times (longer than 9 days), (entry10) using oxygen balloon as opposed to running the reaction open to air, increasing the catalyst loading or increasing temperature led to decomposition of starting material and no desired product. Using freshly prepared CuI and CuCl were also unsuccessful.

Table 3-4. Oxidative coupling conditions for the synthesis of MAPOL.

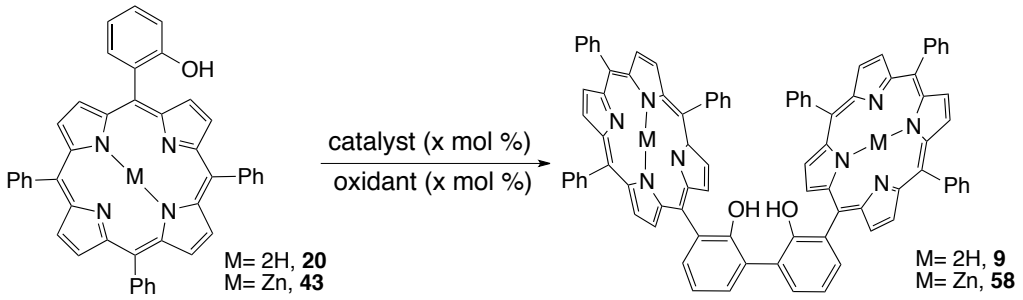

M	conditions	oxidant	time	temp	yield
2H	$CuCl_2$, (1 equiv.) $BnNH_2$ (2 equiv.) MeOH	air	24 h	20 °C	rec. S.M. quant.
Zn	"	"	"	"	rec. **20** quant.
2H	CuCl(OH)•TMEDA (1 mol %), CH_2Cl_2	O_2	8.5 h	0 °C	rec. S.M. quant.
Zn	"	O_2	"	"	rec. **20** quant.
2H	CuCl(OH)•TMEDA (1 mol %), CH_2Cl_2	O_2	20 h	rt.	rec. S.M. quant.
Zn	"	O_2	"	"	rec. **20** quant.
2H	CuCl(OH)•TMEDA (10 mol %), CH_2Cl_2	O_2	20 h	rt.	rec. S.M. quant.
Zn	"	O_2	"	"	rec. **20** quant.
2H	CuCl(OH)•TMEDA (20 mol %), CH_2Cl_2	O_2	20 h	rt.	rec. S.M. quant.
Zn	"	O_2	"	"	rec. **20** quant.
Zn	CuI (10 mol %) L*(10 mol %) DCE	O_2	9 d	40 °C	trace
Zn	CuI (10 mol %) L* (10 mol %) DCE	O_2	> 9 d	40 °C	decomp.

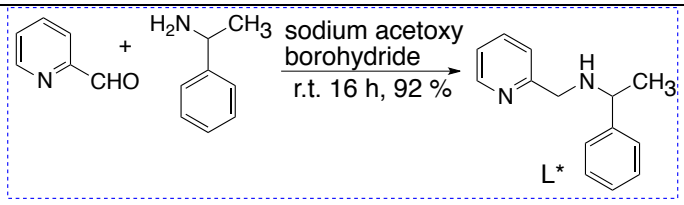

In one final attempt to employ oxidative coupling reaction for the synthesis of MAPOL, we were inspired by an elegant modification reported by Wulff and co-workers (Figure 3-10). In the final step of the synthesis of VANOL and VAPOL, they employ an oxidative phenol coupling of the respective monomers in two ways: first in the small scale synthesis, by dimerization of the starting monomers at 190 °C using air as the oxidant, and the large scale synthesis, by heating the monomers in mineral oil, with the introduction of oxygen by an air flow.[28]

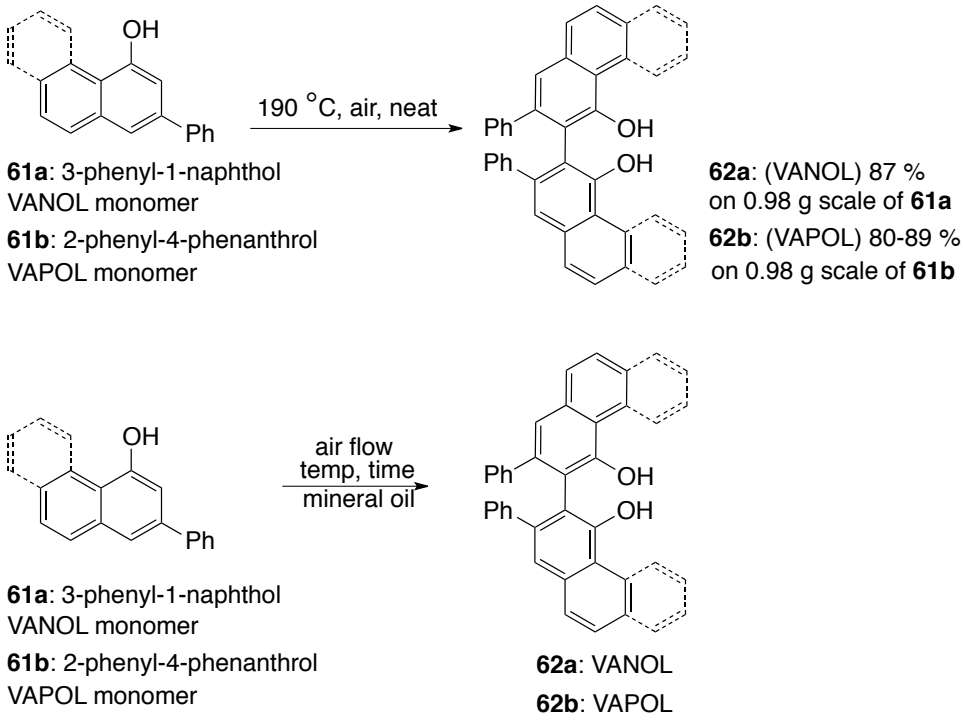

Figure 3-10. Phenolic coupling in the preparation of racemic VANOL and VAPOL.

In our case however, this chemistry failed to work, resulting in black tar-like decomposition material.

3-1.2-C Third generation approach to MAPOL via the 2+2 synthesis.

At this point, it seemed as if our system was not well suited for coupling reactions. So we turned our focus to traditional approaches of porphyrin synthesis, involving the acid-catalyzed condensation of 4 equivalents of pyrrole and 4 equivalents of aldehyde followed by oxidation to provide the porphyrin. We originally had some reservations about this route because of the low yields traditionally obtained. With this in mind, we looked into the MacDonald 2+2 approach for the synthesis of porphyrins.[15]

The backbone of Fischer's classical porphyrin syntheses was the 2+2 synthesis that called for the use of 1-bromo-9-methyldipyrromethenes such as **46** and **47** as intermediates. This coupling reaction involves condensation of the dipyrromethenes in boiling formic acid or in organic melts (succinic, tartaric, etc.) usually requiring temperatures of 200 °C or higher (Scheme 3-8). Not only are these harsh conditions, but also the choice of organic acid to be used is determined by trial and error, based on the temperature required to provide the best yield of porphyrin.

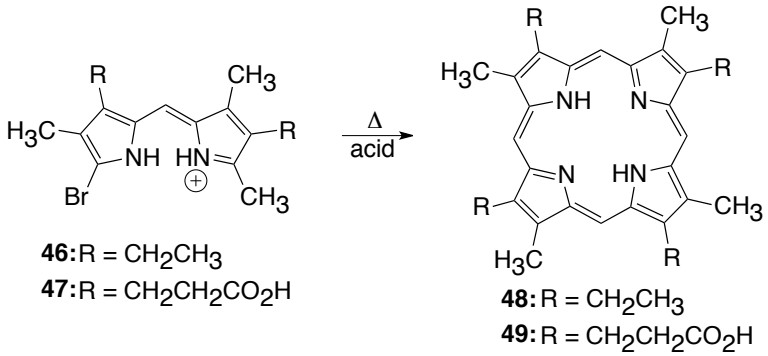

46: R = CH_2CH_3
47: R = $CH_2CH_2CO_2H$

48: R = CH_2CH_3
49: R = $CH_2CH_2CO_2H$

Scheme 3-8. Fischer's synthesis of porphyrins.

Fischer's most famous example of porphyrin synthesis using this approach is his synthesis of deuteroporphyrin **53**, an intermediate that was used in the total synthesis of

hemin **54** by Munich (Scheme 3-9), which was pivotal to Fischer's 1930 Nobel prize award.

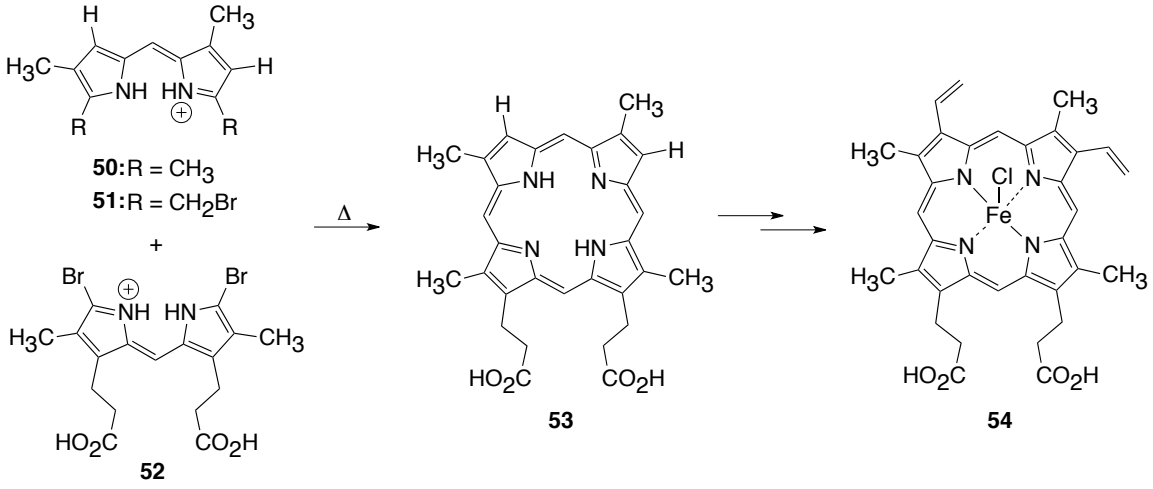

Scheme 3-9. Synthesis of hemin **54** via deuteroporphyrin **53**.

These unfavorably harsh reaction conditions led to development of modifications to Fischer's synthesis. The MacDonald 2+2 synthesis was one pivotal event in porphyrin synthesis.[15, 29] It involves the condensation of 5,5'-diformylpyrromethanes with 5,5'-dihydro dipyrromethanes under mild acidic catalysis. The intermediate porphodimethene is rapidly oxidized to the porphyrin in air (Scheme 3-10).

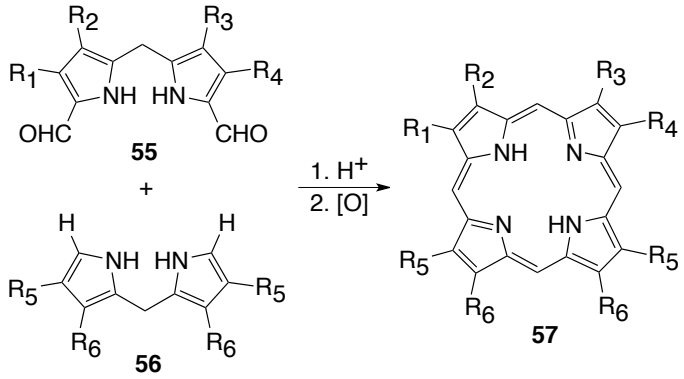

Scheme 3-10. MacDonald's 2+2 porphyrin synthesis.

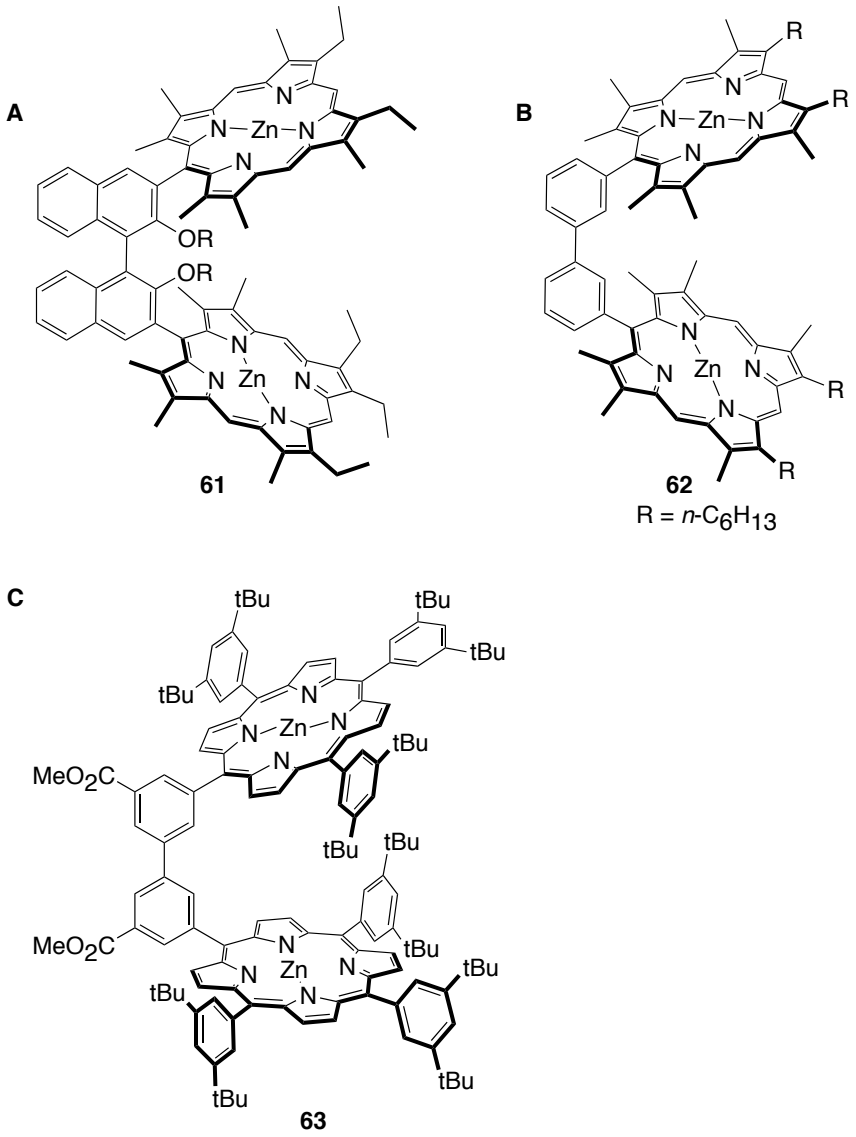

Figure 3-11. Dimeric porphyrins synthesized by Ogoshi.

This method has since been successfully used in the synthesis of a wide range of *meso*-substituted *trans*-porphyrins.[29-30] Several modifications to this method have been developed,[31] one of which is by Ogoshi and coworkers, where instead of the 5,5'-dihydro dipyrromethane, a 5,5'-bis(hydroxybenzyl)dipyrromethane was coupled with a 5,5'-dihydro dipyrromethane to give unsymmetric 5,15-diphenylporphyrins.[32] Furthermore, these condensation conditions have been

employed in the synthesis of BINOL/biphenyl-porphyrin systems.[33] Porphyrin **61** shown in Figure 3-11 A is an example of one such system containing BINOL as a chiral spacer. Porphyrin systems **62** and **63** shown in **B** and **C** are linked by a biphenyl spacer. The synthesis of **62** outlined in Scheme 3-12, involves the condensation of a bis-aldehyde with pyrrole-2-ester, followed by saponification to provide the tetra-acid bis dipyrromethane. Then a MacDonald type condensation with 5,5'-diformyldi-pyrromethane provides **62** in 88% yield.

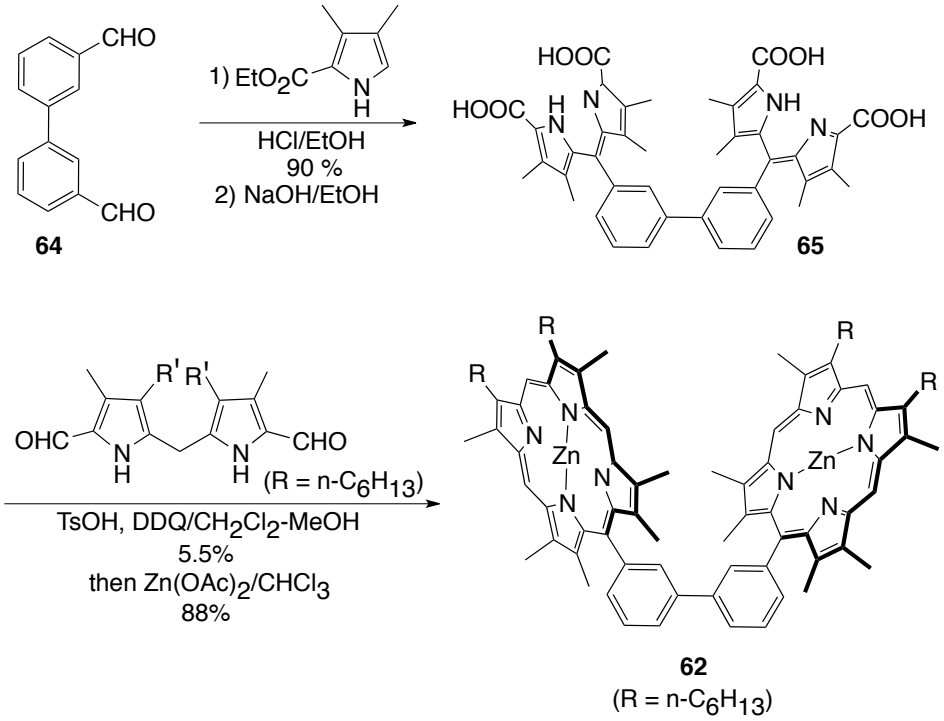

Scheme 3-12. Ogoshi's route to porphyrin B.

Our attempts to synthesize MAPOL via this route begun with the synthesis of diformyldi-pyrromethane **59** by a Vilsmeier-Haack reaction from dipyrrylmethane **38**. This was then employed in a condensation reaction with tetra-acid **60**, obtained by the condensation of bis-aldehyde **59** with methyl 1*H*-pyrrole-2-carboxylate, followed by saponification of the tetra-ester

obtained to provide the tetra-acid bis dipyrromethane **60**. Unfortunately, attempts to carry out the condensation with diformyldi-pyrromethane **59** were unsuccessful (Scheme 3-13). We hypothesized that this could be because of the free rotation of the diformyldi-pyrromethane bond, causing it to not adopt the required conformation for reaction. In the case of Ogoshi's synthesis, their diformyldi-pyrromethane has long alkyl chain substituents on the pyrrole, hindering this rotation.

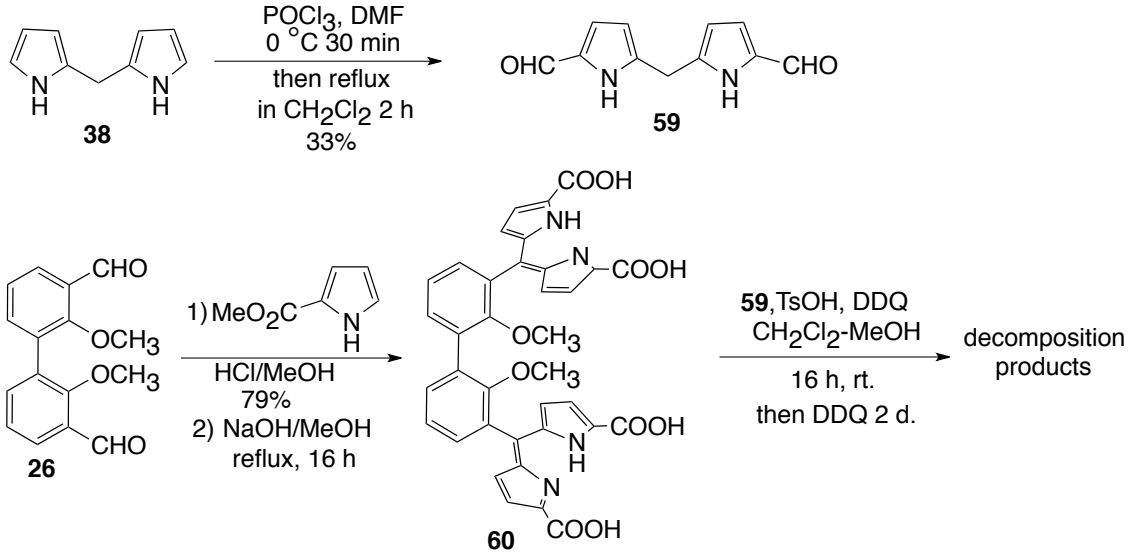

Scheme 3-13. Attempts to synthesize MAPOL using Ogoshi's method.

3-1.2-D Fourth generation approach to MAPOL via Lindsey type condensation.

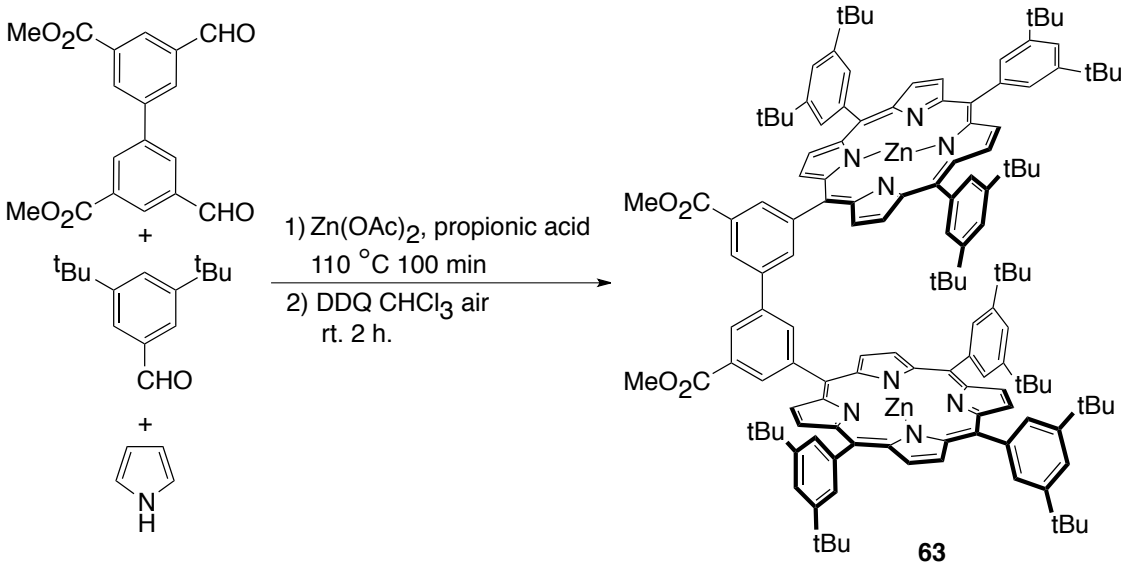

Scheme 3-14. Ogoshi's synthesis of **63**.

An extension of the 2+2 coupling was reported by Ogoshi and co-workers who prepared 5,15-diaryl-β-octaalkylporphyrins by the co-condensation of β-alkyl-5,5'-unsubstituted dipyrromethanes and aromatic aldehydes.[33] They carried out the reactions in refluxing propionic acid in the presence of zinc acetate, and were able to synthesize several porphyrins (obtained as the zinc complex) with substituted phenyl groups in the *meso* positions in 15-25% yield (Scheme 3-14). They obtained even higher yields (30-40%) of porphyrins by running the reactions in benzene with catalytic quantities of trifluoroacetic acid, after air oxidation.

Scheme 3-15 shows the final successful synthesis of MAPOL. We achieved this following Ogoshi's procedure for the synthesis of **62** and **63**. MAPOL was synthesized in three steps from readily accessible starting materials. Ortho-lithiation and subsequent formylation of **37** yields bisaldehyde **26** in good yields. Condensation of bisaldehyde **26**, pyrrole and

benzaldehyde in propionic acid catalyzed by $Zn(OAc)_2$ followed by DDQ oxidation yields methylated Zn-MAPOL in 17% yield. Upon de-methylation and demetallation with BBr_3 we obtained desired MAPOL **9** in 80% yield. Along with MAPOL **9**, all of these synthetic routes also provides Zn-MAPOL **58**, methylated Zn-MAPOL **44**, and the monomer **41** (Figure 3-12) all of which turned out to be useful for investigating the nature of the complex formed between MAPOL **9** and substrates.

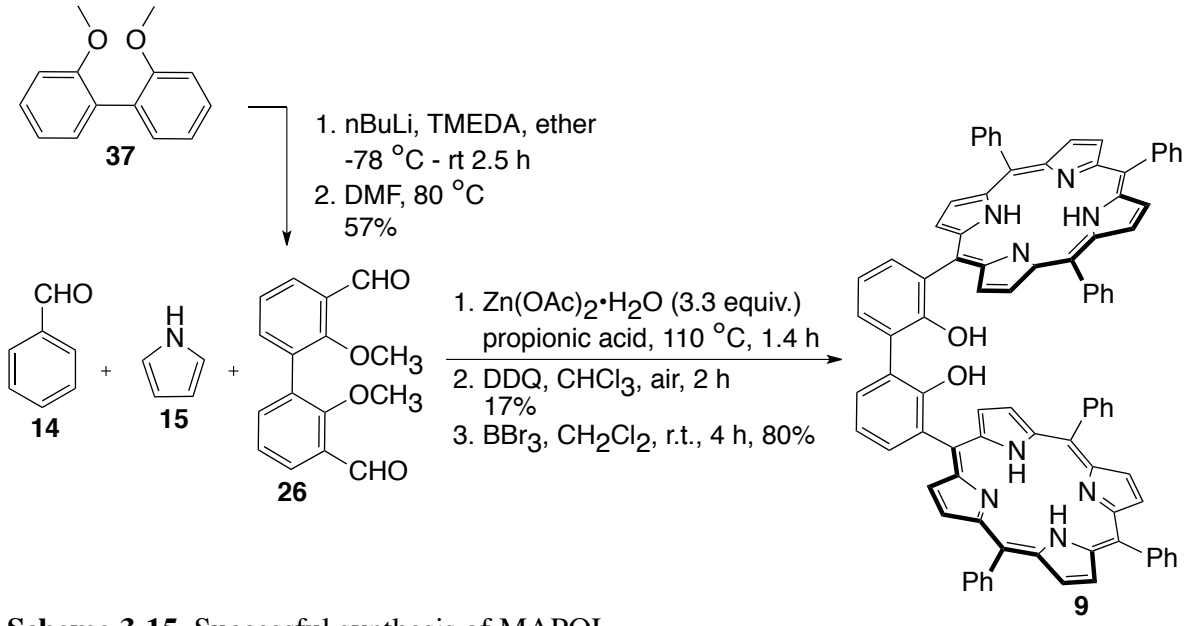

Scheme 3-15. Successful synthesis of MAPOL.

With MAPOL in hand, a series of UV-vis and ECCD studies were done. UV-vis absorption data (λ_{max}) of the newly synthesized porphyrins were obtained in hexane and methyl cyclohexane, and the molar extinction coefficient (ε) was calculated. These solvents were chosen in order to avoid polar solvents that would disrupt hydrogen bonding. Table 3-4 shows the details of this study.

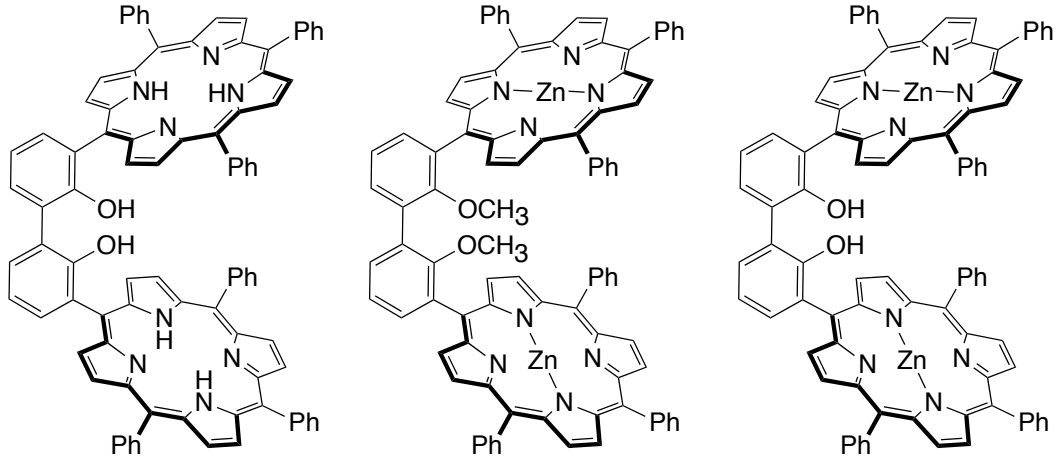

Figure 3-12. Important porphyrins obtained along the way.

Table3-5. UV-vis data for newly synthesized porphyrins.

	hexane		methyl cyclohexane	
	λ, nm	ε	λ, nm	ε
MAPOL **9**	413	420,000	416	298,000
Zn- MAPOL **58**	414	81,100	421	89,000
analogue **44**	412	519,200	420	370,610

Preliminary CD studies were done using the two enantiomers of cyclohexyl ethylamine in both hexane and methyl cyclohexane. No ECCD was obtained with methyl cyclohexane, hence, all CD studies were conducted in hexane.

3-1.3 Investigating the type of interaction and nature of complex formed between MAPOL and amines.

Assuming that the chirality of amines is transferred to MAPOL via non-covalent interactions, we need to determine that the porphyrin units play no part in formation of the complex and that the amines bind to MAPOL solely by hydrogen bonding with the biphenol unit.

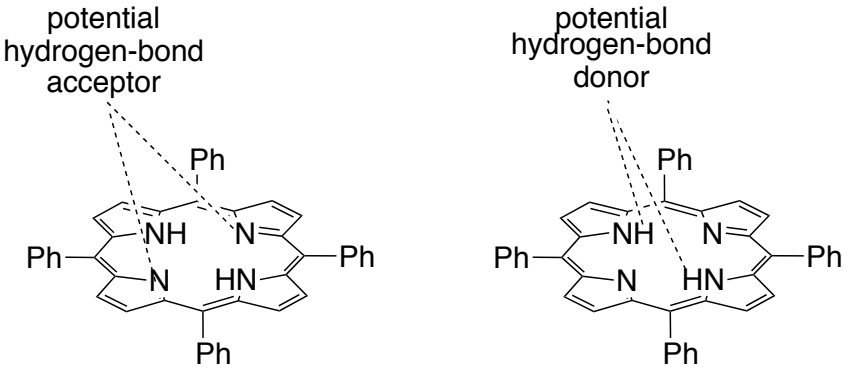

Figure 3-13. Potential sites for hydrogen-bonding on porphyrin unit.

The porphyrin units have two pyrrole protons as well as two nitrogen atoms that could potentially hydrogen bond with the amine (Figure 3-13). In order to use MAPOL as a host for assignment of absolute stereochemistry of amines, there should be no interference with the binding from the porphyrin units. UV-vis, ^{1}H-NMR and CD spectroscopy seemed ideal for investigation of the intermolecular interaction between MAPOL and amines.

UV-vis spectroscopy is a valuable tool for investigating binding.[34] In metallated porphyrin systems, upon titration of an amine into the porphyrin solution, a red-shift of the porphyrin Soret band (B band) is usually observed. This is because of donation of the lone pair electrons of amine to the metal.[1b] In free-base porphyrins however, there is no red-shift of the

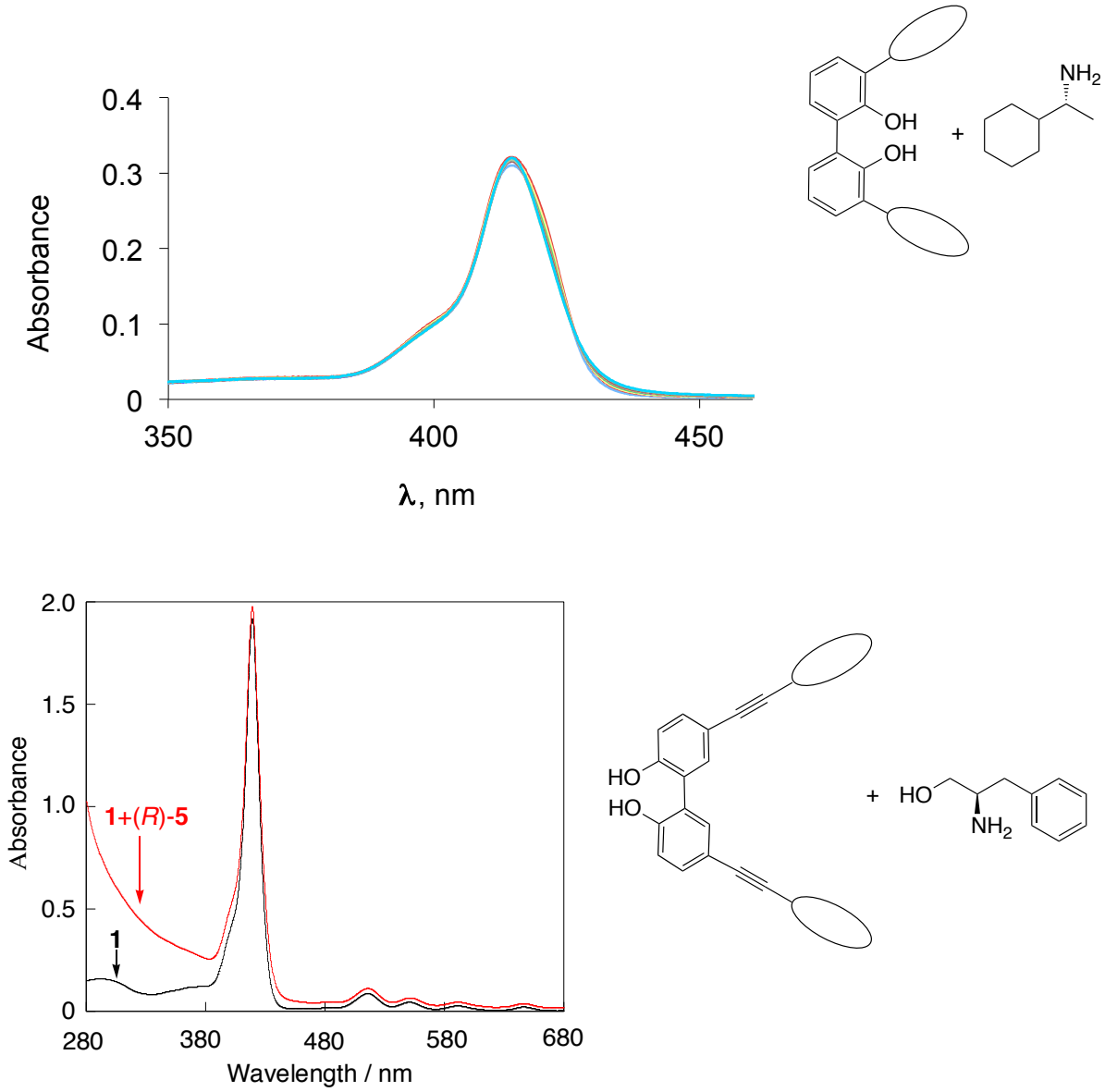

Figure 3-14. UV-Vis curves. A) Titration of MAPOL **9** solution (1 μM) with amine **7** in hexane. B) Ishii's titration of **4** (25 mM) with amino alcohol in DCM. A lack of red-shift indicates that the amine does not bind to the porphyrin.[2]

porphyrin Soret band. If the amines bind to MAPOL via the hydroxyl groups, and have no interaction with the porphyrin units, there should not be any shift in the λ_{max}. But if there is

some interaction between amine and porphyrins, then we can expect to observe a change in the λ_{max}.

Upon titration of MAPOL with amine **2***R* in hexane, the porphyrin Soret band did not undergo a shift. (Figure 3-14 A) This was an initial indication that there was no interaction between the porphyrin and the amine, meaning that the amine does not bind to the prophyrin unit. This lack of porphyrin-guest interaction has previously been demonstrated in similar porphyrin systems. One such example was reported by Ishii and co-workers (discussed earlier Section 3-4). They designed a 2,2'-Biphenyl-bridged bis(free base porphyrin) **4** and employed it as a chirality sensor for chiral amino alcohols.[2] Upon UV-vis titration of **4** with amino alcohol, they do not observe a red-shift. Figure 3-14B shows the UV-vis spectrum obtained by Ishii and co-workers upon titration of amino alcohol with free-base porphyrin **4**. This result, along with additional ^{1}H-NMR data led them to the conclusion that the chiral induction obtained in the form of ECCD sign, was as a result of chirality transfer upon hydrogen-bonding of amino alcohols to the host biphenol unit.

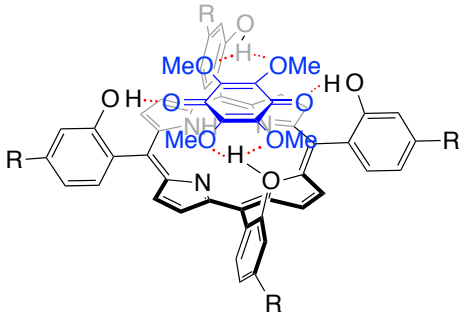

Figure 3-15. Interaction between quinone and porphyrin via multiple hydrogen bonds.

Hydrogen bonding complexes involving porphyrins have also been observed by Hayashi and co-workers.[35] The authors investigated the intermolecular interactions involved in molecular recognition between tetraarylporphyrin and ubiquinone analogues. Specifically, they investigated the type of intermolecular interaction between quinone and porphyrin as a model to understand the behavior of protein-ligand binding.

Second, additional evidence for the hydrogen-bonding interaction between amine and MAPOL was obtained from ^{1}H-NMR spectroscopy, where measurements of **9** with several amines (methyl benzylamine, cyclohexyl ethylamine and 3-methylbutan-2-amine) from 1:1 to 1:100 ratios were taken (see experimental details for full details). Using 3-methylbutan-2-amine as an example (Figure 3-16 A), It was observed that the phenolic OH peak of **1** (sharp singlet ~6 ppm) underwent a dramatic shift to 1.9 ppm. Furthermore, the peak corresponding to the amine NH_2 protons (broad singlet ~1 ppm) significantly shifts downfield (from 1.06 ppm – 2.56 ppm) upon addition of one equivalent of amine.

Additionally, the resonances of the amine protons shift upfield significantly, with the α-proton experiencing the greatest shift. For example, for 3-methylbutan-2-amine shown, the α-proton shifts from 2.67 ppm in the free amine to 1.00 ppm in the bound complex, presumably as a result of lying within the porphyrin shielding cone. Taking a closer look at the ^{1}H-NMR spectrum, the pyrrole protons (broad singlet at -2.8 ppm) remain unchanged throughout the titration process. If the amine were to have any interaction with the porphyrins in MAPOL, we would expect the pyrrole protons to change.

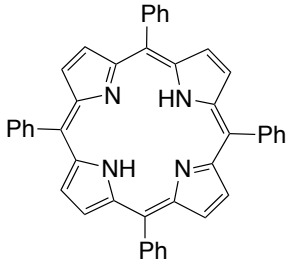

Figure 3-17. A4-TPP porphyrin.

This was supported by using A4-TPP porphyrin as a control (Figure 3-17). This porphyrin has no hydroxyl groups and also has no possible sites for interaction with amine except via the pyrrole protons, hence, there is no possibility of hydrogen bonding. If the amine interacts with the porphyrin, the pyrrole protons of the porphyrin should change. Figure 3-16 B shows the ^{1}H-NMR spectra obtained from titration of TPP with amine **9***S*.

Several observations are notable. First, the pyrrole protons (broad singlet at -2.8 ppm) remain unchanged throughout the titration process, and second, the amine protons do not undergo any shifts. In addition, unlike the MAPOL titration shown in Figure 3-16 A, where both the host and guest ^{1}H-NMR peaks undergo some kind of change, in this case, both these protons remain the same. i.e. there is no observable shift for either the amine protons, or the porphyrin protons. These studies suggest that the amines are situated deep within the cleft between the two porphyrins flanking the binding site, and not within the porphyrin itself.

Additional confirmation that complex formation between MAPOL and amine occurs via hydrogen bonding and not coordination to the porphyrin, was obtained from CD spectroscopy. MAPOL, being a racemic mixture of *P* and *M* atropisomers, was ECCD inactive as expected. However when a chiral amine was added to a solution of MAPOL, the solution became CD active. Moreover, when analogue **44** was used as a control in place of MAPOL **9**, the solution, upon addition of chiral mono amines under similar conditions, induced no CD spectra. From UV-vis titration, amine binds to analogue **44** via zinc coordination, as evidenced by a 12 nm red-shift of the porphyrin Soret band (Figure 3-18). The source of chirality transfer in MAPOL is the rotation around the C-C single bond between the two phenyls. This rotation is brought about upon binding of the chiral amines with MAPOL. Mono amines cannot induce this twist in analogue **44** because they can only bind to one of the porphyrins. On the other hand, when chiral diamine was used with **44**, the complex resulted in a CD signal (Figure 3-19).

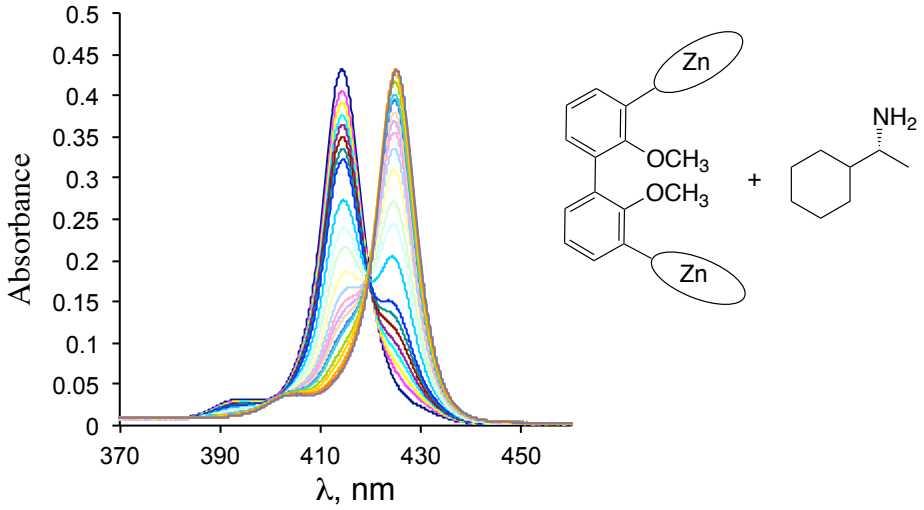

Figure 3-18. UV-Vis titration of Zn-MAPOL **44** solution (1 μM) with amine in hexane. A 12 nm red-shift indicates that the amine binds to the zinc.

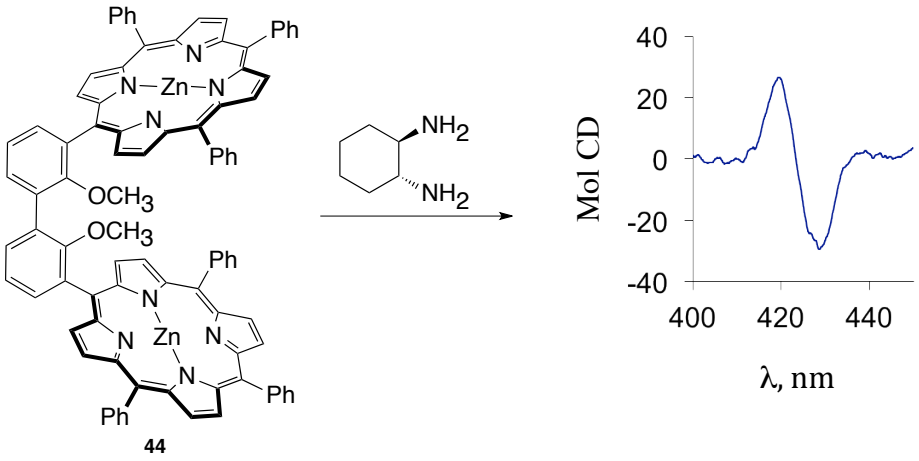

Figure 3-19. ECCD spectrum obtained upon binding of **44** with a chiral diamine.

The structure of the complex formed by MAPOL and amines was studied by ^{1}H-NMR spectroscopy. A complex stoichiometry of **9•amine** in $CDCl_3$ was established at 1:1 by Job's plot analysis from the ^{1}H-NMR titration data[10] (Figure 3-20).

Job's method of continuous variations is a commonly-used analytical technique for determining the composition of coordination complexes in solution.[36] The method involves measuring an intensive property in a series of solutions of constant *total* molarity, but of varying host-to-guest ratio. In practice, two equimolar stock solutions, one of the host and the other of the guest, are prepared. A set of working solutions is then obtained by mixing V_G mL of the stock guest solution with $(V_T - V_G)$ mL of the stock host solution, where V_T is a fixed total volume and V_G is a variable, $0 \leq 2 \leq V_T$. The absorbances of these solutions are then measured at a fixed wavelength, and plotted as a function of mole fraction of guest, (V_G/V_T), or of host, $((V_T - V_G)/V_T)$. The position of maximum absorbance on this plot, in relation to the mole-fraction axis, gives the stoichiometry of the complex.

The data for a Job's plot can also be more conveniently obtained from a regular titration procedure. In titrating a host solution with an *equimolar* guest solution, the total molarity of the host-plus-guest mixture is maintained at a constant value, as the host/guest ratio is varied (additivity of volumes can be assumed for the dilute solutions normally used in these experiments). Thus, the data points from a direct titration actually encompass all of the experimental points corresponding to a Job's plot.

A

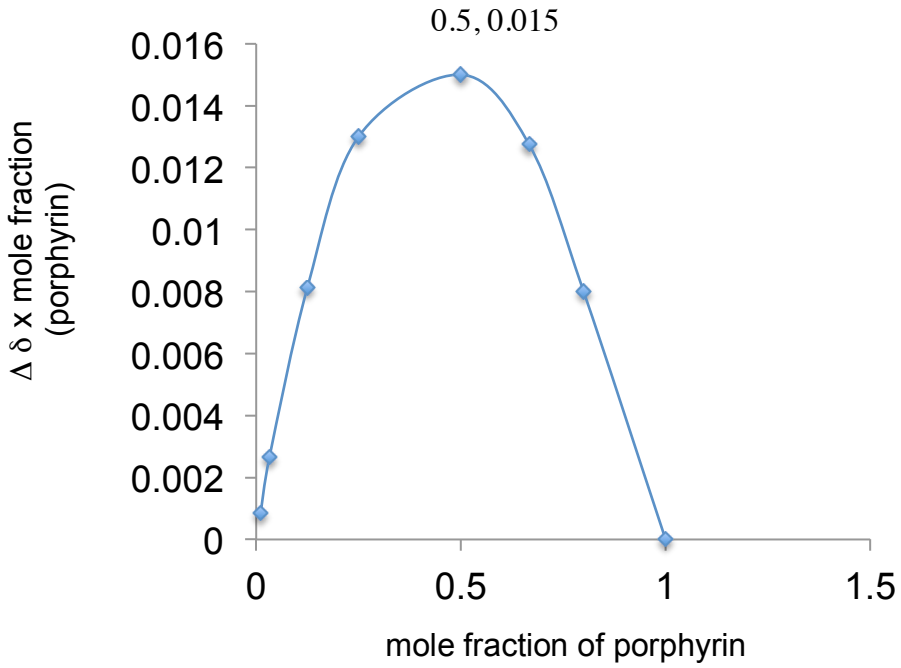

B

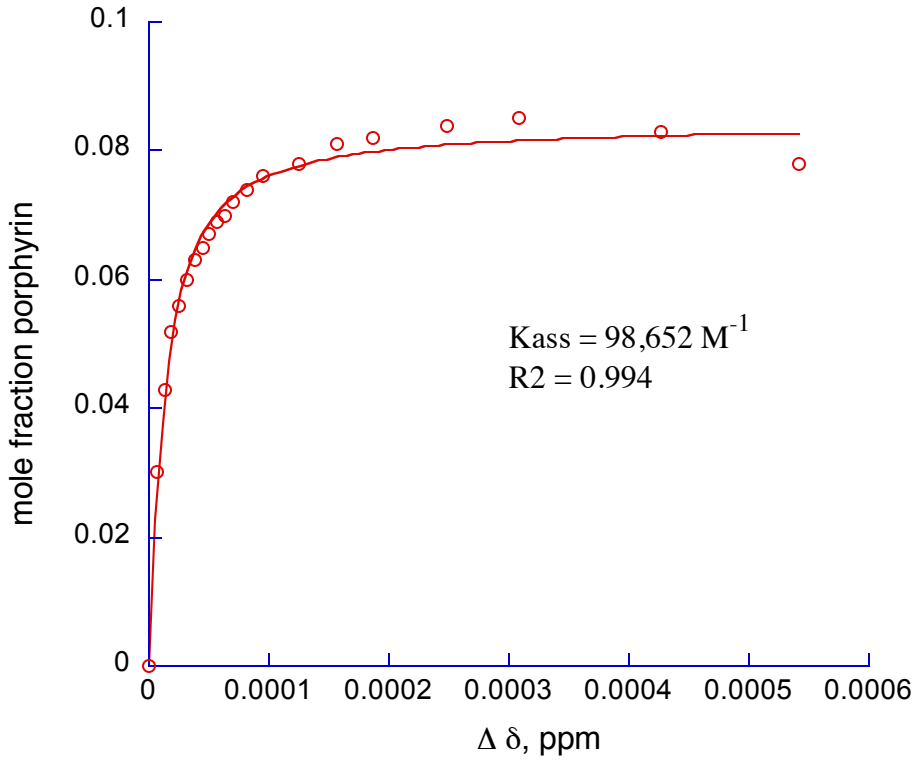

Figure 3-21. A) Job's continuous plot B) The non-linear least square fit of the chemical shift change vs. mole fraction provides the binding constant.

In summary, we developed and synthesized a novel porphyrin host system. This compound demonstrated the ability to form a complex with amines via hydrogen bonding, as shown by both NMR and UV-vis spectroscopy. In addition, a 1:1 stoichiometry of the complex was obtained from a Job's plot analysis. We propose that the new host molesule could provide a direct approach towards chirality sensing of mono coordinating compounds such as carboxylic acids, mono amines and alcohols, and related ECCD studies of these and other substrates will be discussed in the next chapter.

Experimental procedures

Anhydrous CH_2Cl_2 was dried over CaH_2 and distilled. The solvents used for CD measurements were purchased and were spectra grade. All reactions were performed in oven or flame dried glassware under nitrogen. Solvents used for synthesis of substrate were dried as follows: THF dried over Sodium, dichloromethane dried over CaH. Column chromatography was performed using SiliCycle silica gel (230-400 mesh). ^{1}H-NMR spectra were obtained on Varian Inova 300 MHz or 500 MHz instrument and are reported in parts per million (ppm) relative to the solvent resonances (δ), with coupling constants (*J*) in Hertz (Hz). CD spectra were recorded on a JASCO J-810 spectropolarimeter, equipped with a temperature controller (Neslab 111) for low temperature studies, and is reported as λ [nm] ($\Delta\varepsilon_{max}$ [mol^{-1} cm^{-1}]).

Synthesis of **16**

To 30 mL of TMEDA in 550 mL of freshly distilled ether at 25 °C was added 155 mL nBuLi (1.72 M) dropwise. The solution was stirred for 10 min at this temperature and then 2,2'-dimethoxy-biphenyl (19.06 g) was added in. The resultant white suspension was stirred at 25 °C for 2.5 h and then cooled to -78 °C. To this mixture was added iodine (40.69 g) and the reaction maintained at -78 °C for 5 min, after which it was allowed to warm slowly to room temperature and quenched with 500 mL of aqueous Na_2SO_3 solution. Crude mixture was purified by column chromatography (Silica gel, 10% EtOAc in hexane) to give a pure (**16**) in 71 % yield. ^{1}H-NMR ($CDCl_3$, 300 MHz): δ 3.45 (s, 6H), 6.88 (t 2H, J = 7.8), 7.30-7.33 (dd, 2H J_1 = 1.2, J_2 = 7.5),

7.78-7.81 (dd, 2H J_1 = 1.5, J_2 = 7.8); ^{13}C-NMR ($CDCl_3$, 75 MHz): δ 60.6, 92.4, 125.6, 131.8, 132.0, 139.3, 157.0;

Synthesis of **38**

A mixture of paraformaldehyde (1.5 g, 50.0 mmol) and pyrrole (347 mL, 5.0 mol) in a 500 mL round bottom flask was degassed with a stream of argon for 10 min at room temperature. The mixture was then heated at 55 °C for about 10 min under argon until the solution became clear. $InCl_3$ (1.11 g, 5.0 mol) was then added to the mixture, and this was then stirred at 55 °C for 2.5 h the heat source was then removed, and NaOH (6.0 g, 0.15 mol) was added. The mixture was stirred for 1 h and then filtered. The filtrate was concentrated on a rotor evaporator. The recovered pyrrole was distilled for re-use. The crude solid obtained was extracted with a solution of 20% EtOAc in hexane, (5 x 50 mL). After removal of solvent by rotor evaporator, crystallization from methanol/water (4:1) afforded the product as pale white crystals in 45 % yield (3.3 g) ^{1}H-NMR ($CDCl_3$, 300 MHz): δ 3.96 (s, 2H), 6.01-6.03 (m 2H), 6.12-6.15 (m, 2H), 6.63-6.65 (m, 2H), 7.83 (br, s, 2H); ^{13}C-NMR ($CDCl_3$, 75 MHz): δ 26.3, 106.3, 108.3, 117.2, 129.0;

Synthesis of **39**

A flame-dried 500 mL round bottom flask equipped with a magnetic stirring bar was charged with di(1*H*-pyrrol-2-yl)methane **38** (220 mg, 3.0 mmol), benzaldehyde (154 μL, 3.0 mmol), and freshly distilled methylene chloride (293 mL). The solution was degassed with a stream of argon

for 10 min. Trifluoroacetic acid (73.4 μL, 0.97 mmol) was added via syringe and the flask shielded from light with aluminum foil. The solution was stirred for 3 h at room temperature, and then quenched by the addition of *p*-chloranil (486 mg, 3.0 mmol) and the reaction stirred for a further 30 min, after which it was neutralized with triethyl amine (1.4 mL) and poured directly on a silica gel column packed in hexane. The product was eluted with methylene chloride (350 mL). Evaporation of solvent on a rotor evarporator yielded purple crystals that were washed once with hexane, filtered and dried to give **39** in 10 % yield (125 mg). This compound was used without further purification. ^{1}H-NMR ($CDCl_3$, 300 MHz): δ -3.12 (s, 2H), 7.81-7.78 (m 4H), 8.28-8.25 (m, 4H), 9.07 (d, 4H J = 4.5 Hz), 9.38 (d, 4H J = 4.5 Hz), 10.30 (s, 2H).

Synthesis of **43**

Freshly distilled methylene chloride (50 mL) was added to a flame-dried 100 mL round bottom flask equipped with a magnetic stirring bar. 5, 15-diphenyl porphyrin **39** (192 mg, 0.4 mmol), and N-bromosuccinamide (70 mg, 0.4 mmol) were added to the flask at room temperature. The solution was degassed with argon, and left to stir at room temperature for 1 h. Evaporation of solvent on a rotor evaporator yielded crude product as purple solid. The crude mixture was purified by column chromatography (Silica gel, 15% EtOAc in hexane) to give **43** in 71 % yield as purple crystals. ^{1}H-NMR ($CDCl_3$, 300 MHz): δ -2.98 (s, 2H), 7.75-7.80 (m 5H), 8.18-8.21 (m, 5H), 8.93-8.95 (m, 4H) 9.26 (d, 2H J = 5.1 Hz), 9.72 (d, 2H J = 4.8 Hz), 10.15 (s, 1H).

HRMS: calc: 540.0950, 542.0929 exp: 540.9796, 542.9818

Synthesis of **12**

1,2-dichloroethane (3.33 mL) was added to a flame-dried 50 mL round bottom flask equipped with a magnetic stirring bar. (5-bromo-10,20-diphenyl porphyrin)zinc II **43** (20 mg, 0.053

mmol), pinacolborane (40 μL, 0.053 mmol), triethyl amine (60 μL, 0.053 mmol) and trans-dichlorobis-palladium II (3 mg, 10 mol %) were added to the flask at room temperature. The solution was degassed with argon and heated to 90 °C. the mixture was stirred at this temperature for until completion as monitored by TLC. Upon complete consumption of starting material, the reaction was quenched with an aqueous solution of KCl (5 mL), washed with water, and dried (Na_2SO_4). Evaporation of solvent on a rotor evaporator yielded crude product as purple solid. The crude mixture was purified by column chromatography (Silica gel, 100 % DCM) to quantitatively give **12** as purple crystals. ^{1}H-NMR ($CDCl_3$, 300 MHz): δ 1.86 (s, 12H), 7.79-7.78 (m 6H), 8.24-8.23 (dd, 4H J_1 = 0.9 Hz, J_2 = 3.9 Hz), 9.06 (d, 1H J = 2.1 Hz), 9.13 (d, 1H J = 2.1 Hz), 9.37 (d, 1H J = 2.4 Hz), 9.95 (d, 1H J = 2.4 Hz), 10.24 (s, 1H); ^{13}C-NMR ($CDCl_3$, 600 MHz): δ 25.3, 85.2, 107.2, 120.3, 126.5, 127.4, 131.7, 132.0, 132.7, 134.5, 142.7, 148.8, 149.8, 150.2, 153.8; HRMS: calc: 650.1832 exp: 651.2375

Synthesis of **41**

To a flame-dried 3 L round bottom flask equipped with a magnetic stirring bar was added anisaldehyde (0.855 g, 2.3 mmol), benzaldehyde (2 g, 18.8 mmol), pyrrole (1.68 g, 25 mmol) and freshly distilled methylene chloride (2.5 L). The solution was degassed with a stream of argon for 20 min. BF_3•OEt (0.15 mL, 1.25 mmol) was added via syringe and the flask shielded from light with aluminum foil. The solution was stirred for 2 h at room temperature, and then quenched by the addition of *p*-chloranil (12 g, 0.05 mol) and the reaction stirred for a further 2 h. After removal of most of the solvent on a rotor evaporator, the mixture was washed with a solution of 1 M NaOH (2 x 50 mL. The organic layer was extracted with dichloromethane, and

solvents removed on a rotor evarporator to give crude product as purple solid. The crude mixture was purified by column chromatography (Silica gel, 20 % EtOAc in hexane) to give **41** as a purple solid. ^{1}H-NMR ($CDCl_3$, 300 MHz): δ 3.63 (s, 3H), 7.35 (t 2H J = 8 Hz), 7.76-7.71 (m, 10H), 8.01 (d, 1H J = 6.9 Hz), 8.24-8.22 (m, 6H), 8.95-8.89 (m, 8H). HRMS: calc: 706.1711 exp: 706.2531

Synthesis of **20**

HRMS: calc: 630.2420 exp: 631.3031

Synthesis of **26**

Freshly distilled ether (143 mL) was added to a flame-dried 100 mL round bottom flask equipped with a magnetic stirring bar, and cooled to -78 °C. To this flask was added 2,2'-dimethoxy-biphenyl (5 g, 0.023 mol), nBuLi (28 mL, 0.07 mol) and TMEDA (8 mL, 0.07 mol) dropwise. The reaction mixture was kept at this temperature for 5 min, and then allowed to warm to room temperature. The reaction was stirred at this temperature for 2.5 h, after which it was once again cooled to -78 °C, and DMF (10.8 mL, 0.13 mol) added slowly over a 10 min period. The reaction mixture was allowed to warm to room temperature, and immediately quenched with aqueous NH_4Cl solution. The organic layer was extracted with ether, and solvents removed on a rotor evaporator. The crude mixture was purified by column chromatography (Silica gel, 10 % - 15 % EtOAc in hexane) to give **26** as a white solid. ^{1}H-NMR ($CDCl_3$, 300 MHz): δ 3.57 (s, 6H), 7.34-7.29 (td 2H J_1 = 7.5 Hz J_2 = 0.9), 7.64-7.61 (dd, 2H J_1 = 7.5 Hz J_2 = 2.1 Hz), 7.93-7.90 (dd,

2H J_1 = 7.5 Hz J_2 = 1.5 Hz), 10.45 (s, 2H); ^{13}C-NMR ($CDCl_3$, 75 MHz): δ 63.1, 124.3, 128.7, 129.6, 131.5, 137.5, 160.9, 189.7; HRMS: calc: 706.1711 exp: 706.2531

Synthesis of MAPOL **9**

Pyrrole (3.6 mL, 0.052 mol), bisaldehyde **26**, benzaldehyde and $Zn(OAc)_2 \bullet 2H_2O$ were dissolved in propionic acid (270 mL) in a 3 N flask. The mixture was heated to 110 °C, and maintained at this temperature for 100 min. The reaction mixture was then cooled to room temperature and the solvents removed under high vacuum with successive portions of toluene. DDQ (1 g) in chloroform (200 mL) was added to the residue and stirred at room temperature with air bubbling for 2 h. After removal of the solvent on a rotor evaporator, the crude mixture was purified by column chromatography (Silica gel, 10% - 15 % DCM in hexane) to give pure **9**. ^{1}H-NMR ($CDCl_3$, 300 MHz): δ 3.57 (s, 6H), 7.34-7.29 (td 2H J_1 = 7.5 Hz J_2 = 0.9), 7.64-7.61 (dd, 2H J_1 = 7.5 Hz J_2 = 2.1 Hz), 7.93-7.90 (dd, 2H J_1 = 7.5 Hz J_2 = 1.5 Hz), 10.45 (s, 2H). HRMS: calc: 706.1711 exp: 706.2531

REFERENCES

References

1. (a) Huang, X. F.; Fujioka, N.; Pescitelli, G.; Koehn, F. E.; Williamson, R. T.; Nakanishi, K.; Berova, N., Absolute configurational assignments of secondary amines by CD-sensitive dimeric zinc porphyrin host. *Journal of the American Chemical Society* **2002,** *124* (35), 10320-10335; (b) Kurtan, T.; Nesnas, N.; Li, Y. Q.; Huang, X. F.; Nakanishi, K.; Berova, N., Chiral recognition by CD-sensitive dimeric zinc porphyrin host. 1. Chiroptical protocol for absolute configurational assignments of monoalcohols and primary monoamines. *Journal of the American Chemical Society* **2001,** *123* (25), 5962-5973; (c) Proni, G.; Pescitelli, G.; Huang, X. F.; Nakanishi, K.; Berova, N., Magnesium tetraarylporphyrin tweezer: A CD-sensitive host for absolute configurational assignments of alpha-chiral carboxylic acids. *Journal of the American Chemical Society* **2003,** *125* (42), 12914-12927.

2. Ishii, Y.; Onda, Y.; Kubo, Y., 2,2 '-Biphenyldiol-bridged bis(free base porphyrin): synthesis and chiroptical probing of asymmetric amino alcohols. *Tetrahedron Letters* **2006,** *47* (47), 8221-8225.

3. (a) Mizutani, T.; Takagi, H.; Hara, O.; Horiguchi, T.; Ogoshi, H., Axial chirality induction in flexible biphenols by hydrogen bonding and steric interactions. *Tetrahedron Letters* **1997,** *38* (11), 1991-1994; (b) Takagi, H.; Mizutani, T.; Horiguchi, T.; Kitagawa, S.; Ogoshi, H., Efficient axial chirality induction in biphenyldiol triggered by proton-transferred hydrogen bonding with chiral amine. *Organic & Biomolecular Chemistry* **2005,** *3* (11), 2091-2094; (c) Huang, X. F.; Rickman, B. H.; Borhan, B.; Berova, N.; Nakanishi, K., Zinc porphyrin tweezer in host-guest complexation: Determination of absolute configurations of diamines, amino acids, and amino alcohols by circular dichroism. *Journal of the American Chemical Society* **1998,** *120* (24), 6185-6186.

4. (a) Li, X. Y.; Borhan, B., Prompt Determination of Absolute Configuration for Epoxy Alcohols via Exciton Chirality Protocol. *Journal of the American Chemical Society* **2008,** *130* (48), 16126-+; (b) Li, X. Y.; Tanasova, M.; Vasileiou, C.; Borhan, B., Fluorinated porphyrin tweezer: A powerful reporter of absolute configuration for erythro and threo diols, amino alcohols, and diamines. *Journal of the American Chemical Society* **2008,** *130* (6), 1885-1893; (c) Tanasova, M.; Yang, Q. F.; Olmsted, C. C.; Vasileiou, C.; Li, X. Y.; Anyika, M.; Borhan, B., An Unusual Conformation of alpha-Haloamides Due to Cooperative Binding with Zincated Porphyrins. *European Journal of Organic Chemistry* **2009,** (25), 4242-4253; (d) Yang, Q.; Olmsted, C.; Borham, B., Absolute stereochemical determination of chiral carboxylic acids. *Organic Letters* **2002,** *4* (20), 3423-3426.

5. (a) Bell, C. L.; Barrow, G. M., Evidence for a low-lying 2nd potential minimum in hydrogen-bonded systems. *Journal of Chemical Physics* **1959,** *31* (5), 1158-1163; (b) Gurka, D.; Taft, R. W.; Joris, L.; Schleyer, P. V., Regarding proton transfer in hydrogen-

bonded complexes as measured by fluorine nuclear magnetic resonance. *Journal of the American Chemical Society* **1967,** *89* (23), 5957-&; (c) Scott, R.; Depalma, D.; Vinograd.S, Proton-transfer complexes .i. preferential solvation of p-nitrophenol-amine complexes in nonaqueous-solvent mixtures. *Journal of Physical Chemistry* **1968,** *72* (9), 3192-&; (d) Kramer, R.; Lang, R.; Brzezinski, B.; Zundel, G., Proton-transfer in intramolecular hydrogen-bonds with large proton polarizability in 1-piperidinecarboxylic acids - temperature, solvent and concentration-dependence. *Journal of the Chemical Society-Faraday Transactions* **1990,** *86* (4), 627-630; (e) Hanessian, S.; Simard, M.; Roelens, S., Molecular recognition and self-assembly by non-amidic hydrogen-bonding - an exceptional assembler of neutral and charged supramolecular structures. *Journal of the American Chemical Society* **1995,** *117* (29), 7630-7645.

6. (a) Feringa, B. L.; van Delden, R. A., Absolute asymmetric synthesis: The origin, control, and amplification of chirality. *Angewandte Chemie-International Edition* **1999,** *38* (23), 3419-3438; (b) Mason, S., BIOMOLECULAR HOMOCHIRALITY. *Chemical Society Reviews* **1988,** *17* (4), 347-359; (c) Avalos, M.; Babiano, R.; Cintas, P.; Jimenez, J. L.; Palacios, J. C.; Barron, L. D., Absolute asymmetric synthesis under physical fields: Facts and fictions. *Chemical Reviews* **1998,** *98* (7), 2391-2404.

7. (a) Morino, K.; Watase, N.; Maeda, K.; Yashima, E., Chiral amplification in macromolecular helicity assisted by noncovalent interaction with achiral amines and memory of the helical chirality. *Chemistry-a European Journal* **2004,** *10* (19), 4703-4707; (b) Soai, K.; Sato, I.; Shibata, T., Asymmetric autocatalysis and the origin of chiral homogeneity in organic compounds. *Chemical Record* **2001,** *1* (4), 321-332.

8. (a) Yashima, E.; Maeda, K.; Nishimura, T., Detection and amplification of chirality by helical polymers. *Chemistry-a European Journal* **2004,** *10* (1), 42-51; (b) Green, M. M.; Park, J. W.; Sato, T.; Teramoto, A.; Lifson, S.; Selinger, R. L. B.; Selinger, J. V., The macromolecular route to chiral amplification. *Angewandte Chemie-International Edition* **1999,** *38* (21), 3139-3154; (c) Huck, N. P. M.; Jager, W. F.; deLange, B.; Feringa, B. L., Dynamic control and amplification of molecular chirality by circular polarized light. *Science* **1996,** *273* (5282), 1686-1688.

9. (a) Eelkema, R.; Feringa, B. L., Phosphoric acids as amplifiers of molecular chirality in liquid crystalline media. *Organic Letters* **2006,** *8* (7), 1331-1334; (b) Pieraccini, S.; Masiero, S.; Ferrarini, A.; Spada, G. P., Chirality transfer across length-scales in nematic liquid crystals: fundamentals and applications. *Chemical Society Reviews* **2011,** *40* (1), 258-271.

10. Eelkema, R.; Feringa, B. L., Macroscopic expression of the chirality of amino alcohols by a double amplification mechanism in liquid crystalline media. *Journal of the American Chemical Society* **2005,** *127* (39), 13480-13481.

11. Hendrix, M.; Alper, P. B.; Priestley, E. S.; Wong, C. H., Hydroxyamines as a new motif for the molecular recognition of phosphodiesters: Implications for aminoglycoside-RNA interactions. *Angewandte Chemie-International Edition in English* **1997,** *36* (1-2), 95-98.

12. Das, G.; Hamilton, A. D., Molecular, recognition of carbohydrates - strong binding of alkyl glycosides by phosphonate derivatives. *Journal of the American Chemical Society* **1994,** *116* (24), 11139-11140.

13. Onouchi, H.; Maeda, K.; Yashima, E., A helical polyelectrolyte induced by specific interactions with biomolecules in water. *Journal of the American Chemical Society* **2001,** *123* (30), 7441-7442.

14. (a) Verdine, G. L.; Nakanishi, K., PARA-DIMETHYLAMINOCINNAMATE, A NEW RED-SHIFTED CHROMOPHORE FOR USE IN THE EXCITON CHIRALITY METHOD - ITS APPLICATION TO MITOMYCIN-C. *Journal of the Chemical Society-Chemical Communications* **1985,** (16), 1093-1095; (b) Berova, N.; Gargiulo, D.; Derguini, F.; Nakanishi, K.; Harada, N., UNIQUE UV-VIS ABSORPTION AND CIRCULAR DICHROIC EXCITON-SPLIT SPECTRA OF A CHIRAL BISCYANINE DYE - ORIGIN AND NATURE. *Journal of the American Chemical Society* **1993,** *115* (11), 4769-4775; (c) Cai, G. L.; Bozhkova, N.; Odingo, J.; Berova, N.; Nakanishi, K., CD EXCITON CHIRALITY METHOD - NEW RED-SHIFTED CHROMOPHORES FOR HYDROXYL-GROUPS. *Journal of the American Chemical Society* **1993,** *115* (16), 7192-7198.

15. Arsenault, G. P.; Bullock, E.; Macdonald, S. F., Pyrromethanes and porphyrins therefrom. *Journal of the American Chemical Society* **1960,** *82* (16), 4384-4389.

16. (a) Miyaura, N.; Suzuki, A., Palladium-catalyzed cross-coupling reactions of organoboron compounds. *Chemical Reviews* **1995,** *95* (7), 2457-2483; (b) Suzuki, A., Recent advances in the cross-coupling reactions of organoboron derivatives with organic electrophiles, 1995-1998. *Journal of Organometallic Chemistry* **1999,** *576* (1-2), 147-168.

17. (a) Oconnor, S. J.; Williard, P. G., Strategy for the synthesis of the c10-c19 portion of Amphidinolide-A. *Tetrahedron Letters* **1989,** *30* (35), 4637-4640; (b) Marshall, J. A.;

Van Devender, E. A., Synthesis of (-)-deoxypukalide, the enantiomer of a degradation product of the furanocembranolide pukalide. *Journal of Organic Chemistry* **2001,** *66* (24), 8037-8041; (c) Marshall, J. A.; Johns, B. A., Total synthesis of (+)-discodermolide. *Journal of Organic Chemistry* **1998,** *63* (22), 7885-7892; (d) Shirai, T.; Kuranaga, T.; Wright, J. L. C.; Baden, D. G.; Satake, M.; Tachibana, K., Synthesis of a proposed biosynthetic intermediate of a marine cyclic ether brevisamide for study on biosynthesis of marine ladder-frame polyethers. *Tetrahedron Letters* **2010,** *51* (10), 1394-1396; (e) Lepage, O.; Kattnig, E.; Furstner, A., Total synthesis of amphidinolide X. *Journal of the American Chemical Society* **2004,** *126* (49), 15970-15971; (f) Yuan, Y.; Men, H. B.; Lee, C. B., Total synthesis of kendomycin: A macro-C-glycosidation approach. *Journal of the American Chemical Society* **2004,** *126* (45), 14720-14721; (g) Maloney, D. J.; Hecht, S. M., A stereocontrolled synthesis of delta-trans-tocotrienoloic acid. *Organic Letters* **2005,** *7* (19), 4297-4300; (h) Maloney, D. J.; Hecht, S. M., Synthesis of a potent and selective inhibitor of p90 Rsk. *Organic Letters* **2005,** *7* (6), 1097-1099; (i) Maloney, K. M.; Danheiser, R. L., Total synthesis of quinolizidine alkaloid (-)-217A. Application of iminoacetonitrile cycloadditions in organic synthesis. *Organic Letters* **2005,** *7* (14), 3115-3118; (j) O'Connor, S. J.; Barr, K. J.; Wang, L.; Sorensen, B. K.; Tasker, A. S.; Sham, H.; Ng, S. C.; Cohen, J.; Devine, E.; Cherian, S.; Saeed, B.; Zhang, H. C.; Lee, J. Y.; Warner, R.; Tahir, S.; Kovar, P.; Ewing, P.; Alder, J.; Mitten, M.; Leal, J.; Marsh, K.; Bauch, J.; Hoffman, D. J.; Sebti, S. M.; Rosenberg, S. H., Second-generation peptidomimetic inhibitors of protein farnesyltransferase demonstrating improved cellular potency and significant in vivo efficacy. *Journal of Medicinal Chemistry* **1999,** *42* (18), 3701-3710; (k) Smith, A. B.; Xian, M., Design, synthesis, and biological evaluation of simplified analogues of (+)-discodermolide. additional insights on the importance of the diene, the C(7) hydroxyl, and the lactone. *Organic Letters* **2005,** *7* (23), 5229-5232; (l) Arefolov, A.; Panek, J. S., Crotylsilane reagents in the synthesis of complex polyketide natural products: Total synthesis of (+)-discodermolide. *Journal of the American Chemical Society* **2005,** *127* (15), 5596-5603.

18. Stanforth, S. P., Catalytic cross-coupling reactions in biaryl synthesis. *Tetrahedron* **1998,** *54* (3-4), 263-303.

19. Hoye, T. R.; Chen, M. Z.; Hoang, B.; Mi, L.; Priest, O. P., Total synthesis of michellamines A-C, korupensamines A-D, and ancistrobrevine B. *Journal of Organic Chemistry* **1999,** *64* (19), 7184-7201.

20. Mentzel, U. V.; Tanner, D.; Tonder, J. E., Comparative study of the Kumada, Negishi, Stille, and Suzuki-Miyaura reactions in the synthesis of the indole alkaloids hippadine and pratosine. *Journal of Organic Chemistry* **2006,** *71* (15), 5807-5810.

21. (a) Filatov, M. A.; Guilard, R.; Harvey, P. D., Selective Stepwise Suzuki Cross-Coupling Reaction for the Modelling of Photosynthetic Donor-Acceptor Systems. *Organic Letters*

2010, *12* (1), 196-199; (b) Wang, F.; Matsuda, K.; Rahman, A.; Peng, X. B.; Kimura, T.; Komatsu, N., Simultaneous Discrimination of Handedness and Diameter of Single-Walled Carbon Nanotubes (SWNTs) with Chiral Diporphyrin Nanotweezers Leading to Enrichment of a Single Enantiomer of (6,5)-SWNTs. *Journal of the American Chemical Society* **2010,** *132* (31), 10876-10881; (c) Peng, X. B.; Komatsu, N.; Kimura, T.; Osuka, A., Improved optical enrichment of SWNTs through extraction with chiral nanotweezers of 2,6-pyridylene-bridged diporphyrins. *Journal of the American Chemical Society* **2007,** *129* (51), 15947-15953; (d) Chan, K. S.; Zhou, X. A.; Au, M. T.; Tam, C. Y., Synthesis of beta-aryl substituted porphyrins by palladium-catalyzed suzuki cross-coupling reactions. *Tetrahedron* **1995,** *51* (11), 3129-3136; (e) Chung, L. L.; Chang, C. J.; Nocera, D. G., meso-tetraaryl cofacial bisporphyrins delivered by Suzuki cross-coupling. *Journal of Organic Chemistry* **2003,** *68* (10), 4075-4078; (f) Hyslop, A. G.; Kellett, M. A.; Iovine, P. M.; Therien, M. J., Suzuki porphyrins: New synthons for the fabrication of porphyrin-containing supramolecular assemblies. *Journal of the American Chemical Society* **1998,** *120* (48), 12676-12677.

22. Dogutan, D. K.; Ptaszek, M.; Lindsey, J. S., Direct synthesis of magnesium porphine via 1-formyldipyrromethane. *Journal of Organic Chemistry* **2007,** *72* (13), 5008-5011.

23. Cram, D. J.; Degrandpre, M.; Knobler, C. B.; Trueblood, K. N., Host guest complexation .29. expanded hemispherands. *Journal of the American Chemical Society* **1984,** *106* (11), 3286-3292.

24. (a) Li, X. L.; Yang, J.; Kozlowski, M. C., Enantioselective oxidative biaryl coupling reactions catalyzed by 1,5-diazadecalin metal complexes. *Organic Letters* **2001,** *3* (8), 1137-1140; (b) Hovorka, M.; Scigel, R.; Gunterova, J.; Tichy, M.; Zavada, J., The oxidative cross-coupling of substituted 2-naphthols .1. the scope and limitations. *tetrahedron* **1992,** *48* (43), 9503-9516; (c) smrcina, m.; lorenc, m.; hanus, v.; sedmera, p.; kocovsky, p., synthesis of enantiomerically pure 2,2'-dihydroxy-1,1'-binaphthyl, 2,2'-diamino-1,1'-binaphthyl, and 2-amino-2'-hydroxy-1,1'-binaphthyl - comparison of processes operating as diastereoselective crystallization and as 2nd-order asymmetric transformation. *Journal of Organic Chemistry* **1992,** *57* (6), 1917-1920; (d) Wang, H., Recent Advances in Asymmetric Oxidative Coupling of 2-Naphthol and its Derivatives. *Chirality* **2010,** *22* (9), 827-837.

25. (a) Dewar, M. J. S.; Nakaya, T., Oxidative coupling of phenols. *Journal of the American Chemical Society* **1968,** *90* (25), 7134-&; (b) Doussot, J.; Guy, A.; Ferroud, C., Selective synthesis of 1,1 '-binaphthalene derivatives by oxidative coupling with TiCl4. *Tetrahedron Letters* **2000,** *41* (15), 2545-2547; (c) Hwang, D. R.; Chen, C. P.; Uang, B. J., Aerobic catalytic oxidative coupling of 2-naphthols and phenols by VO(acac)(2). *Chemical Communications* **1999,** (13), 1207-1208.

26. Noji, M.; Nakajima, M.; Koga, K., A new catalytic-system for aerobic oxidative coupling of 2-naphthol derivatives by the use of cucl-amine complex - a practical synthesis of binaphthol derivatives. *Tetrahedron Letters* **1994,** *35* (43), 7983-7984.

27. Nakajima, M.; Kanayama, K.; Miyoshi, I.; Hashimoto, S., Catalytic asymmetric synthesis of binaphthol derivatives by aerobic oxidative coupling of 3-hydroxy-2-naphthoates with chiral diamine-copper complex. *Tetrahedron Letters* **1995,** *36* (52), 9519-9520.

28. (a) Bao, J. M.; Wulff, W. D.; Dominy, J. B.; Fumo, M. J.; Grant, E. B.; Rob, A. C.; Whitcomb, M. C.; Yeung, S. M.; Ostrander, R. L.; Rheingold, A. L., Synthesis, resolution, and determination of absolute configuration of a vaulted 2,2'-binaphthol and a vaulted 3,3'-biphenanthrol (VAPOL). *Journal of the American Chemical Society* **1996,** *118* (14), 3392-3405; (b) Ding, Z. S.; Osminski, W. E. G.; Ren, H.; Wulff, W. D., Scalable Syntheses of the Vaulted Biaryl Ligands VAPOL and VANOL via the Cycloaddition/Electrocyclization Cascade. *Organic Process Research & Development* **2011,** *15* (5), 1089-1107.

29. Markovac, A.; Macdonal.Sf, SYNTHESES WITH 5-DIBROMOMETHYL- AND 5-FORMYLPYRROMETHENES. *Canadian Journal of Chemistry* **1965,** *43* (12), 3364-&.

30. (a) Ema, T.; Kuroda, Y.; Ogoshi, H., Selective syntheses of unsymmetrical meso-arylporphyrins. *Tetrahedron Letters* **1991,** *32* (35), 4529-4532; (b) Lindsey, J. S.; Hsu, H. C.; Schreiman, I. C., Synthesis of tetraphenylporphyrins under very mild conditions. *Tetrahedron Letters* **1986,** *27* (41), 4969-4970; (c) Motmans, F.; Ceulemans, E.; Smeets, S.; Dehaen, W., The use of 4,6-disubstituted pyrimidine-5-aldehydes in the synthesis of meso-tetraarylporphyrins. *Tetrahedron Letters* **1999,** *40* (42), 7545-7548; (d) Wallace, D. M.; Leung, S. H.; Senge, M. O.; Smith, K. M., Rational tetraarylporphyrin syntheses - tetraarylporphyrins from the macdonald route. *Journal of Organic Chemistry* **1993,** *58* (25), 7245-7257.

31. (a) Lash, T. D., Porphyrin synthesis by the "3+1" approach: New applications for an old methodology. *Chemistry-a European Journal* **1996,** *2* (10), 1197-1200; (b) Bruckner, C.; Posakony, J. J.; Johnson, C. K.; Boyle, R. W.; James, B. R.; Dolphin, D., Novel and improved syntheses of 5,15-diphenylporphyrin and its dipyrrolic precursors. *Journal of Porphyrins and Phthalocyanines* **1998,** *2* (6), 455-465; (c) Montierth, J. M.; Duran, A. G.; Leung, S. H.; Smith, K. M.; Schore, N. E., The polymer-supported MacDonald-type porphyrin synthesis: coupling of two dissimilar dipyrromethanes. *Tetrahedron Letters* **2000,** *41* (39), 7423-7426; (d) Uno, H.; Kitawaki, Y.; Ono, N., Novel preparation of beta-beta '-connected porphyrin dimers. *Chemical Communications* **2002,** (2), 116-117.

32. Ogoshi, H.; Sugimoto, H.; Nishiguchi, T.; Watanabe, T.; Matsuda, Y.; Yoshida, Z., Syntheses of 5-aryl- and 5,15-diaryl-2,3,7,8,12,13,17,18-octaethylporphines. *Chemistry Letters* **1978,** (1), 29-32.

33. Hayashi, T.; Aya, T.; Nonoguchi, M.; Mizutani, T.; Hisaeda, Y.; Kitagawi, S.; Ogoshi, H., Chiral recognition and chiral sensing using zinc porphyrin dimers. *Tetrahedron* **2002,** *58* (14), 2803-2811.

34. Huang, X. F.; Borhan, B.; Berova, N.; Nakanishi, K., UV-vis spectral changes in the binding of acyclic diamines with a zinc porphyrin tweezer. *Journal of the Indian Chemical Society* **1998,** *75* (10-12), 725-728.

35. (a) Hayashi, T.; Asai, T.; Borgmeier, F. M.; Hokazono, H.; Ogoshi, H., Kinetic and thermodynamic analysis of induced-fit molecular recognition between tetraarylporphyrin and ubiquinone analogues. *Chemistry-a European Journal* **1998,** *4* (7), 1266-1274; (b) Hayashi, T.; Miyahara, T.; Koide, N.; Kato, Y.; Masuda, H.; Ogoshi, H., Molecular recognition of ubiquinone analogues. Specific interaction between quinone and functional porphyrin via multiple hydrogen bonds. *Journal of the American Chemical Society* **1997,** *119* (31), 7281-7290.

36. Derr, P. F.; Stockdale, R. M.; Vosburgh, W. C., Complex ions. II. The stability and activity coefficients of the silver-ammonia ion. *Journal of the American Chemical Society* **1941,** *63*, 2670-2674.

Chapter 4

Determination of Absolute Stereochemistry of α-Chiral Amines

4-1 Background

The determination of absolute stereochemistry of chiral mono amines without the requirement of chemical derivatization is a problem that has long eluded chemists. Chiral mono amines play an increasing importance both in synthetic chemistry as important intermediates in the synthesis of biologically important molecules, as well as in the pharmaceutical industry.[1] There are many examples throughout literature where chiral amines are used as auxiliaries for asymmetric catalysis, and in biologically important roles.[2]

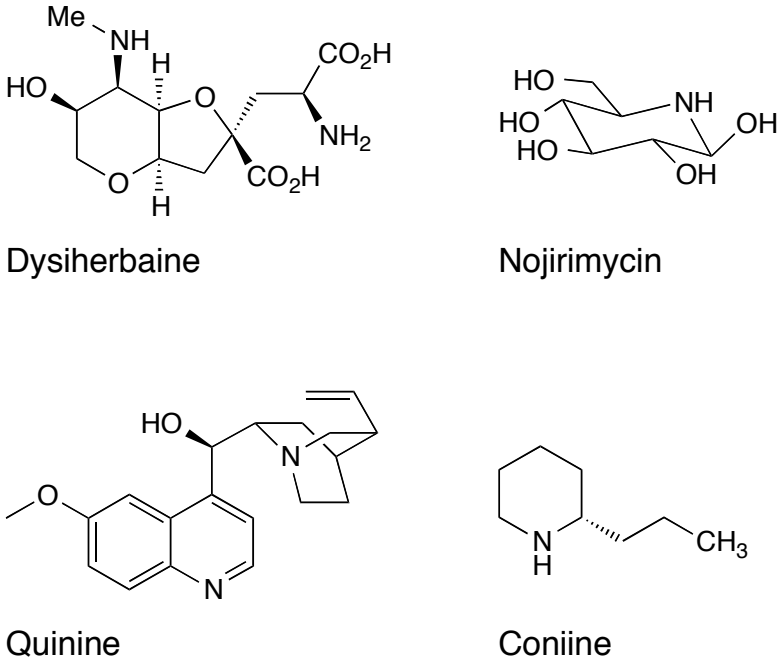

Figure 4-1. Molecules containing the amine functionality.

Due to the pivotal roles that enantiomerically pure amines play in a diverse range of pharmaceutical and organic synthesis, there is considerable effort currently underway to develop efficient methods for assigning their absolute stereochemistry easily and efficiently. For example, Scheme 4-1 shows the use of (*S*)-2-amino-3-methylbutane in a key step as a chiral building block in the key step of the synthesis of Diazoxide BPDZ-44, a tissue selective ATP – sensitive potassium channel opener, that results in inhibition of important physiological processes such as insulin release or muscle tone and contractility.[3]

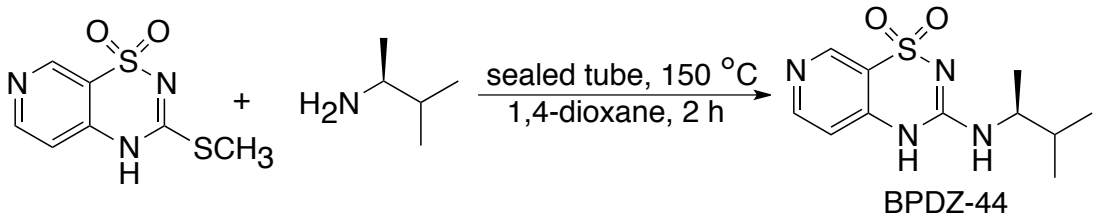

Scheme 4-1. Synthesis of Diazoxide BPDZ-44, using (*S*)-2-amino-3-methylbutane.

The main challenge met in assigning absolute configuration of compounds with one functional group, such as mono amines, is the requirement of derivatization, either with chiral derivatization agents for Mosher analysis protocol, or with achiral carrier molecules for ECCD studies.

4-1-2 Conventional Methods of Assigning Absolute Stereochemistry of α-Chiral Primary Amines

Being that chiral primary and secondary amines only have one site of attachment, they cannot be directly applied in the conventional chiroptical methods used for the absolute configurational assignment of chiral diamines using porphyrin tweezers. With only one amino

group, the sandwiched host-guest complex, in which the chiral substrate is locked inside the tweezer cannot be formed. Consequently, due to the free rotation around the tweezer linker, the two porphyrin chromophores as well as their electric transition dipole moments will be oriented randomly resulting in unpredictable or no CD signals.

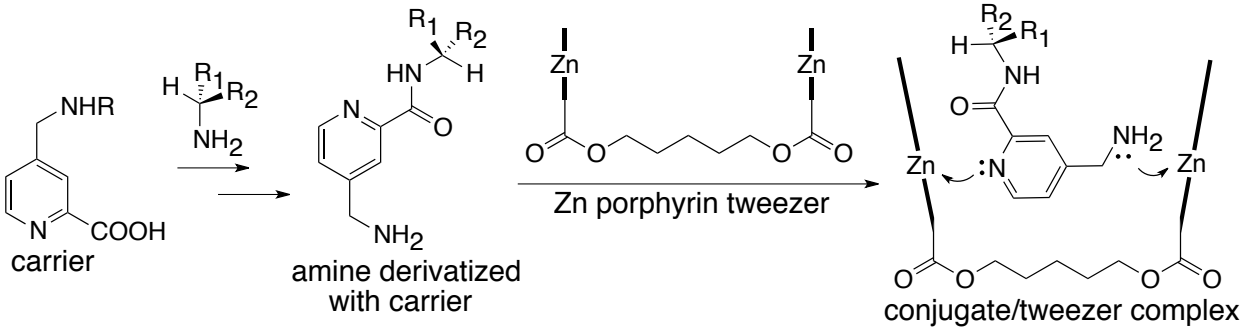

Scheme 4-2. Complex formation between carrier/monoamine conjugate and porphyrin tweezer.

The traditional approach for determining the absolute stereochemistry of α-chiral primary amines using ECCD protocol calls for the monoamine to first be derivatized by a carrier molecule in order to introduce the requisite second binding site (usually nitrogen-containing functionality) (Scheme 4-2).[4] This is not desirable because the substrates are often available in very little amounts and so additional synthetic steps in order to install the carrier and assign the absolute stereochemistry can be time consuming and impractical. A second drawback of this approach is that for each carrier, there's a need for the development of a new mnemonic to relate the observed sign of the ECCD couplet to the absolute stereochemistry of the guest.[5]

In 2001, Inuoe and co-workers designed an octaethyl substituted porphyrin tweezer system with a short ethylene linker, and directly employed it for the assignment of the absolute stereochemistry of monoamines and monoalcohols without the need for derivatization.[6] As

shown in Figure 4-2, the achiral folded *syn* conformer of the ethane-bridged porphyrin switches to the corresponding chiral extended *anti* conformer upon ligand binding.

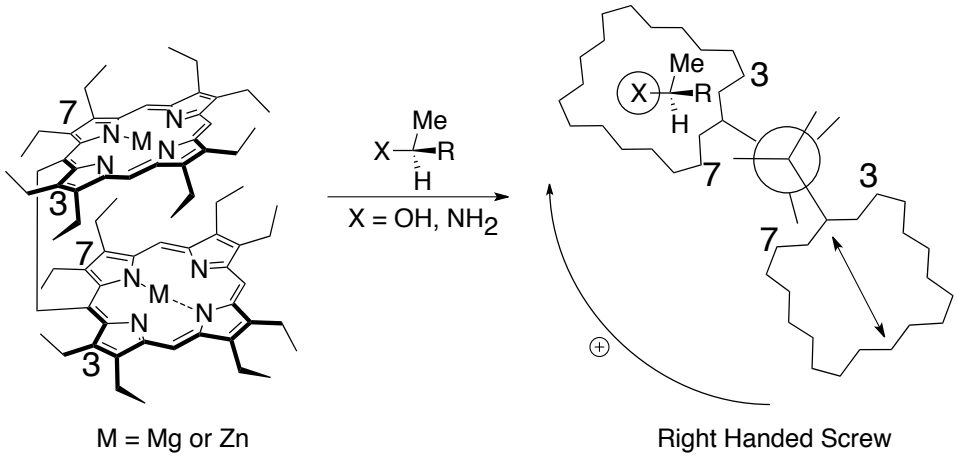

Figure 4-2. Inuoe's porphyrin tweezer for stereochemical determination.

The mechanism of the chiral induction is based on the chiral ligand binding to zinc, and subsequent formation of either right- or left-handed twist, due to steric interactions between the ethyl groups on the porphyrin ring, and the largest substituent on the asymmetric carbon of the ligand. Upon addition of the chiral substrate, it binds to one porphyrin of the tweezer, and the steric interaction between the chiral center and the ethyl groups at 3,7 positions of the non-bound porphyrin drive the non-bound porphyrin to slide away generating a right-handed screw for *S*-substrates and right-handed screw for *R*-substrates. The major drawback of this method is the requirement of an excess of the chiral molecule, as well as low intensity signals for the alcohols.

Perhaps the most commonly used method for assigning absolute stereochemistry of mono amines is the Mosher ester analysis.[7] This method involves the preparation of diastereomeric MTPA (or MPA) amides from the two enantiomers of MTPA and the amine of unknown

configuration. The NMR spectra of the two diastereomeric derivatives are then recorded and the differences in the chemical shifts are calculated. Mosher's proposal of the most relevant conformer in solution is generally accepted. In this proposal, for each diastereomer, the most relevant conformer adopts the *s*-trans arrangement around its N-C-O bonds and the CF_3, carbonyl, NH, and C(1') methane proton groups are all in the same plane, and the CF_3 and the carbonyl units are arranged in a *syn*-periplanar disposition (Figure 4-3). While this is not the only possible conformation, it represents a model that successfully correlates the known results, and as stated by Mosher, the conformation is not intended to represent the preferred ground state conformation of the molecules and may be an average of many conformations.[8] In this proposed model (Figure 4-3), substituent S_2 is shielded in the (*R*)-MTPA amide (Figure 4-3 A). Similarly, substituent S_1 is shielded by the phenyl substituent in the (*S*)-MTPA amide (Figure 4-3 B).

For the amine shown, substituent S_1 has negative $\Delta\delta^{SR}$ values and substituent S_2 has positive values (Figure 4-3 C). In the case where the amine has the opposite configuration, as in case D, the signs for the $\Delta\delta^{SR}$ values of S_1 and S_2 are expected to switch.

While these methods works well for amines and are routinely used, for compounds that are available in short supply (like in the case of initial structural studies of a newly isolated natural product) the requirement for derivatization of the amines before analysis as well as the empirical nature of Mosher analysis is a major limitation. For these reasons, it is desirable to develop methods that avert these drawbacks.

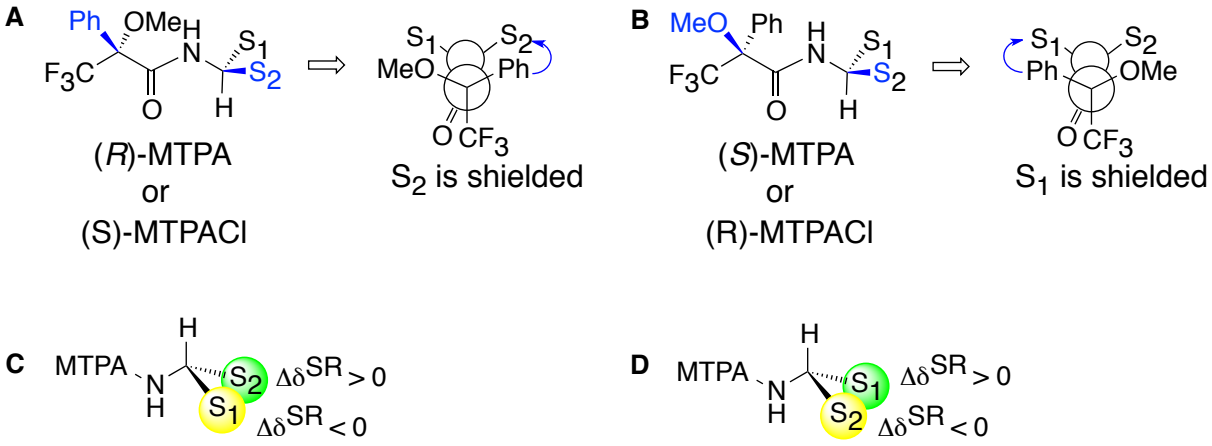

Figure 4-3. (A, B) Mosher's model for correlating the configuration with the ^{1}HNMR shifts. (C, D) expected signs of $\Delta\delta^{SR}$.

4-2 ECCD Studies of Chiral Monoamines Using MAPOL

As mentioned in Chapter 3, biphenols and amines form hydrogen bonding complexes in solution.[9] Therefore it was hypothesized that a chiral mono amine would cause stereodifferentiation in the MAPOL host via the hydrogen bonding interaction. The helicity of MAPOL could be determined by ECCD and this would be related back to the absolute configuration of the amine.

If our designed system works as expected, the principle advantage would be the analysis of absolute stereochemistry without the pre-requisite derivatization as with the tweezer methodologies or Mosher ester analysis. Atropisomers exist as racemic mixtures of the *P* and *M* enantiomers. However, this equilibrium can be perturbed by the introduction of a chiral bias, creating distereomers and causing one confomer to be favored over the other as the complex interacts with the chiral ligands. Our interest in the design of MAPOL is to exploit this phenomenon, while taking advantage of the ability of the porphyrins to couple with each other,

leading to observable ECCD. We could then directly relate the sign of the ECCD to the chirality of the bound amines.

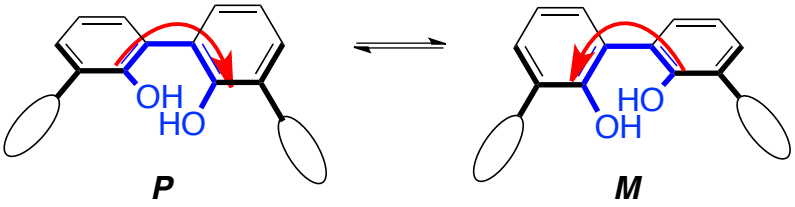

Figure 4-5. *P* and *M* conformers of MAPOL at equilibrium.

MAPOL consists of two porphyrin units and a 2,2'-biphenyl linker. The *P* and *M* helicity of the system is dictated by the rotation around the C-C single bond between the phenyl units (Figure 4-5). At equilibrium, there is a racemic mixture of atropisomers, and if undisturbed, the system can rest in this equilibrium state indefinitely. Additionally, when at equilibrium, MAPOL is inherently ECCD inactive. However, upon introduction of a chiral amine to the system, (based on the results discussed in Chapter 3, indicating a 1:1 amine:host complex formation) we postulate that the chirality of the amine will cause a preferential hydrogen bonding to favor one atropisomer of MAPOL.

Assuming that sterics are responsible for chirality recognition, during the complexation, the largest group on the asymmetric center will position itself in the least sterically encumbered location (Figure 4-6). For both the *P* or *M* atropisomers, there is a large cavity for the largest group to occupy. It is believed that the large group plays no role in stereodiscrimination. Nonetheless, in one helicity of MAPOL, the medium group of the amine will be situated in a more sterically tolerable region, and the smallest group will occupy the most sterically congested area.

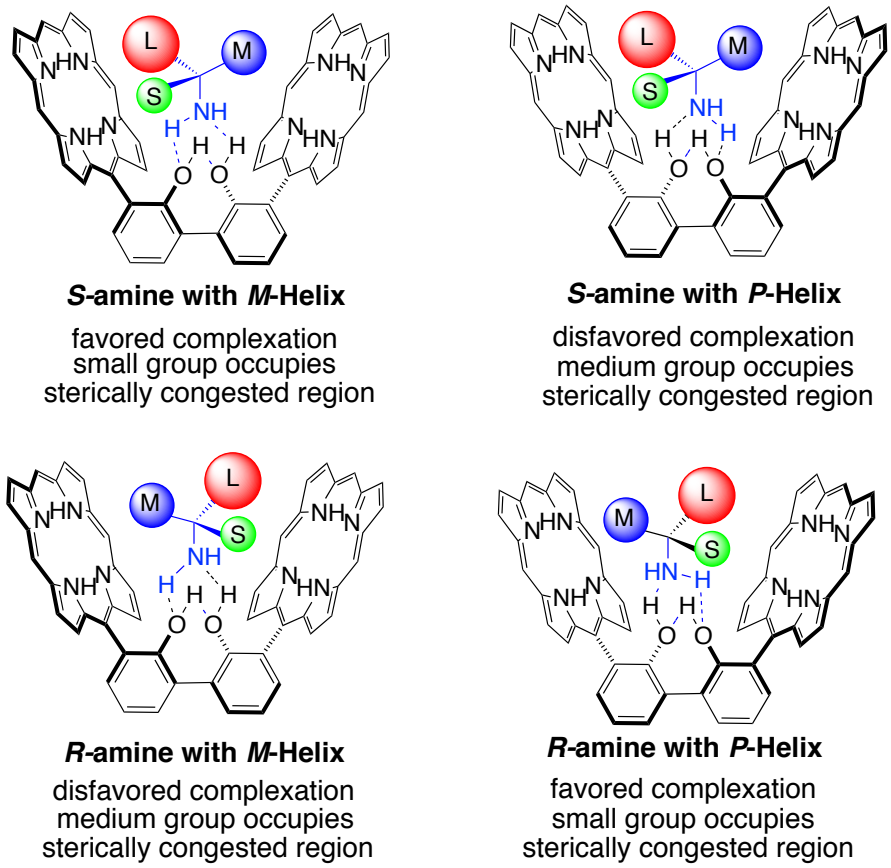

Figure 4-6. Proposed complexation if chiral amine with *P*- and *M*-Helicities of MAPOL.

However, in the other helicity of MAPOL, the opposite would be true, and there will be a more sterically unfavorable interaction with the medium group. In this way, the amine will bind to the MAPOL in the sterically favored helicity. Since the barrier to rotation about the biphenol C-C single bond is small,[10] the equilibrium will shift to create an over-population of the favored helicity. The excess of one helicity over the other will lead to an observed ECCD spectrum as a result of exciton coupling of the porphyrins arranged in a chiral fashion within the sterically preferred complex.

Figure 4-7 shows a proposed enantiodiscimination mechanism using a chiral amine. In A,

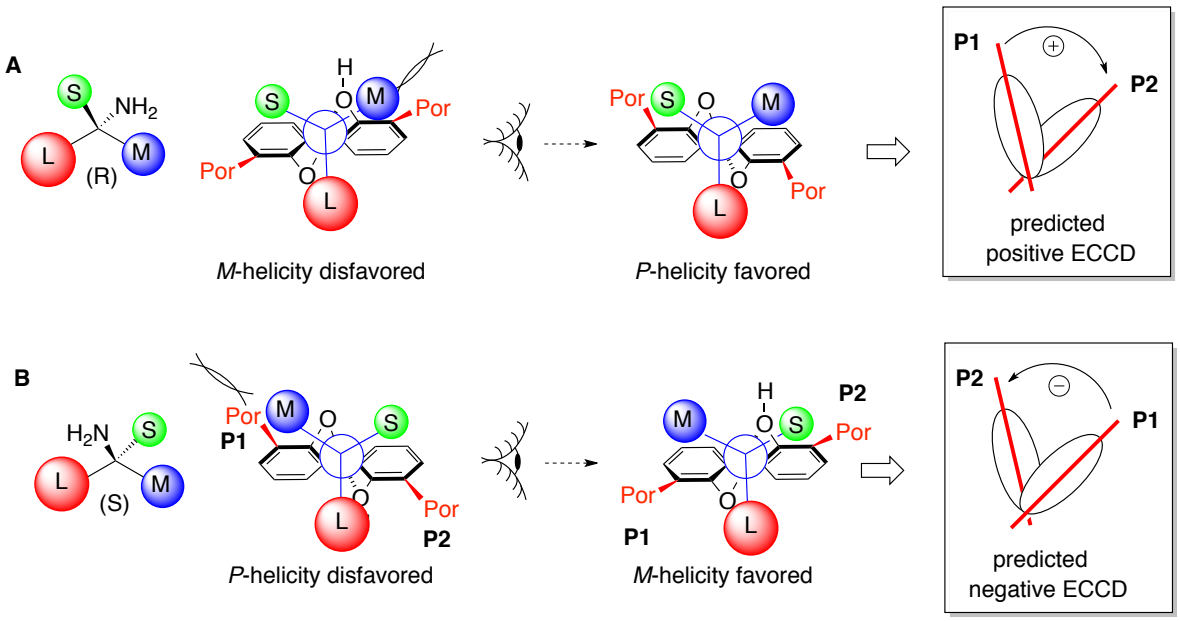

Figure 4-7. Newman projections of a chiral amine complexed with *P*- and *M*-helicities of MAPOL. Inserts: the predicted ECCD signs from the favored conformation. A) (*S*)-amine binds favorably with the *M*-helix, resulting in a predicted negative ECCD. B) (*R*)-amine preferably binds with the *P*-helix, yielding a predicted negative ECCD.

if *S*- amine binds with the P-helix of MAPOL, there would be unfavorable steric interactions between the medium group and the phenyl ring of MAPOL, hence the (*S*)- amine preferably binds with the M-helix. This places the porphyrins in a counterclockwise arrangement that would result in a negative CD sign. On the other hand, the (*R*)- amine preferably binds with the P-helix, avoiding the unfavorable steric interactions that would occur between the medium group and the phenyl ring in the M-helix of MAPOL. In this complex, the porphyrins are arranged in a clockwise manner, resulting in a predicted positive CD sign.

4-2-2 Determination of Chirality for Primary Amines

In light of the above proposal, MAPOL **9** was examined for configurational assignment of a variety of chiral mono amines via the Exciton Coupled Circular Dichroism protocol. To our

delight, consistent and prominent bisignate CD signals at the porphyrin Soret region were observed upon addition of micromolar concentrations of a variety of chiral amines to a solution of MAPOL in hexanes. As shown in Table 4-1, a number of alkyl and aryl primary amines were tested. The *S* amines resulted in negative ECCD spectra while positive signals were observed for the *R* amines. Furthermore, enantiomeric pairs yielded opposite ECCD spectra (compounds **5*R*** and ***S***, **3*R*** and ***S*** and **2*R*** and ***S***). Of particular note is compound **5**, where the system is able to register small differences in size based on their A value (methyl-1.74 vs. ethyl-1.79). In addition, the system is tolerant of other potential H-acceptor groups like esters (**9*S***).

The correlation between substrate chirality and the sign of ECCD is illustrated in Figure 4-8, as shown for (*S*)-cyclohexyl ethylamine. For both the *P* or *M* helicity of the complex, the large cyclohexyl group is positioned in the least sterically encumbered location, while the location of the medium (CH_3) and small (H) groups is dictated by the configuration of the chiral center as illustrated. In A, the medium group (CH_3) is situated in a more sterically tolerable region, while the smallest group (H) occupies the most sterically congested area. On the other hand, the *P* complex would have a sterically unfavorable interaction between the medium (CH_3) group and porphyrin. In this way, the more favorable *M*-helicity is promoted in binding with the *S*-enantiomer. An over-population of the *M* helicity leads to an excess of the counterclockwise orientation of the porphyrins and the observed negative ECCD spectrum (Table 4-1, entry 1).

Table 4-1. ECCD data for chiral amines bound to MAPOL.

entry	amine	predicted sign	MAPOL λ nm, (Δε)	MAPOL A
1	**7***S* 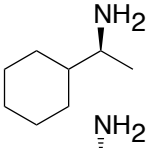	neg	418, -237 409, +257	-494
2	**7***R* 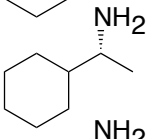	pos	419, +187 410, -345	+532
3	**8***S* 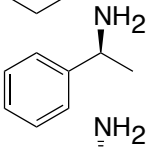	neg	429, -15 420, +46	-61
4	**8***R* 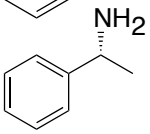	pos	427, +36 409, -12	+48
5	**9***R* 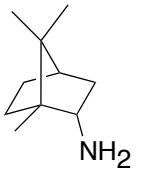	pos	418, +153 420, -62	+215
6	**10***R* 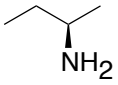	pos	425, +161 412, -177	+338
7	**10***S* 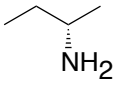	neg	425, -60 411, +108	-168
8	**11***R* 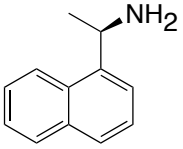	pos	423, +41 414, -26	+67
9	**12***R* 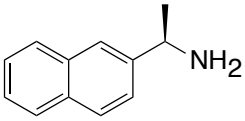	pos	422, +147 414, -59	+206
10	**13***S* 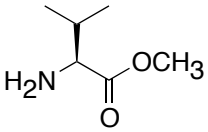	neg	427, -14 415, +24	-38
11	**14***S* 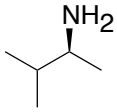	neg	428, -30 412, +90	-120
12	**15***R* 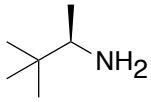	pos	429, +62 412, -121	+183

host:guest ratio – 1:20, 1 μM host concentration in hexane at 0 °C was used for all measurements.

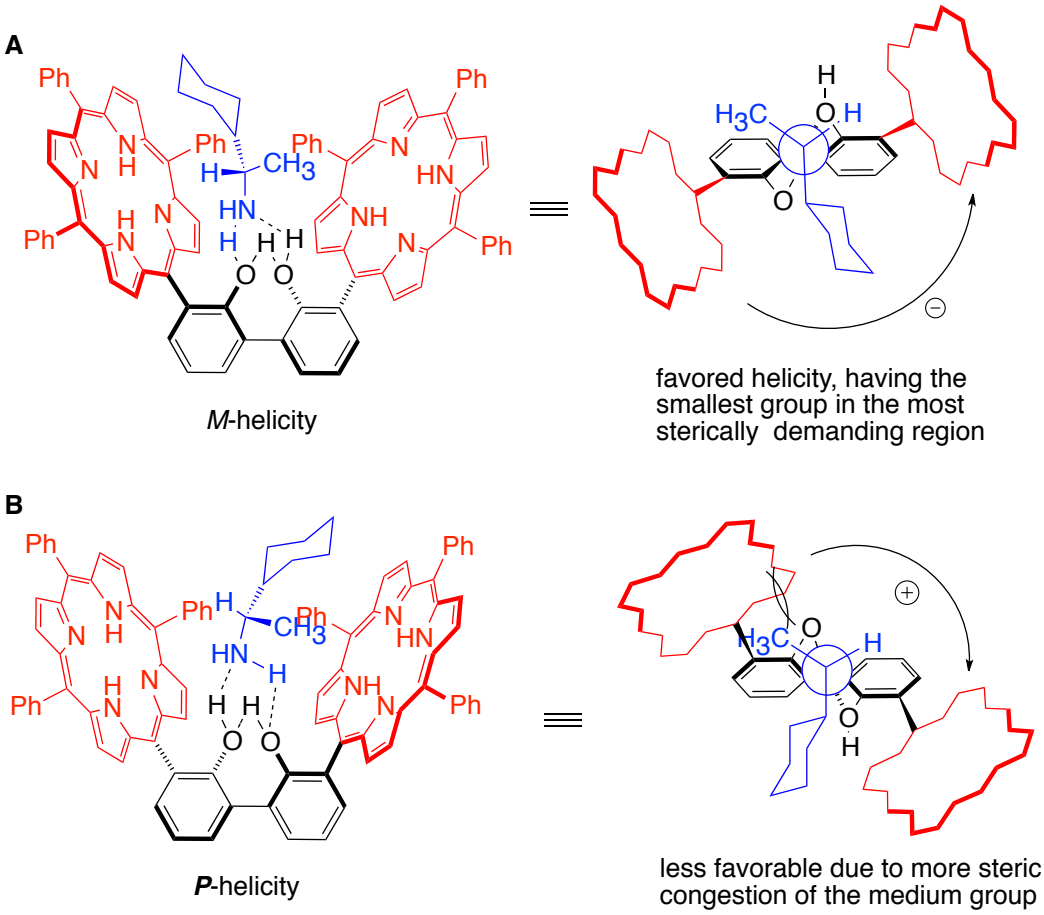

Figure 4-8. Proposed binding model for (*S*)-cyclohexyl ethylamine to MAPOL. In A, the amine binds to the M-helix and in B, the amine binds to P-helix. The complex formed in B is sterically less favorable due to steric congestion between porphyrin and methyl group.

Additional confirmation that complex formation between MAPOL and amine occurs via hydrogen bonding and not coordination to the porphyrin, was supported by the fact that when analogue **44** was used as a control in place of MAPOL **9**, the solution, upon addition of chiral mono amines under similar conditions, induced no CD spectra.[11] Moreover, even though Zn-MAPOL **58** yielded CD signals with primary amines, as shown in Table 4-2, in general, the amplitudes were lower than those obtained with MAPOL **9**.

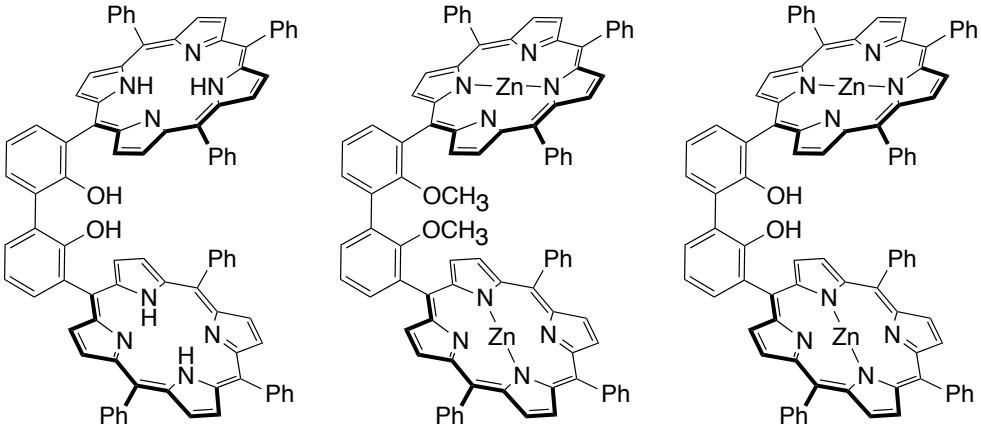

Figure 4-9. MAPOL and analogues of MAPOL used for ECCD studies.

Additionally, a higher concentration of **58** (2 μM) was required in order to obtain ECCD. Even though most of the ECCD signals observed with **58** were consistent with the predicted ECCD signals for **9**, several amines like (**4***R* and **10***S* and **11***R*) did not produce consistent results with **58**. It is important to note that with amines **5***S*, **5***R*, **10***S* and **11***R*, the quality of the signal with **9** is improved to that observed with **58** (Figure 4-10). These inconsistent signs and complex spectra are presumably due to competitive binding to the Zn metal in the porphyrin. Also amine coordination to the zinc could lead to crowding of the binding pocket, preventing efficient hydrogen bonding with the host.

Table 4-2. ECCD data for chiral amines bound to MAPOL[a] and Zn-MAPOL[b] in hexane.

	amine	predicted sign	MAPOL		Zn-MAPOL	
			λ nm, (Δε)	A	λ, nm, (Δε)	A
2*S*	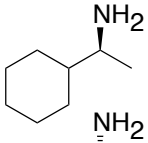	neg	418, -237 409, +257	-494	428, -133 419, +98	-231
2*R*	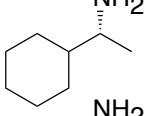	pos	419, +187 410, -345	+532	428, +136 420, -95	+231
3*S*	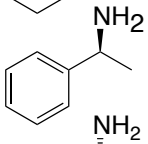	neg	429, -15 420, +46	-61	426, -29 420, +25	-54
3*R*	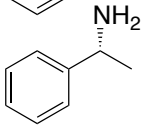	pos	427, +36 409, -12	+48	426, +32 421, -15	+47
4*R*	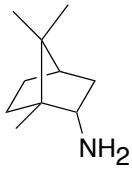	pos	418, +153 420, -62	+215	429, -31 420, +32	-63
5*R*	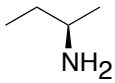	pos	425, +161 412, -177	+338	427, +12 419, -7	+19
5*S*	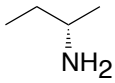	neg	425, -60 411, +108	-168	426, -8 417, +3	-11
6*R*	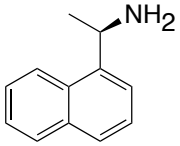	pos	423, +41 414, -26	+67	427, +69 421, -12	+81
7*R*	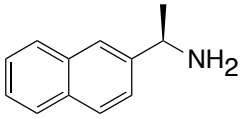	pos	422, +147 414, -59	+206	420, +117 412, -39	+156
8*S*	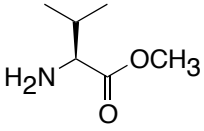	neg	427, -14 415, +24	-38	429, -39 418, +43	-82
10*S*	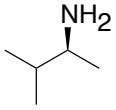	neg	428, -30 412, +90	-120	no ECCD	
11*R*	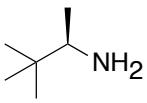	pos	429, +62 412, -121	+183	no ECCD	

host:guest ratio – 1:20, [a]1 μM, [b]2 μM host concentration of host at 0 °C was used

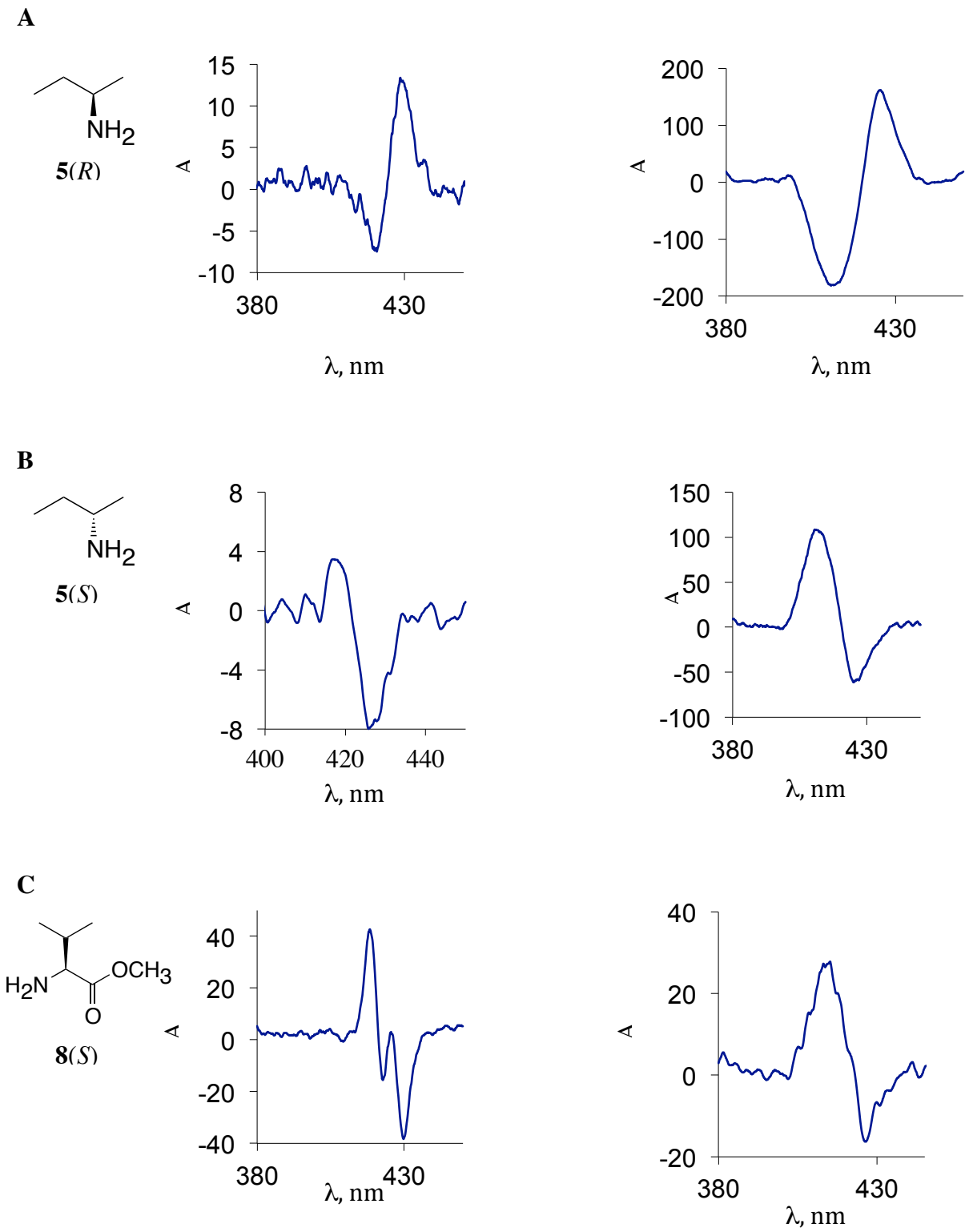

Figure 4-10. CD signals of amines A) **5***R*, B) **5**S, and C) **8***S* with Zn-MAPOL **58** and MAPOL **9**. All amines show better amplitudes and CD spectra with MAPOL.

4-3 Determination of Chirality for Secondary Amines

Following the success of MAPOL for assigning absolute configuration of primary amines, secondary amines seemed like a natural extension of the methodology. Secondary amines, like primary amines, are also of great interest due to their roles as anti-tumor agents, antibiotics, as well as plant growth regulators and promoters.[1] In synthetic chemistry, they have been used as chiral auxiliaries for asymmetric catalysis, chiral resolving agents as well as chiral intermediates in the synthesis of bioactive complex molecules.[12]

4-3-2 Conventional Methods of Assigning Absolute Stereochemistry of α-Chiral Secondary Amines

In a similar manner as for primary amines, the absolute configurational assignment of chiral secondary amines has been achieved by Mosher ester analysis method[13] as well as CD spectroscopy.[14]

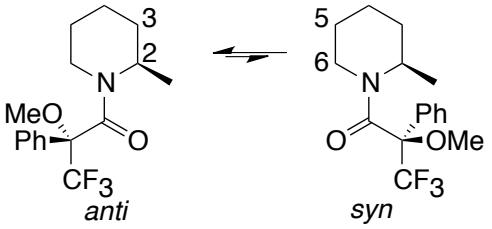

Figure 4-11. The *syn* and *anti* conformers of the (*R*)-MTPA amide of (*R*)-2-methylpiperidine in equilibrium.

Hoye et al. reported a procedure for the assignment of the absolute configuration of *cyclic* secondary amines with the stereocenter located at either the α- or β-positions.[13b] They accomplished this by using the Mosher ester analysis method, using MTPA as the CDA. Their

proposed model follows the standard procedures of comparing the ^{1}H-NMR spectra of the corresponding (*R*)- and (S)-MTPA amides; however the ^{1}H-NMR spectra of these MTPA amides indicated the presence of two rotamers (*syn* and *anti*) in equilibrium with each other shown in Figure 4-11. Therefore, the rules for correlating the NMR shifts and configuration warrant some more explanation. Recalling, Mosher's proposed model[8] of the most relevant conformer discussed in Section 4-1-2 above, the CF_3, carbonyl, NH, and C(1')H groups should all be in the same plane. In addition, the CF_3 and the carbonyl units should be arranged in a *syn*-periplanar manner. Because of this, it is important to differentiate the spectra of the rotamers because, only the signals of the rotamer that has the asymmetric carbon of the MTPA placed *syn* to the asymmetric carbon of the amine should be considered.

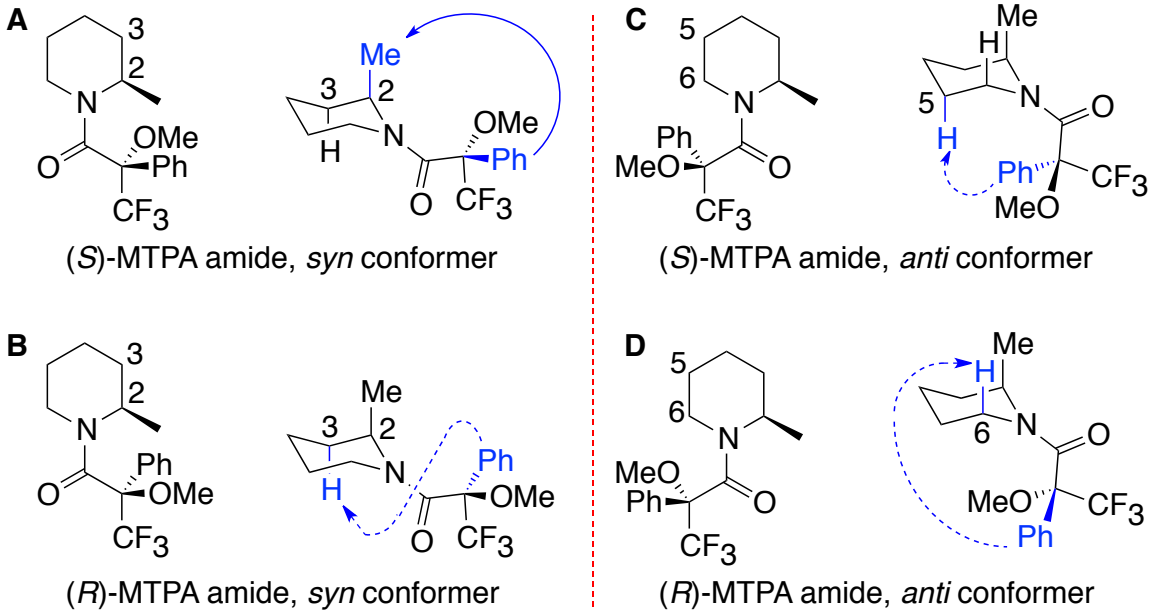

Figure 4-12. *Syn* and *anti* rotamers for the (*S*)- and (*R*)-MTPA amides of (*R*)-2-methylpiperidine.

For example, in the assignment of (*R*)-2-methylpiperidine shown in Figure 4-12, only the signals due to the *syn* rotamer A and B in the (*S*)- and (*R*)-MTPA amides are relevant and only the $\Delta\delta^{SR}$ values corresponding to these rotamers are valid for assignment purposes. In contrast, the *anti* conformers C and D should not be considered.

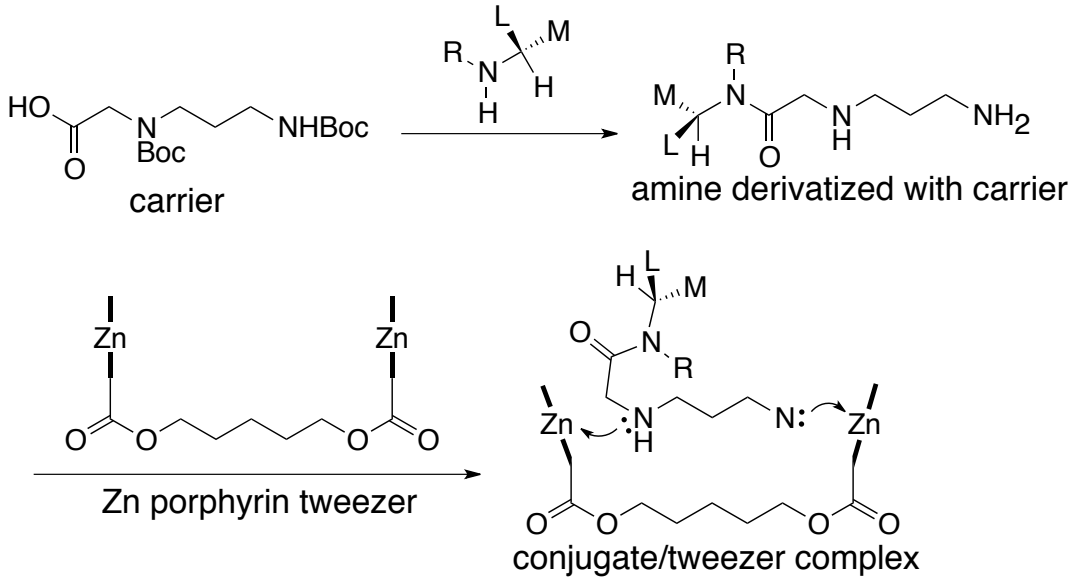

Scheme 4-3. Complex between carrier/monoamine conjugate and porphyrin tweezer.

A second requirement of this method is that only the axial substituents in the *syn* rotamers should be compared to obtain the $\Delta\delta^{SR}$ value. This is because the axial substituents are more exposed to the shielding/deshielding effects of the CDA. For example, after identifying the resonances for the *syn* rotamer in the spectra of the (*S*)- and (*R*)-MTPA amides, the signals due to the axial proton at C-3 (Figure 4-12 A and B) should then be used to obtain the $\Delta\delta^{SR}$ value. Here, the axial methyl group is more shielded in the (*S*)-MTPA amide (Figure 4-12 A) than in the (*R*)-MTPA amide (Figure 4-12 B), and the H-3 proton is more shielded in the (*R*)-MTPA

amide (Figure 4-12 B) than in the (*S*)-MTPA amide (Figure 4-12 A). The resulting $\Delta\delta^{SR}$ values are negative for the methyl at C-2 and positive for the proton at C-3.

The assignment of absolute configuration of secondary amines has also been studied using ECCD spectroscopy (Scheme 4-3). Here, like the case of primary amines, the secondary amines are first derivatized with a carrier molecule in order to provide the required two sites of coordination.[14] The requirement, by both the ECCD methodology and Mosher ester analysis, for derivatized of the sample before analysis, as well as the empirical nature of the Mosher ester analysis method is a major limitation for these methods.

4-3-3 ECCD studies of secondary amines using MAPOL

We envisioned a similar binding and stereo-differentiation mechanism for secondary amines as that of primary amines. Figure 4-13 shows the proposed binding for (*R*)-benzhydrylpyrrolidine, where in both the *P* or *M* helicity of the complex, the large group, (in this case, the methine carbon with the two phenyl groups) is positioned in the least sterically encumbered location.

In the *P* complex (Figure 4-13A), the medium group (chain of ring) is situated in the more sterically tolerable region, while the smallest group (H) occupies the most sterically congested area. On the other hand, the *M* complex would have a more sterically unfavorable interaction between the medium group and porphyrin. In this way, the more favorable *P*-helicity would be promoted in binding with the *R*-enantiomer, leading to a predicted positive ECCD spectrum, while *M*-helicity would be promoted in binding with the *S*-enantiomer and would result in a predicted negative ECCD spectrum.

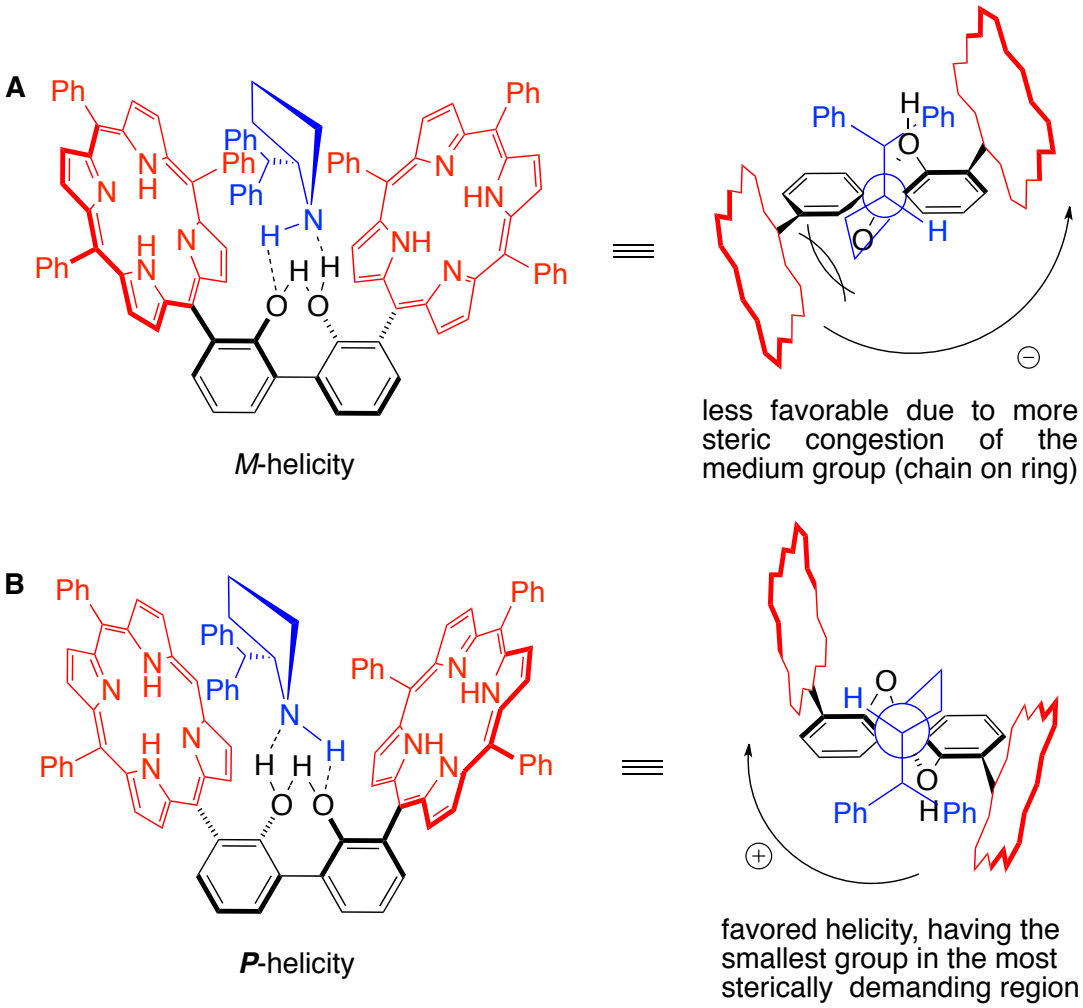

Figure 4-13. Proposed binding model for (*R*)-benzhydrylpyrrolidine to MAPOL. In A, the amine binds to the M-helix and in B, the amine binds to P-helix. The complex formed in A is sterically less favorable due to steric congestion between porphyrin and chain of ring.

To our delight, upon addition of chiral secondary amines to a solution of MAPOL in hexane, prominent CD signals were observed (Table 4-3). However, as can be seen in Table 4-3, the obtained ECCD signs do not match the predicted signs using the same binding model as primary amines. Additionally, no ECCD is observed with substrate **14***R*. Presumably, a different mechanism for enantiodiscrimination is at play for secondary amines than that of primary

amines, and so the working model used for primary amines cannot be used for secondary amines. However, despite this fact, the results were promising, in that amines with opposite stereochemistry yielded opposite CD signals, meaning that whatever the source of enantiodiscrimination is, it is consistent. Therefore, further studies on a larger substrate scope are necessary to investigate trends for MAPOL with secondary amines. Efforts to this end will continue in order to identify the source of enantiodiscrimination that could be used to derive a predictable mnemonic for secondary amines.

Table 4-3. ECCD data of chiral secondary amines bound to MAPOL in hexane.

	amine	predicted sign	λ, nm, (Δε)	A
12*R*	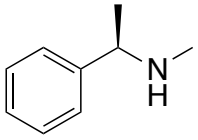	pos	419, -14 412, 47	-61
13*S*	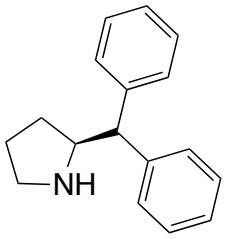	neg	422, 113 411, -42	+155
14*R*	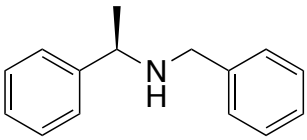	pos	no ECCD	

host:guest ratio – 1:20, 1 μM host concentration at 0°C was used for all measurements.

4-4 Chiral aziridines

Chiral aziridines are useful building blocks for rapid access to nitrogen-containing molecules and heterocycles that are important to pharmaceutical and biologically related fields.

In the past decade, substantial amount of work has focused on the asymmetric synthesis of chiral aziridines[15] as well as their ring-opening reactions.[15a, 16]

Unlike the well developed asymmetric epoxidations of olefin double bond which could afford epoxy alcohols in a straightforward way and provide well-recognized mnemonics facilitating the empirical assignment of chirality for products, there is no direct access to chiral aziridines from olefins and hence no simple mnemonic available for its chirality assignment. Comparing the optical rotations of ring opened products with reported values is also frequently used. The empirical nature of both methods is a major limitation and the latter approach also suffers from extra synthetic work with sensitive molecules. Furthermore, the necessary transformations and derivatizations are inefficient and time consuming. A general non-empirical expedient protocol addressing the absolute stereochemistry of chiral aziridines has not emerged.

4-4:1 ECCD Studies of Chiral Aziridines Using MAPOL

We wish to be employ MAPOL in the absolute stereochemical determination of aziridines.

Table 4-4. ECCD data of chiral aziridines bound to MAPOL in hexane.

	aziridine	predicted sign	MAPOL λ, nm, (Δε)	A
24-trans	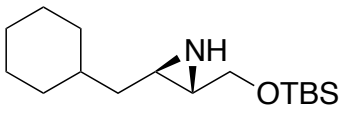	neg	428, -18 409, +21	-39
25-trans	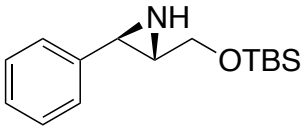	neg	431, +135 422, -79	+214
26-cis	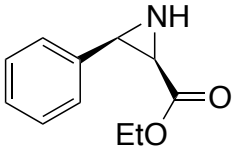	pos	426, +28 418, -18	+46
27-cis	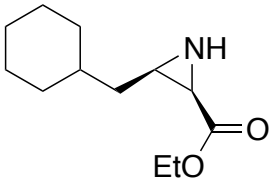	pos	429, -9 420, +21	-30

host:guest ratio – 1:20, 2 μM host concentration at 0 °C was used for all measurements.

The aziridines studies behaved similar to the secondary amines, where, as can be seen in Table 4-4, the obtained ECCD signs do not match the predicted signs using the same binding model as primary amines. Further studies on a larger substrate scope are currently underway to investigate any trends and establish working models for aziridines.

To conclude, we have developed a novel host system and successfully employed it for the absolute stereochemical assignment of primary amines. In addition, we have developed a working model that correlates the observed CD signs to the chirality of the bound primary amines. Moreover, we have demonstrated that MAPOL could potentially be used for absolute configurational assignment of secondary amines and aziridines. However, we have shown that the models that apply to primary amines cannot be applied to secondary amines and aziridines since they predict results opposite to those obtained experimentally. Because of the importance of this class of compounds, additional studies are currently on-going to develop a working model for these two important classes of functional groups, as well as establish a wider substrate scope.

Experimental procedures

The solvents used for CD measurements were purchased from Aldrich and were spectra grade. All reactions were performed in oven or flame dried glassware under nitrogen. Solvents used for synthesis of compounds were dried as follows: THF dried over Sodium, dichloromethane dried over CaH_2. Column chromatography was performed using SiliCycle silica gel (230-400 mesh). ^{1}H-NMR spectra were obtained on Varian Inova 300 MHz, 500 MHz or 600 MHz instruments and are reported in parts per million (ppm) relative to the solvent resonances (δ), with coupling constants (*J*) in Hertz (Hz). IR studies were performed on a Galaxy series FTIR 3000 instrument (Matteson). CD spectra were recorded on a JASCO J-810 spectropolarimeter, equipped with a temperature controller (Neslab 111) for low temperature studies, and is reported as λ [nm] ($\Delta\varepsilon_{max}$ [mol^{-1} cm^{-1}]).

Determination of binding constant

The stock solution of Zn-porphyrin tweezer (1 mM in hexane) was titrated with guest molecule (10 mM in DCM) at different equivalents and the UV-vis spectra was recorded after each addition. The addition of chiral substrate was continued until no visible change in the spectra was observed. Upon formation of the chiral complex, the Soret band of the porphyrin tweezers underwent red-shifts through an isosbestic point. The change of absorption at certain wavelength as a function of the substrate concentration yields an exponential saturation curve, which can be fitted to the following non-linear least square equation:

$$Abs = L * [\frac{(Kx + Ka + 1) - \sqrt{L^2(Kx + Ka + 1)^2 - 4K^2axL^2}}{2 * ka}]$$

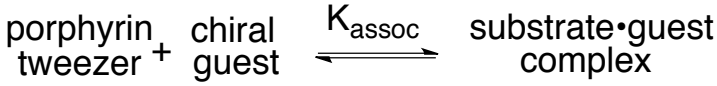

Where:

K = calculated K_{assoc};

Δabs at point of saturation = L;

Total concentration of porphyrin tweezer = a;

Equivalents of chiral substrate added = x (this is the variable);

Assume the concentration of tweezer-substrate formed in equilibrium is A,

Then the concentration of free tweezer is $(a - A)$;

The concentration of free substrate is $(x - A)$;

Since $K_a = \frac{[complex]}{[substrate][tweezer]}$

Then $K_a = \frac{A}{(a-A)(x-A)}$

Thus $A = \frac{(a+x+K_a)-\sqrt{(a+x+K_a)^2-4*a*x}}{2}$

The amount of complex formed, A, could be converted to the absorbance obtained at different concentrations of substrate. When the porphyrin tweezer is saturated with substrate, the amount of absorbance should be the maximum amount of absorbance possible for porphyrin tweezer with concentration of a. And if we assume the absorbance at saturation is L, then the amount of complex formed should be:

$$A = \frac{absorbance}{L} * a$$

Combining the last two equations, the following equation relates absorbance to the amount of substrate added: s

$$Abs = L * [\frac{(ka + kx + 1) - \sqrt{L^2(ka + kx + 1)^2 - 4 * ka * kx}}{2 * ka}]$$

4-4 Synthesis of Chiral Amines

Amine **8** was synthesized from L-Lysine.

All other amines used for the study were obtained from commercial sources and used without further purification.

4-5 Determination of Absolute Stereochemistry of Chiral Carboxylic Acids

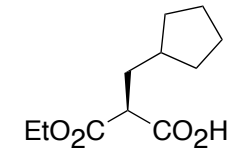

(*S*)-2-Cyclopentylmethyl-propanedioic acid 1-ethyl ester

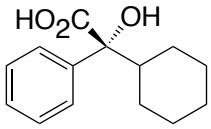

(*R*)-2-Cyclohexyl-2-hydroxy-2-phenylacetic acid

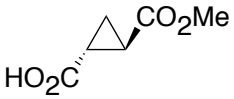

(1*R*,2*R*)-1,2-Cyclopropanedicarboxylic acid monomethyl ester

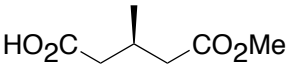

(*R*)-Methyl 3-methylglutalate

Figure 4-14. Examples of some common building blocks containing a carboxylic acid functionality.

Carboxylic acids are commonly found in phamaceuticals and natural products. They play an important role in natural product synthesis and drug development.[17] Some of the different types carboxylic acids found in drugs are salicylic acid, fusidic acid, citric acid, ascorbic acid, benzoic acid and lactic acid. Carboxylic acids are also commonly encountered as intermediates in the synthesis of complex natural products[18] (Figure 4-14). For example, Figure 4-15 shows the final stages of the total synthesis of Swinholide A by Nicolaou.[19] In the synthesis, they made use of the building blocks **15** and **16** in a Yamaguchi esterification to obtain **17** which was then elaborated to the target molecule.

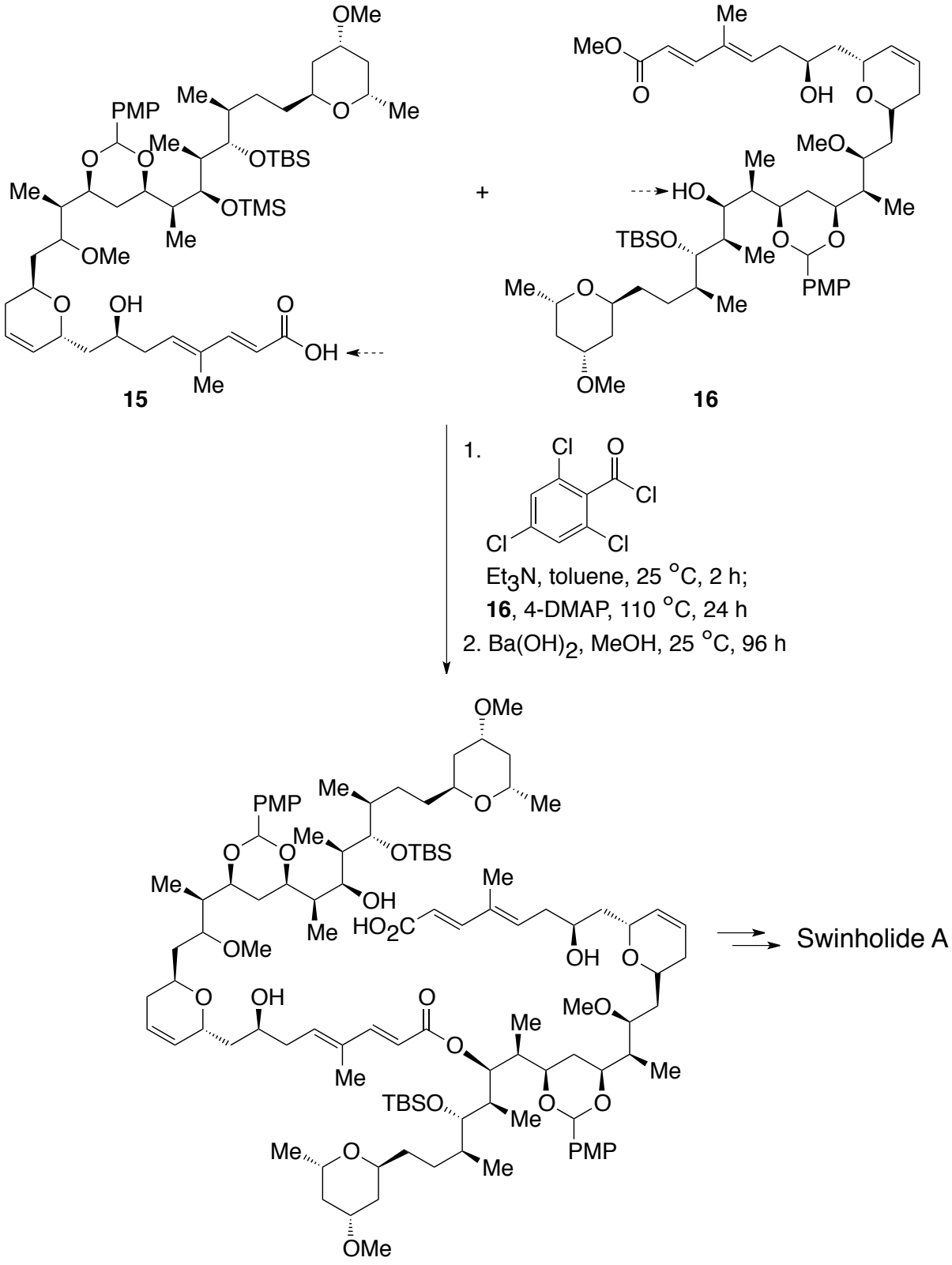

Figure 4-15. Nicolaou's use of a carboxylic acid in the total synthesis of swinholide A.

Chiral carboxylic acids can be divided into two main categories: α-chiral carboxylic acids and carboxylic acids with remote stereocentres, β- and γ-chiral carboxylic acids, each of which will be discussed in more details.

4-5:1 α-Chiral Carboxylic Acids

The most commonly used method for assigning the absolute configuration of α-chiral carboxylic acids is NMR spectroscopy,[20] employing Mosher analysis method (and its modifications). Also the ECCD approach[5b, 21] has been used, after derivatizing the acids with a carrier molecule since the porphyrin tweezer method is not directly applicable to compounds with one site of attachment.

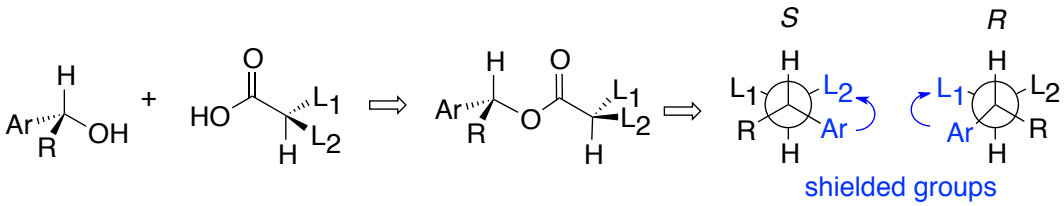

Figure 4-16. Derivatization of an α- chiral carboxylic acid for absolute stereochemical assignment using Mosher analysis.

In the Mosher ester analysis method, the chiral acids are derivatized to either amides or esters, using a chiral derivatizing agent. (CDA)[22] The Mosher analysis method, being empirical, requires the chiral carboxylic acids to be derivatized using both the (*R*)- and (*S*)- enantiomers of the CDA. Figure 4-17 shows some of the more commonly used CDA's. As can be seen, the CDA's usually contain an aryl group that directs its anisotropic cone selectively towards one of the substituents of the asymmetric center of the chiral acid.

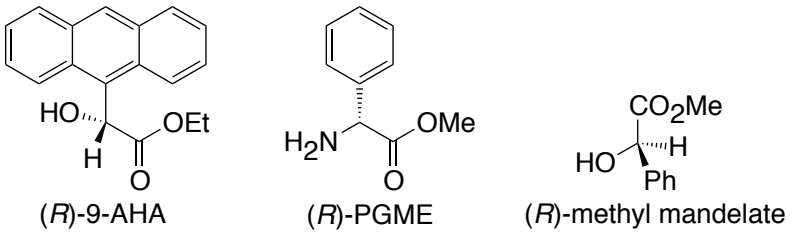

Figure 4-17. Some common CDA's: ethyl 2-(9-anthryl)-2-hydroxyacetate (5, AHA), phenylglycine methyl ester and methyl mandelate.

By comparing the ^{1}H-NMR of the two diastereomeric derivatives, the shielding effect values ($\Delta\delta^{RS}$) for the protons neighboring the chiral center are measured. When using derivatizing agents for the stereochemical determination of α-chiral carboxylic acids, the conformation of the chiral conjugate must be well understood as this could lead to misleading results.[5b, 21] From a practical point, selecting the most suitable reagent for a specific substrate is still problematic and often, the NMR signals of the diastereoisomeric derivatives are too close, requiring extensive conformational analysis to interpret results. In addition, the empirical nature of this method is limiting in cases where the chiral acid is available in limited amounts.

To use chiroptical methods, derivatization of the carboxylic acids with a carrier molecule is usually required. Nakanishi and co-workers[21] first introduced an ECCD protocol for determining the absolute stereochemistry of α-chiral carboxylic acids with derivatization of the substrates as N-γ-aminopropyl amides followed by complexation to a Zn-porphyrin tweezer host, and later Mg-porphyrin host as well[5a] (Figure 4-18 A). Later, Borhan and co-workers[5b] extended this method to work with different carriers (Figure 4-18 B). The choice of carrier plays an

important role, as rigidity/flexibility of the carrier affects the number of possible conformations upon binding to zinc.[5]

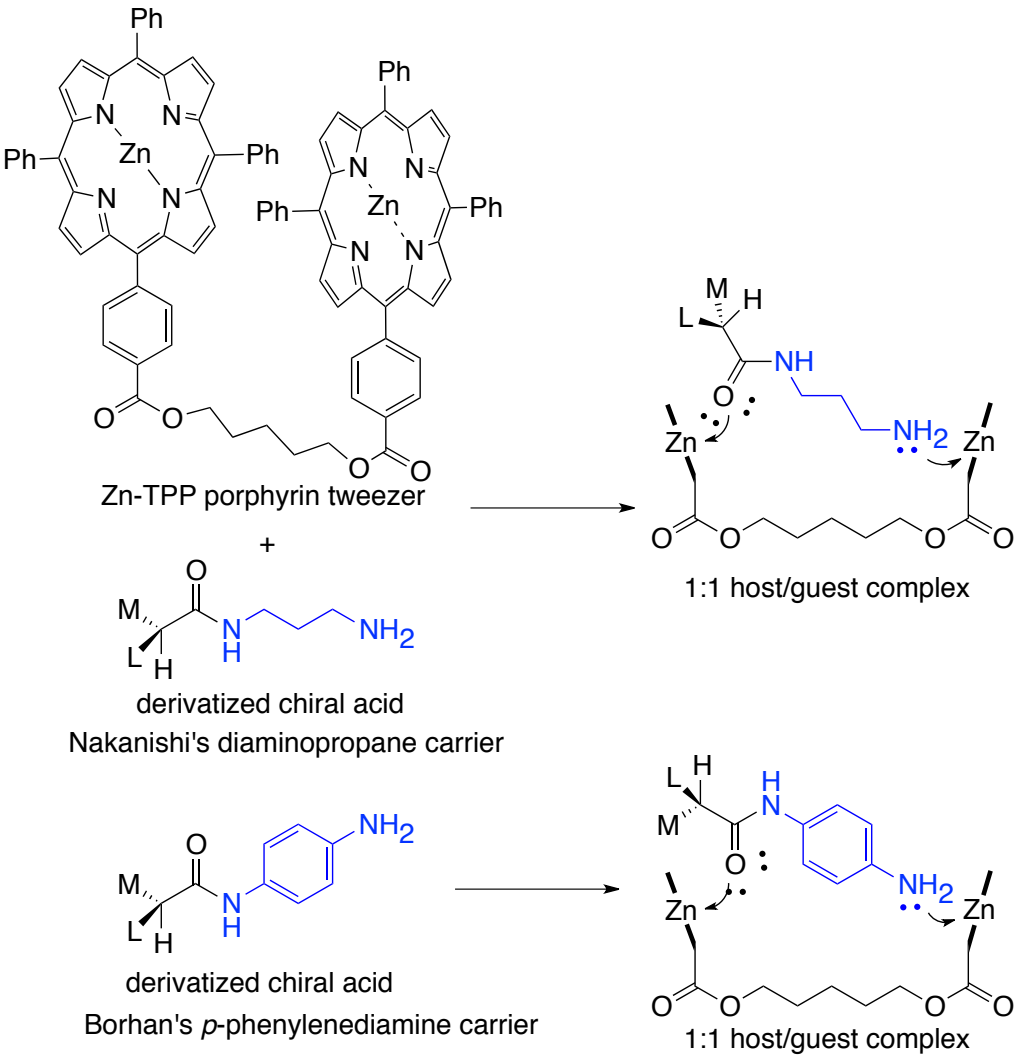

Figure 4-18. Derivatized carboxylic acids with Nakanishi's and Borhan's carriers, for use in CD spectroscopy.

For example, while both carriers above showed consistent ECCD signs with their individual proposed mnemonics, the mnemonics were opposite to each other. This was proposed to be because of the complexes adopting different conformations in solution. Figure 4-19 shows

an example of (*S*)-methyl butyric acid derivatized with both carriers. In Nakanishi's model, the small group (H) is *syn* to the amide hydrogen, and the large (Et) and medium (Me) groups project towards the porphyrin plane, resulting in a positive ECCD. In Borhan's model, the large group (Et) is perpendicular to the carbonyl group, and the medium group (Me) is gauche to the amide hydrogen. The predicted negative ECCD is as a result of the stereodifferentiation between the large and small groups on the chiral centre.

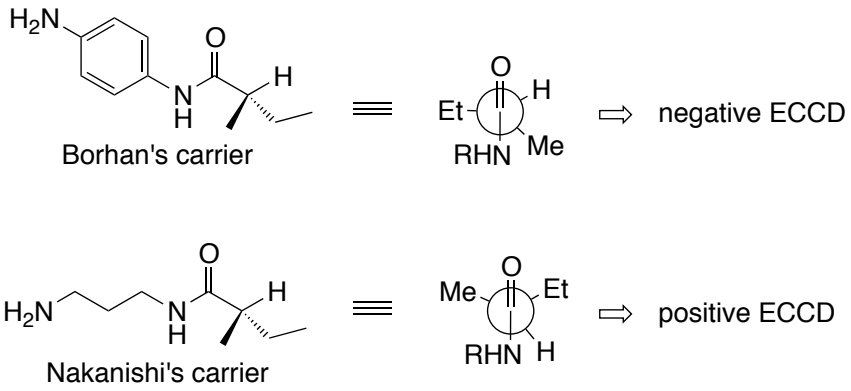

Figure 4-19. Two carriers yielding different ECCD signals.

A recent joint effort from the groups of Canary and Anslyn details a method for determining the absolute configuration of α-chiral carboxylic acids as their carboxylates,[23] without requiring derivatization of the acid. This approach involves complexation of an achiral copper (II) tripodal host shown in Figure 4-20, with the carboxylate of the carboxylic acids. The host system consists of a tri-dentate tripodal ligand with three coordinating arms (chromophores). The

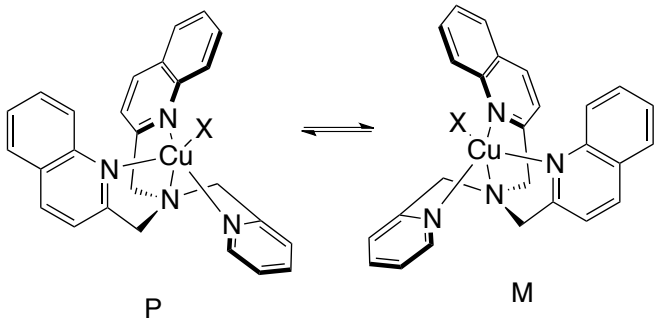

Figure 4-20. At equilibrium, *P* and *M* helices exist in equal amounts.

host, being propeller-shaped, exists in the two enantiomeric forms, *P* and *M* in solution. The ligands occupy four of the five coordination sites of the copper metal, leaving a vacant site for coordination of substrate.

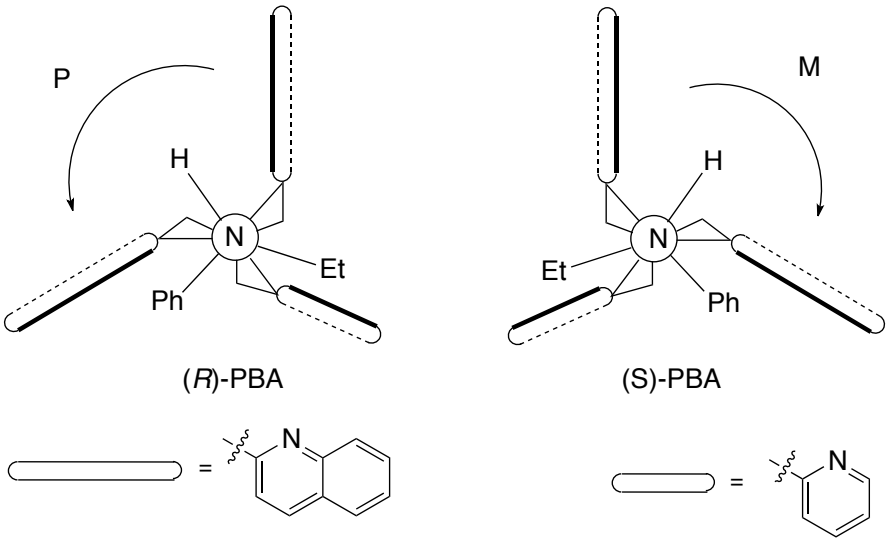

Figure 4-21. Newman projections for triodal system with each enantiomer of PBA bound. An M-propeller gives (+) chirality for the orientation of the quinolone electronic dipole moments.

The substrates are introduced into the host system as the carboxylate form, and upon coordination to the tripod, one twist predominates generating a detectable CD signal. The magnitude and shape of the signal allowed for the assignment of absolute configuration of the carboxylic acids using the pattern recognition protocol LDA.

4-5:2 Use of MAPOL for absolute stereochemical determination of α-chiral carboxylic acids

Following the successful use of MAPOL in assigning the absolute stereochemistry of primary amines, we thought to extend its application to carboxylic acids. Carboxylic acids

cannot directly be assigned using ECCD protocol because they contain only one coordination site. However, as shown in Figure 4-22, the acids can potentially participate in hydrogen bonding with MAPOL.

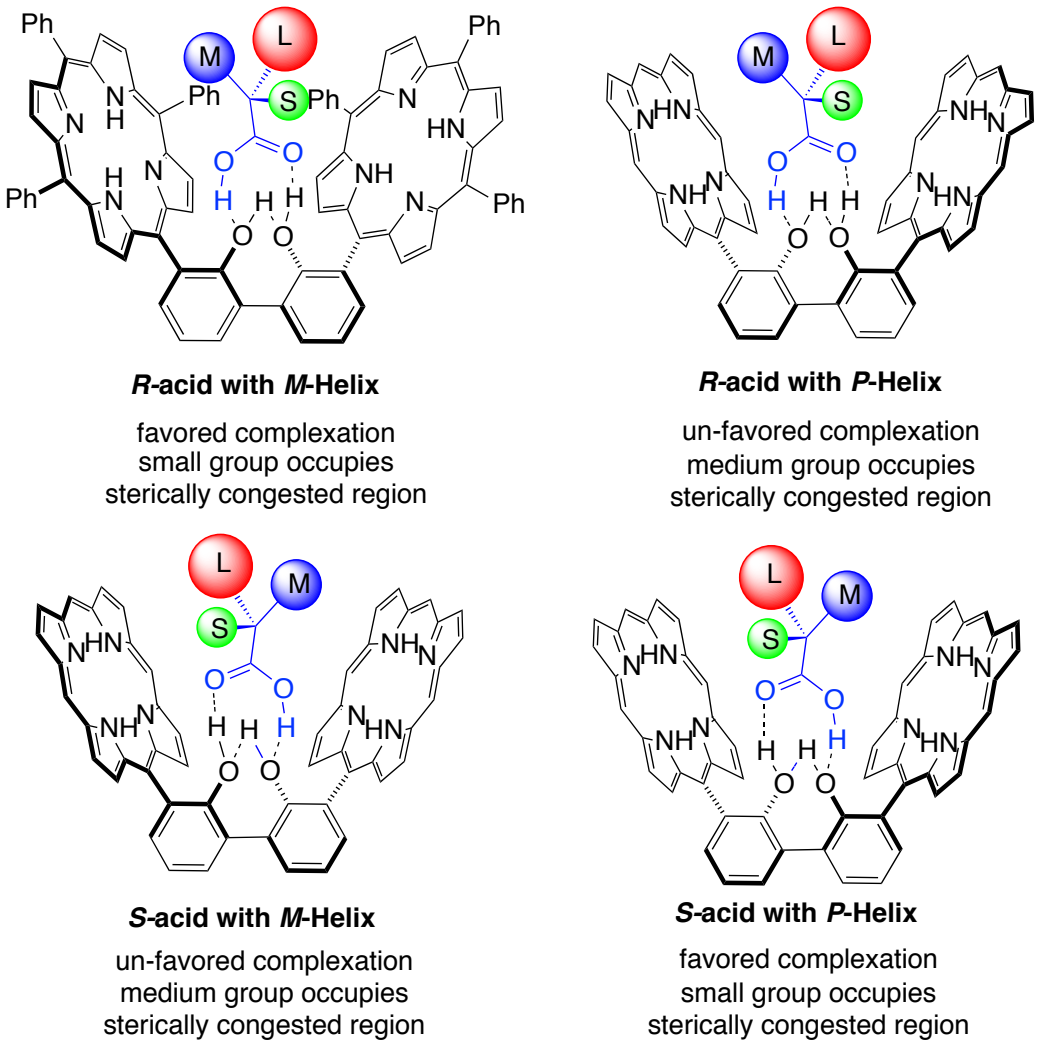

Figure 4-22. Proposed complexation and stereodifferentiation of carboxylic acids with MAPOL.

We postulate that upon introduction of a carboxylic acid to MAPOL in a 1:1 complex, the acid will preferentially bind to one helicity of MAPOL via hydrogen bonding as shown in Figure

4-22. During the complexation, the largest group at the chiral center will position itself in the least sterically encumbered location, which can be achieved in both the *P* or *M* helicities of the complex. Nonetheless, in one helicity, the medium group will be situated in a more sterically tolerable region, and the smallest group will occupy the most sterically congested area. However, in the other helicity, there will be a more sterically unfavorable interaction with the medium group. In this way, the more favorable helicity is promoted in binding with one enantiomer of acid, leading to an over-population of the favored helicity, and ultimately to an observed ECCD spectrum as a result of exciton coupling of the porphyrins due to the chiral twist.

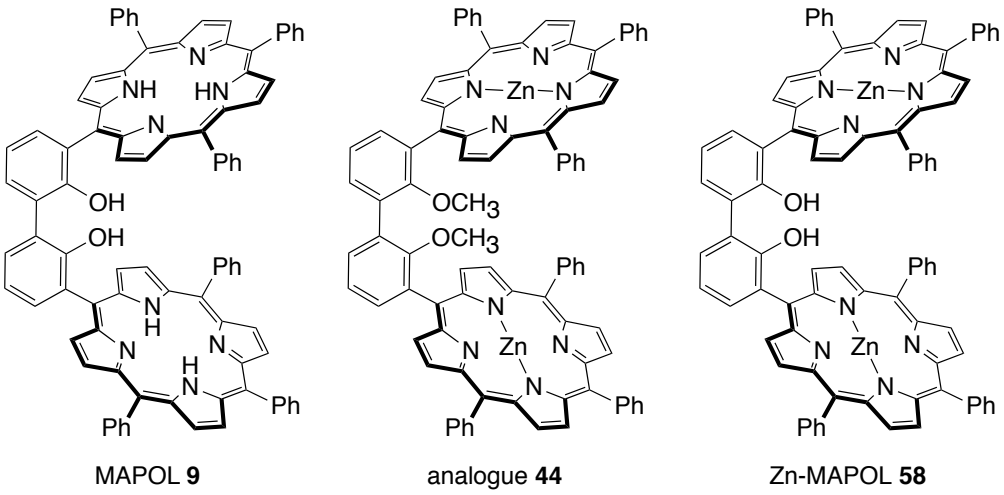

Figure 4-23. MAPOL **9**, MAPOL analogue **44** and Zn-MAPOL **58**.

When several carboxylic acids were tested with MAPOL **9** however, they were ECCD silent. It was proposed that this silence was due to either an inability of the complex to form, or ECCD signals that were too weak to be observed, after formation of the complex. Even more surprisingly, when they were tested with Zn-MAPOL **58**, all of the chiral acids were ECCD active. It is important to note that the CD signals observed with **58** are not from bis-coordination

to both zinc atoms. This is evidenced by a lack of ECCD when analogue **44** was used as a control in place of Zn-MAPOL **58**.

The difference in complexation of MAPOL **9** to amines and carboxylic acids could be explained using acid-base chemistry. In contrast to amines (pKa ~38) that act as the H-acceptor, the carboxylic acids (pKa ~4 – 5) would be the proton donor for MAPOL. For the amines, the complex formed would yield a protonated amine (pKa ~10) while the carboxylic acids would form protonated phenol (pKa ~ -2). Because of this, it would be expected that the hydrogen bonding between MAPOL and carboxylic acids be weaker than the corresponding hydrogen bonding between MAPOL and amines. This weakened hydrogen bonding could explain the lack of ECCD obtained when carboxylic acids were complexed with MAPOL.

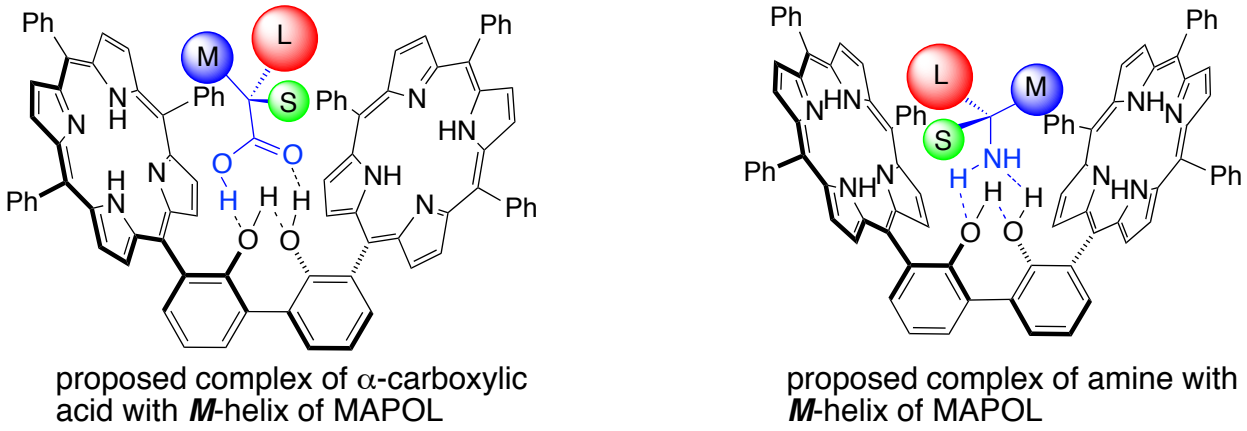

Figure 4-24. Proposed binding of carboxylic acid and amine to MAPOL via hydrogen bonding. The carboxylic acid would act as the H-donor, while the amine would be H-acceptor.

In light of the observations made above with MAPOL and the methylated analogue of MAPOL, we revised the original proposed binding model. Because free base MAPOL did not yield any observable ECCD spectrum with the chiral acids, while Zn-MAPOL did result in

ECCD active complexes with all chiral acids, we propose that unlike the amines, the carboxylic acids bind to host via a two-point complexation involving both the zinc metal and biphenol unit as shown in Figure 4-25.

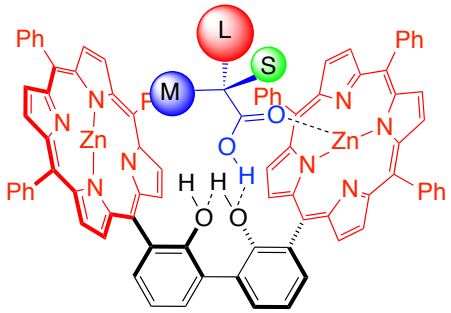

Figure 4-25. α-chiral carboxylic acid involved in both metal coordination and hydrogen-bonding with ***M***-helix of Zn-MAPOL.

There are several advantages to having multi-point recognition sites on a porphyrin host. In addition to the rigid framework of the porphyrin, it is suitable for thermodynamic studies on multipoint molecular recognition because the rotational freedom of the guest alone can be isolated for analysis. In fact, evidence for two-point complexation has been well documented in literature.[24] A common strategy in designing porphyrin receptors is to use a central metal as a Lewis acid site in order to bind a Lewis base functional group of the guest molecule. However, porphyrin receptors bearing multi-point recognition sites have been exploited for the recognition of amino acids, nucleotides, saccharides and other functional groups.[24a, b] In one of the early studies by Ogoshi and co-workers,[24b] they reported a receptor having double recognition sites, the Lewis acid site (zinc), and a Lewis base site (quinolone). In their studies, they investigated the binding of α-amino acid esters to porphyrin hosts with double recognition sites: metal coordination and hydroxyl hydrogen bonding (Figure 4-26).

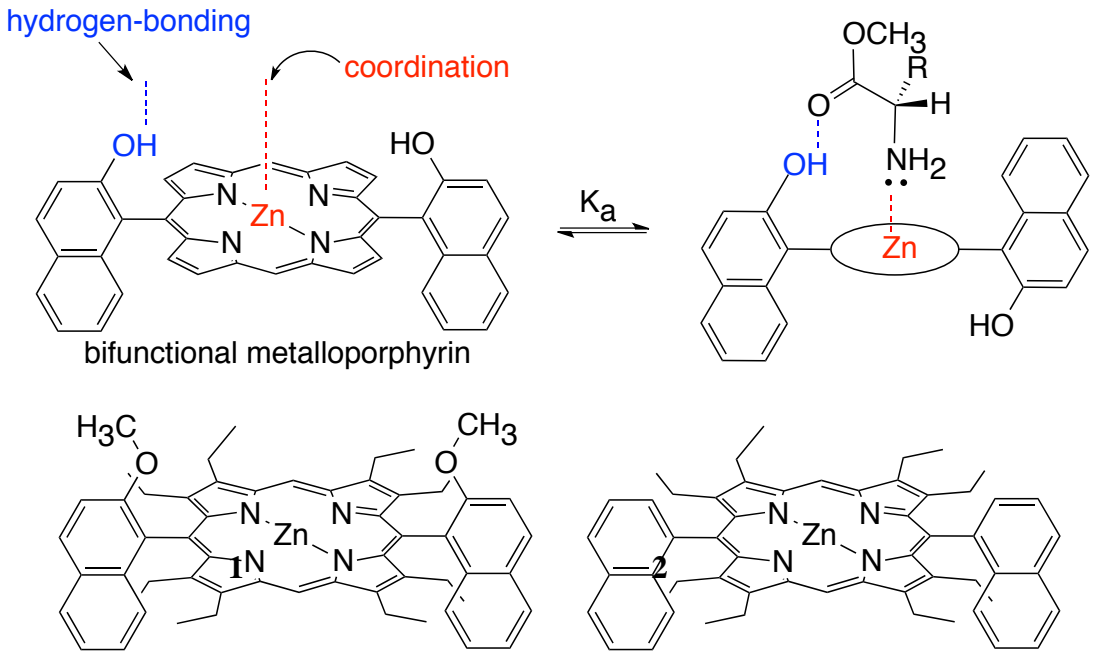

Figure 4-26. Three host porphyrins used by Ogoshi investigated the binding of α-amino acid esters. **1** lacks the hydrogen bond donor site and host **2** lacks the hydrogen bonding site.

In a continuation of this work, the authors looked at the recognition of carbohydrates by zinc porphyrins designed to have double recognition sites.[24a] They designed the host with quinoline moieties, as the hydrogen acceptor site (Figure 4-27, β-ethyl groups omitted for clarity).

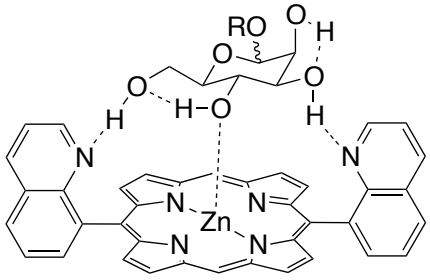

Figure 4-27. Host for carbohydrate recognition.

With this in mind, we propose that the carboxylic acids would bind to Zn-MAPOL, a bifunctional host, via both Zn-metal coordination and hydrogen bonding to the biphenol unit. As shown in Figure 4-28, the carbonyl group is proposed to be involved in metal coordination with the porphyrin, and the acidic proton involved in hydrogen

bonding with the biphenol unit, as a proton donor. Assuming that sterics are responsible for chirality recognition, during the complexation, the large group would be positioned in the least sterically encumbered location in both the *P* or *M* conformers and stereodifferentiation would be between the medium and the small groups. It is believed that the large group plays no role in stereodiscrimination. Nonetheless, in one helicity of Zn-MAPOL, the medium group of the acid will be situated in a more sterically tolerable region, and the smallest group will occupy the most sterically congested area. However, in the other helicity of MAPOL, the opposite would be true, and there will be a more sterically unfavorable interaction with the medium group.

In this way, the carboxylic acid would bind to Zn-MAPOL in the sterically favored helicity. The equilibrium will shift to create an excess of the favored helicity, leading to an observed ECCD spectrum as a result of exciton coupling of the porphyrins arranged in a chiral fashion within the sterically preferred complex. Figure 4-28 shows a proposed enantiodiscimination mechanism for an α-chiral carboxylic acid. In A, if the acid binds with the M-helix of the host, there would be unfavorable steric interactions between the medium group and the host, hence it preferably binds with the P-helix. This places the porphyrins in a clockwise arrangement that would result in a positive CD sign. On the other hand, the enantiomer shown in B preferably binds with the M-helix, avoiding the unfavorable steric interactions that would occur between the medium group and the host in the P-helix of Zn-MAPOL. In this complex, the porphyrins are arranged in a counterclockwise manner, resulting in a predicted negative CD sign.

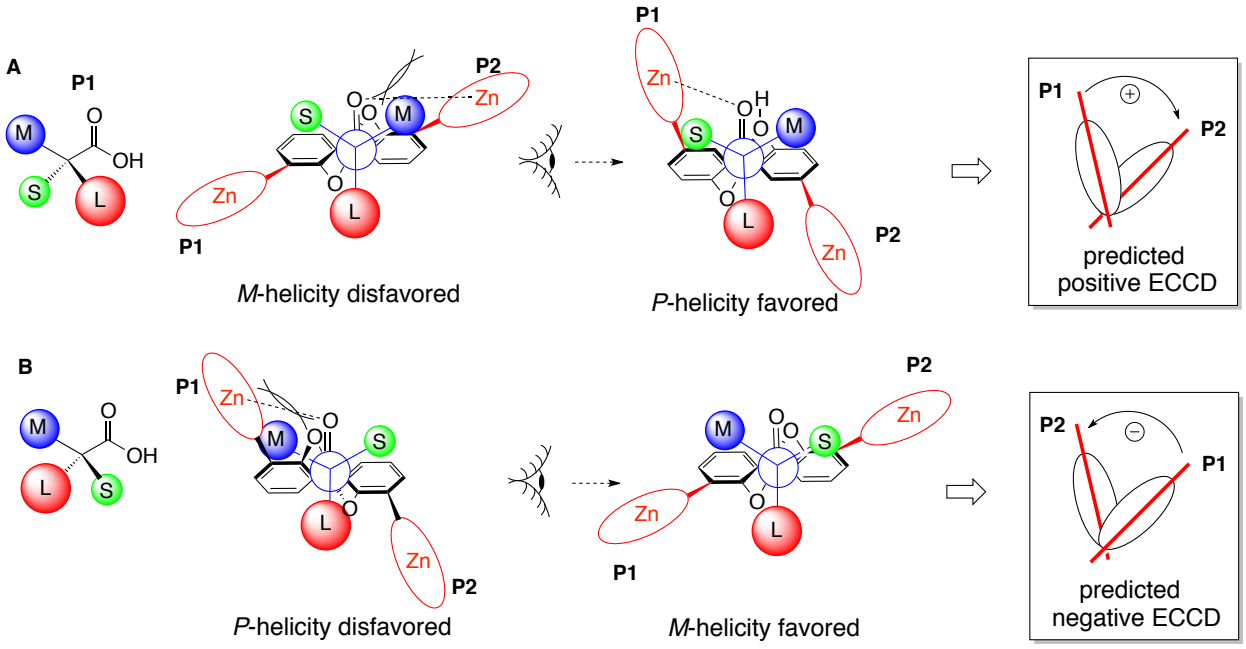

Figure 4-28. Proposed binding model for chiral carboxylic acids to Zn-MAPOL. In A, the acid binds to the P-helix and in B, preferably to M-helix, resulting in the predicted positive and negative CD signs respectively for the two enantiomers.

Based on the above proposal, Zn-MAPOL **44**, was examined for the configurational assignment of a variety of α-chiral carboxylic acids via the ECCD protocol. To our delight, chiral acids bearing different functionalities gave consistent and prominent bisignate CD signals at the porphyrin Soret region, upon addition of micromolar concentrations to a solution of Zn-MAPOL in hexane. As shown in Table 4-5, the signs obtained for entries 1,2 and 3 were consistent with the predicted signs using this proposed model. For substrates bearing an aromatic ring at the chiral center (entries 4 and 5) this model results in predicted signs that are opposite to what is observed. This is proposed to be due to π-π stacking interactions between the aromatic ring and the porphyrin. Such interaction has previously been observed in similar systems.[5b] Looking at substrate **32** (entry 5) the original model above would place the largest group,

(phenyl) in the most sterically accessible location, and the medium group (methyl) in the more sterically congested location, leading to a predicted positive ECCD, however, because of π-π stacking interactions between the phenyl group and porphyrin, the large phenyl group will be positioned in the more sterically congested area placing medium methyl group in the more sterically accessible location, leading to a predicted negative ECCD sign which is observed (Figure 4-29A). Likewise, with favorable π-π stacking interactions in **31**, the large phenyl group would preferentially occupy the more sterically congested area placing medium methoxy group in the more sterically congested location, leading to a predicted negative ECCD sign which is observed (Figure 4-29B).

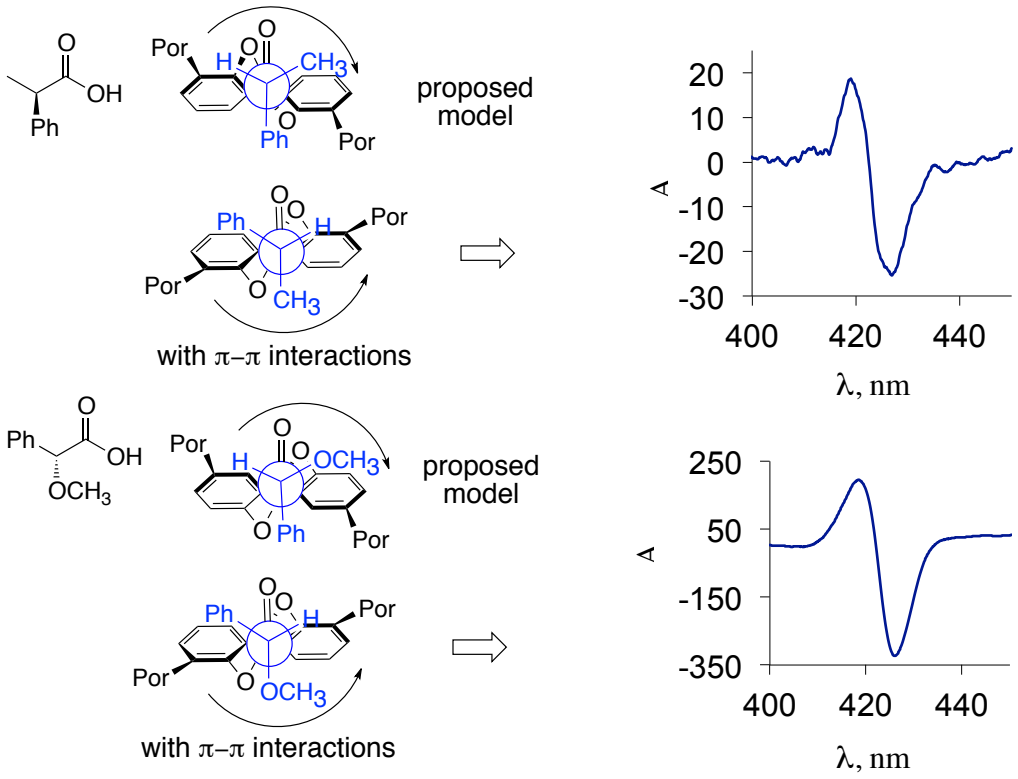

Figure 4-29. Proposed binding of substrates with aromatic groups at chiral center. In both, the models involving π-π interactions between the aromatic group and porphyrin result in predicted sign that are in agreement with the obtained results.

Table 4-5. ECCD data for α-chiral carboxylic acids bound to Zn-MAPOL in hexane.

entry		carboxylic acid	predicted sign	λ, nm, (Δε)	A
1	**28***S*	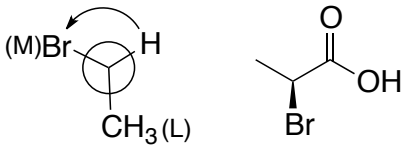	neg	425, -68 416, +45	-113
2	**29***S*	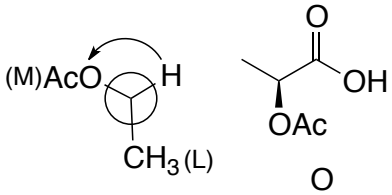	neg	425, -19 415, +21	-40
3	***30S***	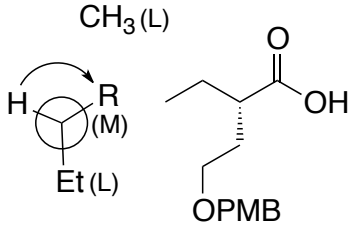	pos	425, +40 416, -34	+74
4	**31***R*	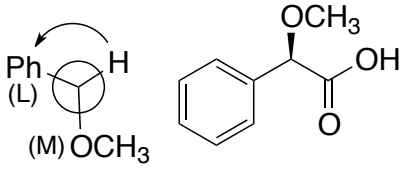	neg	425, -316 417, +185	-501
5	**32***R*	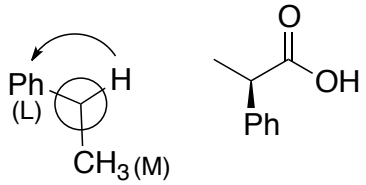	neg	426, -24 418, +16	-40

host:guest ratio – 1:20, 2 μM host concentration at 0 °C was used for measurements.

Figure 4-30 shows the correlation between the chirality of the acid and the sign of ECCD obtained as shown for acid **29**. For both the *P* or *M* helicity of the complex, the large methyl group is situated in the least sterically demanding location, while the location of the medium acetate and small hydrogen groups is dictated by the configuration at the chiral center as illustrated. In the *M* complex (Figure 4-30A), the medium acetate group is situated in a more sterically tolerable region, while the smallest hydrogen group occupies the most sterically congested area.

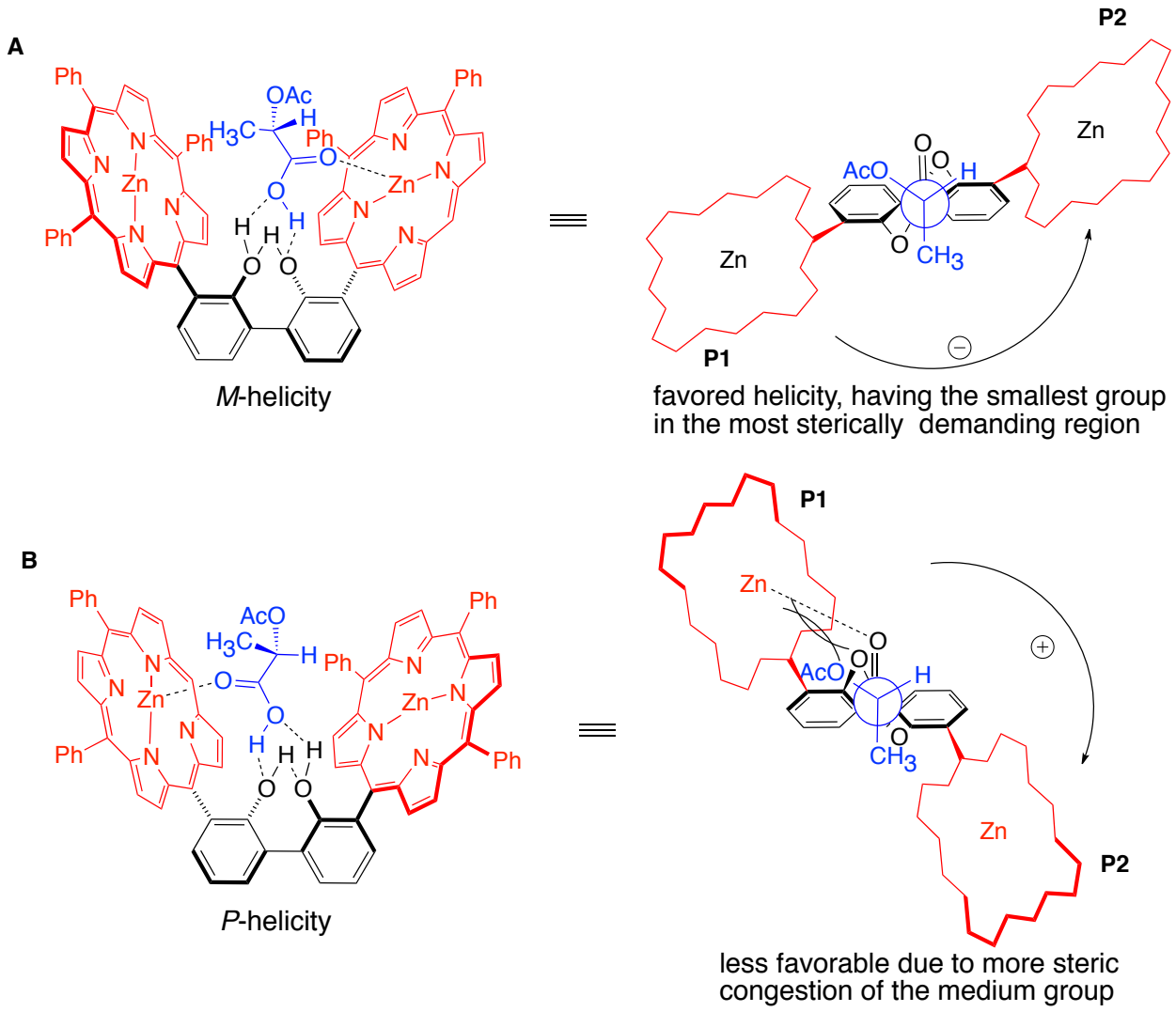

Figure 4-30. Proposed binding model for **29**(*S*) to Zn-MAPOL. In A, the acid binds to the M-helix and in B, it binds to the P-helix. The complex formed in B is less favorable due to steric congestion between porphyrin and the methyl group.

On the other hand, in the *P* complex the methyl group would be positioned in the more sterically unfavorable region. In this way, the more favorable *M*-helicity is promoted in binding with the *S*-enantiomer, leading to the observed negative ECCD spectrum (Table 4-5 entry 2).

Figure 4-31 shows the proposed binding of **32** with Zn-MAPOL. Here, the favored conformer would place the medium methyl group in the more sterically open location, and the

large phenyl group in the more sterically congested location because of favorable π-π stacking interactions. This would lead to a predicted negative ECCD sign.

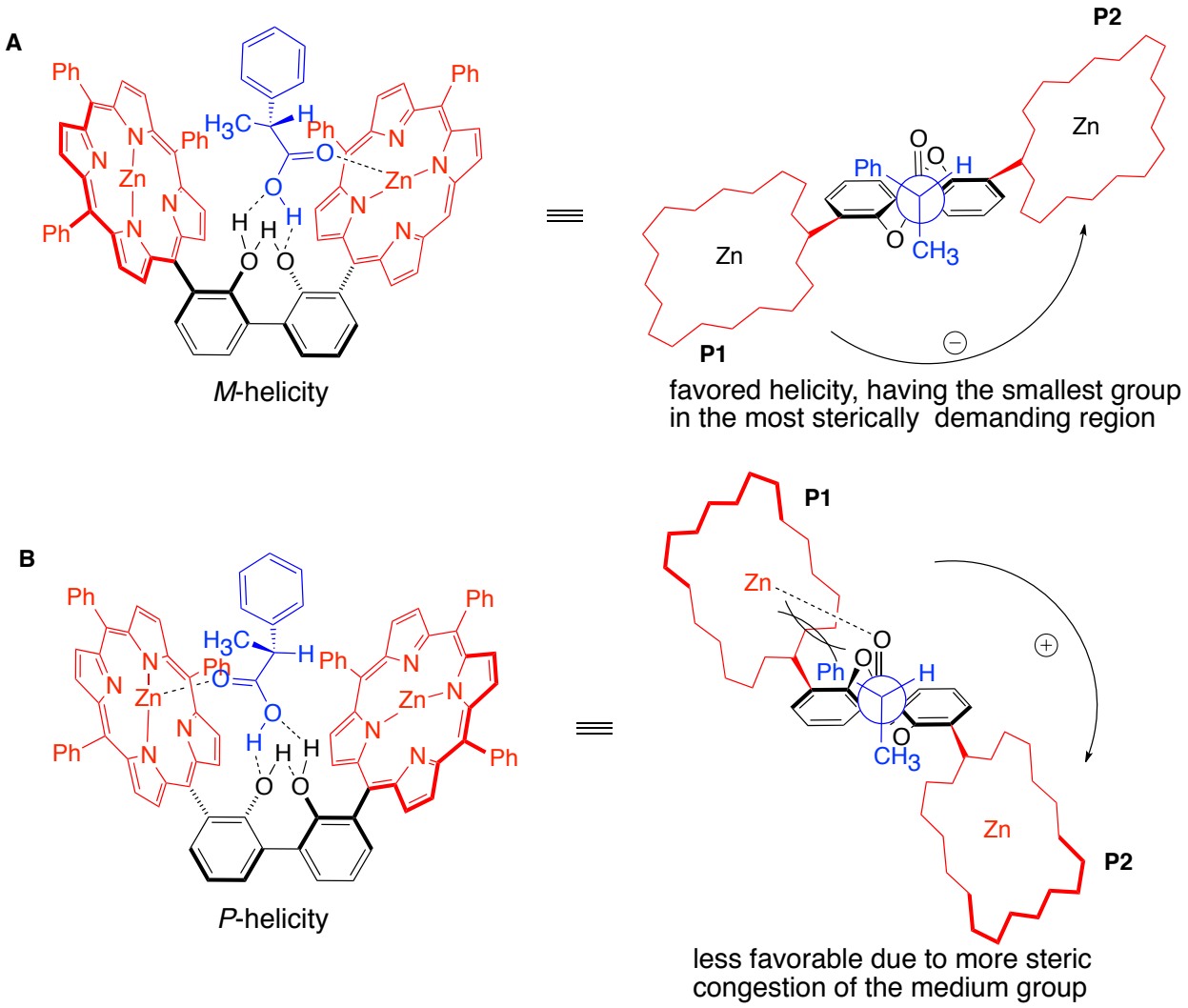

Figure 4-31. Proposed binding model for acid **32** to Zn-MAPOL in a way that places the aromatic ring next to porphyrin for π-π interactions in both helices. In A, the acid binds to theM-helix and in B it binds to the P-helix. The complex formed in B is less favorable due to steric congestion between porphyrin and the phenyl group.

4-5:3 Remote chirality sensing: A case study of β- and γ-chiral carboxylic acids

As an extension of the α-carboxylic acids, we wished to apply Zn-MAPOL to solve the issue of remote chirality sensing. To our knowledge, there are few reports[25] addressing the stereochemical determination of substrates bearing β-stereocenters. Conventionally, the absolute configuration of remote stereocenters has been assigned by ^{1}H-NMR as well as CD spectroscopy.

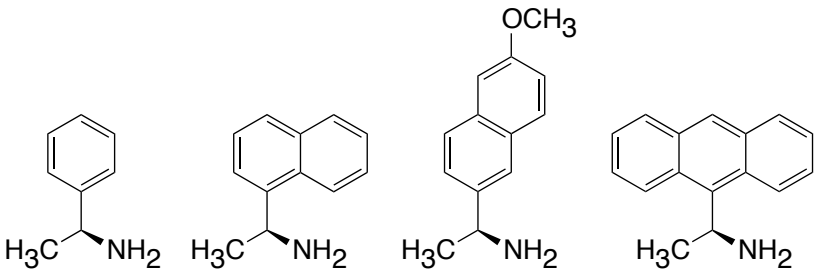

Figure 4-32. 1-arylethylamines used by Hoye as reagents.

Hoye and co-workers,[25-26] report the determination of the absolute stereochemistry of β-chiral carboxylic acids by ^{1}H-NMR spectroscopy. Their approach calls for derivatization of the acids with chiral benzylic amines (Figure 4-32). Analysis of the signs of the chemical shift differences of substituent protons allowed for the determination of absolute configuration. They use the signals of the methyl groups of the amides to assess the effectiveness of these systems as reagents. The authors differentiate two diastereochemical possibilities (*syn* and *anti* diastereomers) according to the relative orientation of the benzylic methyl group and the methyl substituent at the C-3, and calculate Δδ (defined as the difference between the chemical shifts in the *syn* and *anti* diastereomers) for the β-methyl and other groups. Using this method, the β-

methyl groups are always more deshielded in the *syn* series than in the *anti* series, whereas protons in the other β-substituent are more shielded in the *syn* isomers.

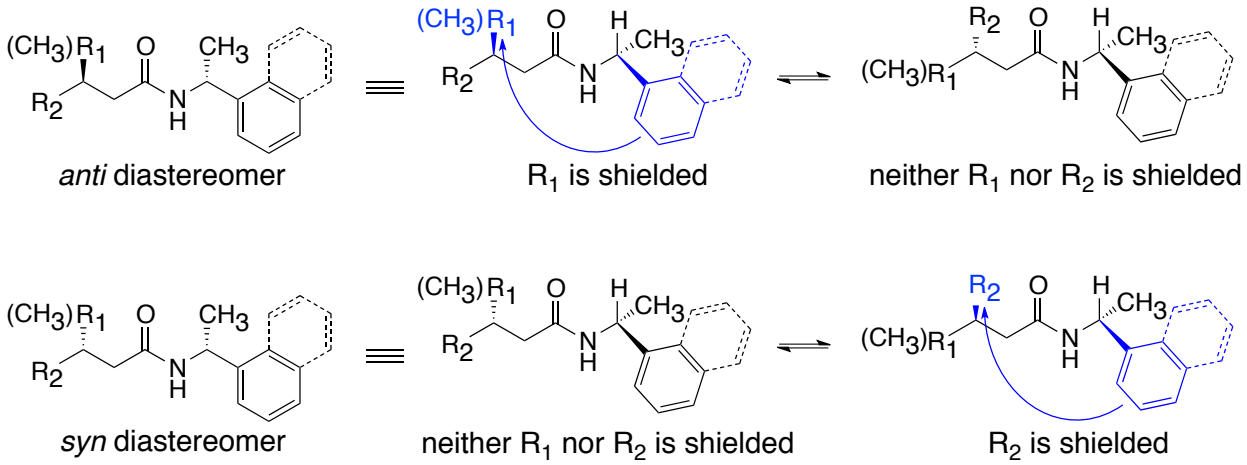

Figure 4-33. Conformational model for the determination of the sign of $\Delta\delta = \delta(syn) - \delta(anti)$ of protons in R_1 an R_2.

They proposed a working model shown in Figure 4-33 based on NMR results and molecular calculations. This model is based on two assumptions: first, the the predominant rotamer around the bond between the benzylic proton is eclipsed with the carbonyl group, and second, one of the two non-hydrogen substituents at C-3 occupies the *anti* position, relative to the carbonyl group. In the case of *anti* diastereomer, R_1 is preferentially shielded, while in the *syn* diastereomer, R_2 is shielded. Consequently, the $\Delta\delta$ values for protons in R_1 are positive and those in R_2 are negative. In an extension of this work, the same authors extend the scope of the methodology to include carboxylic acids with substituents other than a methyl group at C-3.[25]

The methods employing ECCD utilize substrates that carry either an aromatic moiety[27] or contain a group that is potentially derivatizable by the chromophore; a hydroxyl or amino functionality[28] at the stereocenter, thus reducing the problem to determining the stereochemistry adjacent to the chromophoric site stereocenter, i.e. α-chirality. Determining β-stereocenter in the absence of chromophoric/derivatizable sites or sensing remote chirality in general remains a challenging task, where restricting conformational freedom of distal stereocenters is one of the difficulties to overcome.

Our group recently introduced a bulky porphyrin tweezer (Zn-TBP) shown in Figure 4-34, for the assignment of the absolute stereochemistry of a wide variety of β- and γ-chiral carboxylic acids by ECCD protocol.[44] In order to achieve this, the chiral acids were first derivatized with *p*-phenylenediamine carrier in order to introduce the requisite two binding sites.

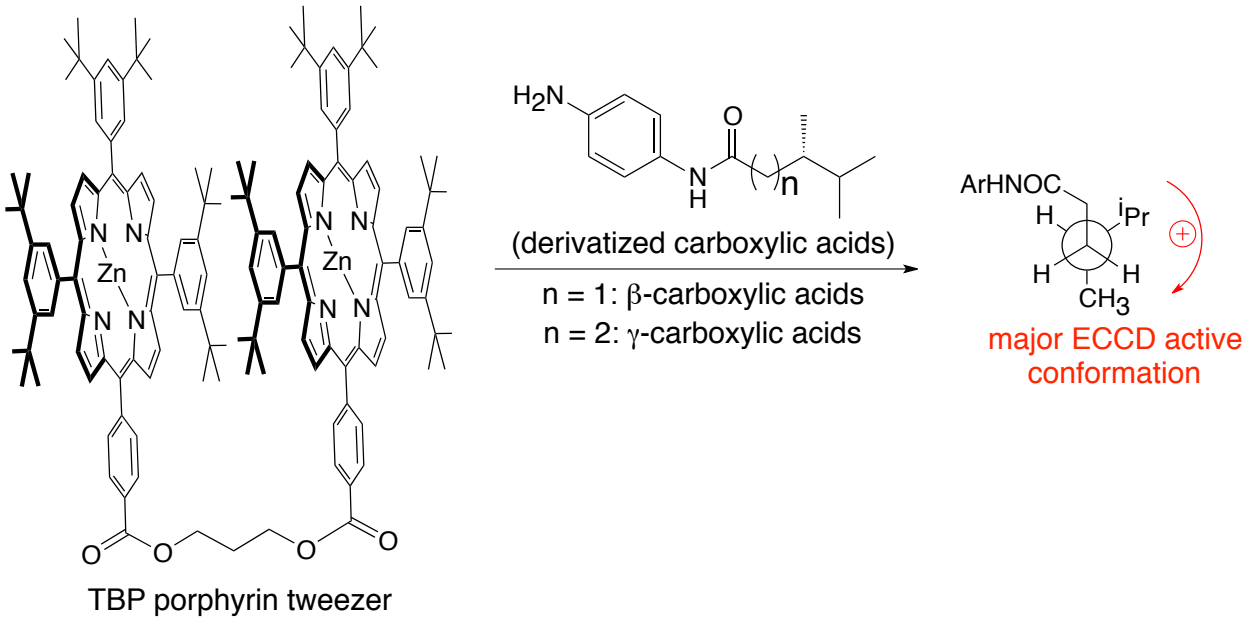

Figure 4-34. TBP porphyrin tweezer used for remote chirality sensing.

Here, the t-butyl substituents on the tweezer provide a better coverage of the tweezer's binding cavity leading to enhanced steric interaction.

4-5:4 Use of Zn-MAPOL for absolute stereochemical determination of β-chiral carboxylic acids

Similar to the α-chiral acids, the β- and γ-chiral carboxylic acids were ECCD silent with MAPOL, however, all acids were ECCD active with Zn-MAPOL. Because of this, it is postulated that they follow a similar binding model and stereodifferentiation as the α-chiral carboxylic acids as shown in Figure 4-35, where the acids coordinate to Zn-MAPOL via a two-point coordination.

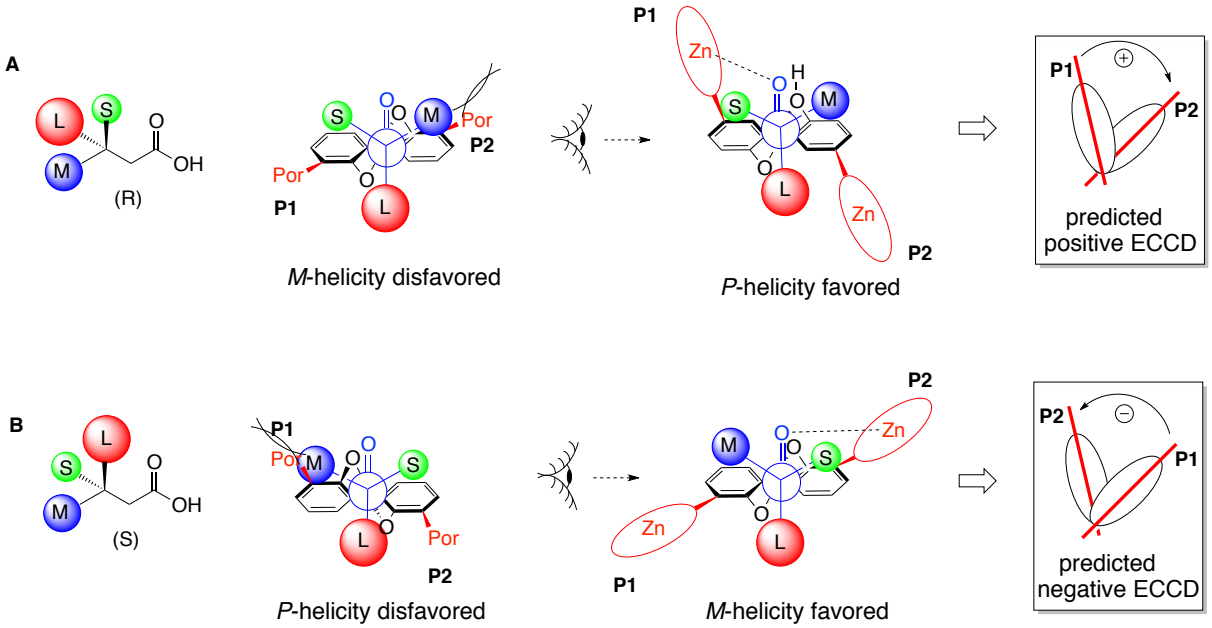

Figure 4-35. Proposed binding model for β-chiral carboxylic acids with Zn-MAPOL. In A, the (*R*)-acid preferable binds to the M-helix and in B, preferably to the P-helix, resulting in the predicted negative and positive CD signs respectively.

It is believed that upon complexation, the large group would be positioned in the least sterically crowded location in both the *P* or *M* conformers, hence it is believed that this group does not take part in the stereodiscrimination process. In one helicity of Zn-MAPOL, the medium group of the acid will be situated in a more sterically tolerable region, and the smallest group will occupy the most sterically congested area. However, in the other helicity, the opposite would be true, and there will be a more sterically unfavorable interaction with the medium group. In this way, the chiral acid would bind to Zn-MAPOL in the sterically favored helicity. The equilibrium will shift to create an excess of the favored helicity. As a result of the chiral twist between the biphenyl unit, the two porphyrins will be oriented in a chiral fashion. Coupling of the porphyrins' electric dipole transition moments leads to an observed ECCD spectrum.

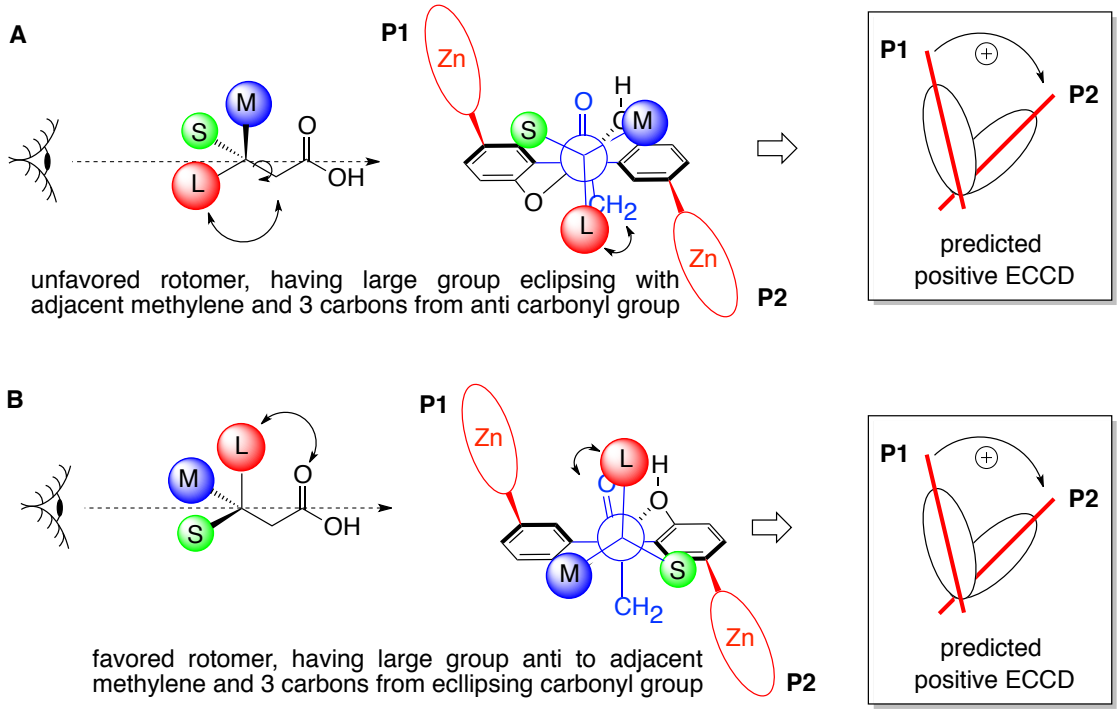

Figure 4-36. Rotomers around the C-C bond.

While it is possible to have bond rotation at the C2 – C3 bond, the rotomer in Figure 4-36A

places the large group in an eclipsing conformation with the methylene that is adjacent. In B, the large group is placed in an eclipsing conformation to the carbonyl group that is three carbons away and is anti to the adjacent methylene. In either case, the expected sign is the same. i.e. positive in this case. However, it is proposed that B is the favored rotomer due to less sterics between the large group on C3 and C2 methylene. The same would hold true for the γ-chiral carboxylic acids as shown in Figure (4-37).

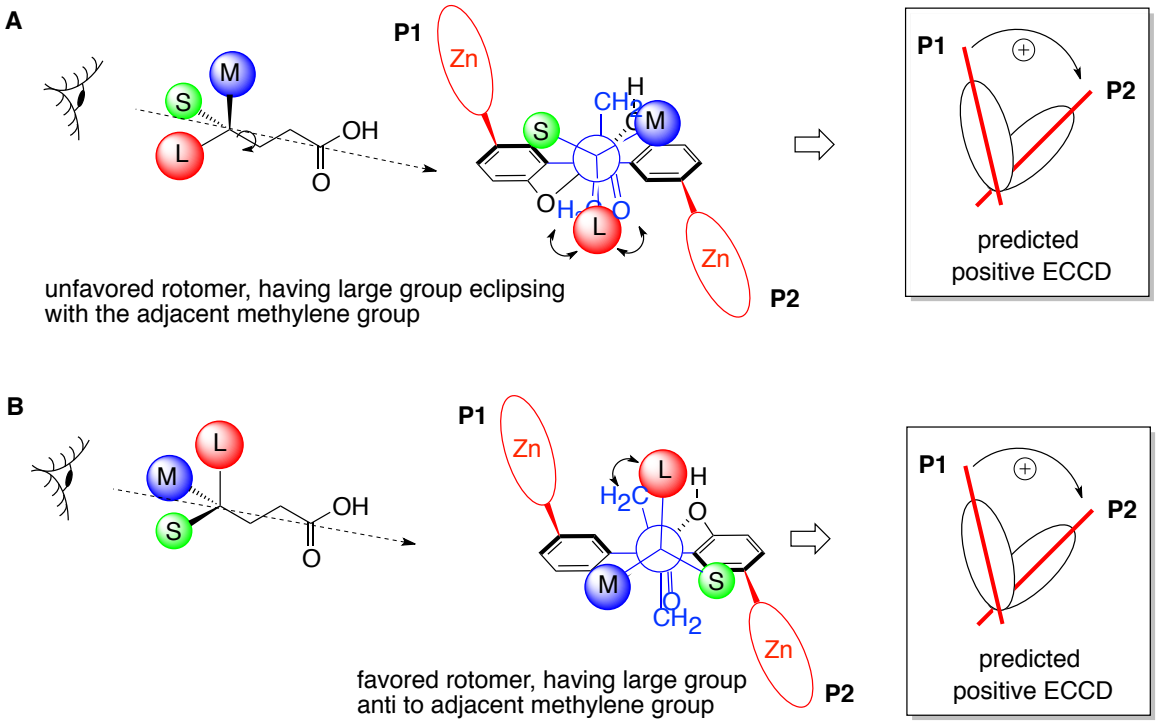

Figure 4-37. Possible rotomers of γ-chiral carboxylic acids.

Zn-MAPOL **44**, was examined for the configurational assignment of a variety of β- and γ-chiral carboxylic acids via the ECCD protocol. All the chiral acids tested gave consistent and

prominent bisignate CD signals at the porphyrin Soret region, upon addition of micromolar concentrations to a solution of Zn-MAPOL in hexane. As shown in Table 4-6, the signs obtained were consistent with the predicted signs.

Figure 4-38, shows the correlation between the substrate chirality and the sign of ECCD obtained as shown for β-carboxylic acid **39**. We propose a similar binding model for β- and γ-carboxylic acids as that for α-carboxylic acids, invoking the two-point coordination. In the *M* complex (Figure 4-38A), the medium group (CH_3) is situated in a more sterically tolerable region, while the smallest group (H) occupies the most sterically congested area. On the other hand, the *P* complex would have a more sterically unfavorable interaction between the medium (CH_3) group and porphyrin. In this way, the more favorable *M*-helicity is promoted in binding with the *R*-enantiomer, leading to the observed negative ECCD spectrum (Table 4-6 entry 3).

Table 4-6. ECCD data of β- and γ-chiral carboxylic acids bound to Zn-MAPOL in hex.

entry		carboxylic acid	predicted sign	λ, nm, (Δε)	A
1	**37***R*	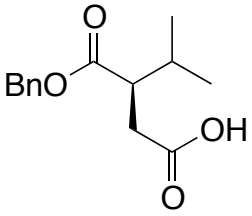	neg	428, -62 418, +55	-117
2	**38***R*	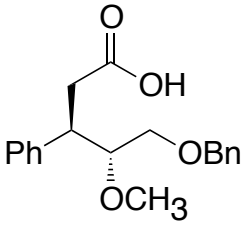	neg	428, -28 418, +11	-39
3	**39***R*	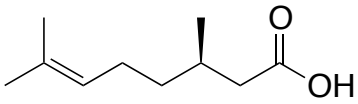	neg	425, -53 417, +30	-83
4	**40***R*	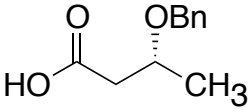	pos	426, +20 420, -12	+32
5	**41***R*	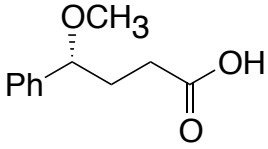	neg	429, -29 419, +26	-55
6	**42***S*	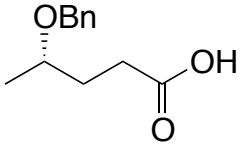	neg	424, -18 418, +13	-31
7	**43***R*	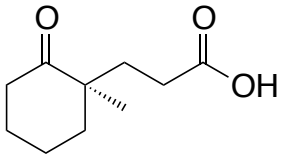	pos	425, +12 418, -15	+27

host:guest ratio – 1:20, 2 μM host concentration at 0 °C was used for measurements.

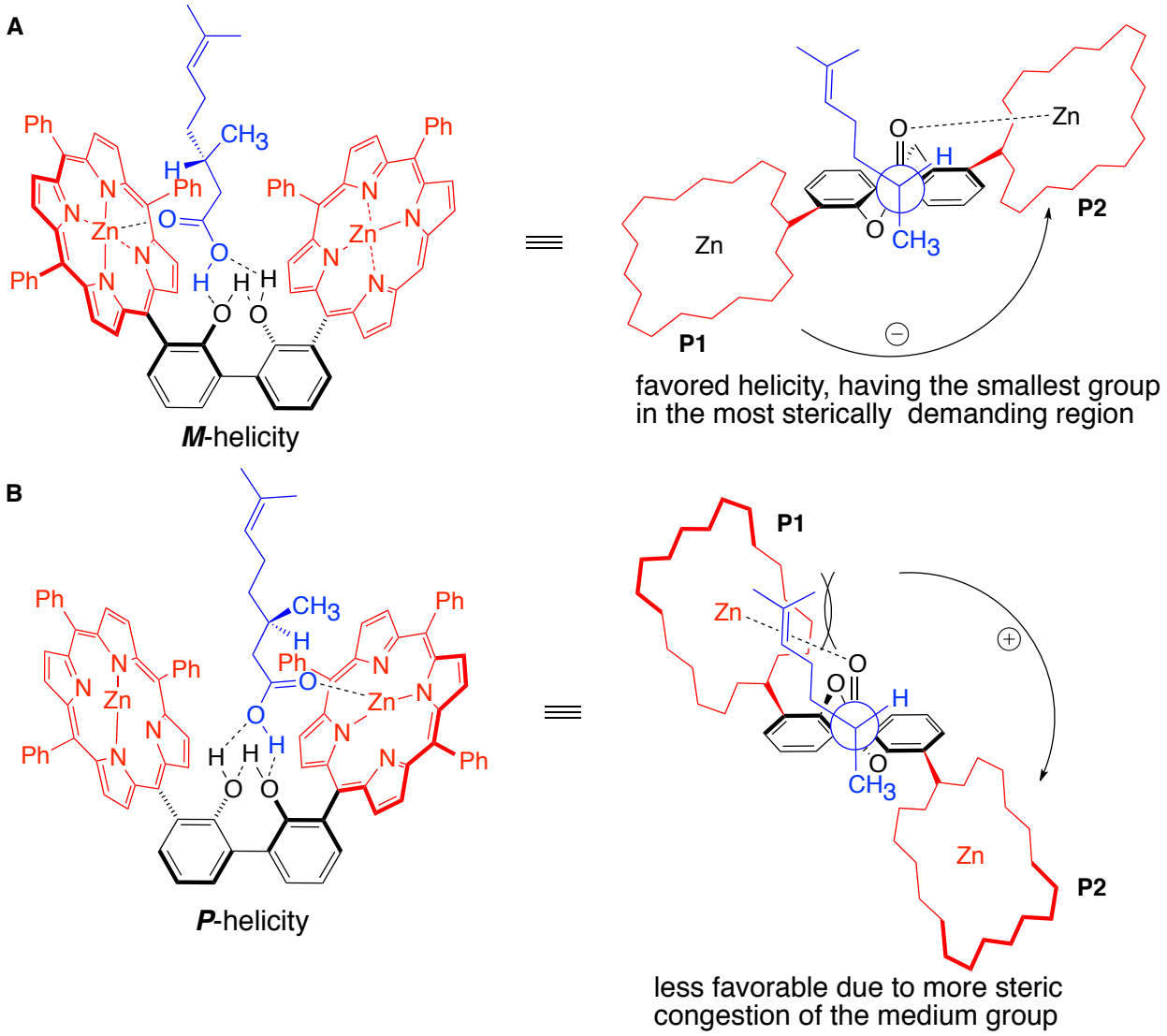

Figure 4-38. Proposed binding model for β-carboxylic acid to Zn-MAPOL by a two-point coordination to zinc and biphenol unit.

In summary, we have demonstrated the prompt and simple method for the assignment of absolute configuration for chiral β- and γ- chiral carboxylic acids. We propose a two-point coordination model utilizing metal coordination to the porphyrin as well as hydrogen bonding with Zn-MAPOL.

4-6 Chiral cyanohydrins

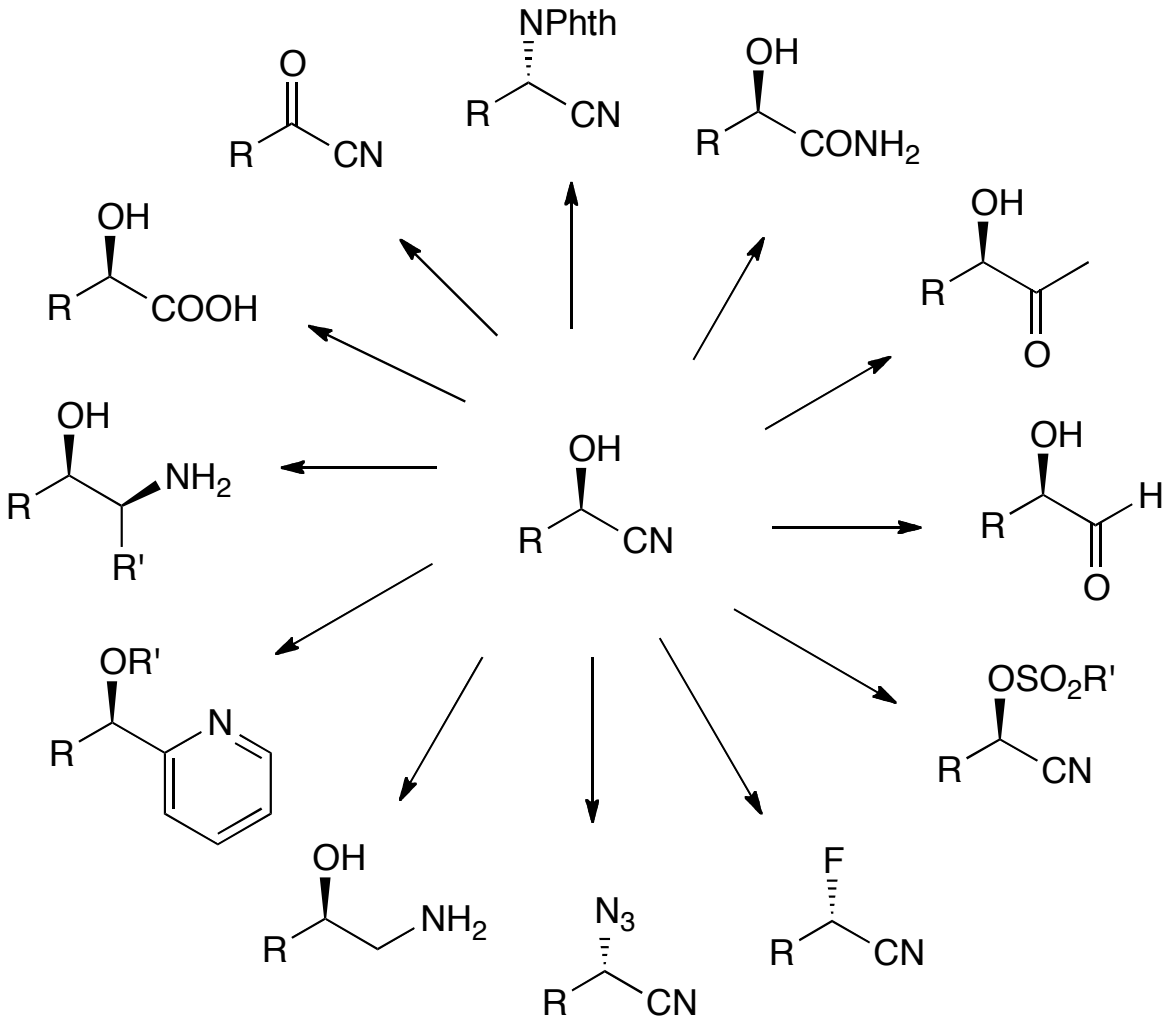

Scheme 4-4. Possible transformations of cyanohydrins.

Chiral cyanohydrins are a common functionality in natural products and are also versatile building blocks in organic synthesis. This is mainly because they are easily synthesized by the addition of cyanide to prochiral carbonyls (aldehydes and ketones) in the presence of chiral catalysts or by enzymatic methods, which can easily be transformed into a range of functional groups (Scheme 4-4).

The more valuable cyanohydrins derived from ketones (ketocyanohydrins) have been used as intermediates in the preparation of compounds with a quaternary center.[9] In fact, a literature search returns an overwhelming amount of publications that deal with either the synthesis or use of chiral cyanohydrins in the total synthesis of natural products.[10] Because of their importance, there is a need for an easy, simple to use, and efficient way for the reliable assignment of the absolute stereochemistry of cyanohydrins.

4-6-1 Conventional Methods of Assigning Absolute Stereochemistry of cyanohydrins

To date, very few attempts are described in literature towards the determination of absolute stereochemistry of chiral cyanohydrins, all of which rely on NMR spectroscopy, in particular Mosher ester analysis method.[29]

The first method applying the use of the Mosher ester analysis method towards chiral cyanohydrins was reported by Riguera's group.[29c] Here, they apply their method to aldocyanohydrins. In their report, they derivatize the cyanohydrins as both the enantiomers of (*R*)- and (*S*)-methoxy-2-phenylacetic acid (MPA) and compare both the ^{1}H and ^{13}C-NMR spectra of the corresponding cyanohydrin MPA ester derivatives. ^{13}C-NMR is necessary because the nitrile group lacks protons and so cannot be analysed by ^{1}H-NMR. In this way, they found that when the (*S*)-MPA was used, the substrate H's were more shielded than the same H's in the (*R*)-MPA ester, leading to a positive difference in chemical shifts ($\Delta\delta^{RS}$). For the nitrile group, the CN carbon is more shielded in the (*R*)-MPA ester derivative than in the (*S*)-MPA ester derivative leading to a negative sign for the difference in chemical shifts ($\Delta\delta^{RS}$) (Figure 4-39).

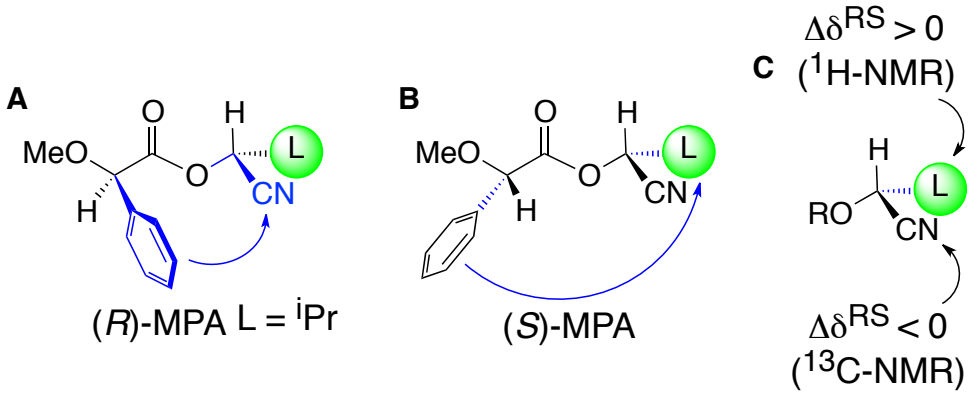

Figure 4-39. NMR representative conformer of A) the (*R*)-MPA ester of an aldehyde cyanohydrin and B) the (*S*)-MPA ester. Shielding effect is shown by a curved arrow. C) Model placing in space the L and CN substituents of the chiral center according to their $\Delta\delta^{RS}$ signs.

The same authors extended this methodology to the ketone cyanohydrins[29a, 29d] and using the same principles, described a method for the determination of absolute stereochemistry of ketone cyanohydrins (Figure 4-40). However while this method worked reliably for most all of their reported aldehyde cyanohydrins, for the ketone cyanohydrins, the α-aryl substituted cyanohydrins showed anomalies from the described model of analysis of the chemical shifts, requiring different sets of protons to be considered for their assignment.

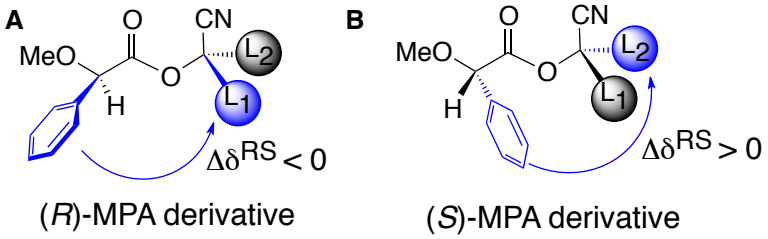

Figure 4-40. Riguera's assignment of keto cyanohydrins using ^{1}H-NMR analysis.

A third method of assigning absolute stereochemistry of cyanohydrins was reported by Bharatam group.[30] In this approach, optically active mandelic acid in the presence of DMAP is used to create a chiral solvating

agent (CSA) for the determination of absolute configuration of cyanohydrins. It should be noted that the magnitude of resolution for ketone cyanohydrins was less compared to aldehyde cyanohydrins but sufficient for the determination of optical purity of these compounds, with resolutions in the order of 0.055-0.112 ppm (16.5-33.6 Hz) for aldo-cyanohydrins and 0.016-0.031 ppm (4.8-9.3 Hz) for keto-cyanohydrins on 300 MHz NMR.

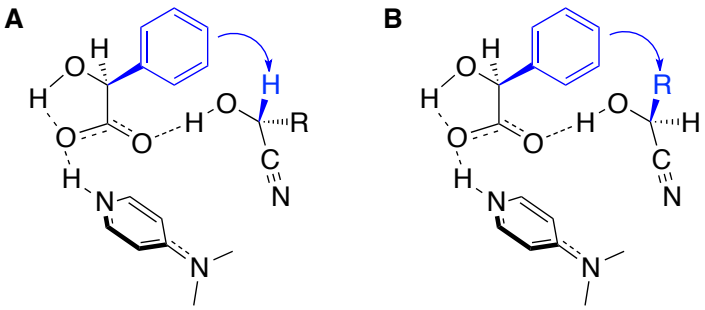

Figure 4-41. Proposed model showing ternary complexes of A) (*R*)- and B) (*S*)-cyanohydrin with (*S*)-mandelate-DMAPH$^+$ ion pair. The H in complex A and the R group in complex B of cyanohydrin are shielded by the phenyl group of mandelate.

In this method, the ^{1}H-NMR spectrum of racemic cyanohydrins in the presence of chiral mandelic acid and DMAP are recorded in $CDCl_3$. Taking mandelonitrile as an example, they first take ^{1}H-NMR of racemic mandelonitrile and both α-protons of the enantiomers of racemic mandelonitrile appear as well resolved singlets. Next the ^{1}H-NMR spectrum of chiral mandelonitrile was recorded with either (*R*) or (*S*)- mandelic acid to determine whether there is any correlation between their absolute configuration and the NMR chemical shift.

Cyanohydrins of *R*- configuration, showed a positive $\Delta\delta^{RS}$ value, whereas cyanohydrins of *S*- configuration showed negative $\Delta\delta^{RS}$ values. Thus, the $\Delta\delta^{RS}$ sign is characteristic for this enantiomeric series and could be used for the assignment of absolute configuration. However, pyridine compounds could not be assigned using this protocol, since the basic nitrogen on pyridine alters the nature of complex formation. Therefore, while these two methods have been developed for the determination of absolute stereochemistry of chiral cyanohydrins, we see that there is need for an improved (reliable), easy to use and fast way that does not require derivatization of the cyanohydrins.

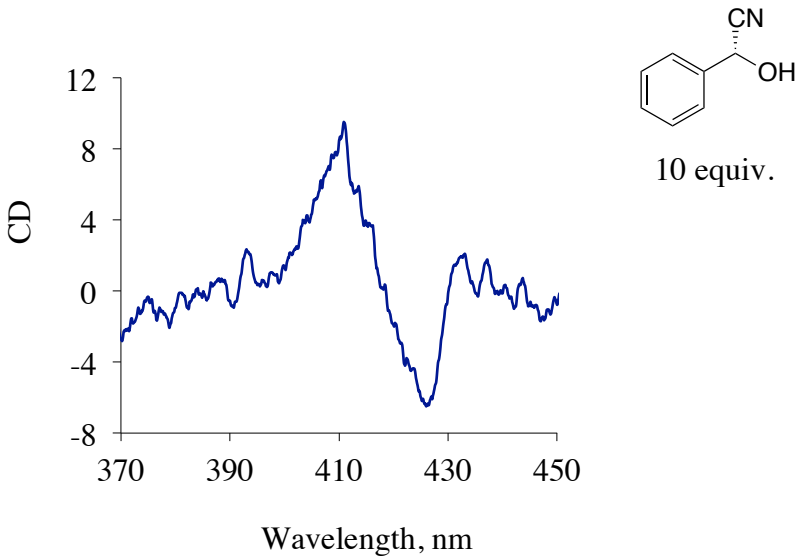

Figure 4-42. CD spectrum obtained for (*R*)-mandelonitrile with TPFP tweezer.

To our knowledge, there is no literature precedence on assigning absolute stereochemistry of cyanohydrins using the ECCD protocol. With the development and successful use of TPFP tweezer with hydroxy ketones and sulfoxides discussed in Chapter 2, we thought to extend the ECCD methodology, using fluorinated TPFP tweezer to cyanohydrins. However,

when cyanohydrins were tested with TPFP tweezers of varying lengths (C-3 to C-7) they were CD silent. One substrate, (*R*)-mandelonitrile, gave a positive result with the long alkyl C-8 tweezer (Figure 4-42). Disappointingly however, none of the other substrates were ECCD active with this tweezer. It is unclear why this is the case. We wished to apply MAPOL in determining the absolute stereochemistry of cyanohydrins.

4-6-2 Use of MAPOL for absolute stereochemical determination of cyanohydrins

The UV-vis titration of mandelonitrile with MAPOL and Zn-MAPOL is shown in Figure 4-44. While the changes are small, for Zn-MAPOL, there seems to be more of an interaction with the porphyrin than with free-base MAPOL. While studies are currently ongoing in order to propose a working model, preliminary results with a number of cyanohydrins however, produced inconsistent results upon binding with host MAPOL. As shown in Table 4-7 entries 1 and 2, no ECCD signals were obtained when chiral cyanohydrins were complexed with MAPOL. In changing the host to Zn-MAPOL however, all four cyanohydrins of same absolute stereochemistry resulted in positive ECCD. This led us to believe that the cyanohydrins could be complexing with Zn-MAPOL in a dual fashion, in a similar way to carboxylic acids.

In the case of cyanohydrins, there are two binding possibilities. One where the hydroxyl group is involved in metal coordination, and the other possibility where the nitrile group is involved in metal coordination. Additional studies including molecular modeling, NMR and IR spectroscopy will be done in order to investigate which of these two possibilities is preferred.

Table 4-7. ECCD data of cyanohydrins bound to Zn-MAPOL in hexane.

entry	cyanohydrin	predicted sign	Zn-MAPOL λ, nm, (Δε)	Zn-MAPOL A	MAPOL λ, nm, (Δε)	MAPOL A
1	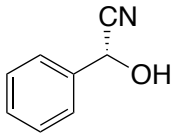	pos	419, +40 412, -20	+60	-	-
2	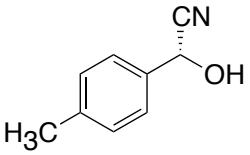	pos	419, +14 412, -13	+27	-	-
3	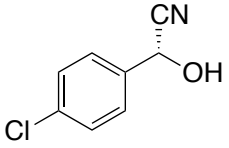	pos	419, +90 412, -21	+101	417, +72 408, -26	+98
4	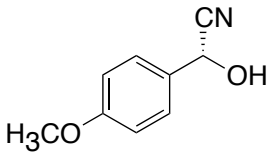	pos	419, +14 412, -11	+25	418, +2 406, -0.5	-2.5

host:guest ratio – 1:20, 2 μM host concentration at 0 °C was used for all measurements.

All tested cyanohydrins were (*R*)-chirality and all resulted in a positive CD signal. Granted, the tested cyanohydrins represent a limited substrate scope (all being derivatives of mandelic acid), however, this is the first example of cyanohydrins succumbing to analysis via ECCD, without the requirement of derivatization. A larger substrate scope, including alkyl cyanohydrins as well as cyanohydrins derived from ketones, needs to be investigated for a binding model to be proposed for this important class of molecules.

4-7 Synthesis of Chiral Cyanohydrins

All cyanohydrins used for the study were obtained from commercial sources and used without further purification.

4-8 Determination of Absolute Stereochemistry for Chiral Alcohols

4-8-1 Background

Enantiomerically pure alcohols are valuable chiral building blocks for synthetic chemists. They form a versatile class of chiral synthons, since they can be incorporated into the biologically active, or natural product structures directly as esters or ethers.

For example, the compounds act as key intermediates in the production of pharmaceuticals, fine chemicals and natural products. Examples of pharmaceuticals with chiral alcohols as intermediates are antihypertensive drugs, calcium and potassium channel blocking drugs, antiarrhythmic agents, β3-receptor agonists, anticholesterol and antiviral drugs. They are important starting materials for the formation of amines, amides, thiols and thioethers. In addition, after transforming the hydroxyl function into a leaving group by way of mesylation, tosylation or triflation, they can be used to form new C–C bonds.

4-8-2 Conventional Methods of Assigning Absolute Stereochemistry of chiral alcohols

Like chiral mono amines, chiral alcohols cannot be directly applied in the conventional chiroptical methods used for the absolute configurational assignment of chiral diols using porphyrin tweezers because they contain only one site of attachment (one hydroxyl group) and so they can only coordinate to one metalloporphyrin.

Traditionally, the absolute stereochemistry of alcohols has been assigned by using Mosher ester analysis,[7-8, 41] or by using ECCD protocol.[42] The use Mosher ester analysis for the determination of absolute configuration of alcohols was first reported in 1973 by Dale and Mosher.[7] Figure 4-45 shows the use of α-methoxy-α-trifluoromethyl-phenylacetic acid (MTPA).

This method involves the coupling of alcohol of interest with each enantiomer of MTPA acid. Alternatively, the acid chlorides can be used.

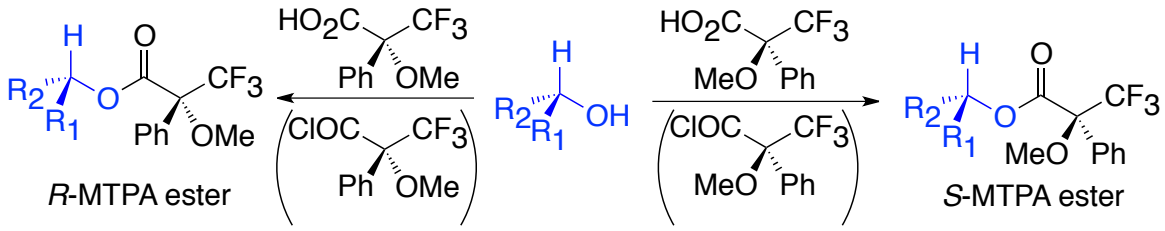

Figure 4-45 Derivatization of a chiral alcohol with R- and S-MTPA acid (and chlorides) for Mosher ester analysis.

However, caution is needed when using the acid chlorides, because when the MTPA acid gets converted to MTPA acid chloride, there is a switch in the priorities of the groups. In the acid, CF_3 >COOH, however, in the MTPA acid chloride, CF_3<COCl. This leads a switch in the absolute stereochemistry of the derivatized mosher ester formed with MTPA acid and MTPA ester. i.e R-Mosher acid results in R-Mosher ester, and S Mosher acid chloride results in R-Mosher ester.

4-8-3-1 ECCD Studies of Chiral Alcohols Using MAPOL

Chiral alcohols cannot directly be assigned by the tweezer methodology using ECCD protocol because they contain only one coordination site. However as shown in figure 4-46, the alcohols could potentially participate in hydrogen bonding with MAPOL. We postulate that upon introduction of a chiral alcohol to MAPOL in a 1:1 complex, the alcohol will preferentially bind to one helicity of MAPOL via hydrogen bonding as

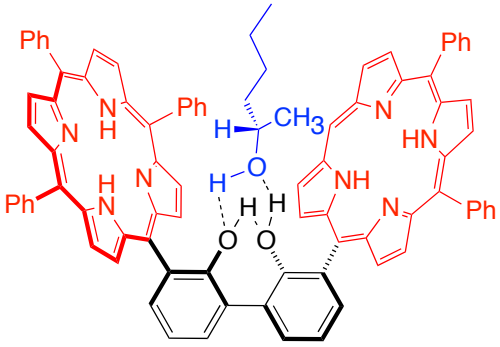

chiral alcohol involved in hydrogen-bonding with ***M***-helix of MAPOL

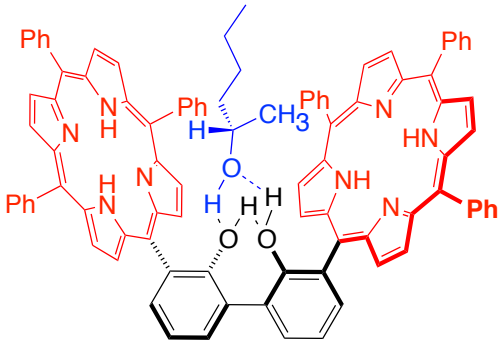

chiral alcohol involved in hydrogen-bonding with ***P***-helix of MAPOL

Figure 4-46. Proposed complexation of chiral alcohols with P and M helices of MAPOL.

shown in Figure 4-46. During the complexation, the largest group at the chiral center will position itself in the least sterically encumbered location, which can be achieved in both the *P* or *M* helicities of the complex. Nonetheless, in one helicity, the medium group will be situated in a more sterically tolerable region, and the smallest group will occupy the most sterically congested area. However, in the other helicity, there will be a more sterically unfavorable interaction with the medium group. In this way, the more favorable helicity is promoted in binding with one enantiomer of acid, leading to an over-population of the favored helicity, and ultimately to an observed ECCD spectrum as a result of exciton coupling of the porphyrins due to the chiral twist.

When subjected to both MAPOL and Zn-MAPOL host systems however, all the chiral alcohols were ECCD silent. This could be either as a result of the alcohols not being able to form a stable hydrogen bonding complex with MAPOL as was observed in the case of carboxylic acids. Here, once again, as was the case of carboxylic acids, the pKa of the alcohols being ~16, would make the alcohols to act as H-donor, making MAPOL the H-acceptor. This would result in formation of a complex with protonated phenol (pKa ~ -2). Because of this, it would be

expected that the hydrogen bonding between MAPOL and alcohols be weaker than the corresponding hydrogen bonding between MAPOL and amines. This weakened hydrogen bonding could explain the lack of ECCD when chiral alcohols were complexed with MAPOL.

4-8-3-2 Tuning the Electronics of MAPOL

The idea was to increase the acidity of the phenolic protons, so that the chiral alcohols can H-bond more easily. To do this, the easiest design was to introduce electron withdrawing nitro groups para to the OH.

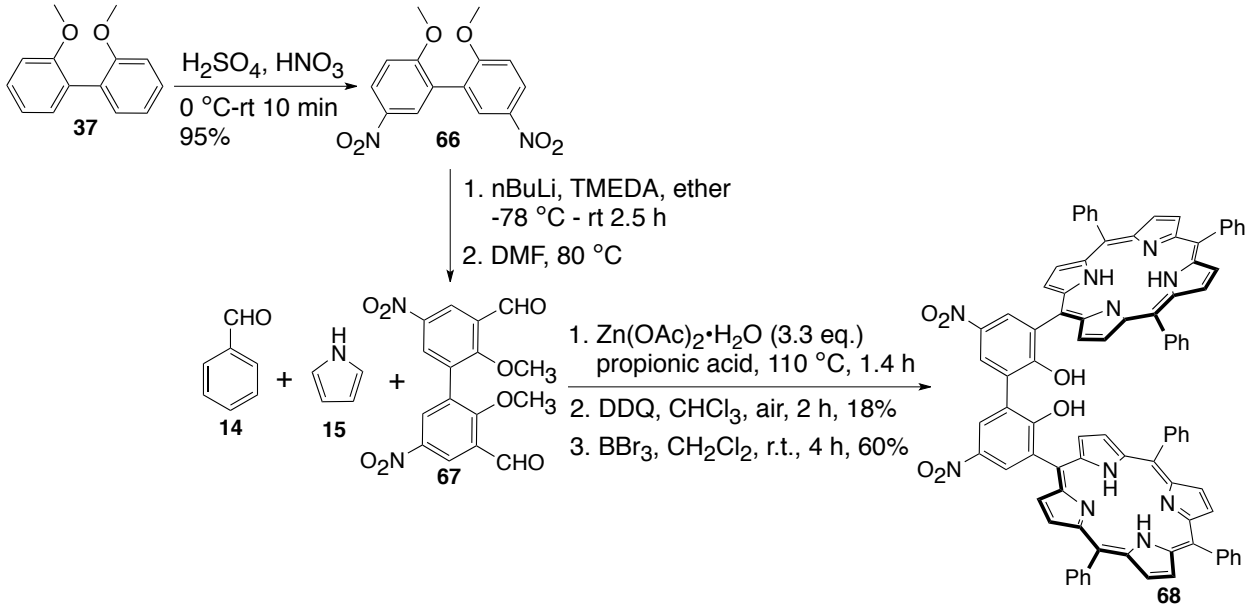

Scheme 4-5. Synthesis of nitro-MAPOL **68**

The synthesis of nitro-MAPOL was accomplished in three steps from commercially available 2,2'-dimethoxybiphenyl. First, nitration of 2,2'-dimethoxybiphenyl, followed by ortho-lithiation and subsequent formylation yields nitro bisaldehyde **67** in good yields. Condensation of nitro bisaldehyde **67**, pyrrole and benzaldehyde in propionic acid catalyzed by $Zn(OAc)_2$

yields methylated Nitro-MAPOL, which upon de-etherification and demetallation with BBr_3 yields desired Nitro-MAPOL **68**.

Uv-Vis titration of nitro-MAPOL with (*S*)-hexan-2-ol results in a spectrum shown in Figure 4-47 below, exhibiting only a drop in amplitude of Soret band. Like the amines, the alcohol does not result in a red-shift. An intense ECCD spectrum is obtained upon CD studies of (*S*)-hexan-2-ol with nitro-MAPOL host. (Fig 4-47 insert)

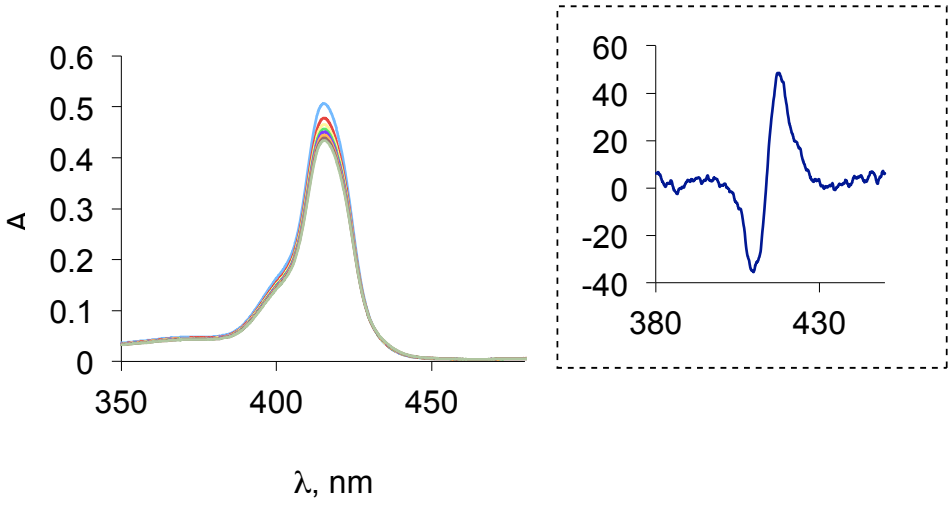

Figure 4-47. UV-Vis titration of nitro-MAPOL solution (1 μM in hexane) with (*S*)-hexan-2-ol (0.01 M in DCM). Insert: obtained ECCD spectrum of (*S*)-hexan-2-ol with nitro-MAPOL, in hexane solvent at 0 °C

Unfortunately, none of the other alcohols showed any ECCD signals. At this point, it is unclear why this is the case.

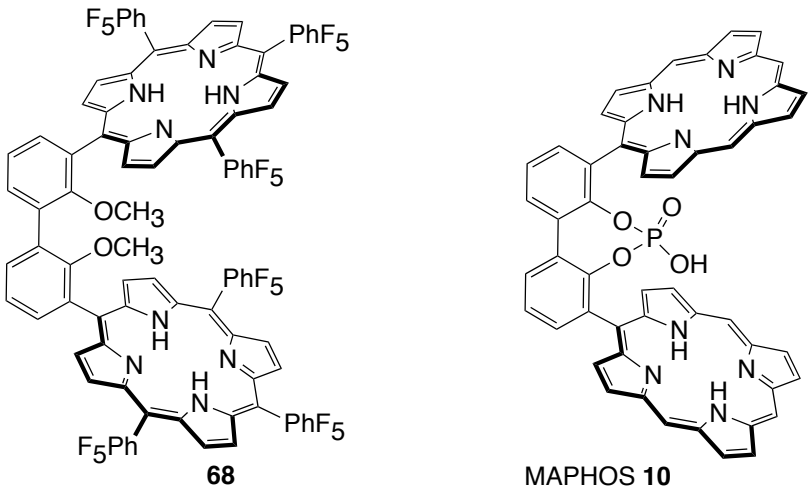

Figure 4-48. Proposed host molecules for assigning absolute stereochemistry of chiral alcohols.

One proposed solution is to make the original MAPHOS, which has the phosphoric acid (Figure 4-48). Another approach would be to mimic TPFP with the introduction of electron withdrawing fluorine on the porphyrins, but in this case, introduce magnesium as a coordinating metal. In other words, go back to the tweezer model. This will be different though because the system is inherently rigid so it should work I think.

Experimental procedures

Anhydrous CH_2Cl_2 was dried over CaH_2 and distilled. The solvents used for CD measurements were purchased from Aldrich and were spectra grade. All reactions were performed in oven or flame dried glassware under nitrogen. Solvents used for synthesis of substrate were dried as follows: THF dried over Sodium, dichloromethane dried over CaH. Column chromatography was performed using SiliCycle silica gel (230-400 mesh). ^{1}H-NMR spectra were obtained on Varian Inova 300 MHz or 500 MHz instrument and are reported in parts per million (ppm) relative to the solvent resonances (δ), with coupling constants (*J*) in Hertz (Hz). IR studies were performed on a Galaxy series FTIR 3000 instrument (Matteson). CD spectra were recorded on a JASCO J-810 spectropolarimeter, equipped with a temperature controller (Neslab 111) for low temperature studies, and is reported as λ [nm] ($\Delta\varepsilon_{max}$ [mol^{-1} cm^{-1}]). Optical rotation $[\alpha]_D^{20}$ was measured on Perkin Elmer Polarimeter 341 (normal aperture, 1 ml cell) at 20 °C.

Synthesis of chiral carboxylic acids

α-carboxylic acids

(*S*)-2-Methylbutyric acid, (*R*)-2-methoxy-2-phenylacetic acid, (*R*)-2-phenylpropanoic acid, (*S*)-2-acetoxypropanoic acid and (*S*)-2-bromopropanoic acid were commercially available and were used without further purification.

(*R*)-2-isopropylpent-4-enoic acid (25) was obtained quantitatively during the process of the synthesis of β-carboxylic acid **30** described below, by basic hydrolysis of **45**.

β-carboxylic acids

(*R*)-Citronellic acid was commercially available from Sigma-Aldrich and was used without further purification.

(*R*)-Methyl 3-(benzyloxy)butanoate (**42**):[31] Dry THF (50 mL) was added into a 100 mL flame dried one necked flask equipped with magnetic stir bar and cooled in an ice bath and NaH (110 mg, 4.4 mmol (NaH was previously washed with pentane and dried over nitrogen)), followed by tetrabutylammonium iodide (154 mg, 0.37 mmol) and BnBr (0.66 g, 4.1 mmol) were added. To this solution a solution of methyl-(*R*)-3-hydroxybutanoate (500 mg, 3.7 mmol) in THF (5 mL) was added in portions. After addition was complete the cooling bath was removed and mixture was stirred at room temperature overnight (8 h). Reaction was then cooled to 0 °C and quenched with water (10 mL). Mixture was stirred for 5 min and dichloromethane (50 mL) was added. Layers were separated with separatory funnel and the aqueous phase was extracted with dichloromethane (20 mL). Organic extracts were combined, washed with brine (50 mL) and water (50 ml), and dried over $NaSO_4$. The mixture was concentrated under reduced pressure on a rotary evaporator (25 °C, 200 mmHg). The crude mixture was purified by column chromatography (Silica gel, 2% EtOAc in hexane, $R_f = 0.32$) to give **23** in 94% (0.79 g) yield. $[\alpha]_D^{20}$ = -23.4 (*c*, 2.06 in DCM); ^{1}H-NMR ($CDCl_3$, 300 MHz): δ 1.24 (d, 3H, $J = 6$), 2.38-2.67 (d of AB quartets 2H, $J_1 = 7.2$, $J_2 = 66.9$, $J_3 = 82.2$), 3.65 (s, 3H), 3.63-4.04 (m, 1H), 4.46-4.57 (AB quartet, 2H, $J = 11.7$), 7.22-7.35 (m, 5H); ^{13}C-NMR ($CDCl_3$, 75 MHz): δ 19.7, 41.7, 51.4, 70.7,

71.7, 127.4, 127.5, 128.2, 138.4, 171.7; MS (DCI): 208.1; IR (neat) 3025, 2900, 1730, 1496, 1370, 1300, 1260, 1180, 1130, 1085, 1025.

(*R*)-3-benzyloxybutanoic acid (33): Ester **42** (500 mg, 2.25 mmol) was placed into a one-necked flask equipped with magnetic stir bar and dissolved in a 1:1 mixture of THF 30 mL and aqueous NaOH (2 M). The mixture was heated at reflux in a heating mantle for 8 h and cooled to room temperature. THF was then removed on a rotary evaporator (25 °C, 100 mmHg). The remaining aqueous phase was extracted once with diethyl ether (10 mL). The aqueous phase was then acidified with 1 N aqueous HCl solution to pH~1 and extracted with dichloromethane (3 x 10 mL). The organic extracts were combined, dried with Na_2SO_4 and concentrated on rotary evaporator at 25 °C and 200 mmHg. The crude acid was obtained in 97% yield (0.42 g) as a colorless liquid. $[\alpha]_D^{20}$ = -28.57 (*c*, 3.22 in DCM); ^{1}H-NMR ($CDCl_3$, 500 MHz): δ 1.31 (d, 3H, J = 7.5), 2.51-2.74 (d of AB quartets, 2H, J_1 = 5.5, J_2 = 15.5, J_3 = 98.5, J_4 = 7.5), 4.01-4.08 (m, 1H), 4.54-4.67 (AB quartet, 2H, J_1 = 11.5, J_2 = 35,), 7.28-7.40 (m, 5H); ^{13}C-NMR ($CDCl_3$, 75 MHz): δ 19.6, 41.6, 70.7, 71.5, 127.5, 127.6, 128.2, 138.1, 177.4; MS (DCI): m/z = 94.

(4*R*, 5*S*)-4-methyl-3-(3-methylbutanoyl)-5-phenyloxazolidin-2-one (47):[32] ^{1}H-NMR ($CDCl_3$, 300 MHz): δ 7.37-7.24 (m, 5H), 5.60 (d, 1H, J = 7.2), 4.72 (p, 1H, J = 6.6), 2.89-2.65 (m, 2H), 2.19 (m, 1H), 0.93 (d, 3H, J = 6.6), 0.83 (d, 3H, J = 6.6); ^{13}C-NMR ($CDCl_3$, 75 MHz): δ 172.3,

152.9, 133.3, 128.6, 125.6, 78.7, 54.6, 43.9, 24.9, 22.4, 22.3, 14.4; HRMS (EI+) $[M+H]^+$: calc'd 262.1443, obs'd 262.1448

(4*R*, 5*S*)-3-((*R*)-2-isopropylpent-4-enoyl)-4-methyl-5-phenyloxazolidin-2-one (37): $[\alpha]_D^{20}$ = +11.4 (*c*, 2.1 in DCM); configuration (*R*); R_f = 0.31 (15 % EtOAc in hexane); dr > 99 %; ^{1}H-NMR ($CDCl_3$, 300 MHz): δ 0.80 (d, 3H, J = 6.6), 0.94 (d, 6H, J = 6.9), 1.89-2.01 (m, 1H), 2.30-2.44 (m, 2H), 3.78-3.86 (m, 1H), 4.75 (p, 1H, J = 6.6), 4.89-5.02 (m, 2H), 5.67-5.81 (m, 1H), 7.22-7.39 (m, 5H); ^{13}C-NMR ($CDCl_3$, 75 MHz): δ 14.4, 19.2, 20.8, 30.2, 33.8, 48.3, 54.9, 78.5, 116.7, 125.6, 128.6, 133.3, 135.4, 152.8, 175.5; HRMS (EI+) $[M+H]^+$: calc'd 302.1756, obs'd 302.1761

(*R*)-benzyl 2-isopropylpent-4-enoate (38): $[\alpha]_D^{20}$ = -8.6 (*c*, 2.1 in DCM); configuration (*R*); R_f = 0.24 (2 % EtOAc in hexane); ^{1}H-NMR ($CDCl_3$, 300 MHz): δ 0.90 (d, 3H, J = 6.6), 0.93 (d, 3H, J = 6.6), 1.87 (m, 1H, J = 6.6), 2.24-2.38 (m, 3H), 4.94-5.10 (dd, J_1 = 17.2, J_2 = 20.7), 5.01-5.79 (m, 1H), 7.28-7.35 (m, 5H); ^{13}C-NMR ($CDCl_3$, 75 MHz): δ 20.1, 20.3, 30.2, 33.9, 52.4, 65.8, 116.4, 128.0, 128.2. 128.4, 135.8, 136.1, 174.7; MS (DCI) m/z = 232

(*R*)-benzyl 2-isopropyl-4-oxobutanoate (39): configuration (*R*); R_f = 0.24 (2 % EtOAc in hexane); ^{1}H-NMR ($CDCl_3$, 500 MHz): δ ^{13}C-NMR ($CDCl_3$, 125 MHz): δ 22.4, 23.3, 33.1, 43.1, 48.6, 70.6, 73.1, 75.6, 127.3, 127.5, 128.2, 138.2, 179.1, 202.4;

(*R*)-3-(benzyloxycarbonyl)-4-methylpentanoic acid (40): $[\alpha]_D^{20}$ = -8.0 (*c*, 0.78 in DCM); ^{1}H-NMR ($CDCl_3$, 500 MHz): δ 0.89 (d, 3H, J = 7), 0.91 (d, 3H, J = 7), 2.00-2.03 (m, 1H), 2.42-2.48 (m, 1H), 2.75-2.82 (m, 2H), 5.12 (AB q, 2H, J_1 = 12, J_2 = 3.5), 7.28-7.34 (m, 5H), 8.68 (s, br, 1H); ^{13}C-NMR ($CDCl_3$, 125 MHz): δ 19.4, 20.0, 30.0, 32.7, 47.2, 66.3, 128.1, 128.4, 132.1, 135.9, 174.1, 177.7; MS (DCI) m/z = 250

(*2R, 3S*)-(3-Phenyl-oxiranyl)-methanol (**49**):[33] 4Å molecular sieves (6 g) were placed into a one-necked 500 mL round bottom flask and heated on heating mantel at 300 °C under reduced pressure for 10 h. The flask was then cooled under nitrogen atmosphere and dry dichloromethane (200 mL) was added, stirred for 5 min and cooled to –23 °C. To the cold solution was added L-(+)-diisopropyl tartrate (1.5 mL, 5.6 mmol) followed by Ti(O^iPr)$_4$ (1.5 mL, 5.2 mmol). The catalyst was allowed to age for 30 min and *t*-BuOOH solution in toluene (3.3M, 42 mL) was then added via syringe and the mixture was allowed to stir for another 30 min. Cinnamyl alcohol (3.9 g, 29.1 mmol) was dissolved in dry dichloromethane (20 mL) and slowly added to the main solution over 1 h. The reaction mixture was stirred at –23 °C for 7 h,

warmed to –12 °C and quenched with 40% solution of NaOH in brine (16 g NaOH, 40 ml H_2O and 2 g NaCl) (40 mL). The cooling bath was removed and after 20 min $MgSO_4$ was added and stirring was continued for 10 min. The reaction mixture was allowed to warm to room temperature and filtered through pad of Celite. The filtrate was dried over Na_2SO_4 and concentrated under reduced pressure. The crude mixture was purified by column chromatography (Silica gel) using 5% EtOAc in hexane solution as eluent to give epoxyalcohol **49** in 94% (5 g) yield. $[\alpha]_D^{20}$ = -48 (*c*, 1.0 in $CHCl_3$) [literature value, $[\alpha]_D^{20}$ = -49 (*c*, 0.01 in CH_2Cl_2)[33]]; ^{1}H-NMR ($CDCl_3$, 300 MHz): δ 2.17 (dd, 1H, J_1 = 5, J_2 = 6), 3.26-3.28 (m, 1H), 3.79-3.88 (ddd, 1H, J_1 =4, J_2 = 8, J_3 = 12), 3.97 (d, 1H, J = 2.1), 4.05-4.12 (ddd, J_1 = 2, J_2 = 5, J_3 = 13), 7.26-7.42 (m, 5H); ^{13}C-NMR ($CDCl_3$, 75 MHz): δ 55.6, 61.2, 62.5, 125.6, 128.2, 128.3, 136.6.

((2*S*, 3*S*)-3-phenyloxiran-2-yl)methanol (**50**):[34] To dry THF (100 mL) into a 250 mL flame dried one necked flask equipped with magnetic stir bar and cooled on ice bath was added NaH (0.48 g, 20 mmol, prior to use, NaH was washed with pentane and dried over nitrogen)), followed by tetrabutylammonium iodide (0.5 g, 1.33 mmol) and BnBr (2.4 g, 14 mmol). To this solution a solution of epoxyalcohol **49** (2 g, 13.3 mmol) in THF (10 mL) was added dropwise. After addition was complete the cooling bath was removed and the mixture was stirred at room temperature overnight (8 h). The reaction was then cooled to 0 °C and quenched with water (10 mL). The mixture was stirred for 5 min and dichloromethane (50 mM) was added. The layers

were separated and the aqueous phase was extracted with dichloromethane (2 x 20 mL). The organic extracts were combined, washed with brine (50 mL) and water (50 mL), and dried over $NaSO_4$. The mixture was concentrated under reduced pressure on a rotary evaporator (25 °C, 200 mmHg), and the crude mixture purified by column chromatography (Silica Gel, 2% EtOAc in hexane, R_f = 0.35) to give pure **50** in 95% (3 g) yield. $[\alpha]_D^{20}$ = –38.9 (*c* 0.82, $CHCl_3$) [literature value $[\alpha]_D^{20}$ = –38.9 (*c*, 0.82 in $CHCl_3$)[35]]; ^{1}H-NMR ($CDCl_3$, 300 MHz): δ 3.24-3.27 (m, 1H), 3.61-3.66 (dd, 1H, J_1 = 5.1, J_2 = 11.4), 3.80-3.89 (ddd, 1H, J_1 = 2.1, J_2 = 3.3, J_3 = 13.8), 4.64 (d, 2H, *J* = 2.7), 7.26-7.38 (m, 10 H); ^{13}C-NMR ($CDCl_3$, 75 MHz): δ 55.8, 61.1, 69.8, 73.3, 125.6, 127.7, 127.8, 128.1, 128.3, 128.4, 136.8, 137.8; HRMS (EI+): $C_{16}H_{16}NaO_2$ ($M+Na^+$): 263.1048; found: 263.1048

(2*R*, 3*R*)-1-(benzyloxy)-3-phenylhex-5-en-2-ol (**51**):[35] Epoxide **50** (3 g, 15.6 mmol) was placed into a one-neck round bottom flask (flame dried and cooled under nitrogen), dissolved in dry dichloromethane (100 mL) and cooled with ice bath. To the cold solution was added 2 M solution of allylmagnesium chloride (12 mL, 23.4 mmol) dropwise under nitrogen atmosphere. After compete addition ice bath was removed and reaction mixture was allowed to stir at room temperature for 10 h (overnight). The reaction flask was then cooled on an ice bath and quenched with aqueous saturated solution of NH_4Cl (100 mL). After 10 min of stirring organic layer was separated and aqueous phase was extracted with dichloromethane (3 x 25 mL). The organic extracts were combined, dried over Na_2SO_4 and concentrated on a rotary evaporator. Column

chromatography with 5% EtOAc in hexane afforded the alcohol **51** (R_f = 0.25) in 72% (2.6 g) yield. $[\alpha]_D^{20}$ = -6.9 (*c*, 0.92 in CH_2Cl_2), ^{1}H-NMR ($CDCl_3$, 500 MHz): δ 2.19 (s, 1H (OH)), 2.50-2.56 (m, 1H), 2.60-2.66 (m, 1H), 2.87-2.91 (m, 1H), 3.30-3.32 (dd, 1H, J_1 = 9.5, J_2 = 9.3), 3.49-3.51 (dd, 1H, J_1 = 4, J_2 = 5.5), 4.09-4.12 (m, 1H), 4.52 (s, 2H), 4.97-5.07 (m, 2H), 5.66-5,75 (m, 1H), 7.26-7.40 (m, 10 H); ^{13}C-NMR ($CDCl_3$, 125 MHz): δ 36.3, 48.0, 72.2, 72.8, 73.3, 116.3, 126.6, 127.7, 128.2, 128.4, 128.9, 136.5, 137.9, 140.5; HRMS (FAB) $C_{19}H_{23}O_2$ ($M+H^+$): calc'd 283.1698, obs'd 283.1690.

((2*R*, 3*R*)-1-(benzyloxy)-2-methoxyhex-5-en-3-yl)benzene (**44**): Alcohol **51** (2 g, 8.5 mmol) was placed into a round bottom flask (100 mL, flame dried and cooled under nitrogen atmosphere), dissolved in dry THF (60 mL) and cooled on ice bath. To this solution NaH (0.3 g, 12.2 mmol, NaH was washed with pentane and dried over nitrogen) was added, followed by iodomethane (2.4 g, 12.7 mmol). After addition was complete the cooling bath was removed and the mixture was stirred at room temperature overnight (8 h). Reaction was then cooled to 0 °C and quenched with water (10 mL). The mixture was stirred for 5 min and dissolved with dichloromethane (50 mL). Layers were separated with separatory funnel and the aqueous phase was extracted with dichloromethane (2 x 20 ml). Organic extracts were combined, washed with brine (50 mL) and water (50 mL), and dried over $NaSO_4$. Mixture was concentrated under reduced pressure on a rotary evaporator (25 °C, 200 mmHg). The crude mixture was purified by column chromatography (Silica gel, 2% EtOAc in hexane, R_f = 0.32) to give an olefin **52** in 98%

(2.05 g) yield. $[\alpha]_D^{20}$ = -5.0 (*c*, 1.23 in CH_2Cl_2), ^{1}H-NMR ($CDCl_3$, 500 MHz): δ 2.52-2.58 (m, 1H), 2.61-2.67 (m, 1H), 2.98-3.02 (m, 1H), 3.33-3.36 (m, 1H), 3.44-3.47 (m, 1H), 3.48 (s, 3H), 3.62-3.66 (q, 1H, *J* = 4.5), 4.49 (s, 2H), 4.5-76 (d, 1H, *J* = 10.5), 5.07 (d, 1H, *J* = 17), 5.70, 5.78 (m, 1H), 7.22-7.40 (m, 10 H); ^{13}C-NMR ($CDCl_3$, 125 MHz): δ 36.4, 47.4, 59.1, 70.8, 73.3, 82.1, 116.1, 126.3, 127.5, 126.6, 127.9, 128.2, 129.2, 136.9, 138.2, 141.0

(3*R*, 4*R*)-5-(Benzyloxy)-4-methoxy-3-phenylpentanoic acid (31): Olefin **52** (1.5 g, 0.5 mmol) was placed in a 100 ml one-neck round bottom flask and dissolved in dry CH_2Cl_2 (50 mL). The solution was cooled to –78 °C on dry ice-acetone bath and ozone was purged through the solution via glass pipette until the appearance of intense blue color in the reaction solution. The ozone source was then removed and the reaction mixture was flushed with nitrogen until clear colorless solution was observed. To the obtained ozonide at –78 °C was added 50% solution of H_2O_2 (5 mL) and mixture was allowed to warm and stirred for 2 h at room temperature. The reaction mixture was concentrated and submitted to the column chromatography (Silica, 10% EtOAc in Hexanes) to provide compound (**31**) 67% yield. $[\alpha]_D^{20}$ = +2.2 (*c*, 0.98 in CH_2Cl_2), ^{1}H-NMR ($CDCl_3$, 300 MHz): δ 2.79-3.01 (d of AB quartet, 2H, J_1 = 6, J_2 = 34.8, J_3 = 65.4), 3.30-3.46 (d of AB quartet, 2H, J_1 = 5.4, J_2 = 15, J_3 = 47.4), 3.5 (s, 3H), 3.65-3.69 (q, 1H, *J* = 5.4), 4.48 (s, 2H), 7.26-7.40 (m, 10H); ^{13}C-NMR ($CDCl_3$, 75 MHz): δ 36.19, 43.14, 59.09, 70.28,

73.20, 81.92, 126.56, 127.52, 127.56, 127.59, 127.71, 128.07, 128.26, 128.32, 128.54, 128.74, 129.51, 137.89, 139.49

γ-Chiral carboxylic acids:

(*S*)-Methyl 2-(benzyloxy)propanoate (53):[36] To the solution of (*S*)-ethyl lactate (5 g, 42 mmol) in dry dichloromethane (150 mL) was added benzylbromide (7.9 g, 45 mmol) and silver oxide (10 g, 43 mmol). The reaction mixture was stirred at room temperature for 24 h and filtered through a pad of Celite. The filtrate was concentrated and the obtained crude oil was purified by column chromatography (eluted with 2% EtOAc in hexane) to afford compound **53** in 64% yield (5.6 g): $[\alpha]_D^{20}$ = -72.7 (*c*, 6.6 in $CHCl_3$) [literature value $[\alpha]_D^{20}$ = -74.5 (*c*, 2.92 in $CHCl_3$), *ee%* = 99][36]; ^{1}H-NMR ($CDCl_3$, 300 MHz): δ 1.32 (t, 3H, *J* = 7.6), 1.44 (d, 3H, *J* = 6.9), 4.05 (q, 1H, *J* = 7), 4.22 (q, 2H, *J* = 7), 4 57 (AB quartet, 2H, J_1 = 11.7, J_2 = 49.2), 7.25-7.33 (m, 5H); ^{13}C-NMR ($CDCl_3$, 75 MHz): δ 14.2, 19.5, 60.6, 72.2, 74.0, 127.8, 128.0, 128.5.

(*S*)-2-(Benzyloxy)propan-1-ol (54):[37] Ester **53** (2.5 g, 12 mmol) was dissolved in dry THF (100 mL) and cooled on ice bath. To this solution LAH (0.5 g, 13 mmol) was added portionwise and reaction mixture stirred at room temperature for 4 h. Cooled on ice bath reaction mixture was then quenched slowly with water (30 ml), diluted with EtOAc (50 mL) and stirred for 30 min. The layers were separated, the aqueous layer was extracted with EtOAc (20 mL) and the combined organic extracts were dried and concentrated. Purification of the crude mixture with

column chromatography (Silica Gel, 10% EtOAc in hexane) afforded the alcohol **54** in 95% yield (1.9 g). $[\alpha]_D^{20}$ = +42.8 (*c*, 5 in CH_2Cl_2) [literature value $[\alpha]_D^{20}$ = +45.86 (*c*, 6 in $CHCl_3$)[37]]; ^{1}H-NMR ($CDCl_3$, 300 MHz): δ 1.5 (d, 3H, J = 6), 2.07 (s, br, 1H (OH)), 3.44-3.60 (m, 2H), 3.62-3.68 (m, 1H), 4.44-4.64 (AB quartet, J_1 = 11.7, J_2 = 49.2), 7.25-7.33 (m, 5H); ^{13}C-NMR ($CDCl_3$, 75 MHz): δ 15.1, 66.3, 70.7, 75.5, 127.5, 127.7, 128.4, 138.4.

(*S*)-2-(benzyloxy)propanal (55): Aldehyde was obtained via DMP oxidation of alcohol **54** in dry DCM in 87% yield. $[\alpha]_D^{20}$ = -64 (*c*, 2 in $CHCl_3$) [literature value[38] $[\alpha]_D^{20}$ = -66 (*c*, 6 in $CHCl_3$)]; ^{1}H-NMR ($CDCl_3$, 300 MHz): δ 1.34 (d, 3H, J = 7), 3.90 (qd, 1H, J_1 = 7, J_2 = 1.7), 4.60 (d, 1H, J = 11.7), 4.66 (d, 1H, J = 11.7), 7.25-7.33 (m, 5H); ^{13}C-NMR ($CDCl_3$, 75 MHz): δ 15.3, 71.9, 79.4, 127.9, 128.0, 137.2, 203.4; MS (DCI) *m/z*: 164.1.

(*S*,*E*)-Ethyl 4-(benzyloxy)pent-2-enoate (56): A solution of aldehyde **55** (2 g, 13 mmol) and Wittig reagent (4.7 g, 13.1 mmol) were dissolved in dry dichloromethane (150 mL) and stirred at room temperature for 18 h. The solvent was removed under reduced pressure and the remaining mixture was purified with column chromatography (Silica Gel, 10% EtOAc in hexane) to afford an ester **56** as a yellow liquid in 84% yield (2.4 g). $[\alpha]_D^{20}$ = +20.3 (*c*, 5.1 in CH_2Cl_2); ^{1}H-NMR ($CDCl_3$, 300 MHz): δ 1.29 (t, 3H, J = 7), 1.31 (d, 3H, J = 6.6), 4.08-4.12 (m, 1H), 4.38 (q, 2H, J = 7.2), 4.41 (d, 1H, J = 12), 5.46 (d, 1H, J = 12), 5.98-6.03 (dd, 1H, J_1 = 1.5, J_2 = 15.9), 6.84-

6.91 (dd, 1H, J_1 = 6, J_2 = 15.9), 7 23-7.36 (m, 5H); ^{13}C-NMR ($CDCl_3$, 75 MHz): δ 14.2, 20.6, 60.5, 70.7, 73.8, 121.3, 126.9, 127.6, 127.7, 128.4. 138.1, 149.2, 166.3; MS (DCI) *m/z*: 234.1

(*S*)-Ethyl 4-(benzyloxy)pentanoate (57): To the solution of unsaturated ester **56** (1 g, 4.2 mmol) in ethyl acetate was added Pd/C (10 mg). The reaction mixture was stirred under hydrogen atmosphere for 3 h and was filtered through pad of Celite. The filtrate was concentrated under reduced pressure to give **57** in quantitative yield (no benzyl cleavage was detected). $[\alpha]_D^{20}$ = +21.3 (*c*, 6.26 in $CHCl_3$); ^{1}H-NMR ($CDCl_3$, 300 MHz): δ 1.25 (d, 3H, J = 6), 1.27 (t, 3H, J = 7), 1.89 (q, 2H, J = 7.2), 2.43-2.46 (dt, 2H, J_1 = 3, J_2 = 7.5), 3.60 (m, 1H, J = 6), 4.47 (d, 1H, J = 11.7), 4.62 (d, 1H, J = 11.7), 7.29-7.40 (m, 5H); ^{13}C-NMR ($CDCl_3$, 75 MHz): δ 14.1, 19.3, 30.3, 31.6, 60.1, 70.3, 73.7, 127.4, 127.6, 128.2, 138.7, 173.6; MS (DCI) *m/z*: 236.

(*S*)-4-(Benzyloxy)pentanoic acid (36): Ester **57** (0.3 g, 1.27 mmol) was dissolved in THF (5 mL) and 2M NaOH (3 ml) and refluxed overnight. THF was then removed under reduced pressure and the remaining solution acidified with 10% HCl and extracted with DCM (3 x 10 mL). Extracts were combined, dried over Na_2SO_4 and concentrated to give a crude acid in ~96% yield. $[\alpha]_D^{20}$ = (*c*, 6.26 in $CHCl_3$); ^{1}H-NMR ($CDCl_3$, 300 MHz): δ 1.22 (d, 3H, J = 6), 1.84 (q, 2H, J = 7.5), 2.47 (dt, 2H, J_1 = 2.1, J_2 = 7.5), 3.60 (m, 1H, J = 6), 4.41-4.68 (AB q, 2H, J_1 = 11.4, J_2 = 46.8), 7.28-7.39 (m, 5H); ^{13}C-NMR ($CDCl_3$, 75 MHz): δ 19.4, 30.2, 31.3, 70.4, 73.6, 127.5, 127.7, 128.3, 138.5, 179.7.

(*S*)-Methyl 2-methoxy-2-phenylacetate (59):[39] To the solution of **58** (3 g, 18 mmol) in dry dichloromethane (50 mL) was added iodomethane (3.6 g, 21.6 mmol) and silver oxide (5 g, 21.6 mmol). The reaction mixture was stirred at room temperature for 24 h and filtered through a pad of Celite. The filtrate was concentrated and the obtained crude oil was purified by column chromatography (eluted with 2% EtOAc in hexane) to afford compound **59** in 77% yield (2.5 g): $[\alpha]_D^{20}$ = (c, DCM); ^{1}H-NMR ($CDCl_3$, 500 MHz): δ 3.37 (s, 3H), 3.69 (s, 3H), 4.74 (s, 1H), 7.31-7.42 (m, 5H); ^{13}C-NMR ($CDCl_3$, 125 MHz): δ 52.2, 57.3, 82.5, 127.2, 128.6, 128.7, 136.1, 171.1

(S)-2-Methoxy-2-phenylethanol (60): To the ice cold solution of **59** (2 g, 11 mmol) in dry THF (60 mL) was added LAH (0.5 g, 13.3 mmol) portion-wise and the reaction mixture was stirred at room temperature for 4 h. The mixture was then cooled back to 0 °C and was slowly quenched with cold water. After 30 min Na_2SO_4 (10 g) was added and mixture was stirred for additional 30 min. The solution was then filtered through a pad of Celite, the filter cake was washed with dichloromethane (2 x 25 mL) and the filtrate was dried with Na_2SO_4 and concentrated. Flash chromatography (10% EtOAc in hexane) afforded alcohol **60** in 95% yield (1.6g). $[\alpha]_D^{20}$ = +113.2 (*c*, 3.57 in DCM); ^{1}H-NMR ($CDCl_3$, 500 MHz): δ 2.54 (s, 1H (OH)), 3.28 (s, 3H), 3.57-3.68 (m, 2H), 4.27-4.30 (dd, 1H, J_1 = 4, J_2 = 8), 7.27-7.36 (m, 5H); ^{13}C-NMR ($CDCl_3$, 125 MHz): δ 56.8, 67.3, 84.6, 126.8, 128.1, 128.5, 138.3.

(*S*)-2-Methoxy-2-phenylacetaldehyde (61): To the solution of alcohol **60** in dry dichloromethane (50 mL) was added DMP and mixture stirred at room temperature under nitrogen atmosphere for 4 h. The mixture was filtered through Celite and concentrated. Column chromatography (Silica Gel, 5% EtOAc in hexane) afforded aldehyde **61** in 87% yield. $[\alpha]_D^{20}$ = (c, DCM); ^{1}H-NMR ($CDCl_3$, 500 MHz): δ; ^{13}C-NMR ($CDCl_3$, 125 MHz):

(*R*, *E*)-Methyl 4-methoxy-4-phenylbut-2-enoate (62):[40] Solution of aldehyde **61** (0.5 g, 3.3 mmol) in dry dichloromethane (50 mL) and ylide (1 g, 3.6 mmol) was stirred at room temperature for 12 h, concentrated and directly transferred into the Silica Gel column. The resulting ester was washed out with 2% EtOAc in hexane in 97% (0.66 g) yield. ^{1}H-NMR ($CDCl_3$, 500 MHz): δ 1.25 (t, 3H, J = 7.2), 3.31 (s, 3H), 4.16 (q, 2H, J = 7.2), 4.74-4.77 (dd, 1H), 6.02-6.08 (dd, 1H, J_1 = 1.2, J_2 = 15.9), 6.90-6.97 (dd, 1H, J_1 = 5.4, J_2 = 15.6), 7.26-7.41 (m, 5H); ^{13}C-NMR ($CDCl_3$, 125 MHz): 14.1, 20.1, 42.0, 60.3, 120.2, 127.0, 127.6, 128.9, 143.6, 152.9, 167.0; MS (DCI) *m/z* 206.

(*R*)-Methyl 4-methoxy-4-phenylbutanoate (63): Olefin **62** (0.6 g, 2.9 mmol) was dissolved in methanol and Pd/C was added (12 mg). The reaction mixture was stirred under hydrogen atmosphere for 4 h and filtered through Celite. The filtrate was concentrated to afford ester **63** in quantitative yield. $[\alpha]_D^{20}$ = +48.6 (*c*, 3.40 in DCM); ^{1}H-NMR ($CDCl_3$, 500 MHz): δ 1.25 (t, 3H, J = 7.2), 3.31 (s, 3H), 4.16 (q, 2H, J = 7.2), 4.74-4.77 (dd, 1H), 6.02-6.08 (dd, 1H, J_1 = 1.2, J_2 =

15.9), 6.90-6.97 (dd, 1H, J_1 = 5.4, J_2 = 15.6), 7.26-7.41 (m, 5H); 14.1, 20.1, 42.0, 60.3, 120.2, 127.0, 127.6, 128.9, 143.6, 152.9, 167.0; MS (DCI) *m/z* 208.

(*R*)-4-Methoxy-4-phenylbutanoic acid (33): ^{1}H-NMR ($CDCl_3$, 500 MHz): δ 1.97-2.17 (m, 2H), 2.47-2.52 (m, 2H), 3.26 (s, 3H), 4.20-4.25 (dd, 1H, J_1 = 5.1, J_2 = 7.1), 7.29-7.43 (m, 5H), 11.26 (s, br, 1H (OH)); ^{13}C-NMR ($CDCl_3$, 125 MHz): δ 30.4, 32.8, 56.7, 82.7, 126.5, 127.8, 128.4, 128.5, 141.3, 179.6

REFERENCES

References

1. Saidi, M. R.; Azizi, N.; Zali-Boinee, H., A simple one-pot three-component reaction for preparation of secondary amines and amino esters mediated by lithium perchlorate. *Tetrahedron* **2001,** *57* (31), 6829-6832.

2. Fukui, H.; Fukushi, Y., NMR Determinations of the Absolute Configuration of alpha-Chiral Primary Amines. *Organic Letters* **2010,** *12* (12), 2856-2859.

3. Khelili, S.; de Tullio, P.; Lebrun, P.; Fillet, M.; Antoine, M. H.; Ouedraogo, R.; Dupont, L.; Fontaine, J.; Felekidis, A.; Leclerc, G.; Delarge, J.; Pirotte, B., Preparation and pharmacological evaluation of the R- and S-enantiomers of 3-(2 '-butylamino)-4H- and 3-(3 '-methyl-2 '-butylamino)-4H-pyrido 4,3-e -1,2,4-thiadiazine 1,1-dioxide, two tissue selective ATP-sensitive potassium channel openers. *Bioorganic & Medicinal Chemistry* **1999,** *7* (8), 1513-1520.

4. (a) Gargiulo, D.; Cai, G. L.; Ikemoto, N.; Bozhkova, N.; Odingo, J.; Berova, N.; Nakanishi, K., CD Exciton chirality method - new chromophores for primary amino-groups. *Angewandte Chemie-International Edition in English* **1993,** *32* (6), 888-891; (b) Huang, X. F.; Borhan, B.; Rickman, B. H.; Nakanishi, K.; Berova, N., Zinc porphyrin tweezer in host-guest complexation: Determination of absolute configurations of primary monoamines by circular dichroism. *Chemistry-a European Journal* **2000,** *6* (2), 216-224; (c) Kurtan, T.; Nesnas, N.; Li, Y. Q.; Huang, X. F.; Nakanishi, K.; Berova, N., Chiral recognition by CD-sensitive dimeric zinc porphyrin host. 1. Chiroptical protocol for absolute configurational assignments of monoalcohols and primary monoamines. *Journal of the American Chemical Society* **2001,** *123* (25), 5962-5973.

5. (a) Proni, G.; Pescitelli, G.; Huang, X. F.; Nakanishi, K.; Berova, N., Magnesium tetraarylporphyrin tweezer: A CD-sensitive host for absolute configurational assignments of alpha-chiral carboxylic acids. *Journal of the American Chemical Society* **2003,** *125* (42), 12914-12927; (b) Yang, Q.; Olmsted, C.; Borham, B., Absolute stereochemical determination of chiral carboxylic acids. *Organic Letters* **2002,** *4* (20), 3423-3426.

6. Borovkov, V. V.; Lintuluoto, J. M.; Inoue, Y., Supramolecular chirogenesis in zinc porphyrins: Mechanism, role of guest structure, and application for the absolute configuration determination. *Journal of the American Chemical Society* **2001,** *123* (13), 2979-2989.

7. Dale, J. A.; Mosher, H. S., Nuclear magnetic-resonance enantiomer reagents - configurational correlations via nuclear magnetic-resonance chemical-shifts of diastereomeric mandelate, o-methylmandelate, and alpha-methoxy-alpha-trifluoromethylphenylacetate (mtpa) esters. *Journal of the American Chemical Society* **1973,** *95* (2), 512-519.

8. Sullivan, G. R.; Dale, J. A.; Mosher, H. S., Correlation of configuration and f-19 chemical-shifts of alpha-methoxy-alpha-trifluoromethylphenylacetate derivatives. *Journal of Organic Chemistry* **1973,** *38* (12), 2143-2147.

9. (a) Scott, R.; Vinograd.S, Proton-transfer complexes .2. role of solvent polarity and specific solvation of p-nitrophenol-amine complexes in aqueous solutions. *Journal of Physical Chemistry* **1969,** *73* (6), 1890-&; (b) Scott, R.; Depalma, D.; Vinograd.S, Proton-transfer complexes .i. preferential solvation of p-nitrophenol-amine complexes in nonaqueous-solvent mixtures. *Journal of Physical Chemistry* **1968,** *72* (9), 3192-&; (c) Hudson, R. A.; Vinograd.Sn; Scott, R. M., Hydrogen-bonded complex-ion-pair equilibria in 3,4-dinitrophenol-amine-aprotic solvent system. *Journal of Physical Chemistry* **1972,** *76* (14), 1989-&; (d) Hanessian, S.; Simard, M.; Roelens, S., Molecular recognition and self-assembly by non-amidic hydrogen-bonding - an exceptional assembler of neutral and charged supramolecular structures. *Journal of the American Chemical Society* **1995,** *117* (29), 7630-7645.

10. (a) Ferrarini, A.; Ferroni, F.; Pieraccini, S.; Rosini, C.; Superchi, S.; Spada, G. P., Central-to-Axial Chirality Transfer Revealed by Liquid Crystals: A Combined Experimental and Computational Approach for the Determination of Absolute Configuration of Carboxylic Acids with an alpha Chirality Centre. *Chirality* **2011,** *23* (9), 736-743; (b) Sahnoun, R.; Koseki, S.; Fujimura, Y., Density functional theoretical study on enantiomerization of 2,2 '-biphenol. *Journal of Physical Chemistry A* **2006,** *110* (7), 2440-2447; (c) Kranz, M.; Clark, T.; Schleyer, P. V., Rotational barriers of 1,1'-binaphthyls - a computational study. *Journal of Organic Chemistry* **1993,** *58* (12), 3317-3325.

11. Ishii, Y.; Onda, Y.; Kubo, Y., 2,2 '-Biphenyldiol-bridged bis(free base porphyrin): synthesis and chiroptical probing of asymmetric amino alcohols. *Tetrahedron Letters* **2006,** *47* (47), 8221-8225.

12. Whitesell, J. K., C2 Symmetry and asymmetric induction. *Chemical Reviews* **1989,** *89* (7), 1581-1590.

13. (a) Hoye, T. R.; Renner, M. K., Applications of MTPA (Mosher) amides of secondary amines: Assignment of absolute configuration in chiral cyclic amines. *Journal of Organic Chemistry* **1996,** *61* (24), 8489-8495; (b) Hoye, T. R.; Renner, M. K., MTPA (Mosher) amides of cyclic secondary amines: Conformational aspects and a useful method for assignment of amine configuration. *Journal of Organic Chemistry* **1996,** *61* (6), 2056-2064.

14. Huang, X. F.; Fujioka, N.; Pescitelli, G.; Koehn, F. E.; Williamson, R. T.; Nakanishi, K.; Berova, N., Absolute configurational assignments of secondary amines by CD-sensitive dimeric zinc porphyrin host. *Journal of the American Chemical Society* **2002,** *124* (35), 10320-10335.

15. (a) Tanner, D., Chiral aziridines - their synthesis and use in stereoselective transformations. *Angewandte Chemie-International Edition in English* **1994,** *33* (6), 599-619; (b) Tanner, D.; Andersson, P. G.; Harden, A.; Somfai, P., C-2 Symmetrical bis(aziridines) - a new class of chiral ligands for transition metal-mediated asymmetric-synthesis. *Tetrahedron Letters* **1994,** *35* (26), 4631-4634; (c) Tanner, D.; Birgersson, C.; Gogoll, A.; Luthman, K., On the use of C-2 symmetrical aziridines as chiral auxiliaries. *Tetrahedron* **1994,** *50* (32), 9797-9824; (d) Muller, P.; Fruit, C., Enantioselective catalytic aziridinations and asymmetric nitrene insertions into CH bonds. *Chemical Reviews* **2003,** *103* (8), 2905-2919.

16. Pineschi, M., Asymmetric ring-opening of epoxides and aziridines with carbon nucleophiles. *European Journal of Organic Chemistry* **2006,** (22), 4979-4988.

17. (a) Nicolaou, K. C. S., E. J., *Classics in Total Synthesis;* . VCH: Weinheim: 1996; (b) Liu, M.; Sibi, M. P., Recent advances in the stereoselective synthesis of beta-amino acids. *Tetrahedron* **2002,** *58* (40), 7991-8035; (c) Kato, D.; Mitsuda, S.; Ohta, H., Microbial deracemization of alpha-substituted carboxylic acids: Substrate specificity and mechanistic investigation. *Journal of Organic Chemistry* **2003,** *68* (19), 7234-7242.

18. (a) Custar, D. W.; Zabawa, T. P.; Hines, J.; Crews, C. M.; Scheidt, K. A., Total Synthesis and Structure-Activity Investigation of the Marine Natural Product Neopeltolide. *Journal of the American Chemical Society* **2009,** *131* (34), 12406-12414; (b) Nicolaou, K. C.; Nold, A. L.; Milburn, R. R.; Schindler, C. S.; Cole, K. P.; Yamaguchi, J., Total synthesis of marinomycins A-C and of their monomeric counterparts monomarinomycin A and iso-monomarinomycin A. *Journal of the American Chemical Society* **2007,** *129* (6), 1760-1768.

19. Nicolaou, K. C.; Ajito, K.; Patron, A. P.; Khatuya, H.; Richter, P. K.; Bertinato, P., Total synthesis of swinholide A. *Journal of the American Chemical Society* **1996,** *118* (12), 3059-3060.

20. (a) Latypov, S. K.; Seco, J. M.; Quinoa, E.; Riguera, R., Conformational structure and dynamics of arylmethoxyacetates - dnmr spectroscopy and aromatic shielding effect. *Journal of Organic Chemistry* **1995,** *60* (3), 504-515; (b) Ferreiro, M. J.; Latypov, S. K.; Quinoa, E.; Riguera, R., Assignment of the absolute configuration of alpha-chiral carboxylic acids by H-1 NMR spectroscopy. *Journal of Organic Chemistry* **2000,** *65* (9), 2658-2666; (c) Seco, J. M.; Quinoa, E.; Riguera, R., A practical guide for the assignment of the absolute configuration of alcohols, amines and carboxylic acids by NMR. *Tetrahedron-Asymmetry* **2001,** *12* (21), 2915-2925; (d) Ferreiro, M. J.; Latypov, S. K.; Quinoa, E.; Riguera, R., The use of ethyl 2-(9-anthryl)-2-hydroxyacetate for assignment of the absolute configuration of carboxylic acids by H-1 NMR. *Tetrahedron-Asymmetry* **1997,** *8* (7), 1015-1018.

21. Proni, G.; Pescitelli, G.; Huang, X. F.; Quraishi, N. Q.; Nakanishi, K.; Berova, N., Configurational assignment of alpha-chiral carboxylic acids by complexation to dimeric Zn-porphyrin: host-guest structure, chiral recognition and circular dichroism. *Chemical Communications* **2002,** (15), 1590-1591.

22. (a) Nagai, Y.; Kusumi, T., New chiral anisotropic reagents for determining the absolute-configuration of carboxylic-acids. *Tetrahedron Letters* **1995,** *36* (11), 1853-1856; (b) Yabuuchi, T.; Ooi, T.; Kusumi, T., Application of phenylglycine methyl ester (PGME) to determination of the absolute configuration of carboxylic acids having phenylalkyl group. *Chirality* **1997,** *9* (5-6), 550-555.

23. Joyce, L. A.; Maynor, M. S.; Dragna, J. M.; da Cruz, G. M.; Lynch, V. M.; Canary, J. W.; Anslyn, E. V., A Simple Method for the Determination of Enantiomeric Excess and identity of Chiral Carboxylic Acids. *Journal of the American Chemical Society* **2011,** *133* (34), 13746-13752.

24. (a) Mizutani, T.; Kurahashi, T.; Murakami, T.; Matsumi, N.; Ogoshi, H., Molecular recognition of carbohydrates by zinc porphyrins: Lewis acid Lewis base combinations as a dominant factor for their selectivity. *Journal of the American Chemical Society* **1997,** *119* (38), 8991-9001; (b) Mizutani, T.; Ema, T.; Yoshida, T.; Kuroda, Y.; Ogoshi, H., Recognition of alpha-amino-acid esters by zinc porphyrin derivatives via coordination and hydrogen-bonding interactions - evidence for 2-point fixation from thermodynamic and induced circular-dichroism spectroscopic studies. *Inorganic Chemistry* **1993,** *32* (10), 2072-2077; (c) Mizutani, T.; Murakami, T.; Ogoshi, H., Dynamics of molecular recognition of multi-point host-guest complex. *Tetrahedron Letters* **1996,** *37* (30), 5369-5372; (d) Rudkevich, D. M.; Shivanyuk, A. N.; Brzozka, Z.; Verboom, W.; Reinhoudt, D. N., A self-assembled bifunctional receptor. *Angewandte Chemie-International Edition in English* **1995,** *34* (19), 2124-2126.

25. Hoye, T. R.; Hamad, A. S. S.; Koltun, D. O.; Tennakoon, M. A., An NMR method for determination of configuration of beta-substituted carboxylic acids. *Tetrahedron Letters* **2000,** *41* (14), 2289-2293.

26. Hoye, T. R.; Koltun, D. O., An NMR strategy for determination of configuration of remote stereogenic centers: 3-methylcarboxylic acids. *Journal of the American Chemical Society* **1998,** *120* (19), 4638-4643.

27. Yashima, E.; Nimura, T.; Matsushima, T.; Okamoto, Y., Poly((4-dihydroxyborophenyl)acetylene) as a novel probe for chirality and structural assignments of

various kinds of molecules including carbohydrates and steroids by circular dichroism. *Journal of the American Chemical Society* **1996,** *118* (40), 9800-9801.

28. (a) Gimple, O.; Schreier, P.; Humpf, H. U., A new exciton-coupled circular dichroism method for assigning the absolute configuration in acyclic alpha- and beta-hydroxy carboxylic acids. *Tetrahedron-Asymmetry* **1997,** *8* (1), 11-14; (b) Hor, K.; Gimple, O.; Schreier, P.; Humpf, H. U., Absolute configurational assignment of acyclic hydroxy carboxylic acids: A new strategy in exciton-coupled circular dichroism. *Journal of Organic Chemistry* **1998,** *63* (2), 322-325.

29. (a) Louzao, I.; Garcia, R.; Manuel Seco, J.; Quinoa, E.; Riguera, R., Absolute Configuration of Ketone Cyanohydrins by (1)H NMR: The Special Case of Polar Substituted Tertiary Alcohols. *Organic Letters* **2009,** *11* (1), 53-56; (b) Louzao, I.; Manuel Seco, J.; Quinoa, E.; Riguera, R., (13)C NMR as a general tool for the assignment of absolute configuration. *Chemical Communications* **2010,** *46* (42), 7903-7905; (c) Louzao, I.; Seco, J. M.; Quinoa, E.; Riguera, R., The assignment of absolute configuration of cyanohydrins by NMR. *Chemical Communications* **2006,** (13), 1422-1424; (d) Louzao, I.; Seco, J. M.; Quinoa, E.; Riguera, R., The Use of a Single Derivative in the Configurational Assignment of Ketone Cyanohydrins. *European Journal of Organic Chemistry* **2010,** (34), 6520-6524.

30. (a) Moon, L. S.; Jolly, R. S.; Kasetti, Y.; Bharatam, P. V., A new chiral shift reagent for the determination of enantiomeric excess and absolute configuration in cyanohydrins. *Chemical Communications* **2009,** (9), 1067-1069; (b) Moon, L. S.; Pal, M.; Kasetti, Y.; Bharatam, P. V.; Jolly, R. S., Chiral Solvating Agents for Cyanohydrins and Carboxylic Acids. *Journal of Organic Chemistry* **2010,** *75* (16), 5487-5498.

31. Seebach, D. B., U.; Schnurrenberger, P.; Przybyski, M., High-yielde synthesis of 20-, and 25-membered macropentolide, hexolide, and -heptolide, respectrively, from (R)- or (S)-3-hydroxybutanoic acid under Yamaguchi's macrolactonization condirions. *Helvetica Chimica Acta* **1988,** *71* (1), 155-167.

32. Braddock, D. C.; Brown, J. M., Asymmetric synthesis and Lewis acid mediated type II carbonyl ene cyclisations of (R)-2-isopropyl-5-methylhex-5-enal. *Tetrahedron-Asymmetry* **2000,** *11* (17), 3591-3607.

33. Nandy, J. P.; Prabhakaran, E. N.; Kumar, S. K.; Kunwar, A. C.; Iqbal, J., Reverse turn induced pi-facial selectivity during polyaniline-supported cobalt(II) salen catalyzed aerobic epoxidation of N-cinnamoyl L-proline derived peptides. *Journal of Organic Chemistry* **2003,** *68* (5), 1679-1692.

34. VidalFerran, A.; Moyano, A.; Pericas, M. A.; Riera, A., Synthesis of a family of fine-tunable new chiral ligands for catalytic asymmetric synthesis. Ligand optimization through the enantioselective addition of diethylzinc to aldehydes. *Journal of Organic Chemistry* **1997,** *62* (15), 4970-4982.

35. Tanaka, T.; Hiramatsu, K.; Kobayashi, Y.; Ohno, H., Chemo- and stereoselectivity in titanium-mediated regioselective ring-opening reaction of epoxides at the more substituted carbon. *Tetrahedron* **2005,** *61* (28), 6726-6742.

36. Aragozzini, F.; Maconi, E.; Potenza, D.; Scolastico, C., Enantioselective Microbial Reduction of Monoesters of 1,3-Dihydroxypropanone - Synthesis of (S)-1,2-O-Isopropylideneglycerol and (R)-1,2-O-Isopropylideneglycerol. *Synthesis-Stuttgart* **1989,** (3), 225-227.

37. Takai, K.; Heathcock, C. H., Acyclic Stereoselection .32. Synthesis and Characterization of the Diastereomeric (4s)-Pentane-1,2,3,4-Tetrols. *Journal of Organic Chemistry* **1985,** *50* (18), 3247-3251.

38. SolladieCavallo, A.; Bonne, F., Synthesis of enantiomerically pure threo 1-alkyl-2-benzyloxy-propylamines. *Tetrahedron-Asymmetry* **1996,** *7* (1), 171-180.

39. Annunziata, R.; Cinquini, M.; Cozzi, F.; Gilardi, A.; Cardani, S.; Poli, G.; Scolastico, C., Double Stereoselection in the Aldol-Type Synthesis of Gamma-Methyl and Gamma-Alkoxy Beta-Hydroxy Ketones Mediated by Alpha-Sulfinyl Hydrazones. *Journal of the Chemical Society-Perkin Transactions 1* **1985,** (2), 255-259.

40. Bull, S. D.; Davies, S. G.; Domingez, S. H.; Jones, S.; Price, A. J.; Sellers, T. G. R.; Smith, A. D., Diastereoselective [2,3]-sigmatropic rearrangements of lithium N-benzyl-O-allylhydroxylamides bearing a stereogenic centre adjacent to the migration terminus. *Journal of the Chemical Society-Perkin Transactions 1* **2002,** (19), 2141-2150.